THE BIOSYNTHESIS OF *CIS*-CARBAPENEMS AND THE DEVELOPMENT OF PENEM ANTIBIOTICS FOR THE TREATMENT OF TUBERCULOSIS

by
Evan P. Lloyd

A dissertation submitted to Johns Hopkins University in conformity with the requirements for the degree of Doctor of Philosophy

Baltimore, Maryland

February, 2017

Abstract

Inspired by their naturally occurring members, the carbapenem class of β-lactam antibiotics have been heavily researched over the past forty years, resulting in the development of a set of broad-spectrum, β-lactamase resistant, last resort antibiotics for the treatment of severe bacterial infections. Manufactured by total synthesis, carbapenems are limited to their use in the first world due to their high cost. As antibacterial resistance increases, the need for these drugs is rising.

To combat the high price of manufacture, fermentation or semi-synthetic methods that take advantage of the enzymatic machinery of their biosynthesis to assemble the carbapenem core would reduce the number of synthetic steps and ultimately the cost of production. The key biosynthetic steps to assemble the carbapenem core, however, remain unknown. In this dissertation, we studied the MM 4550 biosynthetic gene cluster to examine how carbapenems are made by comparative genomics and we uncovered clues about how *cis*-carbapenems might diverge from thienamycin. Total syntheses of *cis*-carbapenems were completed for activity assays with newly discovered enzymes in the MM 4550 gene cluster; CmmSu, Cmm17 and CmmPah. Additionally, 2-thioalkyl carbapenam substrates were synthesized for assays with ThnK *in vitro*, which was found to perform sequential double methylation of carbapenam substrates for the installation of the 6-ethyl sidechain of thienamycin. The function of ThnK has provided a path forward to uncovering the remaining biosynthetic steps carries out by the function of ThnL and ThnP.

In collaboration with Prof. Gyanu Lamichhane at the Johns Hopkins Medical Institute, a new class of cell wall crosslinking transpeptidases in *Mycobacteria*, L,D-

transpeptidases (Ldts), was screened for their inhibition by commercially available β-lactam antibiotics using intact protein analysis electrospray ionization high-resolution mass spectrometry. We found that carbapenems form covalent adducts with Ldts and through efficient inhibition are potent drugs against *Mycobacterium tuberculosis*. Faropenem was found to be the most potent inhibitor of Ldts, however, unlike carbapenems, was unsuccessful against Tuberculosis infection *in vivo.* As a result, we synthesized new penems that take advantage of the best carbapenem structural features with the goal to retain both the high potency of penems but the *in vivo* success of carbapenems. Our lead compound has been found to have highly potent antibacterial activity, as evidenced by MIC_{90} data against *M. tuberculosis* and other pathogenic bacteria. The results of *in vivo* tests in an animal model of the disease will be forthcoming.

Thesis advisor:

Professor Craig A. Townsend, Department of Chemistry

Dissertation Committee:

Professor John P. Toscano, Department of Chemistry

Professor John D. Tovar, Department of Chemistry

Acknowledgements

I have many people to thank for helping me along my journey through graduate school. I must first thank Dr. Craig Townsend. Dr. Townsend has taught me how to study problems with a critical eye. Through his encouragement, I've learned how to conduct scientific research at a high level using all the resources at my disposal. I especially thank him for his patience and unwavering support for me in my career. He has always been understanding of my needs scientifically and personally, and I can't thank him enough for his hard work every day. I'd also like to thank our collaborators, Dr. Gyanu Lamichhane and Dr. Squire Booker. Gyanu has provided me with many opportunities to contribute to his great project, and through collaboration with his lab we have learned a lot about the power of synthetic chemistry for drug discovery. Dr. Booker was so welcoming to us each time visiting his lab and provided us with his expertise and facilities without which we would have never learned anything about ThnK,

There is nobody I know other than Dr. Rongfeng Li who has as much knowledge and expertise in biological research. He has helped me throughout my graduate career with a unique perspective. Rongfeng is always excited to talk about research with me and has been a big influence in my education as a chemical biologist.

My work with Dr. Daniel Marous on ThnK was my favorite project during my Ph.D. Due to his friendship, I had fun on our trips to Penn State even though those weeks were some of the longest hours I spend in lab.

Dr. Kristos Moshos was a very patient mentor when I first joined the lab. Through his guidance I quickly refined my synthetic skills during my summer rotation in 2010, and without his help I wouldn't have accomplished much in my first few years.

Dr. Andrew Buller, Dr. Courtney Hastings and Dr. Jesse Li helped mentor me as a scientist and a young professional early in my Ph.D. Darcie Long, Doug Cohen, Ryan Oliver and Jacob Kravitz have become my best friends in the lab, and besides talking at length about science, I appreciate the time I spent with them outside of lab.

I also thank the next generation of graduate students, particularly Hunter Batchelder, Erica Sinner and Trevor Zandi who will continue the projects I worked on for so many years. I wish Hunter luck with the *cis*-carbapenem biosynthesis project, Trevor with the Tuberculosis collaboration, and Erica with the radical SAMs. Their future work will solve the remaining mysteries of carbapenem biosynthesis and generate important new drugs.

Without the Johns Hopkins chemistry department staff I wouldn't be able to conduct the experiments needed to make any of the progress discussed in this dissertation. I thank Dr. Phil Mortimer for keeping the mass spectrometers up and running, and Dr. Cathy Moore, Dr. Joel Tang, Dr. Chuck Long, and Dr. Ananya Majumdar for their help with NMR spectroscopy. As administrative staff, Rosalie Elder, Lauren McGhee, Jean Goodwin and John Kidwell were always generous with providing help when I needed it. Our facilities manager Boris Steinberg works as hard as anyone in the department and his enthusiasm and broad skill set has solved a lot of technical issues needed to keep our work moving forward, from tracking down missing packages to assisting me with using the drill press in the machine shop.

Most of all, I have to thank my family. Without my wife Christina, none of the work described here would be possible. She has encouraged me through the frustrating times and celebrated with me every success. I can't wait to begin the next chapter of my

life with Christina and our son, Darren. My parents and sister, Emma, have always been confident in my abilities even when I wasn't, and I am grateful that I know I can lean on them whenever necessary. My best friends Spencer and Drew provided much needed relief and relaxation, and their perspective on the world outside of lab keeps me grounded.

Nobody can accomplish anything worth achieving without support from their friends, family and coworkers. The best lesson I learned was to never be afraid to ask for help; whether it's from a fellow student in lab or a professor at a different university. I've come to appreciate collaboration with others, and working with people to solve complex problems using our combined experiences and skill sets is my favorite aspect of scientific research. I am fortunate to have worked with all of those listed in the above paragraphs; a few words cannot describe how grateful I am for each person who has influenced my education.

For Christina

"People who work together will win, whether it be against complex football defenses, or the problems of modern society"

-Vince Lombardi-

Publications Drawing Upon This Thesis

1. R. Li, **E.P. Lloyd**, K.A. Moshos, C.A. Townsend. "Identification and characterization of the carbapenem MM 4550 and its gene cluster in *Streptomyces argenteolus* ATCC 11009." *ChemBioChem*, 2014, 15 (2), 320-31.

2. M.J. Bodner, R.M. Phelan, M.F. Freeman, K.A. Moshos, **E.P. Lloyd**, C.A. Townsend. "Definition of the common and divergent steps in carbapenem β-lactam antibiotic biosynthesis." *ChemBioChem,* 2011, 12 (14), 2159-65.

3. D.R. Marous, **E.P. Lloyd**, A.R. Buller, T.L. Grove, A.J. Blaszczyk, S.J. Booker, C.A. Townsend. "Consecutive radical *S*-adenosylmethionine methylations form the ethyl side chain in thienamycin biosynthesis." *Proc. Natl. Acad. Sci. U.S.A.*, 2015, 112 (33), 10354-8.

4. L.A. Basta, A Ghosh, Y. Pan, J Jean, **E.P. Lloyd**, C.A. Townsend, G. Lamichhane, M.A. Bianchet. "Loss of a functionally and structurally distinct L,D-transpeptidase LdtMt5, compromises cell wall integrity in *Mycobacterium tuberculosis.*" *J. Biol. Chem.*, 2015, 290 (42), 25670-85.

5. P. Kumar, A. Kaushik, **E.P. Lloyd**, S-G. Li, R. Mattoo, N. Ammerman, D. Bell, A. Perryman, T. Zandi, S. Ekins, S. Ginell, C.A. Townsend, J. Freundlich, G. Lamichhane. "Non-classical transpeptidases yield insight into new antibacterials." *Nat. Chem. Biol.,* 2017, 13, 54-61.

6. R. Mattoo, **E.P. Lloyd**, A. Kaushik, P. Kumar, J.L. Brunelle, C.A. Townsend, G. Lamichhane. "A molecular vulnerability in *Mycobacterium avium:* L,D-transpeptidase orthologue in *Mycobacterium avium* is constitutively expressed and inhibited by carbapenems." *Future Microbiol.,* 2017 *in press.*

Submitted or In Preparation:

7. Y.H. Pan, L.A. Basta, H.G. Saaverdra, **E.P. Lloyd**, P. Kumar, R. Mattoo, C.A. Townsend, M.A. Bianchet, G. Lamichhane. "Structural insight into the mechanism of inhibition of *Mycobacterium tuberculosis* L,D-transpeptidase 2 by Biapenem and Tebipenem." *Manuscript submitted for review.*

8. D.R. Marous, **E.P. Lloyd**, R. Li, A.J. Blaszczyk, K.A. Moshos, S.J. Booker, and C.A. Townsend. "Placement of RS Enzymes and Implications for Attachment of Extended, CoA-Derived Thiols in Complex Carbapenem Biosynthesis." *Manuscript nearing submission.*

9. **E.P. Lloyd**, A. Kaushik, P. Kumar, H. Batchelder, T. Zandi, E. Nuremberger, G. Lamichhane, C.A. Townsend. "Novel penems are effective against multi-drug resistant ESKAPE pathogens and *Mycobacteria in vivo*." *Manuscript nearing submission.*

Table of Contents

List of Figures

List of Schemes

List of Tables

Chapter 1

Introduction to β-Lactam Antibiotics

Discovery of β-Lactam Antibiotics

The discovery of penicillin by Alexander Fleming is the most impactful contribution to modern medicine in the early 20th century. One of the most meaningful findings in scientific history was the serendipitous discovery that fungal contamination of *Staphylococcus aureus* plates was found to have an inhibitory growth effect on the bacterial culture[1]. Fleming not only took note of this discovery, but he had the foresight to publish this important observation and predict in that first article that some agent produced by the fungus could be a valuable antibacterial substance. Although Fleming stated in his Nobel Prize lecture that he "didn't truthfully have this foresight at the time", his speculation about the impact of this happy accident was enough to spark a pharmaceutical revelation when it came to curing bacterial infection that so commonly resulted in the loss of life or limb at the time[2].

Research associated with Fleming's *Penicillium* mold continued for another decade, but it wasn't until the necessities of World War II launched a monumental effort between Great Britain and the United States in the scale-up of penicillin fermentation to produce the massive quantities of antibiotic needed to treat wounded soldiers overseas. By the end of the war, the technologies of fermentation were advanced to the point of antibiotic distribution being commonplace. However, despite this mammoth effort, it wasn't until Dorothy Hodgkin's crystal structure in 1945 that the previously proposed β-lactam ring was confirmed as the central piece to the penicillin mystery[3].

The importance of the β-lactam structure cannot be overstated. In 1957 former Merck scientist John Sheehan, then at MIT, proved leading chemists wrong with his paramount synthesis of penicillin, which had been deemed "impossible". It took him 9 years, due to the state of organic chemistry at the time that the necessary chemical reactions needed to synthesize such a complex molecule had not yet been discovered. Sheehan and his lab were able to make penicillin V using dicyclohexylcarbodiimide (DCC) as the key step in forming the β-lactam ring (Scheme 1.1)[4]. Sheehan was quoted to say that using traditional chemistry to assemble the structure was like "placing an anvil on top of a house of cards[5]." Despite Sheehan's triumph, penicillin and its derivatives are still produced by non-synthetic fermentation methods and, unfortunately, no pharmaceutical use came from this synthesis.

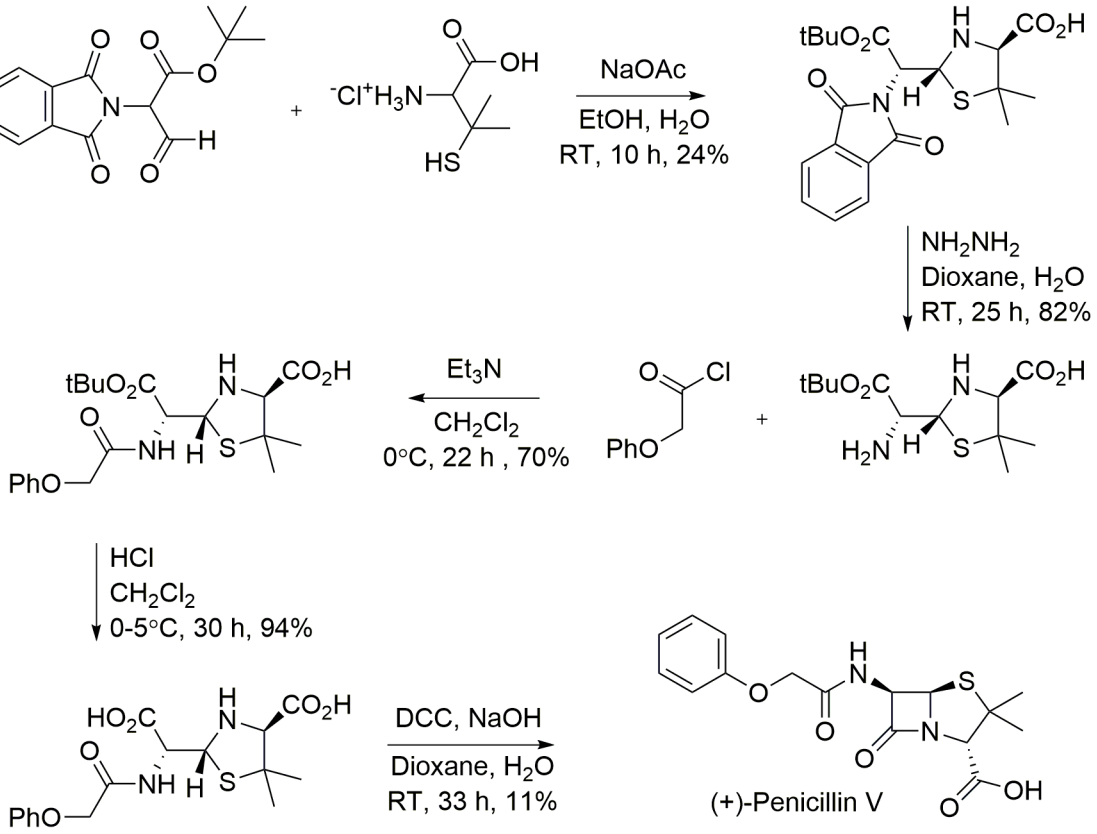

Scheme 1.1: First total synthesis of (+)-penicillin V[4]

Mode of action

The "magic" of penicillin is its β-lactam core. Traditionally, amide bonds are extremely stable to hydrolysis or to any nucleophilic attack whatsoever. This heightened stability relative to the more electrophilic aldehydes, esters, thioesters or ketones is attributed to amide resonance. The electrophilicity of carbonyls can be ranked using a comparison of measured pKa values for α-protons as shown in Figure 1.1.

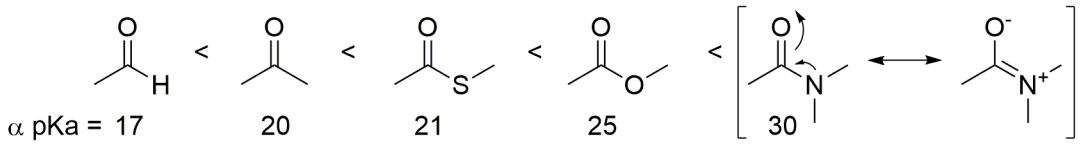

Figure 1.1: Alpha proton pKa values for common acyl intermediates including amide resonance

Resonance structures are a useful tool to understand the significant electronic contributors to a covalently bonded structure, and for a significant contributing structure to include the nitrogen lone pair as a part of a π-bond with the carbonyl carbon, planarity across that bond is necessary. Remarkably, nature has provided a natural product that includes an amide bond as part of a 4-membered ring such that planarity of amide resonance is difficult to achieve due to steric constraints, weakening the stability of the bond. In addition, the presence of a fused 5-membered ring forces the amide even further out of plane. A typical amide bond, such as those that comprise the backbone of proteins and polypeptides, has a hydrolysis half-life at room temperature and neutral pH of >500 years. In comparison, the half-life of penicillin is on the order of 48 h under the same conditions[6]. This presents a problem of stability when the drug is stored or administered in the clinic, but the reactivity is critical as a reactive acylation agent that allows for the inhibition of bacterial cell wall biosynthesis.

The bacterial cell wall is critical for prokaryotic structural stability. For single-celled organisms to survive and reproduce in a variety of environmental conditions, the cell wall ensures that the more fragile interior cell membrane remains intact. This structural entity is comprised of a *N*-acetyl glucosamine (NAG) linked to *N*-acetyl muramic acid (NAM) in β-1,4 fashion to form a polymeric backbone. This backbone is ultimately attached to the cell membrane through the Van der Waals interactions between the cellular membrane and an attached undecaprenyldiphosphate lipid. This complex is referred to as lipid II, which is biosynthesized in the cellular cytoplasm before it is localized in the cytosolic membrane and then translocated across the membrane to the outer leaflet thus presenting itself as a substrate for peptidoglycan biosynthesis (Figure 1.2). The polysaccharide backbones are interlinked periodically by the second structural component, where periodically an ether linkage is formed between the polypeptide strand and the NAM carboxylate. The critical polypeptide cross-links that provide the structural integrity of the cell wall are catalyzed through transpeptidases, related evolutionarily and in their mechanism of action to serine proteases. The target of penicillin, these transpeptidases were first discovered through their inhibition, therefore these enzymes are referred to as penicillin-binding proteins (PBPs). Typically, small molecule inhibitors are bound to their targets through favorable polar and non-polar interactions; however the "binding" that occurs in the interaction between penicillin and PBPs is covalent; a result of the extraordinary reactivity of the β-lactam[7,8].

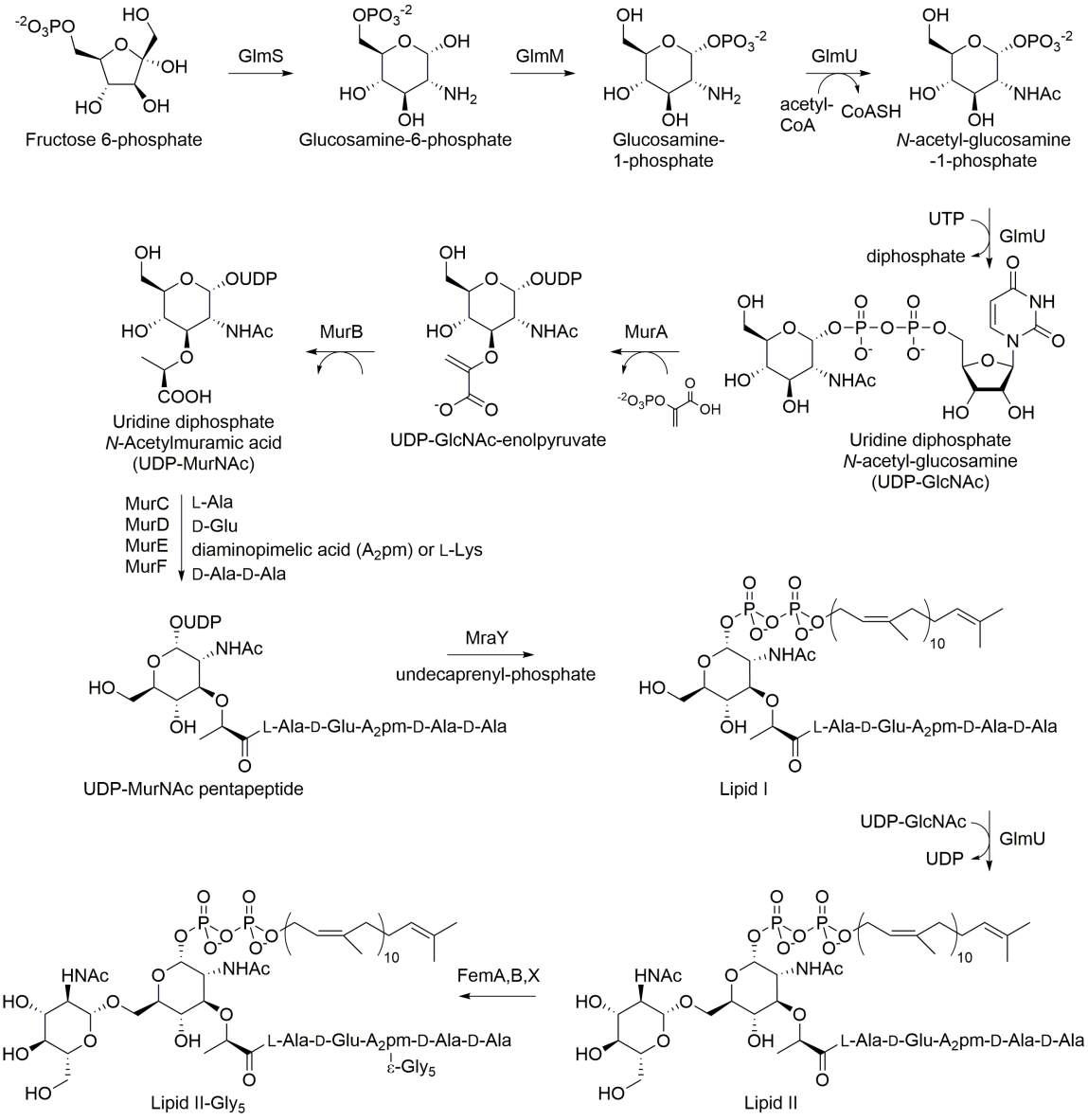

Figure 1.2: Stepwise cytosolic biosynthesis of Lipid II from Fructose-6-phosphate[7]

The polypeptide chain consists of a sequence NAM-L-Ala-γ-D-Glu-L-Lys[ε-Gly-Gly-Gly-Gly-Gly]-D-Ala-D-Ala in Gram-positive bacteria. Before translocation of lipid II across the cell membrane and outside of the cytoplasm, the polypeptide chain matures by the addition of an ε-linked pentaglycine structure commonly referred to as the "bridge" structure. In the pentaglycine bridge, where the length and sequence can vary

considerably from species to species, the addition of glycine residues occurs through the action of the FemA, B and X non-ribosomal peptidyl transferases[7]. with glycyl-tRNA acting as the substrate. In the case represented in Figure 1.3, the terminal glycine residue is shown as the nucleophile in the transpeptidation reaction. Although the nucleophile may vary, most often the electrophile is at the amide bond between D-Ala-D-Ala at the polypeptide terminus; this linkage is referred to as a 4,3-polypeptide cross-link. More recently, novel transpeptidases were found in *Mycobacterium tuberculosis* to create a different crosslink at the electrophilic terminus, in which nucleophilic attack ultimately occurs at the third amide bond. These transpeptidases, namely 3,3-transpeptidases, or L,D-transpeptidases, have since been discovered and characterized in addition to the traditional 4,3-transpeptidases in many species of bacteria and are thought of as a possible mode of resistance and resilience against cell-wall targeted antibiotics[9,10]. This alternative pathway for peptidoglycan synthesis will be discussed further in Chapters 5 and 6.

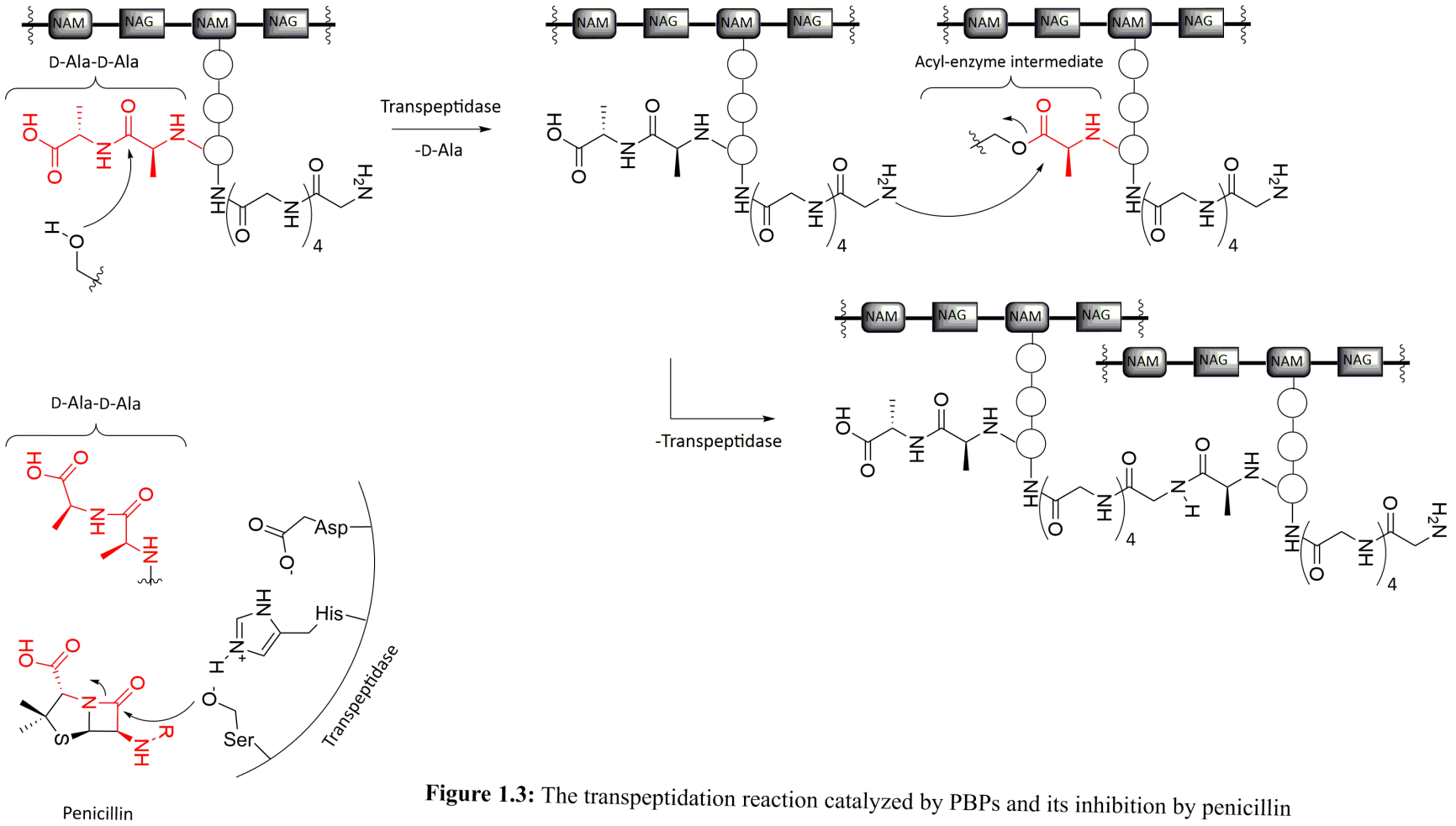

Figure 1.3: The transpeptidation reaction catalyzed by PBPs and its inhibition by penicillin

Prokaryotes require a cell wall and its biosynthesis for growth and proliferation, yet eukaryotic human cells have none of these processes, making for an ideal antibacterial target for bacterial infection in humans. While other drugs have been explored to inhibit bacterial growth through cell wall biosynthetic targets, the β-lactams have stood the test of time as champions of the antibiotic industry for their broad spectrum, ease of use and unequivocal success in curing infection with minimal side effects in most patients.

β-lactamases

As the natural product β-lactams evolved, so did the ability to defeat competing bacteria that produce them[11]. Chemical warfare between competing bacterial colonies in the environment is common: the culture that can successfully proliferate will persist and evolve. Once β-lactams allow a species to dominate the ecosystem by killing its competition, other species developed β-lactam-hydrolyzing enzymes, known as β-lactamases, as a mode of resistance. As new β-lactams appeared as a result, new β-lactamases co-evolved. This cycle continues today. In Alexander Fleming's 1945 Nobel lecture, he cautioned the world on the use of penicillin[2]. He estimated that one day antibiotics would be available on store shelves and their common administration would allow bacterial resistance to develop. He was right; the widespread use of β-lactam antibiotics have brought on resistant infectious strains and the β-lactam/β-lactamase cycle that evolved over millions of years has accelerated in the past half-century. Even carbapenemases have been identified, enzymes that provide resistance to our current last-line of defense antibiotics, which are reserved for only the most highly resistant strains of nosocomial infections[11].

Carbapenems

Carbapenems form a class of β-lactams that were first discovered in soil bacteria, *Streptomyces,* in 1976. Fortuitously, the first carbapenem characterized was none other than thienamycin, which was isolated from *Streptomyces cattleya* by researchers at Merck Sharp and Dohme Research Laboratories[12]. The efficacy of the natural product against difficult-to-treat strains such as *Pseudomonas* and its resistance to β-lactamases caused a major impact in the height of the golden age of antibiotics research. With the discovery coming nearly 50 years after penicillin in 1928, synthetic chemistry moved at a blazing pace in comparison. By 1978 the first total synthesis of racemic thienamycin was completed, an impressive achievement considering its complexity and susceptiblity to hydrolysis under neutral conditions and degradation by intermolecular reaction upon concentration[13].

In the years following the discovery of thienamycin, more than 50 carbapenems have been isolated and characterized from natural sources[12,14–23]. Modifications of the core structure include alkylation, oxidation and sulfonation at the C-6 sidechain, acetylation, oxidation, and chain length variation at the C-2 thiol sidechain, and diversification of the C-6 and C-8 stereocenters. A representation of the natural carbapenem antibiotics is shown in Figure 1.4.

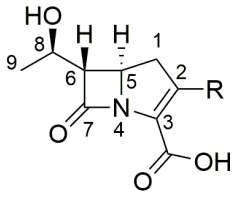

R = $SCH_2CH_2NH_2$, Thienamycin
(*Z*) SCH=CHNAc, *N*-acetyldehydrothienamycin
SCH_2CH_2NHAc, *N*-acetylthienamycin
Pantetheine, OA-6129B_2

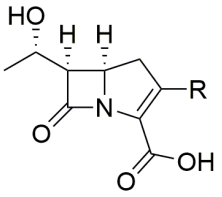

R = SCH_2CH_2NAc, Epithienamycin A
(*Z*) SCH=CHNAc, Epithienamycin B
(*Z*) SOCH=CHNAc, Epithienamycin B sulfoxide
SO_3^-, Pluracidomycin D
Pantetheine, OA-6129B_1

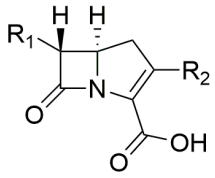

R_1,R_2 = H, (3*S*,5*S*)-Carbapenem-3-carboxylic acid
R_1 = ethyl
R_2 = $SCH_2CH_2NH_2$, deshydroxy-thienamycin
R_2 = SCH_2CH_2NAc, PS-5
R_2 = (*Z*) SCH=CHNAc, PS-7
R_2 = pantetheine, OA-6129A
R_1 = isopropyl
R_2 = SCH_2CH_2NAc, PS-6
R_2 = (*Z*) SCH=CHNAc, PS-8

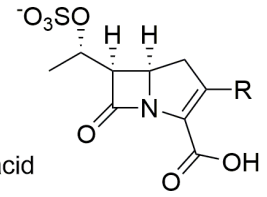

R = $SCH_2CH_2NH_2$, 8U-207
SCH_2CH_2NAc, Epithienamycin F
(*Z*) SCH=CHNAc, Epithienamycin E
(*E*) SCH=CHNAc, AB-110-D
(*Z*) SOCH=CHNAc, MM4550
SO_3^-, Pluracidomycin A
SO_2^-, Pluracidomycin A_2
$SOCH2CO_2^-$, Pluracidomycin B
SOCHCOH, Pluracidomycin C_1
$SOCH_2CH_2OH$, Pluracidomycin C_2
$SOCH_2CH_2NAc$, Pluracidomycin C_3
Pantetheine, OA-6129C

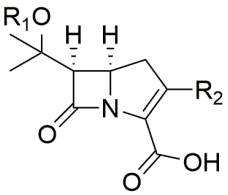

R_1 = H
R_2 = SCH_2CH_2NAc, KA-6643-G
R_2 = (*Z*) SOCH=CHNAc, Carpetimycin A
R_2 = $SOCH_2CH_2NAc$, Carpetimycin C
R_1 = SO_3^-
R_2 = SCH_2CH_2NAc, KA-6643-D
R_2 = (*Z*) SOCH=CHNAc, Carpetimycin B
R_2 = $SOCH_2CH_2NAc$, Carpetimycin D
R_2 = (*Z*) SCH=CHNAc, KA-6643-F

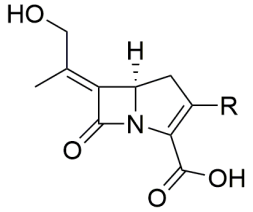

R = SCH_2CH_2NAc, 6643-X
(*Z*) SOCH=CHNAc, Asparenomycin A
$SOCH_2CH_2NAc$, Asparenomycin B
(*Z*) SCH=CHNAc, Asparenomycin C

Figure 1.4: Representative carbapenem natural products. The core structure of thienamycin is numbered, as convention dictates.

As anti-infective therapeutic agents, carbapenems were first sold in 1987 after Primaxin I.V. (imipenem/cilastatin) was approved by the FDA (Figure 1.5). Much effort was contributed by Merck Sharp and Dohme to be the first "last line of defense" drug for the treatment of drug-resistant nosocomial infections. Imipenem, like all natural carbapenems, was found to be highly susceptible to hydrolysis by renal dehydropeptidase-1 (RDH-1), an enzyme in human kidneys. Without administration of an RDH-1 inhibitor, cilastatin, the half-life of imipenem is greatly reduced and patients undergoing treatment can succumb to complications with the kidneys or even organ failure. As a result, imipenem is administered as a combination with an equal amount of cilastatin, and is sold under the name Primaxin.

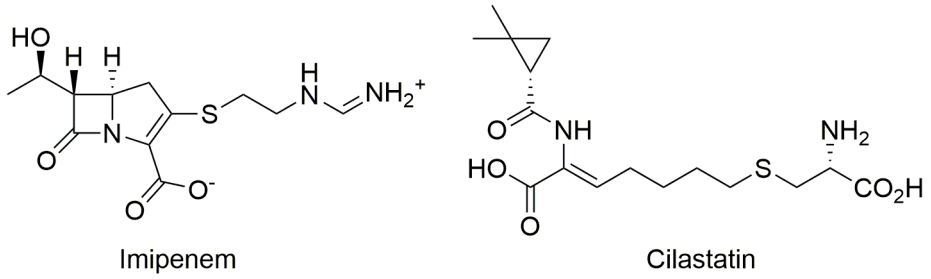

Figure 1.5: Structures of imipenem and cilastatin

Syntheses of imipenem

Unlike penicillin or cephalosporin derivatives produced on an industrial scale, efforts to achieve the fermentation or semi-synthesis of carbapenems failed[24]. The natural producers of carbapenems are primarily *Streptomyces*, which produce secondary metabolite carbapenems in 1-10 mg/liter quantities. Increased sensitivity of the carbapenems to heat, acid, base and concentration is also a hindrance to isolation efforts. Merck was never able to bring fermentation titers above 100 mg/liter. A Merck chemist,

Dr. Edward J.J. Grabowski, quoted Dr. Edward L. Paul, the head of Chemical Engineering on the imipenem-thienamycin project, as saying "to produce 40,000 kg of imipenem per year, we would have to run the thienamycin fermentation in Lake Erie and pump to Lake Ontario for the workup!"[25] As a result, the carbapenem total synthesis effort was initiated and to this day carbapenems produced for the pharmaceutical market are made entirely by total synthesis.

The first total synthesis of imipenem, by chemists at Merck Sharp and Dohme, was achieved as shown in Scheme 1.2[13].

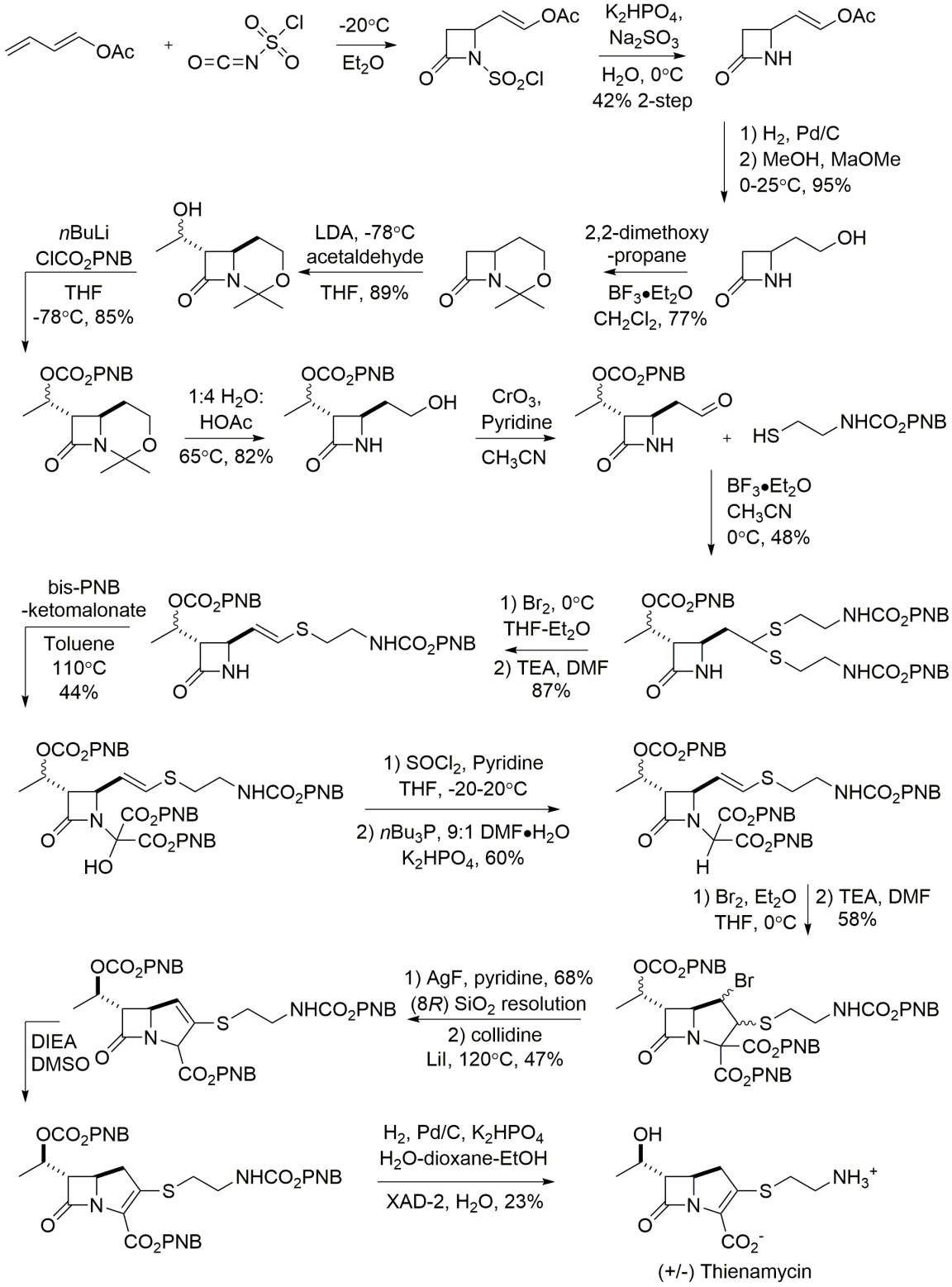

Scheme 1.2: First total synthesis of (+/-) thienamycin[13]

The remarkable carbene mediated insertion from an α-diazo intermediate to form the [2.3.0] ring system evolved from the chemistry used in the first total synthesis[26]. It was incorporated into the synthesis of thienamycin based on acetone dicarboxylate and ultimately this synthesis was modified into a chiral synthesis that eventually became the process used for industrial thienamycin production for many years[25]. The acetone dicarboxylate synthesis of (+) thienamycin is shown in Scheme 1.3[27].

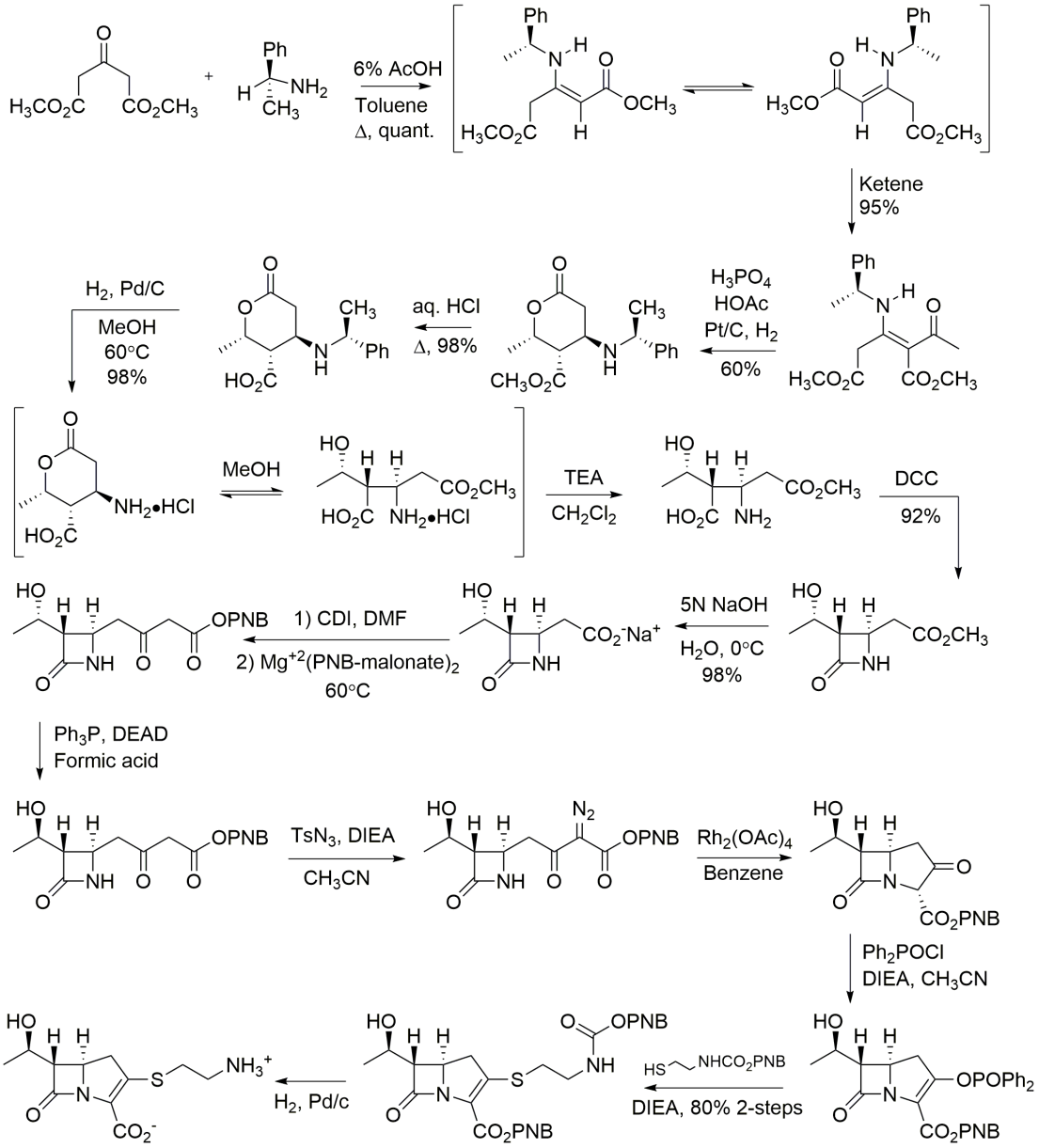

Scheme 1.3: Chiral synthesis of (+)-thienamycin from acetone dicarboxylate[27]

An additional synthetic strategy took advantage of commonly available and inexpensive penicillin as a starting material for thienamycin synthesis[28]. To build the necessary α-diazo-β-keto-ester for the diazoinsertion reaction required for 5 membered ring closure, a new method was developed to react the silylenolether of benzyl-acetoacetate with a *N*-acyliminium electrophilic intermediate of the β-lactam ring. The chemistry described, as well as the methodology to convert penicillin to thienamycin, is presented in Scheme 1.4.

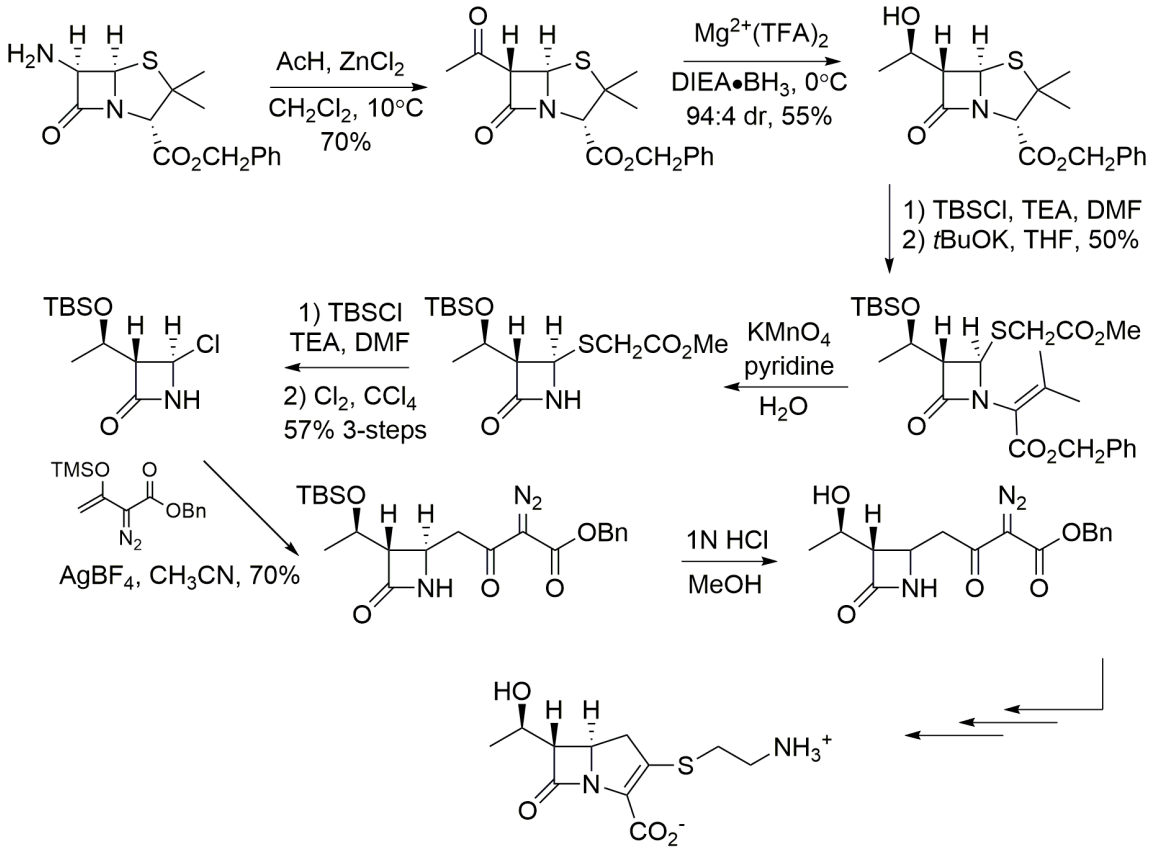

Scheme 1.4: Chiral synthesis of (+)-thienamycin from penicillin[28]

The route from penicillin, although not practical enough to outperform the already established acetone dicarboxylate process, brought the critical component of *N*-

acyliminium chemistry in the construction of the carbapenem bicycle. The convergent nature of this synthetic approach allowed for a new synthesis to be derived, using aspartic acid as a source of chirality in the construction of the β-lactam. Grabowski described the modern acetoxyazetidinone process for imipenem synthesis as a "Frankenstein" process, because it stole key chemical steps from the effort by many groups at Merck who developed 6 different total syntheses for thienamycin[24]. The [2.3.0] ring construction using the diazoinsertion reaction was "stolen" from the early medicinal chemical efforts of thienamycin synthesis and brought to practicality by its use in the acetone dicarboxylate synthesis that made plant scale production successful. The *N*-acyliminium chemistry was "stolen" from the penicillin synthesis. Finally, the use of the 4-acetoxyazetidinone intermediate which has been so critical in carbapenem production in the modern process to imipenem was "stolen" from the aspartic acid synthesis[29].

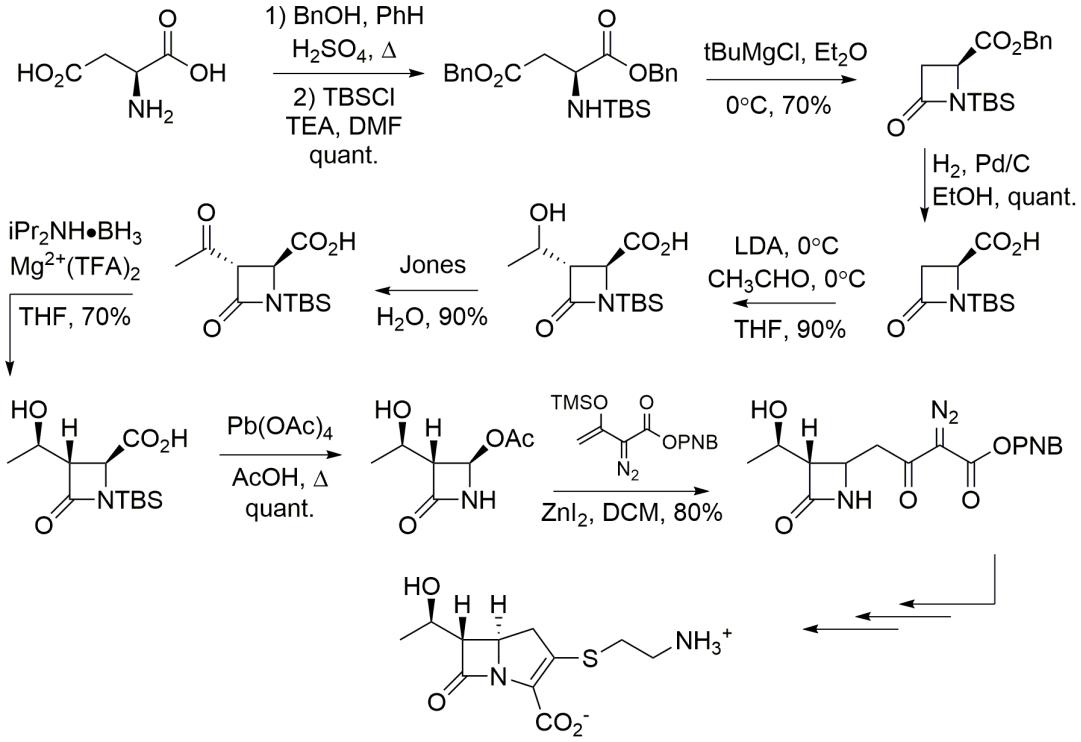

Scheme 1.5: Chiral synthesis of (+)-thienamycin from L-aspartic acid[29]

The modern acetoxyazetidinone process shown in Scheme 1.6 takes advantage of all of the aforementioned chemistry, and utilizes a now commercially available intermediate. (3*R*,4*R*)-4-Acetoxy-3[(*R*)-1-(tert-butyldimethylsilyloxy)ethyl]azetidin-2-one is manufactured by the Japanese companies Takasago and Nisso and is readily available[24].

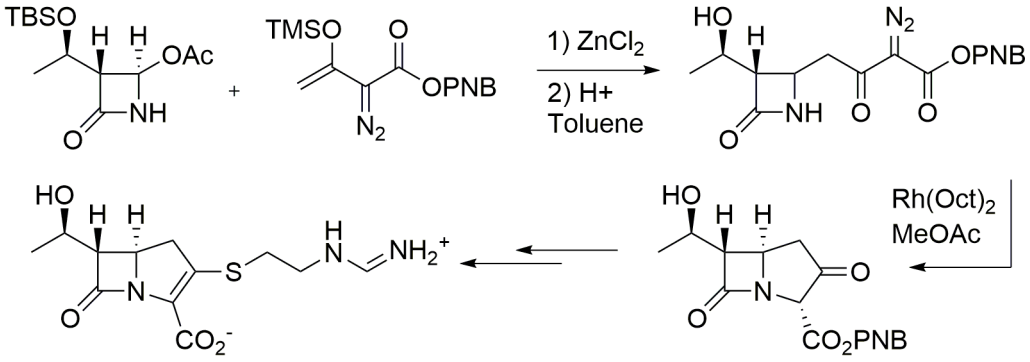

Scheme 1.6: The current acetoxyazetidinone process to imipenem

The unification of all these synthetic achievements into what is now one efficient and convergent process to imipenem highlights the high level of work done in the Merck Process group over the years, and underlines the importance of collaboration to solve important problems in pharmaceutical drug development.

Second-generation carbapenems

In a parallel attempt to make carbapenems for the pharmaceutical market, Sumitomo Dainippon Pharma of Japan developed meropenem as a result of in depth structure-activity relationship studies from over 50 newly synthesized carbapenem

compounds by their lead optimization research group. They found that a cation in the C-2 side chain was important for resistance to RDH-1, and discovered that further stability to the renal enzyme was achieved with the addition of a 1-β-methyl group on the carbapenem bicyclic core. The result of their study was meropenem, as a 3-hydroxyproline-derived substituent linked to the C-2 thiol provided low central and renal toxicities *in vivo*. As nephrotoxicity was a problem for patients treated with carbapenems for a long period of time (>2 weeks), meropenem had the advantage. Additionally, the need for cilastatin co-administration was no longer necessary[30].

Since imipenem was approved, meropenem, ertapenem and doripenem have been approved in the United States. To date, biapenem and panipenem are approved for use in Japan. Other carbapenems have been developed and some are still in clinical trials, like tebipenem whose prodrug ester, tebipenem pivoxil is orally available. Razupenem is an example of a carbapenem that failed clinical trials.

There is great promise in the development of new carbapenems that may have heightened antibacterial activity in comparison to the currently used carbapenems. Through optimization of the C-6 and C-2 sidechains, as well as taking into account the possibility of oral carbapenem administration through study of carbapenem prodrug esters, the reign of the carbapenem as the last, best, hope against drug-resistant strains is far from over.

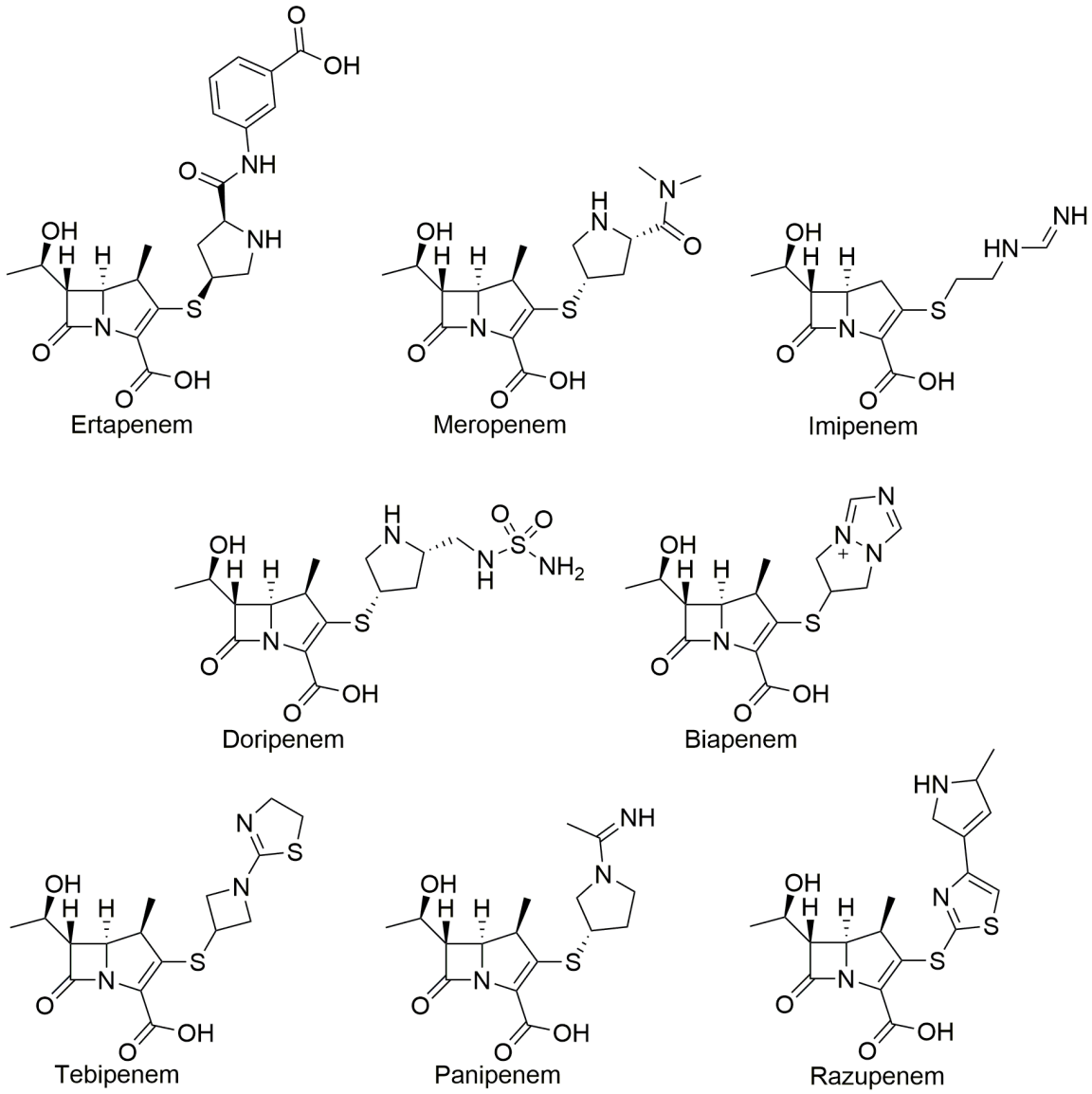

Figure 1.6: Structures of clinically administered carbapenems

Early studies on the biosynthesis of thienamycin

As previously noted, fermentation efforts to obtain carbapenems from *Streptomyces* yielded titers that were far too low for fermentation to be a process from which sufficient quantities could be produced for the pharmaceutical market. In order to diverge from the exemplary, but still expensive, total synthesis process methods, the use of enzymes for the semi-synthesis of carbapenems is proposed to provide a more green,

direct and inexpensive method for carbapenem production. Unfortunately, the biosynthesis of carbapenem antibiotics remains largely unknown.

In the 1980s, early studies on the biosynthesis of carbapenems were attempting to better understand how these molecules are made by their producers. One particular study in 1984 had success in changing the antibiotic profile by random mutational analysis of the strain *S. fulvuviridis* A933[31]. Knocking out an enzyme involved in the truncation of the carbapenem C-2 thiol side chain, carbapenems with pantetheine as the thioether at C-2 were isolated. These carbapenems and a proposed biosynthetic pathway among them is shown in Scheme 1.7.

OA-6129A is thought of as a direct precursor for the C-6 ethyl carbapenem PS-5, OA-6129B_2 for *N*-acetyl thienamycin, OA-6129B_1 for epithienamycin A, and OA-6129C for MM 17880. Likely, these carbapenems are also intermediates for each other and a proposed biosynthesis pathway from the isolated carbapenam OA-6129D to MM 17880 is shown in Scheme 1.7.

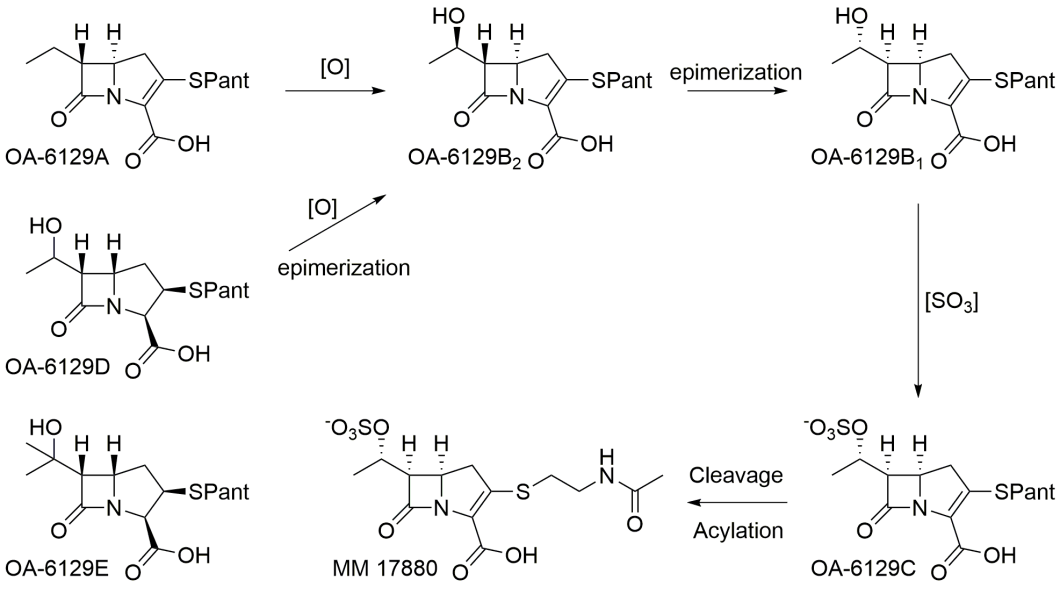

Scheme 1.7: Isolated compounds of *S. fulvuveridis* mutants and proposed biosynthetic pathway between them. SPant = pantetheine

In 1985, Merck chemists examined the biosynthetic precursors of thienamycin through radioactive and stable isotope substrates[32]. It was found that the carbapenem bicyclic core was assembled from acetyl-CoA and glutamic acid. The C-8 and C-9 carbons of the C-6 hydroxyethyl sidechain each come from the methyl group of methionine, and the C-2 sidechain incorporated radiolabeled cysteamine. These studies, along with other work, produced an early biosynthetic proposal to thienamycin, are summarized in Scheme 1.8.

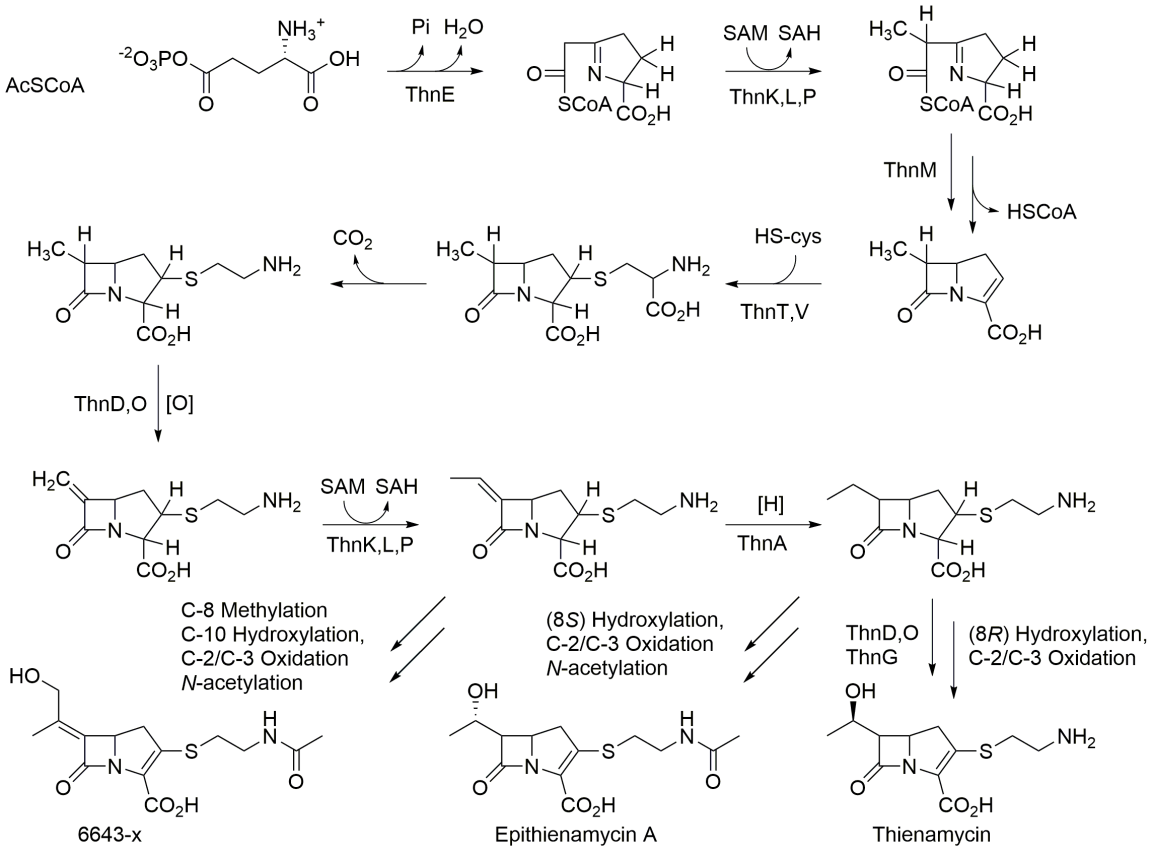

Scheme 1.8: Early proposal of thienamycin biosynthesis by Merck Sharp and Dohme[32] and proposed enzymatic function by Salas *et al.*[33]

Some inconsistencies exist in the Merck biosynthetic proposal when all the data available in the literature at the time are taken into account. With no gene sequence or bioinformatics analysis at their disposal as researchers commonly use today, Merck did their best to match isotopic labeling and isolation experiments with a biosynthetic proposal. From their experiments, an attempt was made to explain the vast diversity of carbapenem natural products that had been isolated, for example, asparenomycins, epithienamycins, and thienamycin. However, stereochemical divergence at C-6 was ignored. The most egregious mistake was perhaps their disregard for the critical OA-6129 series of isolated carbapenems. Instead of suggesting that a larger C-2 sidechain may be added at C-2 for all carbapenems, their proposal merely suggests that the OA-6129 series are outliers, and the biosynthetic pathway must occur differently for those compounds. What was missed from this proposal, however, was that the OA-6129 compounds were isolated from mutants of a strain, *S. fulvuveridis* that normally produces epithienamycins and compounds such as PS-5, 6 and 7. Those carbapenems with truncated C-2 sidechains must derive from those with pantetheine at C-2. The mistake, however, is forgivable because the authors were attempting to justify their own data that the C-2 thioether incorporated radiolabeled ^{13}C originated from cysteine. Apparently unbeknownst to them at the time, experiments in CoA biosynthesis had revealed that bacteria have the capability to construct CoA using cysteine as a building block in a condensation with pantothenic acid to produce pantetheine.

Modern biosynthetic studies of carbapenems

The advent of inexpensive DNA sequencing stimulated in part by the human genome sequencing project at the turn of the 21st century afforded researchers with the ability to sequence entire biosynthetic gene clusters for secondary metabolites, and indeed, entire bacterial genomes. In 1997, the Salmond group of the University of Cambridge sequenced and analyzed the gene cluster for the simplest carbapenem, carbapenem-3-carboxylic acid in *Pectobacterium carotovora*[34]. Mutational analysis of the gene cluster revealed that the only genes out of the 8 in the cluster that caused a loss of antibiotic production when knocked-out were *carA*, *carB*, and *carC*. The earliest effort from the Townsend lab on carbapenem biosynthesis examined the roles of these three enzymes, where Rongfeng Li and Anthony Stapon published, in a series of JACS Communications, that the transformations catalyzed by CarA, B and C were all that was necessary to make carbapenem-3-carboxylic acid from acetate and L-glutamate as shown in Scheme 1.9[35–37]. CarB was discovered as important in condensing pyrrolidine 5-carboxylate with malonyl-CoA. CarC, an α-ketoglutarate dependent non-heme iron oxygenase, was found through rigorous study to both epimerize the C-5 bridgehead position of the (3*S,5R*)-carbapenam-3-carboxylic acid and desaturate the C-2/C-3 bond successively.

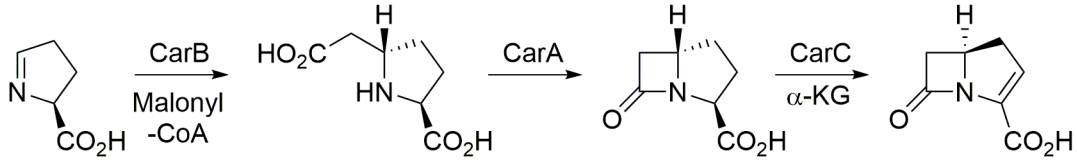

Scheme 1.9: Biosynthesis of (5*R*)-carbapenem-3-carboxylic acid in *E. carotovora*

As for thienamycin biosynthesis, the gene cluster was discovered in *S. cattleya* and published by the Salas group at the University of Oviedo, Spain, in 2003[33]. Analysis of the 22 open reading frames revealed putative functions for most enzymes. Of these, *thnE* and *thnM* had high sequence homology to *carA* and *carB*, respectively, the enzymes responsible for the biosynthesis of the carbapenam bicycle in the simple carbapenem gene cluster from *E. carotovora*. Strikingly, no CarC homologue was encoded in the thienamycin gene cluster. However, two non-heme iron oxygenases were encoded, *thnG* and *thnQ*, but with shared homology to known hydroxylases. *ThnK, thnL* and *thnP* encoded putative radical SAM methyltransferases, and *thnF* an *N*-acetyltransferase. Ruling out a putative transport protein, two transcriptional activators and a β-lactamase in *thnJ*, *thnI*, *thnU*, and *thnS* respectively, the remaining enzymes of unknown function were *thnH*, *thnN*, *thnO*, *thnR*, *thnT* and *thnV* were used to fill in the remaining chemistry based on the biosynthetic pathway proposed in Scheme 1.8.

A major contribution by Dr. Michael F. Freeman and Dr. Kristos A. Moshos was achieved to carbapenem biosynthesis revealed the function of four enzymes, ThnR, H, T and F, which were found by *in vitro* enzyme assays to be responsible for the truncation of coenzyme A in thienamycin biosynthesis, confirming that the C-2 cysteamine sidechain is derived from coenzyme A, not cysteine as thought for many years[38]. As previously stated, this finding does not contradict the early isotopic labeling experiments where radiolabeled cysteine that was incorporated into at C-2. ThnF, as expected by sequence homology, was confirmed as the *N*-acylase to produce *N*-acetylcarbapenems[38]. The others, ThnR, H and T were found to truncate CoA to cysteamine in the order of ThnR, which cleaves CoA to provide phosphopantetheine, then ThnH, which cleaves the

terminal phosphate to produce pantetheine, and ThnF, the responsible amidohydrolase that cleaves pantetheine to cysteamine. The results published in 2008, combined with unpublished *in vitro* enzyme activity assays using CoASH and phosphopantetheine substituted carbapenams, prove that the tailoring of CoA can occur with the carbapenam/em structure attached[39]. ThnH, for example, requires the carbapenem structure present to successfully cleave the terminal phosphate. The results of these experiments are outlined for the state of thienamycin biosynthesis in 2011 in Scheme 1.10[39].

To support the hypothesis that ThnE and ThnM function in parallel to CarB and CarA, respectively, despite low sequence identity of 37 and 25%, Micah Bodner, Ryan Phelan, Kristos Moshos and I synthesized pyrrolidine and carbapenam substrates for enzyme activity assays of compounds with varying substitution patterns and stereochemistry[40]. As there is not a CarC homologue encoded by the thienamycin biosynthetic cluster, the hope was that more diverse substrates would be accepted as the preferred substrates for ThnE and ThnM to solve the mysteries of how epimerization and desaturation might occur. The results of these assays, along with kinetic analysis, revealed that ThnE and ThnM had unambiguous preferences for the natural substrates of CarB and CarA. This key set of observations confirmed that all of the chemistry required for C-2 thioalkylation, C-5 epimerization, and C-2/C-3 desaturation must occur after formation of the β-lactam ring.

To find the enzyme(s) responsible for C-5 epimerization in the absence of a CarC homologue, Micah Bodner and Ryan Phelan also investigated the function of the non-heme iron oxygenases encoded in the thienamycin gene cluster, ThnG and ThnQ[41]. Both

enzymes were tested individually against (5*R*) 2-*N*-acetyl-carbapenams in hopes that one or both would epimerize C-5 or desaturate the C-2/C-3 bond. Where these substrates failed to provide enzymatic turnover, carbapenem substrates showed successful hydroxylation of the C-8 position when incubated with ThnQ and sulfoxidation and desaturation of the 2-alkylthio group was observed in assays with ThnG[41]. Dual functionality of enzymes can never be ruled out; however it was clear at the time that ThnG and ThnQ were not involved in the synthesis of the (5*S*)-carbapenem core.

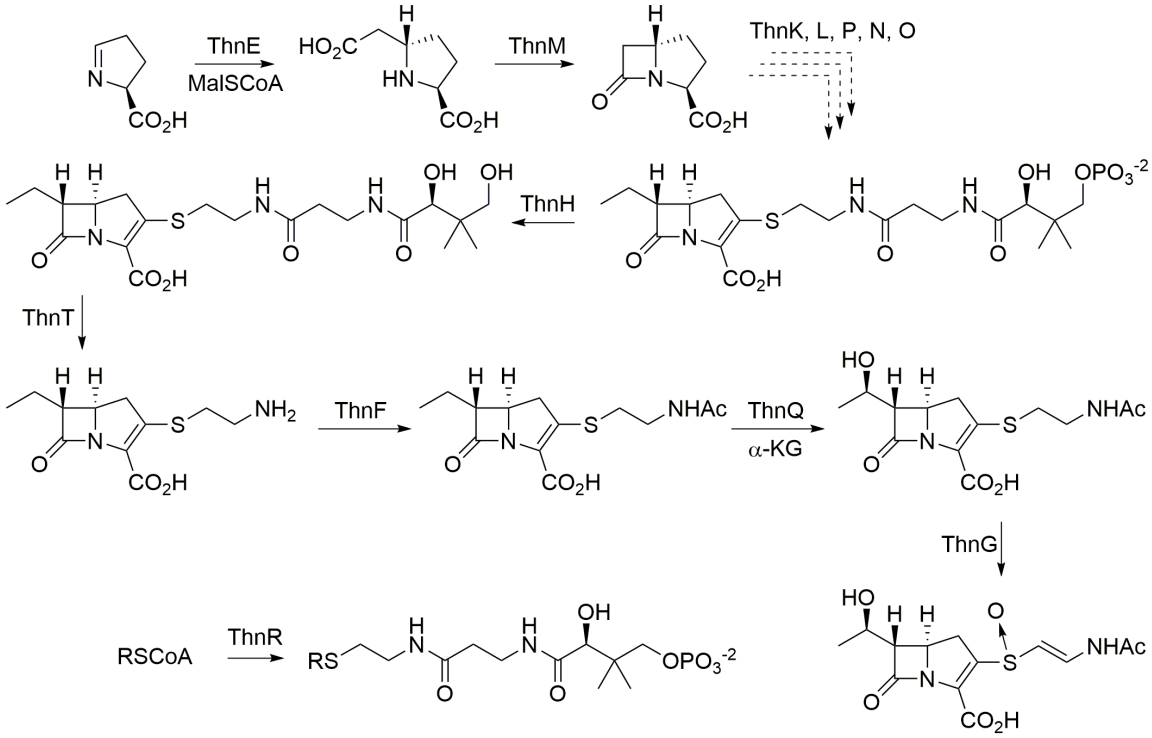

Scheme 1.10: A proposal of thienamycin biosynthesis based on confirmation of enzymatic substrates and products in combination with experiments highlighted in the literature up to 2011. R = H or carbapenam/em,

Thesis aims

The goals of this thesis are to investigate further the steps of carbapenem biosynthesis. Chapter 2 reports investigations of mutational analysis of a *cis*-

carbapenem-producing gene cluster and the determination of a biosynthetic pathway is proposed based on the analysis of gene-disruption mutants. Further synthetic and enzymatic analyses of *cis*-carbapenems and *O*-sulfonation reaction are explored in Chapter 3. Investigations of sequential double methylation of C-2 thioalkyl carbapenems by ThnK are described in Chapter 4. The inhibition of a L,D-transpeptidases (Ldts) in *Mycobacterium tuberculosis* by intact protein mass spectrometry is analyzed in Chapter 5, and the resulting directed syntheses of penem antibiotics and success in the optimization of lead compounds, provided new penem anibiotics that are markedly effective against *Mycobacteria* and other pathogens that express Ldts is explored in Chapter 6.. In large measure, this work is based upon publications. Chapters 2, 4, and 5 mirror their respective publications on the MM 4550 gene cluster, ThnK enzymology, and *in vitro* inhibition of Ld_{Mt2} by carbapenems. Chapter 6 is written in the format of a manuscript as its contents are expected to be ready for publication shortly after the submission of this thesis.

References

1. Fleming, A. On the antibacterial action of cultures of a penicillium, with special reference to their use in the isolation of B. influenzae. 1929. *Bull. World Health Organ.* **79,** 780–790 (2001).
2. Alexander Fleming. Penicillin. *Nobel Lect.* (1945).
3. Woodward, R. B. & Lecture, N. Recent advances in the chemistry of natural products. (1965).
4. Sheehan, J. C. & Henery-Logan, K. R. the Total Synthesis of Penicillin V. *J. Am. Chem. Soc.* **79,** 1262–1263 (1957).
5. Professor John C. Sheehan Dies at 76. *MIT Tech Talk* **36,** (1992).
6. Macek, T. J., Hanus, E. J. & Feller, B. A. The Stability of Penicillin G Sodium in Aqueous Solution. *J. Am. Pharm. Assoc. (Scientific ed.)* **37,** 322–327 (1948).
7. van Heijenoort, J. Lipid Intermediates in the Biosynthesis of Bacterial Peptidoglycan. *Microbiol. Mol. Biol. Rev.* **71,** 620–635 (2007).

8. Testero, S. A., Fisher, J. F. & Mobashery, S. in *Burger's Medicinal Chemistry and Drug Discovery* (John Wiley & Sons, Inc., 2010). doi:10.1002/0471266949.bmc226

9. Gupta, R. *et al.* The Mycobacterium tuberculosis protein LdtMt2 is a nonclassical transpeptidase required for virulence and resistance to amoxicillin. *Nat. Med.* **16,** 466–9 (2010).

10. Lamichhane, G. Novel targets in M. tuberculosis:search for new drugs. *Trends Mol. Med.* **17,** 25–33 (2011).

11. Fisher, J. F., Meroueh, S. O. & Mobashery, S. Bacterial resistance to beta-lactam antibiotics: Compelling opportunism, compelling opportunity. *Chemical Reviews* **105,** 395–424 (2005).

12. Kahan, J. S. S. *et al.* Thienamycin, a new beta-lactam antibiotic. I. Discovery, taxonomy, isolation and physical properties. *J. Antibiot. (Tokyo).* **32,** 1–12 (1979).

13. Johnston, D. B. R., Schmitt, S. M., Bouffard, F. A. & Christensen, B. G. Total synthesis of (.+-.)-thienamycin. *J. Am. Chem. Soc.* **100,** 313–315 (1978).

14. Hood, J. D., Box, S. J. & Verrall, M. S. Olivanic acids, a family of beta-lactam antibiotics with beta-lactamase inhibitory properties produced by Streptomyces species. II. Isolation and characterisation of the olivanic acids MM 4550, MM 13902 and MM 17880 from Streptomyces olivaceus. *J. Antibiot. (Tokyo).* **32,** 295–304 (1979).

15. Okamura, K. *et al.* PS-5, a new beta-lactam antibiotic. I. Taxonomy of the producing organism, isolation and physico-chemical properties. *J. Antibiot. (Tokyo).* **32,** 262–271 (1979).

16. Shibamoto, N. *et al.* PS-6 and PS-7, new beta-lactam antibiotics. Isolation, physicochemical properties and structures. *J. Antibiot. (Tokyo).* **33,** 1128–1137 (1980).

17. Cassidy, P. J. *et al.* Epithienamycins. II. Isolation and structure assignment. *J. Antibiot. (Tokyo).* **34,** 637–648 (1980).

18. Box, S. J., Hood, J. D. & Spear, S. R. Four further antibiotics related to olivanic acid produced by Streptomyces olivaceus: fermentation, isolation, characterisation and biosynthetic studies. *J. Antibiot. (Tokyo).* **32,** 1239 (1980).

19. Shoji, J. *et al.* Asparenomycins A, B and C, new carbapenem antibiotics. II. Isolation and chemical characterization. *J. Antibiot. (Tokyo).* **35,** 15–23 (1982).

20. Harada, S., Nozaki, Y., Shinagawa, S. & Kitano, K. C-19393 E5, a new carbapenem antibiotic. Fermentation, isolation and structure. *J. Antibiot. (Tokyo).* **35,** 957–962 (1982).

21. Bycroft, B. W., Maslen, C., Box, S. J., Brown, A. G. & Tyler, J. W. The isolation and characterisation of (3R,5R)- and (3S,5R)-carbapenam-3-carboxylic acid from Serratia and Erwinia species and their putative biosynthetic role. *J. Chem. Soc. Chem. Commun.* 1623 (1987).

22. Wilson, K. E., Kempf, A. J., Liesch, J. M. & Arison, B. H. Northienamycin and 8-epi-thienamycin, new carbapenems from Streptomyces cattleya. *J. Antibiot. (Tokyo).* **36,** 1109–1117 (1983).

23. Nakayama, M. *et al.* New beta-lactam antibiotics, carpetimycins C and D. *J. Antibiot. (Tokyo).* **36,** 943–949 (1983).

24. Grabowski, E. J. J. Enantiopure drug synthesis: From methyldopa to imipenem to efavirenz. *Chirality* **17,** S249–S259 (2005).

25. Grabowski, E. J. J. Reflections on Process Research. *ACS Symp. Ser. Chem. Process Res.* **870,** 1–21 (2003).

26. Salzmann, T. N., Ratcliffe, R. W., Christensen, B. G. & Bouffard, F. A. A stereocontrolled synthesis of (+)-thienamycin. *J. Am. Chem. Soc.* **102,** 6161–6163 (1980).

27. Melillo, D. G., Cvetovich, R. J., Ryan, K. M. & Sletzinger, M. An enantioselective approach to (+)-thienamycin from dimethyl 1,3-acetonedicarboxylate and (+)-.alpha.-methylbenzylamine. *J. Org. Chem.* **51,** 1498–1504 (1986).

28. Amato, J. S., Karady, S. & Weinstock, L. M. Stereospecific synthesis of thienamycin from penicillin. (1984).

29. Reider, P. J. & Grabowski, E. J. J. Total synthesis of thienamycin: a new approach from aspartic acid. *Tetrahedron Lett.* **23,** 2293–2296 (1982).

30. Prashad, A. S., Vlahos, N., Fabio, P. & Feigelson, G. B. A highly refined version of the α-keto ester based carbapenem synthesis: The total synthesis of meropenem. *Tetrahedron Lett.* **39,** 7035–7038 (1998).

31. Yoshioka, T. *et al.* Structures of OA-6129A, B1, B2 and C, new carbapenem antibiotics produced by Streptomyces sp. OA-6129. *J. Antibiot. (Tokyo).* **36,** 1473–1482 (1983).

32. Williamson, J. M. *et al.* Biosynthesis of the beta-lactam antibiotic, thienamycin, by Streptomyces cattleya. *J. Biol. Chem.* **260,** 4637–47 (1985).

33. Núñez, L. E., Méndez, C., Braña, A. F., Blanco, G. & Salas, J. A. The Biosynthetic Gene Cluster for the β-Lactam Carbapenem Thienamycin in Streptomyces cattleya. *Chem. Biol.* **10,** 301–311 (2003).

34. McGowan, S. J. *et al.* Analysis of the carbapenem gene cluster of *Erwinia carotovora* : definition of the antibiotic biosynthetic genes and evidence for a novel β-lactam resistance mechanism. *Mol. Microbiol.* **26,** 545–556 (1997).

35. Rongfeng Li *et al.* Three Unusual Reactions Mediate Carbapenem and Carbapenam Biosynthesis. *J. Am. Chem. Soc.* **122,** 9296–9297 (2000).

36. Stapon, A. *et al.* Carbapenem Biosynthesis: Confirmation of Stereochemical Assignments and the Role of CarC in the Ring Stereoinversion Process from l-Proline. *J. Am. Chem. Soc.* **125,** 8486–8493 (2003).

37. Stapon, A., Li, R. & Townsend, C. A. Synthesis of (3S,5R)-Carbapenam-3-carboxylic Acid and Its Role in Carbapenem Biosynthesis and the Stereoinversion

Problem. *J. Am. Chem. Soc.* **125,** 15746–15747 (2003).

38. Freeman, M. F., Moshos, K. A., Bodner, M. J., Li, R. & Townsend, C. A. Four enzymes define the incorporation of coenzyme A in thienamycin biosynthesis. *Proc. Natl. Acad. Sci. U. S. A.* **105,** 11128–11133 (2008).

39. Moshos, K. A. Design and Synthesis of Substrates and Standards Used to Elucidate Activities of Enzymes in Carbapenem Gene Clusters. (Johns Hopkins University, 2011).

40. Bodner, M. J. *et al.* Definition of the Common and Divergent Steps in Carbapenem β-Lactam Antibiotic Biosynthesis. *ChemBioChem* **12,** 2159–2165 (2011).

41. Bodner, M. J., Phelan, R. M., Freeman, M. F., Li, R. & Townsend, C. A. Non-Heme Iron Oxygenases Generate Natural Structural Diversity in Carbapenem Antibiotics. *J. Am. Chem. Soc.* **132,** 12–13 (2010).

Chapter 2

Identification and Characterization of the Carbapenem MM 4550 and its Gene Cluster in *Streptomyces argenteolus* ATCC 11009

It has been reported that 50-60% of the more than two million nosocomial infections in the USA each year are caused by antimicrobial-resistant bacteria[1]. β-lactam antibiotics are critically important as pharmaceutical agents to combat these bacterial pathogens. Among these, carbapenems are the most potent subclass of these antibacterials due to their rapid penetration across bacterial cell membranes, high affinity to penicillin-binding proteins and resistance to a broad range of β-lactamases. With the rapid spread of multidrug resistance and abandoned anti-infective research and development programs in pharmaceutical companies, there are few antibiotics available for treatment and even fewer drugs in the antibiotic pipeline.

To date, all currently used carbapenems such as imipenem and meropenem are manufactured by total synthesis, in part because fermentation efforts have failed to obtain commercially viable amounts of thienamycin and knowledge of their biosynthesis is far from complete. Therefore treatment of severe infections with carbapenems is very costly. An important role could be played by the development of semi-synthetic approaches to provide large quantities of carbapenems at reduced cost.

The complex carbapenems are composed of a (5*R*)-carbapenem-3-carboxylic acid core that is commonly diversified by a sulfur-linked side chain at C-2 and an alkyl substituent at C-6. The nature of these substituents, often highly oxidized, gives rise to approximately 50 known natural carbapenem products; the simplest and best understood of which is (5*R*)-carbapenem-3-carboxylic acid. The biosynthesis of (5*R*)-carbapenem-3-carboxylic acid (Figure 2.1) in *Pectobacterium carotorovum* has been discovered to be

exquisitely efficient requiring only three enzymes, CarA, CarB and CarC. CarB is a member of the crotonase superfamily and catalyzes the formation of (*2S,5S*)-carboxymethylproline (CMP), the first committed intermediate in the pathway, from malonyl-CoA and L-pyrroline-5-carboxylate (L-P5C)[1]. CarA, carbapenam synthetase, cyclizes CMP to yield the (*2S,5S*)-carbapenam nucleus coupled to the hydrolysis of adenosine triphosphate (ATP)[2]. Finally, CarC, a non-heme iron α-ketoglutarate (α-KG)-dependent oxygenase, catalyzes both epimerization at the C-5 bridgehead and C-2/C-3 desaturation of the carbapenam to produce the final simple carbapenem[3–5].

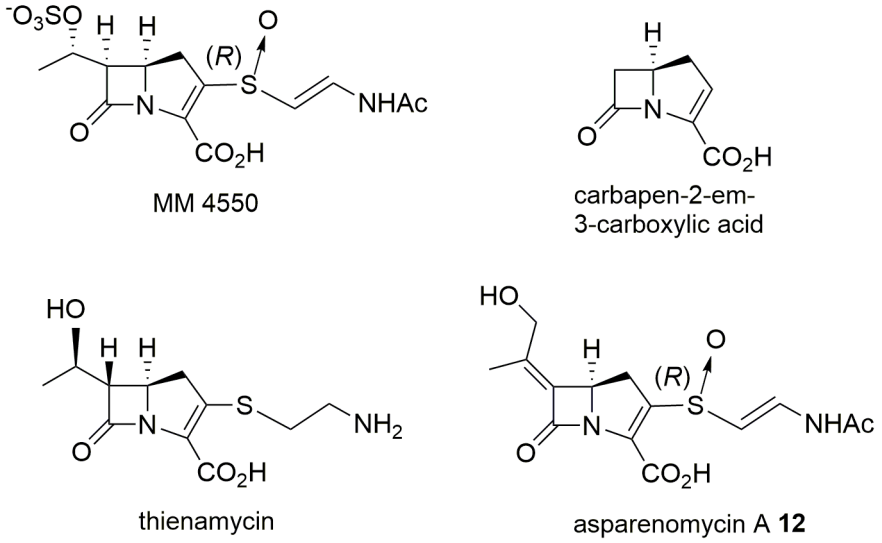

Figure 2.1: Representative carbapenems.

The discovery of the gene cluster for thienamycin (Scheme 2.1) in *Streptomyces cattleya* led to the assignment of 23 genes (*thnA-V*), 21 of which are not present in the simple carbapenem gene cluster[6]. Biochemical analysis has shown that the activity of ThnE and ThnM mirror that of CarB and CarA, respectively, and are capable of producing the common bicyclic core. Additionally, ThnQ is involved in the hydroxylation of the C-6 side chain of PS-5 to produce *N*-acetyl thienamycin[7–9]. Efforts aimed at revealing the biosynthesis of the C-2 substituent have shown that ThnR, ThnH

and ThnT incrementally cleave CoA to 4-phosphopantetheine, pantetheine and cysteamine, respectively[8,10]. ThnF acts as an acetyltransferase to convert thienamycin to *N*-acetyl thienamycin. In addition, ThnG is responsible for the further modification of the C-2 side chain as a desaturase and an oxygenase[8]. Gene inactivations have indicated that *thnL, thnN, thnO*, and *thnP* are absolutely necessary for the biosynthesis of thienamycin. However, reported mutational analyses give seemingly contradictory results as thienamycin production was still observed in *thnG, thnR* and *thnT* disruption mutants, suggesting that these genes are not required for thienamycin biosynthesis[11]. Finally, two pathway regulatory proteins, ThnI and CepU, positively regulate the expression of 10 genes in the thienamycin cluster and the biosynthesis of cephamycin in *S. cattleya*, respectively[12].

These recent advances notwithstanding, many questions remain about the biosynthesis of complex carbapenems including how, and in what order, epimerization of the carbapenam bridgehead, introduction of the double bond at carbons C-2/C-3, incorporation of CoASH at C-2 and alkylation at C-6 occur. Enzymatic analysis has demonstrated that the differences in the level of oxidation of the C-6 and C-2 side chains and C-6 stereochemistry give rise to many structural combinations[13–18]. It remains unknown how these differences are genetically encoded to produce potent antibiotics, distinct from thienamycin. Genetic differences across different species would explain these structural alterations. Apart from the silent gene cluster discovered in the *S. flavogriseus* genomic sequencing project, the thienamycin cluster in *S. cattleya* so far remains the only openly available gene cluster functionally associated with a specific complex carbapenem. Thus, exploration of the comparative genomics of the structurally

advanced carbapenems would not only give greater insight into the biosynthesis of these metabolites, but also provide an opportunity to apply combinatorial biosynthesis to generate new carbapenems with potentially improved properties.

In the early 1980's *S. argenteolus* ATCC 31589 was reported to be a producer of asparenomycin A (**12**), another potent carbapenem[19,20]. In this chapter, we establish that MM 4550 rather than asparenomycins is the major carbapenem produced in a related strain of *S. argenteolus* ATCC 11009. In addition, we provide detailed information on the identification, bioinformatic analysis, and mutational analysis of the gene cluster responsible for the biosynthesis of MM 4550.

Asparenomycins are not produced by *S. argenteolus* ATCC 11009

Asparenomycin A, B and C (Scheme 2.1) were isolated from two *Streptomyces* strains, *S. tokunonensis* ATCC 31569 and *S. argenteolus* ATCC 31589[20]. However, a query of the ATCC and NRRL catalogs did not yield *S. argenteolus* ATCC 31589, but a different strain of *S. argenteolus,* ATCC 11009. *S. argenteolus* ATCC 11009 was also reported to produce carbapenems and carbapenams such as an olivanic acid complex and 17927 D[15,20,21], but identifications have not been published[22]. We expected *S. argenteolus* ATCC 11009 to produce the asparenomycins as well, due to the similarity to the acquired strain with *S. argenteolus* ATCC 31589. As the most direct route to confirming the produced carbapenem(s), the total synthesis of asparenomycin A and C was performed through the route shown in Scheme 2.1 in an attempt to simply compare retention time of the metabolite with our synthetic standards without isolation from the *S. argenteolus* medium.

To synthesize asparenomycin A, the synthesis of Ona *et al.*[23] was found to be reliable and

reproducible in both products formed and yields reported in the original publication. Stirring 1,4 pentadiene with chlorosulfonylisocyanate for three days in a sealed pressure tube yielded (±) 4-allyl-2-azetidinone **1** in 61.9% yield after reductive workup of the azetidinone sulfate with sodium sulfite at neutral pH and at 0 °C. Protection of the amide with tert-butyldimethylsilyl chloride (TBSCl) proceeded in quantitative yield to produce **2**. Trimethylsilyl (TMS) protected acetol was prepared from 2-hydroxyacetone and trimethylsilyl chloride in the presence of dimethylaminopyridine (DMAP) and triethylamine (TEA) in 80% yield after distillation. Enolate addition of (±)-4-allylazetidin-2-one **1** to TMS acetol provided the alcohols **3a** and **3b** after acidic workup in a 2:1 ratio over two steps with a yield of 54%. Two diastereomers were produced from each enantiomer, resulting in a total of four stereoisomers. No 3,4-*cis*-compounds were detected by NMR spectroscopy, in agreement with the literature findings by Ona and coworkers[23]. It was important at this stage to separate the diastereomers by silica gel chromatography, so that the separate pathways may converge in the later steps of the synthesis.

The resulting 1,2-diols **3a** and **3b** were protected as the 1,3-dioxolidinone with 0.4 equivalents triphosgene and 2.2 equivalents pyridine and without purification the TBS groups were removed with TBAF and acetic acid to yield the azetidinones **4a** and **4b** in 64% yield after silica gel chromatography. **4a** and **4b** were further purified by recrystallized from toluene/ether.

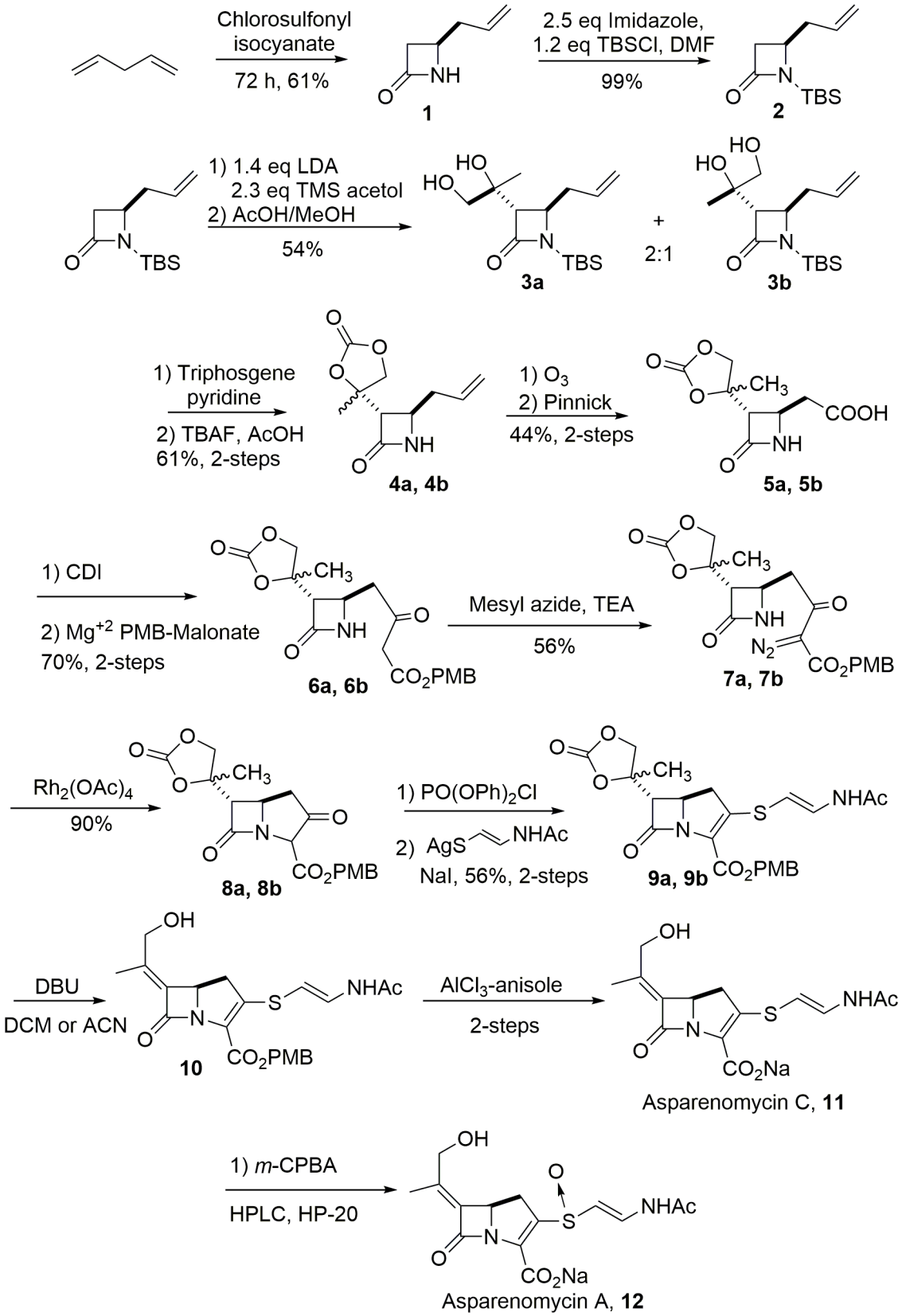

Scheme 2.1: Synthesis of (±) Asparenomycins A and C[23].

Ozonolysis of the 4-allyl group of **4a** or **4b** in dichloromethane and methanol proceeded cleanly at -78 °C and without purification the ozonide was reduced to the aldehyde and immediately oxidized to the carboxylic acid under Pinnick conditions[24]. Ona and coworkers used potassium dichromate in sulfuric acid (Jones reagent) in the original publications[23], however it was found that the product acid **5a** and **5b** was difficult to purify from contaminating chromate salts. Pinnick conditions were chosen due to the mild nature of the reaction and ease of purification by acidic workup and subsequent extraction. The products were crystallized from EtOAc/Ether to give the carboxylic acids **5a** and **5b** in 47% yield.

1,1-carbonyldiimidazole was used to activate the carboxylic acid for nucleophilic addition of the malonic acid mono-4-methoxybenzyl ester monomagnesium salt α-carbon, prior to spontaneous decarboxylation. Diazotization of the resulting β-keto esters **6a** and **6b** with mesyl azide afforded the α-diazo-β-keto esters **7a** and **7b**, thus priming the side chain for carbene addition into the amide N-H bond in the presence of catalytic rhodium (II) acetate. Diphenylchlorophosphate (DPCP) addition to the 2-oxopenams **8a** and **8b** activated the ring system for addition of silver-(*E*)-2-acetamido-1-ethenethiolate and spontaneous elimination of the phosphate produced the carbapenems **9a** and **9b**.

DBU was used to deprotonate the C-6 hydrogen for the elimination of the cyclic carbonates **9a** and **9b** to evolve CO_2 in the presence of bis-silylacetamide (BSA). BSA wass necessary to cap the free alcohol with TMS during the course of the reaction, so intermolecular polymerization of the produced alkoxide did not hamper yields, as was evidenced in literature reports[25]. Choice of solvent, dichloromethane or acetonitrile, dictates the mechanism of elimination, E2 or E1cb respectively, such that the required *E* isomer is made[26]. The separated diastereomers, **3a** and **3b**, produced earlier in the pathway converge to the enantiomers **10**.

As hydrogenolysis might negatively impact the yield of deprotection of the benzyl ester in the presence of the double bond on the C-2-thiol side chain, the 4-methoxybenzylester was

used to allow deprotection methods that would not compete with other functional groups in the molecule. $AlCl_3$-anisole provided the appropriate Lewis-acidic conditions for cleavage of the PMB ester in non-acidic non-reducing conditions as established by the work of Ohtani *et al*.[27]. Tsuji and coworkers[28] designed this protection / deprotection methodology for use in β-lactams chemistry, proposing that the strong affinity for aluminum halides for oxygen would draw electron density away from the ester bond, thus allowing the formation of a benzyl cation. It just so happens that the *p*-methoxybenzyl system is sufficiently electron rich to stabilize a formal positive charge at the benzyl position, affording good yields while retaining high selectivity. Desalting was achieved through elution from Diaion® HP-20 polystyrene resin and lyophilization afforded (±) asparenomycin C **11** from the cyclic carbonate as a white powder in 15% yield from **9a**. Intermediate **10** was not purified so no yield obtained, but crude mass suggests that compared to the elimination step, $AlCl_3$-deprotection was the more efficient of the two reactions.

It was possible to convert this antibiotic to asparenomycin A **12** simply by the addition of 1 equivalent of *m*-chloroperbenzoic acid (*m*CPBA) in water. Reverse-phase preparatory HPLC was necessary to purify the resulting sulfoxide diastereomers. A size-exclusion desalting column was used to remove excess salts to provide asparenomycin A **12** as the (*R*)-sulfoxide in 20% yield from asparenomycin C **11**. Though the yield of 20% seems very low, it is common to lose a great deal (>50%) of compound by HPLC purification. Investigations on suspect compound recovery from HPLC purification have been inconclusive.

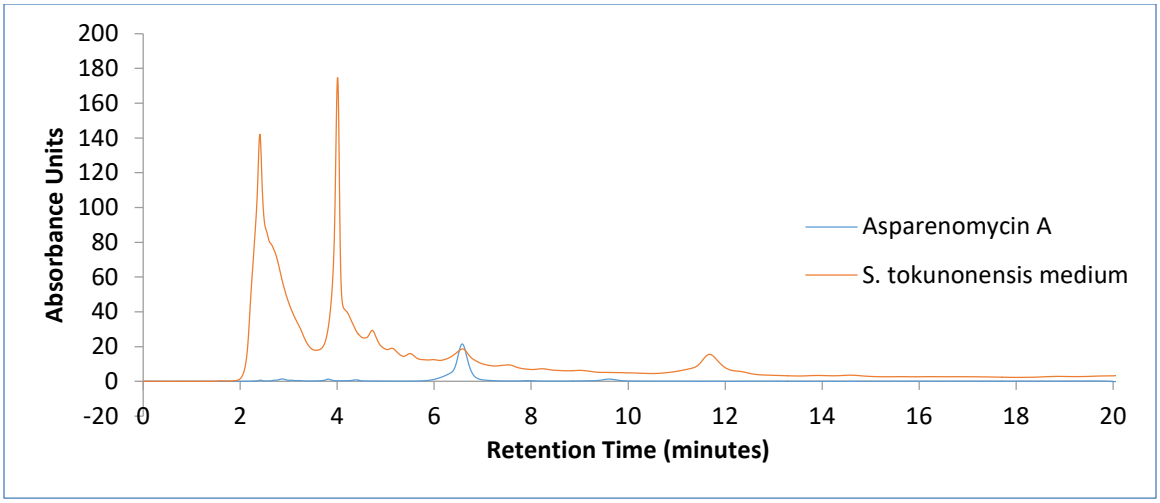

Figure 2.2: Elution of Asparenomycin A at 6.4 min as a synthetic standard (blue) and the fermentation product of *S. tokunonensis* (red)

Co-injection of the fermentation medium of *S. argenteolus* and either asparenomycin A or C showed no overlap of secondary metabolites with our synthetic standards (data not shown). As a proof of concept, the fermentation broth of *S. tokunonensis* was analyzed for asparenomycin production, so as to validate that this experiment could determine the presence of asparenomycins in the culture medium. *S. tokunonensis*, a known asparenomycin producer, was found to produce asparenomycin A in good titers, as was evidenced by overlap of a peak in the HPLC chromatogram with our synthetic standard, shown in Figure 2.2 The peak at 6.4 minutes, when isolated, produced a zone of inhibition on *E. coli* ESS plates indicating the presence of antibiotic.

It was concluded that asparenomycin A is not the major carbapenem product of *S. argenteolus*, so it was decided to formally isolate the major carbapenem produced from a large scale fermentation and determine its structure. The following experiments were carried out in close collaboration with Dr. Rongfeng Li. Work not done either by either myself alone or done together with Dr. Li is explicitly stated.

Identification of the carbapenems produced in *S. argenteolus* ATCC 11009

As the first step in our investigation, we conducted small-scale fermentations of *S. argenteolus* ATCC 11009 in OMYM and ISP4^{+} media, which showed antibiotic activity against the β-lactam super-sensitive *E. coli* ESS and inhibition of the β-lactamase in *Klebsiella pneumoniae* subsp. *pneumoniae* ATCC 29665 (data not shown). Bioassay of the fractions collected from HPLC by direct injection of supernatant broth indicated that the active product(s) resided in only one narrow region of the chromatogram (data not shown).

Our initial efforts to identify the β-lactam product failed owing to the low titer from the wild-type *S. argenteolus* ATCC 11009. To improve production, Dr. Rongfeng Li took a genetic engineering approach by the overexpression of three positive regulatory genes, *cmmI*, *cmm22* and *cmm23* (see below). The expression of each gene was individually controlled by an *ermE*p* constitutive promoter and the final expression construct containing all three genes, pMS82/cmmI-22-23 was integrated into the ϕBT1 site of the genome. Bioassay of his engineered strain against *E. coli* ESS showed an enlarged zone of inhibition, and HPLC analysis revealed that this altered strain still produced the same product as the wild-type (Figure 2.5), but in a nearly 4-fold improved yield based on comparison of peak areas for the active fraction. In addition, the maximal production in the engineered strain was at 48 h and 56 h in 50-mL and 1.3-L scale fermentations, respectively, compared to the wild-type strain at 72 h and 80 h.

S. argenteolus cmmI-22-23 was used for characterization of the carbapenem produced. A large-scale fed-batch fermentation procedure was developed using a modified minimal medium (ISP4^{++}) to give maximal production that also minimized

impurities during product purification. To make large-scale growth applicable to laboratory purification techniques, a long-chain quaternary ammonium salt was used as a phase transfer catalyst to extract negatively charged carboxylates into a small volume of organic solvent. Back-extraction of the resulting organic mixture with aqueous potassium iodide allowed recovery of the antibiotic into a volume 100 times more concentrated than the original fermentation filtrate. It was found that a 5% solution of Aliquat 336 in dichloromethane was highly effective in extracting the antibiotic where only two 300 mL washes were required to extract almost all of the antibiotic from 13 L of fermentation filtrate as monitored by *E. coli* ESS bioassay. The concentrated KI solution was then lyophilized, and the crude salt obtained was further purified by anion exchange chromatography over Dowex resin. Anion exchange chromatography was critical at this stage to remove the majority of impurities, salts, and residual Aliquat. Most importantly, this procedure resulted in highly concentrated fractions for further purification and analysis by HPLC.

Reverse-phase (C18) HPLC analysis of the active fractions resolved only one bioactive peak, as determined by bioassay on *E. coli* ESS plates, with a retention time of 16.3 min (Figure 2.5). Co-injection with a synthetic asparenomycin A standard showed a different retention time and UV spectrum, again supporting that the asparenomycins originally reported from *S. argenteolus* ATCC 31589 are not produced in *S. argenteolus* ATCC 11009[14,20]. Reaction with hydroxylamine resulted in the loss of that peak, consistent with the presence of a β-lactam in the active product. Additional bioactive material was collected by HPLC for further characterization.

The UV spectrum showed the product had not only a typical carbapenem absorbance signature at 288 nm but also an additional absorbance band was noted at 245 nm. A search of available UV data across all natural carbapenems resulted in only one potential compound that matched the spectrum of the isolated antibiotic. ^{1}H NMR spectroscopy identified the compound as MM 4550, as both chemical shifts and coupling constants were consistent with the published characterization of this compound[29,30] as is referenced in the experimental. Furthermore, two-dimensional ^{1}H-^{1}H COSY, ROESY, and TOCSY experiments confirmed the assignments of all protons made in the original publication[31]. Electrospray ionization mass spectrometry provided accurate mass of 407.0226 (±0.5 ppm; calculated 407.0224) for the anion of MM 4550.

Cloning of the MM 4550 biosynthetic gene cluster

Dr. Li did all of the cloning, cosmid library generation, and sequence analysis described in this section. Sequence analysis suggested and biochemical studies confirmed that ThnE and ThnM in the thienamycin biosynthetic pathway mirror the chemistry of CarB and CarA in the simple carbapenem pathway[7,8]. Alignment of CarA (*P. carotovorum*), β-LS (*S. clavuligerus*), β-LS3 (*S. antibioticus*), CpmA (*P. luminescens*), ThnM (*S. cattleya*), and several Asn-B (asparagine synthetase) revealed two motifs (M1 and M2) highly conserved in the β-lactam forming enzymes but either absent or present at distinctly lower homology in asparagine synthetases (Asn-B). Using the CODEHOP program (http://blocks.fhcrc.org/codehop.html)[30], two degenerate primers were designed, thnM-DEG-5 and thnM-DEG-3 (Figure 2.2), to these regions. A specific PCR product with the expected size of ~350 bp was obtained from *S. argenteolus* gDNA.

This PCR product showed an incomplete open reading frame (ORF) encoding a truncated protein of 108 amino acids with 74% identity to ThnM of *S. cattleya*, and 32% identity to CarA of *P. carotovorum*. A BLASTP alignment also showed that the two highly conserved motifs, M1 and M2, were present in the partial protein. These results strongly suggested that a partial *thnM* orthologous gene had been cloned from *S. argenteolus*.

A)

```
AsnB1 318 YVKVILSGEGA 329 - 100aa - 429 EFAQGCASSTVLE 441
AsnB2 318 YVKVILTGEGA 329 - 100aa - 429 QFDEGSGTVDLLV 441
AsnB3 318 YVKVVLSGEGA 329 - 100aa - 429 EFAQGCASSGVLE 441
AsnB4 353 GPLRILTGYGA 363 -  96aa - 459 GIHEGSGTTSAWT 471

           Motif M1                        Motif M2
BLS3  330 SGRRILTGYGA 340 - 96 aa - 436 GVHEGSGVTAAFT 448
BLS   339 PERRILTGYGA 349 - 96 aa - 445 GVHEGSGTTSSFS 457
CarA  336 QVSCMLTGYGS 346 - 99 aa - 445 GIHEGSSVNQAFA 457
CpmA  333 KVNSLITGYGS 343 - 99 aa - 442 GIHEGSSVNKSFA 454
ThnM  295 ARQVMLSGYGA 305 - 96 aa - 401 GIHEGTAMSRMFA 413
PluM  313 DRQVLLSGYGA 323 - 96 aa - 419 GIHEGTAMSRMFA 430
              :::***:                   *:***:. .  *:
```

B)

```
Primers:
 thnM-DEG-5: 5′-GCGCCAGTGCATGCTGwsnggntaygg-3′
 thnM-DEG-3: 5′-CATGGCGGTGCCCtcrtgdatncc-3′
```

Figure 2.3: (a) The two conserved motifs in the β-lactam ring-closing enzymes. The names and access numbers are as follows: BLS3, *Streptomyces antibioticus* (AFH74298.1); BLS, *Streptomyces clavuligerus* ATCC 27064 (ZP_05002824.1); CarA, *Pectobacterium carotovorum* subsp. *brasiliensis* PBR1692 (ZP_03825848.1); CpmA: *Photorhabdus luminescens* subsp. *laumondii* TTO1 (NP_927548.1); ThnM, *Streptomyces cattleya* NRRL 8057 (YP_004920124.1); PluM, *Streptomyces sulfonofaciens* NRRL 16438 (unpublished); AsnB1, *Nodularia spumigena* CCY9414 (YP_003135129.1); AsnB2, *Cyanothece* sp. CCY0110 (ZP_01729766.1); AsnB3, *Leptolyngbya* sp. PCC 7375 (ZP_18904938.1). BLS: β-lactam synthetase; AsnB: asparagine synthetase. The beginning and ending numbers indicate the position of amino acids in the proteins, and the numbers between the motifs indicate the separation in amino acid residues. **(b)** Primers designed for the M1 and M2 motifs according to the CODEHOP program. N: A/T/G/C; Y: C/T; M: A/C; R: A/G.

A cosmid gDNA library of *S. argenteulos* ATCC 11009 was constructed and screened using the ~350-bp gene fragment as a probe. Fourteen positive clones were obtained from a 2000 clone library. The sequencing analysis revealed that the T_3 and T_7

ends of the insert in cosmid 5D1 and 12B9 encoded a MarR-family transcriptional regulator and an AsnC-family transcriptional regulator, respectively. These proteins are not encoded by genes in the thienamycin gene cluster, indicating that cosmids 5D1 and 12B9 likely contained a whole carbapenem gene cluster. Cosmid 5D1 was chosen for further investigation.

Cosmid 5D1 was sequenced in its entirety. Five gaps between five contigs were bridged by PCR amplification and Sanger sequencing to give the full, circular cosmid. Overall, we ascertained that 5D1 contained the putative MM 4550 biosynthetic genes, which spanned almost 43.8 kb of the *S. argenteolus* genome. Computer-assisted analysis of the sequence revealed 31 complete open reading frames (ORFs) (Figure 2.4).

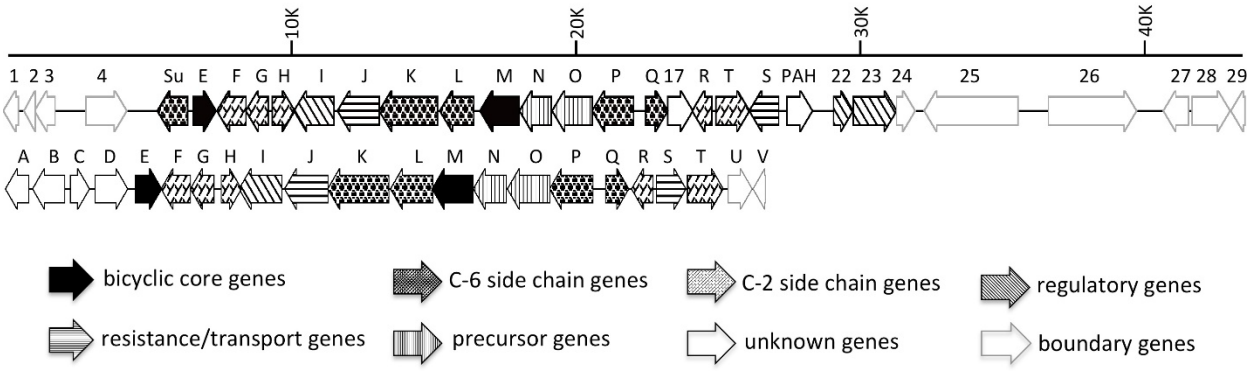

Figure 2.4: Gene organization of the MM 4550 and the thienamycin gene clusters in *S. argenteolus* ATCC 11009 (top) and *S. cattleya* NRRL8057 (below). The direction of transcription and the proposed functions of individual ORFs are indicated.

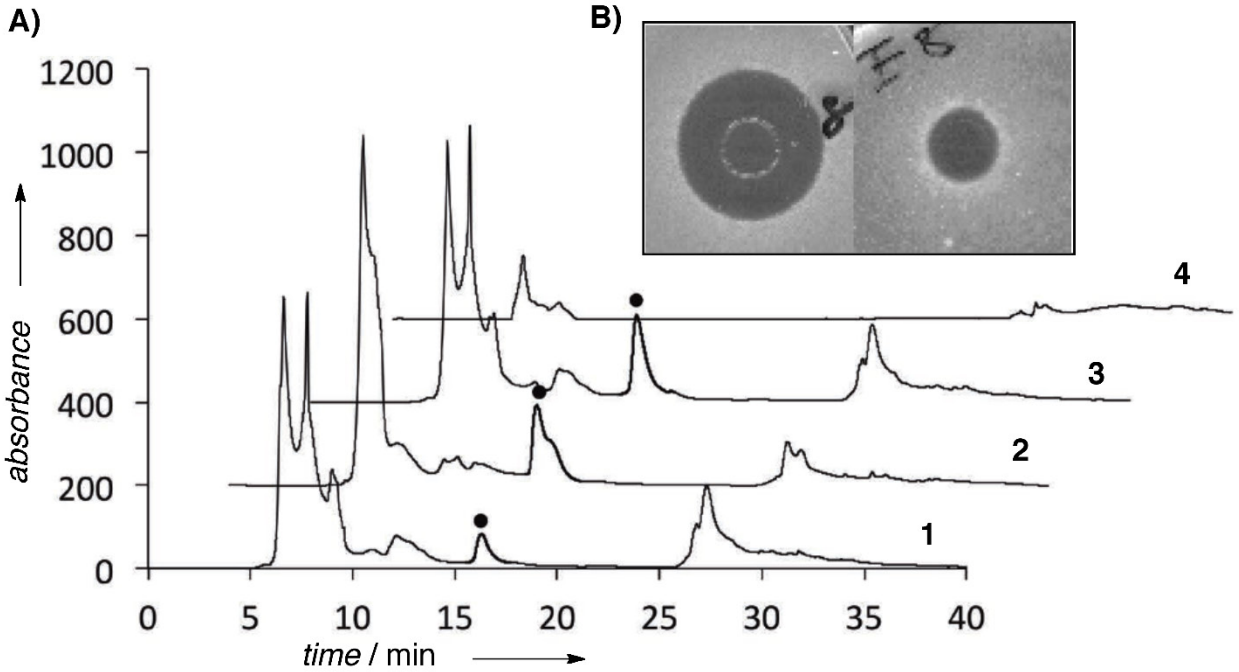

Figure 2.5: (a) HPLC analysis of *S. argenteolus* extracts. **1.** Wild-type *S. argenteolus* ATCC 11009; **2.** *S. argenteolus* cmmI-22-23; **3.** Wild-type *S. argenteolus* ATCC 11009 spiked with isolated peak from *S. argenteolus* cmmI-22-23; **4.** argE8 disruption mutant. Peaks (absorbance in arbitrary units) corresponding to MM4550 are indicated by a heavy dot (●). (b) Bioassay of the 16.3-min HPLC fractions of *S. argenteolus* cmmI-22-23 (left) and argE8 (right).

In order to confirm the cloned gene cluster was responsible for the biosynthesis of MM 4550, *cmmE*, whose gene product showed 76% and 40% identity to ThnE and CarB, respectively, was inactivated by a PCR targeting strategy with an *oriT-aac(3)IV* cassette to generate a gene replacing mutant argE8. The intended disruption of *cmmE* was confirmed by Southern hybridization with *cmmE* and *oriT-aac(3)IV* probes. As expected, when *Pml*I-digested gDNA was tested with the *cmmE* probe, a 1.65-kb positive fragment was observed in the wild-type but not the argE8 mutant gDNAs. Correspondingly this fragment was replaced with a 2.2-kb band in the argE8 mutant when hybridized with the *oriT-aac(3)IV* probe, but this band was missing in the wild-type gDNA (Figure 2.5). Bioassay on *E. coli* ESS plates showed that the argE8 mutant failed to produce

antibacterial products when fermented in ISP4^{+} medium (Table 2.2, Figure 2.4B). I performed HPLC analysis of the extract from the argE8 fermentation medium to show that the peak corresponding to MM 4550 in the wild-type *S. argenteolus* was absent (Figure 2.4A). These results strongly suggested that the gene cluster cloned in cosmid 5D1 is responsible for the biosynthesis of MM 4550 in *S. argenteolus*.

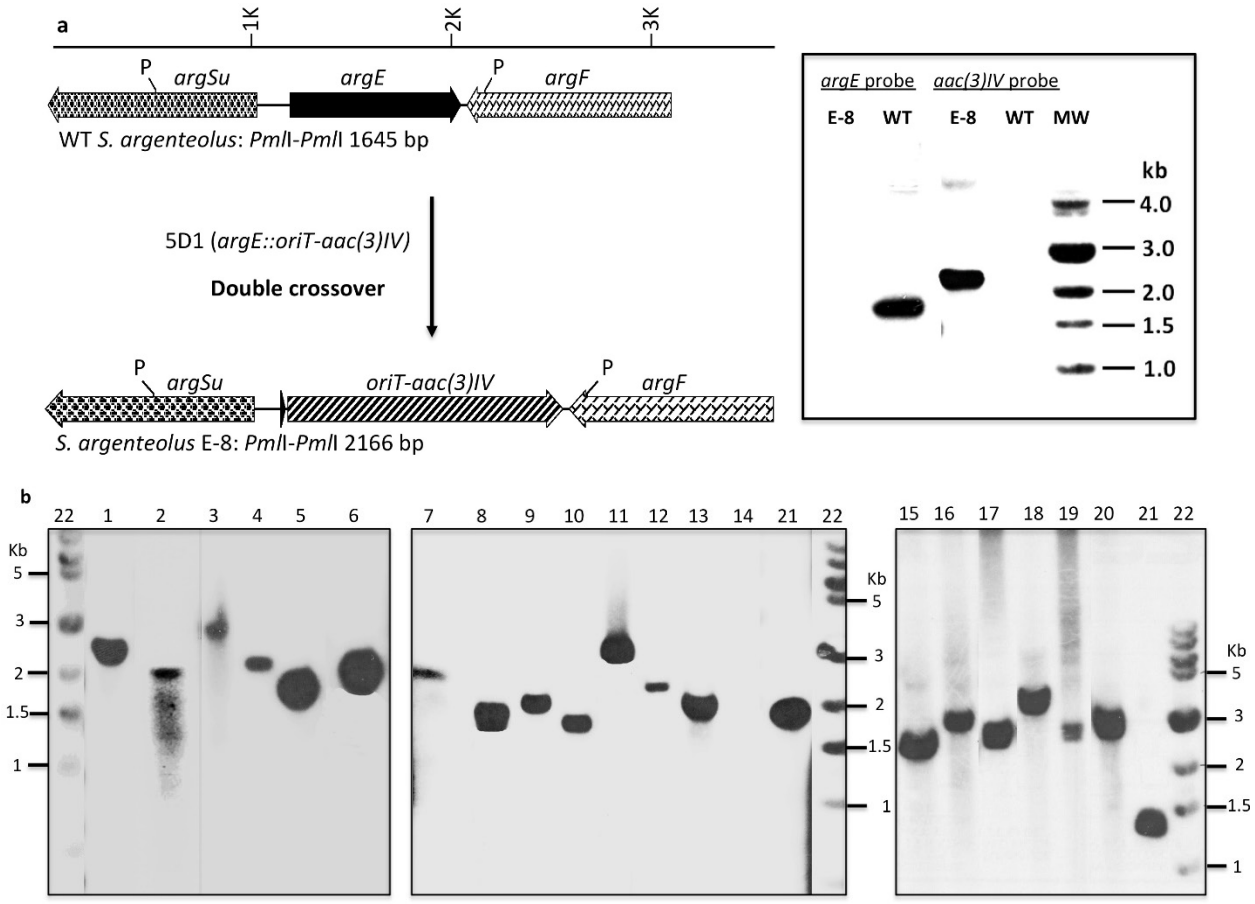

Figure 2.6: (a) The organization of *cmmSu, cmmE,* and *cmmF* in cosmid 5D1 and the construction of the argE8 disruption mutant. The restriction maps of the wild-type *cmmE* gene and its disrupted copy in the mutant are shown. (b) Southern analysis of the wild-type and the argE8 (*ΔE8*) mutant, showing the positive hybridizing bands to the *cmmE* and the *oriT-aac(3)IV* probes, respectively.

The DNA sequences of MM 4550 gene cluster have been deposited in the NCBI nucleotide sequence database with accession number KF042303.

Sequence analysis of the MM 4550 biosynthetic gene cluster

Dr. Rongfeng Li also examined the sequences and searched for the putative functions of the deduced gene products summarized in Table 1. The overall architecture and some gene products of the MM 4550 gene cluster are highly similar to a cryptic cluster in *S. flavogriseus* ATCC 33331 identified by gene scanning[32]. However, because no product is known from this cluster and none of the enzymes encoded by it have been characterized, analysis of the MM 4550 gene cluster focused principally on comparison with the thienamycin gene cluster.

Table 2.1: Deduced functions of proteins encoded by the MM 4550 biosynthetic gene cluster

Protein	Amino acids	Proposed function	Sequence similarity (identity/positive)	Identity/ positive to ATCC 33331(%)
Orf1	238	Unknown	No similar sequences	--/--[a]
Orf2	475	arabinofuranosidase	SMCF_639, *Streptomyces coelicoflavus* ZG0656 (89/92)	--/--
CmmSu	353	sulfotransferase	Sfla_0165, *S. flavogriseus* ATCC 33331 (87/92)	87/92
CmmE	263	carboxymethylproline synthase	ThnE, *S. cattleya* NRRL 8057 (69/80)	93/96
CmmF	338	N-acetyltransferase	ThnF, *S. cattleya* NRRL 8057 (58/66)	86/89
CmmG	263	oxidoreductase	ThnG, *S. cattleya* NRRL 8057 (70/80)	87/92
CmmH	229	HAD-superfamily hydrolase	ThnH, *S. cattleya* NRRL 8057 (57/69)	82/87
CmmI	466	LysR family transcriptional regulator	ThnI, *S. cattleya* NRRL 8057 (51/64)	83/87
CmmJ	487	Transporter protein	ThnJ, *S. cattleya* NRRL 8057 (56/68)	89/93
CmmK	680	radical SAM methyltransferase	ThnK, *S. cattleya* NRRL 8057 (79/86)	95/96

CmmL	394	radical SAM methyltransferase	ThnL, *S. cattleya* NRRL 8057 (67/72)	82/86
CmmM	459	Carbapenam synthetase	ThnM, *S. cattleya* NRRL 8057 (64/76)	86/91
CmmN	369	AFD class I superfamily protein, acyl-CoA synthase	ThnN, *S. cattleya* NRRL 8057 (86/91)	95/97
CmmO	467	aldehyde dehydrogenase	ThnO, *S. cattleya* NRRL 8057 (75/82)	90/94
CmmP	482	radical SAM methyltransferase	ThnP, *S. cattleya* NRRL 8057 (83/91)	97/98
CmmQ	259	putative oxigenase	ThnQ, *S. cattleya* NRRL 8057 (72/81)	93/94
Cmm17	292	enoyl-CoA hydratase	Kyg_13766, *Acidovorax* sp. NO-1 (34/46)	89/93
CmmR	228	nudix hydrolase	ThnR, *S. cattleya* NRRL 8057 (55/66)	75/82
CmmT	388	hydrolase	ThnT, *S. cattleya* NRRL 8057 (69/75)	87/90
CmmS	334	β-lactamase	Orf11, *S. clavuligerus* ATCC 27064 (63/71)	80/87
CmmPah	298	proclavaminate amidino hydrolase	PAH, *S. clavuligerus* ATCC 27064 (52/65)	86/90
Cmm22	227	two-component system response regulator	SPW_1836, *Streptomyces* sp. W007 (84/90)	--/--
Cmm23	506	two-component system sensor kinase	Sacte_5700, *Streptomyces* sp. SirexAA-E (89/93)	--/--
Cmm24	217	unknown	Sacte_5699, *Streptomyces* sp. SirexAA-E (74/79)	--/--
Orf25	1094	putative peptidase	Sacte_5698, *Streptomyces* sp. SirexAA-E (81/88)	--/--
Orf26	1029	putative glycosyl hydrolase	Szn_17732, *Streptomyces zinciresistens* K42 (78/88)	--/--
Orf27	294	putative RNA polymerase sigma factor	Sfla_6134, *S. flavogriseus* ATCC 33331 (88/93)	--/--
Orf28	441	putative serine/threonine phosphatase	Sfla_6135, *S. flavogriseus* ATCC 33331 (85/91)	--/--

Orf29	164	putative MarR family transcriptional regulator	S.fla_6136, *S. flavogriseus* ATCC 33331 (93/95)	--/--

a. --/--: not in the cluster.

As shown in Figure 2.2, among the 31 complete ORFs present in the insert of 5D1, 17 clear homologues are also present in the thienamycin gene cluster[7]. Genes *cmmE-Q* show the same organization as *thnE*-Q in the thienamycin gene cluster. Notable genes *cmmR, cmmS* and *cmmT* are also shared between the two clusters. However, in the MM 4550 gene cluster, they are organized as *cmmR-cmmT-cmmS* with *cmmR* and *cmmS* transcribed in the opposite orientation to *cmmT.* A new gene, *cmm17*, is inserted between *cmmQ* and *cmmR* in the MM 4550 gene cluster. In addition to *cmm17*, four more new genes, *cmmSu, cmmPah. cmm22* and *cmm23* are present in the MM 4550 cluster with *cmmSu* located upstream of *cmmE* at one end and the other three genes are downstream of *cmmS* at the other end of the cluster. Bioinformatic analysis indicated that genes upstream of *cmmSu* and downstream of *cmm24* encode proteins that are not related to the biosynthesis of carbapenems or are not present in known carbapenem gene clusters (Table 2.1). Finally, *thnA-D* and *thnV,* whose roles in the thienamycin biosynthetic pathway have not been determined, and *cphU*, which encodes a SARP-like regulator for cephamycin biosynthesis[12], are all absent from the MM 4550 gene cluster.

It has been reported that thienamycin and (5*R*)-carbapenem-3-carboxylic acid share the first two steps in their biosynthetic pathways to make the carbapenam bicyclic core. The orthologous genes in the MM 4550 cluster encode proteins sharing 69%, 37% and 64%, 22% identity to ThnE, CarB and ThnM, CarA, respectively, and active site residues are also conserved, indicating CmmE and CmmM catalyze the same reactions in

MM 4550 biosynthesis[2,7,8,11,33].

The three putative radical-SAM enzymes encoded by *cmmK, cmmL* and *cmmP* are also highly conserved in the MM 4550 gene cluster and share 79%, 67%, and 83% amino acid identities to ThnK, ThnL and ThnP, respectively. CmmQ shows sequence homology to ThnQ that has been shown to be a Fe(II)/α-KG-dependent oxygenase responsible for the hydroxylation of the C-6 ethyl side chain of thienamycin[9]. To explain the difference between the C-8 sulfate of MM 4550 and C-8 hydroxyl of thienamycin, a BLASTP search revealed that CmmSu has 38% identity and 52% positive to the putative sulfotransferase in *S. blastmyceticus*[34]. A conserved 5'-phosphosulfate-binding sequence (5'-PSB), ^{17}RC**G**STM^{23}, was located in a strand-loop-helix (PSB-loop) motif. A second motif, ^{89}G**R**YAAGEVPAI**S**L^{101}, similar to the conserved 3'-phosphate binding sites in sulfotransferases is also present in CmmSu[35–37]. These conserved motifs strongly suggest that CmmSu acts as a sulfotransferase required for sulfonation of the C-6 side chain in MM 4550. Together, we propose that some or all of *cmmK, cmmL, cmmP, cmmQ* and *cmmSu* are involved in the biosynthesis of the C-6 side chain in MM 4550.

A set of genes were designated as *cmmR, cmmH, cmmT, cmmF* and *cmmG*, whose products show high similarity to ThnR, ThnH, ThnT, ThnF and ThnG in the thienamycin biosynthetic pathway. Their roles in the biosynthesis of the C-2 cysteaminyl side chain in thienamycin have been demonstrated through stepwise cleavage of CoA by ThnR, ThnH and ThnT[11]. Furthermore, the acetyltransferase ThnF, is responsible for the *N*-acetylation of the cysteaminyl side chain from acetyl-CoA[38]. Finally, CmmG shares 70% identity with ThnG in the thienamycin biosynthetic pathway. *In vitro* characterization of ThnG has shown that it catalyzes the desaturation and sulfoxidation of the *N*-acetyl-2-

cysteaminyl side chain of *N*-acetyl-thienamycin to form the sulfoxide of PS-7[8]. Consistent with its structure, the C-2 side chain of MM 4550 is likely to be processed by these five enzymes in the order of CmmR, CmmH, CmmT, CmmF and CmmG.

cmmI encodes a putative LysR-family positive regulator, which shares 50% and 26% identities to ThnI and ClaR in the biosynthetic pathways of thienamycin and clavulanic acid, respectively[12,39,40]. Two new genes, *cmm22* and *cmm23,* located at the right end of the gene cluster encode proteins homologous to the two-component regulatory systems in a wide range of microorganisms. The amino acid sequence of Cmm22 (227 aa) shows end-to-end similarity to response regulators, including an aspartate residue (Asp^{52}) typically phosphorylated inside the *N*-terminal phosphorylation domain, a *C*-terminal DNA binding domain, and several other key characteristic residues (Asp^{9}, Asp^{10}, Thr^{80} and His^{101})[41–43]. As observed in most two-component regulatory systems, *cmm23* encodes a protein (506 aa) with full-length homology to sensory histidine kinases and is located immediately downstream of *cmm22*. Cmm23 contains three conserved domains including the H-box (^{269}**H**ELRTPL^{275}) (His^{269} is a putative phosphorylation site), the N-box (^{376}NLVGNA^{381}), and the G-box (^{405}VRDSGPGI^{412}) [35]. Structural prediction using TopPred 0.01 (http://mobyle.pasteur.fr/cgi-bin/portal.py?#forms::toppred)[44] identified three possible transmembrane domains in Cmm23: domain I (residues 14-34, score 1.96), II (147-167, score 1.26) and III (181-201, score 1.26). The sensor domain is generally located at the *N*-terminus in most histidine kinases; therefore, domain I is likely the sensor domain of Cmm23. The organization and likely properties of Cmm22 and Cmm23 suggested that they belong to the OmpR family of two-component response regulators[42].

Two genes, *cmm17* and *cmmPah*, absent in the thienamycin gene cluster were also identified. *cmm17* is located directly downstream of and in the same orientation as *cmmQ* in the gene cluster and encodes a 292-amino acid protein. BLASTP analysis showed Cmm17 has appreciably high similarity (35-38% identity and 50-55% similarity) to enoyl-CoA hydratases from a number of microorganisms. Cmm17 possesses most residues important for substrate binding and catalysis including Glu^{128}. However, a His^{148} residue is present instead of the Glu residue that is typically conserved in most enoyl-CoA hydratases[33,45]. *cmmPah* is located between *cmmT* and *cmmS* and is transcribed in the opposite direction to *cmmT* and *cmmS*. Its gene product comprises 298 amino acids and belongs to the arginase-like/histone-like hydrolase superfamily[46]. A BLASTP search showed that CmmPah has significant similarity to agmatinases, a subgroup of the arginase superfamily and a key enzyme in an alternative metabolic pathway of arginine in microorganisms and plants[47]. The highest homology (46-52% identity and 60-67% similarity) is to proclavaminate amidino hydrolase (PAH), an enzyme in the clavulanic acid and 5*S* clavam biosynthetic pathways from *S. clavuligerus* and *S. antibioticus*[48,49]. However, alignment of CmmPah with three PAH enzymes from *S. clavuligerus* and *S. antibioticus* and two arginases from *A. flavithermus* and *S. viridis* showed that only one of the six Mn^{2+}-binding residues (Asp^{222}) is conserved in CmmPah. Only one of the three guanidino binding residues (Thr^{232}) and one of the four α-amino acid binding residues (Gly^{147}) conserved in arginases and PAHs is present in CmmPah[50]. The Gly-Gly-Asp-His-Ser motif conserved in all arginases is changed to ^{116}Gly-Gly-Gly-Arg-Ser^{120} in CmmPah. Finally, secondary structure prediction (http://bioinf.cs.ucl.ac.uk/psipred/) showed that the *N*-terminal secondary structure of CmmPah is similar to the PAHs and

arginases, but the *C*-terminal region is different[50].

Mutational analysis of genes in the MM 4550 gene cluster

To better understand the role of each individual gene in the biosynthesis of MM 4550, Dr. Li generated gene-replacing mutants for twenty genes in the proposed biosynthetic gene cluster using λ-RED-mediated PCR mutagenesis[51]. Each targeted gene was replaced with a FRT-*oriT-aac(3)IV*-FRT cassette in its resultant mutant. Mutants derived from double crossover events with the targeted genes, and their disrupted copies on 5D1 were selected according to their apramycin-resistant/ kanamycin-sensitive (Am^R /Km^S) phenotype. To confirm the genotype of the mutants, gDNA was digested with restriction enzymes and hybridized with a *oriT-acc(3)IV* probe. As expected, the gDNA of wild-type *S. argenteolus* did not hybridize to the probe, but positive hybridization was observed from all tested mutants and the size of each resultant band was as predicted by restriction analysis. The digested gDNA of each mutant was also hybridized against the gene-specific probe. No hybridization was observed from any potential mutant (data not shown), confirming that targeted gene replacement had occurred in each case. One mutant in each disruption of a specific gene was chosen for further characterization.

Table 2.2: Analysis of the disruption mutants of *S. argenteolus*

Disruption mutants	*E. coli* ESS	*B. licheni-formis*	Nitrocefin
argSu13	+	-	+
argE8	-	-	-
argF7	-	-	-
argG5	+	+	+
argH8	+	+	+
argJ4	-	-	-

argK11	-	-	-
argL2	-	-	-
argM7	-	-	-
argN7	-	-	-
argO2	-	-	-
argP4	-	-	-
argQ4	+	-	+
arg17-4	-	-	+
argR8	-	-	-
argT3	-	-	-
argS6	+	+	+
argPah9	-	-	-
arg22-6	-	-	-
arg24-3	+	+	+
WT	+	+	+

Together, we characterized all disruption mutants by fermentation in ISP4^{+} medium and analyzed for antibacterial activity on *E. coli* ESS or β-lactamase induction on *B. licheniformis* using nitrocefin as indicator[52]. We observed that, in addition to antibiotic activity against *E. coli* ESS, MM 4550 also exhibits moderate β-lactamase-inducing activity in *B. licheniformis*. I further analyzed bioactive intermediates in disruption mutants by UPLC-MS (Table 2.3).

As summarized in Table 2, bioassay on *E. coli* ESS showed that disruption of *cmmE* and *cmmM* completely eliminated production of MM 4550 during 7-day fermentation. nitrocefin assays showed that β-lactamase induction was only at background levels compared with the wild-type, consistent with no carbapenem(s) being produced in these mutants. Moreover, HPLC analysis confirmed that the peak corresponding to MM 4550 was completely absent in the argE8 mutant (Figure 2.3). Similar results were also obtained from argK11, argL2 and argP4 mutants, suggesting that these enzymes are also necessary for biosynthesis (Table 2.2). Bioassay against *E.*

coli ESS showed that the disruption mutant of *cmmQ*, argQ4, consistently produced a bioactive product during its fermentation, but in reduced amount or potency in comparison to the wild-type. The nitrocefin assay showed that argQ4 still maintains β-lactamase induction activity, but loses detectable antibacterial activity against *B. licheniformis* (Table 2.2). The active fraction of extracted fermentation broth shared both the same retention time and mass with synthetic PS-5, confirming that PS-5 is accumulated in argQ4 (Table 2.3)[9]. BLASTP analysis suggested that CmmSu is the most likely candidate in the gene cluster to catalyze C-6 sulfonation to MM 4550. Interestingly, the disruption mutant of *cmmSu*, argSu13, still produced antibacterial products. However, unlike the wild-type *S. argenteolus*, the supernatant of the argSu3 only showed β-lactamase induction activity rather than antibacterial activity on *B. licheniformis*, indicating that the product is likely not MM 4550. UPLC-MS analysis of the bioactive material in argSu13 revealed a mass for the non-sulfonated derivative of MM4550 (Table 2.3).

Mixed results were obtained from genes potentially involved in the biosynthesis of the C-2 side chain. Mutants argR8, argT3 and argF7, disrupted at *cmmR, cmmT* and *cmmF,* respectively, were unable to produce MM 4550 at any time point during the fermentation, while the *cmmH* and *cmmG* mutants, argH8 and argG5, still produced bioactive products as indicated by bioassay on *E. coli* ESS (Table 2.2). The nitrocefin assay showed that both the argG5 and argH8 mutants had similar antibacterial and β-lactamase induction activities as the wild type. UPLC-MS analysis showed the active intermediate in argG5 has the same mass as MM 17880 (Table 2.3). These results indicate that *cmmH, cmmG*, *cmmR*, *cmmT* and *cmmF* are essential for the production of

MM 4550.

Table 2.3: HPLC-MS analysis of carbapenems from *S. argenteolus*

Strain	Found (m/z)	Calculated (m/z)	Molecular Formula	Proposed Structure
WT	407.0215	407.0224	$C_{13}H_{15}N_2O_9S_2^-$	MM 4550
argSu13	313.0848	313.0858	$C_{13}H_{17}N_2O_5S^-$	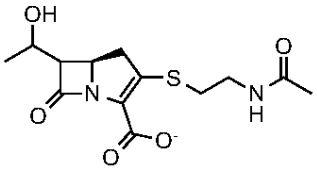 Epithienamycin A
argQ4	297.0909	297.0909	$C_{13}H_{17}N_2O_4S^-$	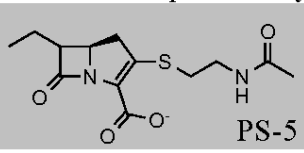 PS-5
argG5	393.0404	393.0426	$C_{13}H_{17}N_2O_8S_2^-$	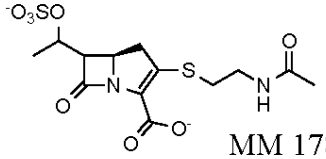 MM 17880
argE8	n/a	n/a	n/a	no carbapenem masses found

Dr. Li disrupted gene *cmm22* to investigate if the two-component response regulators are involved in the MM 4550 biosynthesis. Both antibacterial and β-lactamase induction activities from the disruption mutant, arg22-6, were negative, suggesting that the two-component regulators encoded by *cmm22/23* are essential for the biosynthesis of MM 4550 (Table 2.2). Thus, the biosynthesis of MM 4550 is regulated by at least two regulatory mechanisms; LysR-type transcription activation and the two-component response system, in *S. argenteolus*[6,12].

Dr. Li also studied the involvement of two new genes, *cmm17* and *cmmPah*, in the biosynthesis of MM 4550 through gene inactivation. Disruption of *cmm17* generated

a mutant (arg17-4) that was unable to produce any metabolites active against *E. coli* ESS and *B. licheniformis*. However, the fermentation supernatant showed strong β-lactamase induction activity as shown by the nitrocefin assay, indicating a β-lactam ring-containing intermediate accumulated in the mutant. On the other hand, bioassays and β-lactamase induction assay showed that the *cmmPah* disruption mutant (argPah9) failed to produce metabolites positive against *E. coli* ESS and *B. licheniformis*, or induce β-lactamase expression. While the role of CmmPah in the biosynthesis is unknown, extensive mass spectroscopic analyses were unable to detect intermediates in the mutants. Notwithstanding, the results demonstrated that these two new genes are essential for the biosynthesis of MM 4550 (Table 2.2). Finally, analysis of CFEs of mutants arg17-4 and argPah9 showed that they displayed similar antibacterial and β-lactamase induction activities as their fermentation supernatants (data not shown).

Disruption of *cmm24* by Dr. Li resulted in a mutant with the same phenotype of antibacterial and β-lactamase induction activities as the wild-type *S. argenteolus*. Combined with the BLASTP analysis (Table 1), *cmm24* may not be involved in the biosynthesis of MM 4550 and likely to be the 3' boundary of the gene cluster. The ORF analysis also showed that the intergenic region upstream of *cmmSu* is nearly 1 kb and the gene (*orf4*) upstream of *cmmSu* encodes a protein similar to sugar metabolism that is clearly unrelated to carbapenem biosynthesis (Table 2.1). Thus, we propose that the MM 4550 gene cluster harbors 21 genes involved in its biosynthesis, resistance and regulation (Figure 2.3).

Discussion

Olivanic acids, including MM 4550, MM 13902 and MM 17880, were originally identified from *S. olivaceus* ATCC 31126 and *S. olivaceus* ATCC 21379. Although it has been mentioned that olivanic acids are also produced by other *Streptomyces* strains, including *S. argenteolus* ATCC 11009, no further information has been reported[15,31,53]. By combining genetic engineering approaches with modified extraction protocols and structural analysis, we have demonstrated, for the first time, that MM 4550 is the major carbapenem produced by *S. argenteolus* ATCC 11009. This finding contrasts with the two *S. olivaceus* strains in which three compounds of the olivanic acid complex are produced in similar titers[31]. NMR and UV spectroscopy, and mass spectrometry support the structure of the final product in *S. argenteolus* as MM 4550.

The MM 4550 gene cluster is only the second gene cluster determined to be involved in the biosynthesis of a complex carbapenem that has been characterized. In comparison with thienamycin, MM 4550 is more highly functionalized, with a sulfate at the C-8 hydroxyl as well as an oxidatively modified C-2 side chain. The syn relationship across the C-5/C-6 bond is another feature that differs, and many carbapenems have been discovered having this stereochemistry. This structural feature suggests a potential fundamental difference in their biosynthetic pathways, despite the similarity of the gene clusters for thienamycin and MM 4550.

Although genes presumed to be involved in the biosynthesis of the bicyclic core and the C-6 and C-2 side chains are conserved between the two gene clusters, there are differences that stand out. First, the genes *thnA-D, cepU* and *thnV* in the thienamycin gene cluster are all missing in the MM 4550 cluster. It is known that *cepU* is a regulatory

gene for cephamycin biosynthesis, but the functions of the other genes in this group are yet to be determined in *S. cattleya*. Second, we found that the biosynthesis of MM 4550 is regulated by two regulatory mechanisms with proteins encoded by *cmmI* and *cmm22/23*. A helix-turn-helix (HTH) DNA-binding domain and the rare TTA codon are shared by ThnI and CmmI, indicating similar regulatory roles in their biosynthetic pathways[12]. Two-component regulatory systems are generally global regulators in the biosynthesis of secondary metabolites[54,55]. Disruption of *cmm22* clearly showed that *cmm22/23* is involved in MM 4550 biosynthesis, presumably through phosphorylation of the regulator (Cmm22) by the membrane-bound phosphokinase (Cmm23). In addition, overexpression of *cmmI* and *cmm22/23* improved the production of MM 4550, confirming their positive regulatory roles. Lastly, three putative biosynthetic genes that are unique in the MM 4550 gene cluster were identified.

The first, *cmmSu,* encodes a putative sulfotransferase as predicted by sequence analysis. Sulfotransferases are a superfamily of enzymes catalyzing sulfonation of a variety of endogenous and exogenous substrates. In contrast to humans and other mammals, little is known about bacterial sulfotransferases[36]. BLASTP analysis suggested that CmmSu is PAPS-dependent owing to the presence of a putative PBS-loop and the 3'-phosphate binding sites. Disruption of *cmmSu* resulted in a mutant with a different antibacterial spectrum from MM 4550. Mass-spectroscopic analysis showed the accumulation of a non-sulfonated derivative of MM 4550 in the argSu13 mutant, as expected. An earlier analysis of the OA-6129 group of carbapenems identified in a series of random mutants of *S. fulvoviridis* processing at C-6 and C-8 that was thought to be ordered as C-8 hydroxylation, C-6 isomerization and C-8 sulfonation. The substrate of

the sulfonation enzyme, OA-6129B_1, was demonstrated to be bioactive[56]. MM 4550 possesses the same C-6 side chain as OA-6129C, suggesting that the C-6 side chain of MM 4550 is processed through a similar biosynthetic sequence as the OA-6129 carbapenem group.

Structurally, the major difference that distinguishes MM 4550 from thienamycin is the syn-relationship across C-5 and C-6. The remaining enzymes that could be involved in establishing this alternate stereochemistry are Cmm17 and CmmPah as they are present in *S. argenteolus* but not in *S. cattleya*. Cmm17 shows high sequence homology to enoyl-CoA hydratases. It is known that the acid/base chemistry for this type of enzymes can hydrate α, β-unsaturated double bonds or perform the reverse reaction[46]. Interestingly, disruption of *cmm17* resulted in the loss of antibacterial activities against *E. coli* ESS and *B. licheniformis* but gained stronger β-lactamase induction activity compared to the wild-type and other disruption mutants, indicating that a β-lactam-containing intermediate was accumulated in the mutant. We propose that Cmm17 could be involved in the epimerization of the C-6 side chain and, therefore, produce a different ultimate stereochemical outcome in MM 4550 biosynthesis (Scheme 1.3). Although CmmPah displays high sequence similarity to arginases and PAHs, almost all the amino acid residues involved in substrate binding and co-factor binding in the comparison enzymes are absent from CmmPah, strongly suggesting that CmmPah catalyzes a different reaction(s) in the biosynthesis of MM 4550 from the arginases and PAHs.

It is important to note that the disruption mutants for *cmmG* and *cmmQ* resulted in the detection of intermediates with masses for MM 17880 and PS-5, respectively, in the mutants (Table 2.3). As shown previously in *S. cattleya*, ThnQ hydroxylates the bioactive

substrate PS-5 to generate *N*-acetyl thienamycin, and the latter is further oxidized by ThnG to produce *N*-acetyl dehydrothienamycin. ThnG also catalyzes the oxidation of PS-5 to produce PS-7 and PS-7 sulfoxide[9]. Thus, in keeping with this *in vitro* analysis, CmmG is responsible for the oxidation of MM 17880 to produce MM 13902 and further to produce MM 4550 (Scheme 2.3), CmmQ is likely involved in the C-8 hydroxylation of MM 4550 as observed in the OA-6129 group of carbapenems. Thus, a bioactive intermediate with the mass and UPLC retention of PS-5 is accumulated when *cmmQ* was knocked-out.

Importantly, disruption of *cmmR* and *cmmT* led to MM 4550 non-producers in *S. argenteolus.* This finding contradicts reports in *S. cattleya* in which inactivation of orthologous genes *thnR* and *thnT* retained thienamycin production in the mutants[12]. Biochemical studies have shown that both ThnR and ThnT are involved in the incremental truncation of the C-2 side chain in thienamycin[11]. Our gene inactivation results support the *in vitro* analysis and confirmed that *cmmR* and *cmmT* are essential for the biosynthesis of MM 4550. ThnR and ThnT are similar to Nudix hydrolases and peptidases, respectively. Searching the recently sequenced genome of *S. cattleya* showed five putative Nudix hydrolases and 46 putative peptidases. Thus, the continued production of thienamycin in *thnR* and *thnT* disruption mutants could result from *in trans* complementation.

The questions that remain in the biosynthesis of complex carbapenems include the mechanism and timing of inversion of the C-5 carbapenam bridgehead, the desaturation of the C-2/C-3 bond, and the attachment of the C-2 and C-6 side chains. Like the thienamycin cluster, there are no obvious candidates to catalyze these steps in the MM

4550 gene cluster. As both thienamycin and MM 4550 require these transformations, it is probable that enzymes conducting these steps are among those encoded in common by both gene clusters. Our gene disruption results ruled out the involvement of *cmmQ* and *cmmG* in the epimerization/desaturation as has been hypothesized[9] because the disruption mutants retain the ability to produce bioactive intermediates.

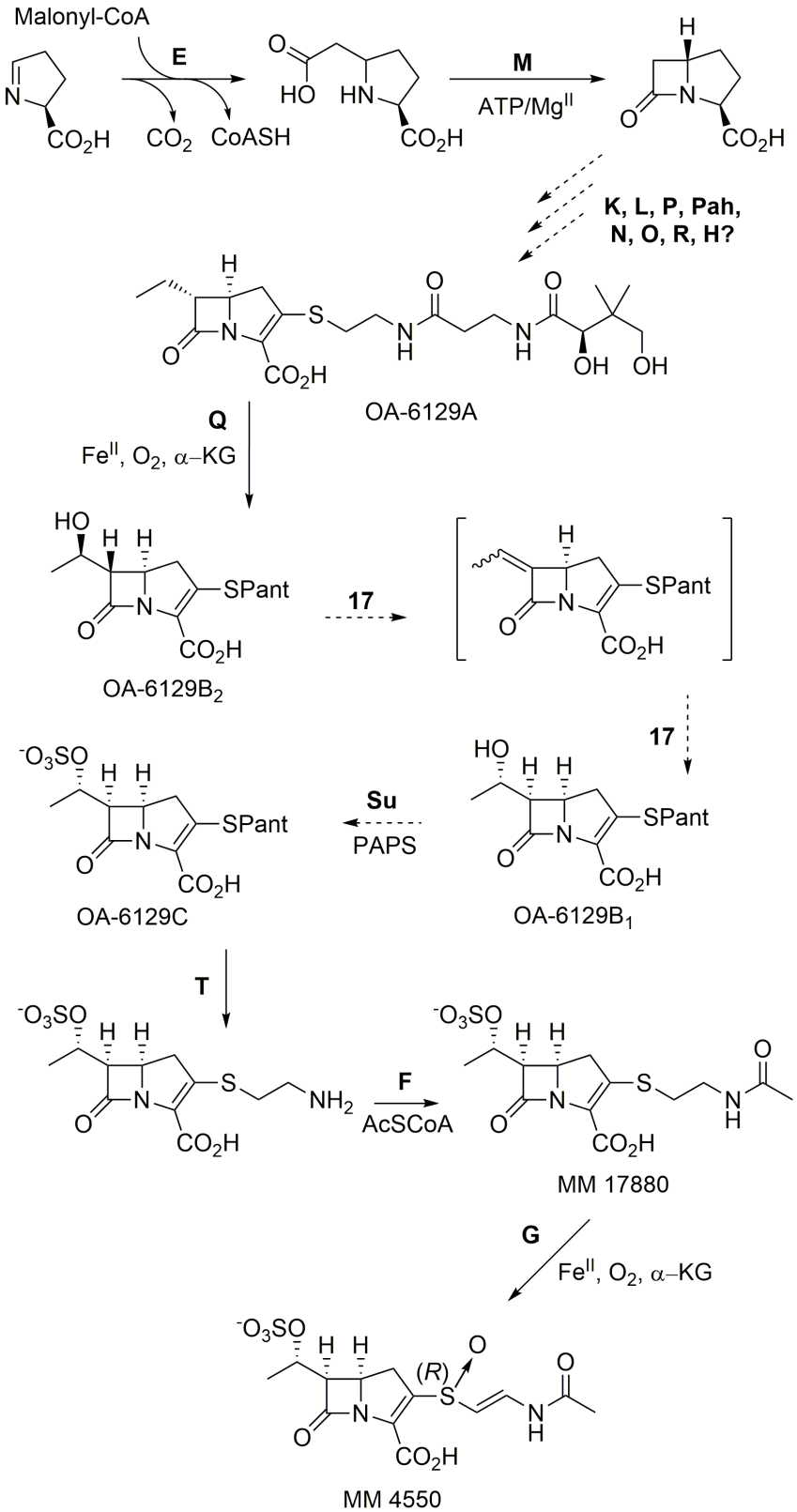

Scheme 2.2: Proposed biosynthetic pathway to MM 4550 in *S. argenteolus* ATCC 11009. Solid arrows indicate steps thought to correspond to those in thienamycin biosynthesis in *S. cattleya.* (Pant = pantetheine)

Based on previous reports and the results of our earlier experiments, we propose a biosynthetic pathway to MM 4550 shown in Scheme 2.2. Many of the early steps are almost certainly shared with thienamycin biosynthesis, but diverge to achieve stereochemical inversion of the C-6 and C-8 stereocenters and the addition of SO_3, likely through the action of Cmm17 and CmmSu. The OA-6129 group of carbapenems identified from mutagenesis studies in *S. fulvoviridis* includes the C-2 side chain prior to pantethiene cleavage by a ThnT orthologue[57]. These accumulated products, presumed intermediates, provide possible insight into the sequence of CmmQ hydroxylation, dehydration/rehydration of the C-6 sidechain and *O*-sulfonation. The OA-6129 carbapenems are shown as possible intermediates in Scheme 2.2. Additionally, the occurrence of the asparenomycin group of carbapenems in *Streptomyces* suggests the possibility of an ene-carbapenem intermediate during the proposed C-6 and C-8 epimerization[21]. The origin of the structural diversity of many isolated carbapenems across the entire family can in part be rationalized by this scheme.

It has been shown that the stereochemical relationship across C-5 and C-6 influences both antibacterial activity and stability toward β-lactamases where the presence of a sulfate in C-8 also appears to enhance stability toward β-lactamases[58]. Fully understanding the biosynthesis of MM 4550 in *S. argenteolus* will surely provide information for rational development of novel carbapenems in the future.

Conclusion

The isolation and characterization of the carbapenem MM 4550 from *S. argenteolus* ATCC 11009 coupled with the data resulting from DNA sequence and

individual gene disruptions provide insights into the biosynthesis of the structurally complex carbapenem antibiotics. The consistencies and inconsistencies apparent in comparisons with the thienamycin gene cluster point to specific gene products to account for the structural differences between thienamycin and MM 4550. The absence of genes homologous to *thnA-D* and *thnV* suggest that their corresponding proteins are not involved in the assembly of the carbapenem, but the additional genes *cmmSu*, *cmm17* and *cmmPah* may well be responsible for the differing stereochemical features of the C-6 side chain. The knowledge provided by the sequencing of multiple carbapenem-producing gene clusters can offer insights into their genetic diversity and how that diversity translates into antibiotic structural variation. Exploration of this diversity may provide cost-effective fermentation methods to produce antibiotics or semi-synthetic strategies for the synthesis of new antibiotics to combat the ever-developing resistance of bacterial pathogens.

Experimental

General methods:

Restriction enzymes, DNA modifying enzymes, and PCR reagents were obtained from New England Biolabs (Ipswich, MA). Plasmid kits were from Thermo Scientific (Waltham, MA). *E. coli* DH5α (Invitrogen) was usually used for DNA cloning and ThnK expression was done in *E. coli Rosetta 2*(DE3) (Novagen). Plasmid DNA was sequenced by the Synthesis and Sequencing Facility of the Johns Hopkins University. Solvents and reagents were purchased from Sigma Aldrich or Fisher Scientific in purity of ≥98%. Silica gel chromatography was performed using 60Å silica gel from Sorbtech. Thin layer

chromatography (TLC) was performed using 250 μm Analtech GHLF silica plates. A Bruker Avance (Billerica, MA) 300 or 400 MHz spectrometer was utilized for all ^{1}H and ^{13}C NMR spectra, which are reported in parts per million (δ) referenced against a TMS standard or residual solvent peak. The JHU Chemistry Department Mass Spectrometry Facility determined exact masses by fast atom bombardment (FAB) or electrospray ionization (ESI).

Cloning of *thnM/carA* homologous gene in *S. argenteolus*: Degenerate PCR primers *thnM*-DEG-5 and *thnM*-DEG-3 were designed using the CODEHOP program[30] (Figure 2.1). The PCR reaction was performed using a ‘‘touchdown’’ program, which consisted of (1) denaturation at 98 °C for 5 min, (2) 7 cycles of 40 s at 98 °C, 40 s at 63–56 °C (decreasing 1 °C every cycle) and 1 min at 72 °C, (3) 30 cycles of 40 s at 98 °C, 40 s at 56 °C and 1 min at 72 °C, and (4) 10min at 72 °C. The 300-bp PCR product was cloned into pBluescript SK(+) and the resulting recombinant was subjected to DNA sequence analysis.

Disruption of *S. argenteolus* genes by λ-RED-mediated PCR targeting mutagenesis: A λ RED mediated PCR mutagenesis system developed by Gust et al. was employed for the inactivation of genes in the targeted gene cluster in *S. argenteolus*[52]. The extended *FRT-oriT-aac(3)IV-FRT* cassette amplified by PCR was used to target each individual gene on cosmid 5D1 in *E. coli*. For the overlapped ORFs in the gene cluster, primers were designed from outside the overlapped regions but the translation remained in-frame. The PCR products were used to replace the corresponding genes in the cluster in *E. coli*

BW25113 (pIJ790) by homologous recombination. The mutated cosmid was introduced into *E. coli* ET12567 (pUZ8002) for conjugation into wild-type *S. argenteolus*[52]. Disruption mutants generated by double crossover events were confirmed by a Km^S/Am^R phenotype and eventually by Southern hybridization using the gene-specific and *oriT-aac(3)IV* probes.

Construction of *S. argenteolus* cmmI-22-23: *cmmI, cmm22*, and *cmm23* were cloned by PCR from cosmid 5D1 (see Supporting Information) and cloned into pBluescript SK(+) to give recombinants pBS/*cmmI*, pBS/*cmm22*, and pBS/*cmm23,* respectively. *cmmI* was excised from pBS/*cmmI* with *Nde*I-*Hind*III and inserted into pUWL201PW digested with the same enzymes to generate plasmid pUWL201/*cmmI*. *cmm23* was also inserted into pUWL201PW at *Nde*I-*Eco*RI sites to yield plasmid pUWL201/*cmm23*. pUWL201/*cmm23* was digested with *Kpn*I and blunt-ended with Klenow DNA polymerase followed by digestion with *Eco*RI. The blunt-*Eco*RI *ermE*p-cmm23* was cloned downstream of *cmmI* in pUWL201/*cmmI* at *Hind*III/Klenow-*Eco*RI sites to give recombinant pUWL201/*cmmI-cmm23*. *cmm22* was excised as a *Nde*I-*Hind*III fragment from pBS/*cmm22* and inserted into pET28(b) to yield plasmid pET28(b)/*cmm22*. The RBS-*cmm22* obtained by digesting pET28(b)/*cmm22* with *Xba*I-*Hind*III was inserted into pIJ4070 to give plasmid pIJ4070/*cmm22*. The *ermE*p*-RBS-*cmm22* was excised as a blunt-end fragment by digestion of pIJ4070/*cmm22* with *Eco*RI-*Pst*I and followed by treatment with Klenow DNA polymerase. The *ermE*p*-RBS-*cmm22* was inserted into the blunt-ended *Hind*III site in pMS82 to give plasmid pMS82/*cmm22*. Finally, the *ermE*p-cmmI-ermE*p-cmm23* was excised as a *Xho*I-*EcoR*I fragment and blunt-ended with Klenow DNA polymerase and inserted into pMS82/*cmm22* at the blunt-ended

*Eco*RI site to give the final integrative expression vector pMS82/*cmmI-22-23*.

S. argenteolus cmmI-22-23 was constructed by conjugating the wild-type *S. argenteolus* with *E. coli* ET12567 (pUZ8002, pMS82/*cmmI-22-23*).

Fermentation and detection of the wild-type, genetic-engineered and disruption mutants of *S. argenteolus*: The wild-type *S. argenteolus* and its derived strains were grown at 30 °C on S/P medium (1% glycerol, 1% yeast extract, 2% agar, pH 7.0) for solid cultivation, and on tomato paste-oatmeal agar for sporulation[59]. For liquid cultivation, mycelia or spores were inoculated in S/P liquid medium and grown for 72 h at 30 °C. Antibiotics were added in cultures if necessary at the following final concentrations: apramycin (50 μg/mL); nalidixic acid (20 μg/mL); hygromycin (50 μg/mL). For the general antibacterial activity test, 2.5 mL seed culture was transferred to 50 mL fermentation medium of either modified ISP4 medium ($ISP4^{+}$: ISP4 plus 6 mg/L $CoCl_2 \bullet 6H_2O$ and pH 7.7) or OMYM medium [22]. For isolation, purification, and characterization of intermediates or final products, the fermentation was carried out in a 1.3-L × 10 scale as follows: 100 mL S/P medium (containing antibiotics if necessary) was inoculated with 100 μL of spores at a concentration of ~10^{6-9}/mL and grown at 30 °C for 48-56 h and 10 mL of seed culture was transferred into 1.3 L modified ISP4 medium ($ISP4^{++}$: ISP4 plus 6 mg/L $CoCl_2 \bullet 6H_2O$ and 1 mg/L methylcobalamin, pH 7.7). The fermentation was carried out at 30 °C for 52-56 h with 250 rmp rotation.

A 2-mL sample was taken every 24 h from each culture, and supernatant (250 μL) was added to a micro-cylinder on top of nutrient agar seeded with β-lactam supersensitive *E. coli* ESS[60]. The carbapenem MM 4550 and its bioactive intermediates

could be visualized as inhibition zones after incubating at 37 °C for 15 h. The production of carbapenems was also detected with induction of β-lactamases in *Bacillus licheniformis* ATCC 14580 in a colorimetric assay with nitrocefin[52].

Isolation and identification of MM 4550 in *S. argenteolus*: Isolation and purification steps were performed at 4 °C, with the exception of preparatory HPLC, which was performed at room temperature. K_2HPO_4 buffer (20 mM, pH = 7.0) containing ethylenediamenetetraacetate (EDTA, 0.5 mM) was used to make all aqueous solutions in order to maintain the pH and provide a neutral environment to avoid degradation of carbapenem products.

To extract antibiotics from media, the filtrate from of fermentation broth (13 L) was first washed with dichloromethane (600 mL). The resultant washed medium was then extracted with Aliquat 336 (5%, 300 mL) in dichloromethane. The medium was tested for bioactivity by *E. coli* ESS bioassay before and after extraction, which confirmed efficient extraction. The organic phase was then back-extracted with aqueous potassium iodide (KI, 4 × 25 mL), each of 1%, 3%, 5% and 10%. The 3% and 5% KI fractions contained the greatest quantity of antibiotic as shown by bioassay on *E. coli* ESS, and were collected and lyophilized.

The crude powder was dissolved in phosphate buffer and loaded onto a column of anion-exchange resin (Dowex 1 x 2, 200 x 20 mm, 100 mesh). The antibiotic was eluted with NaCl (1 M) and the bioactive fractions were lyophilized and dissolved in a minimum amount of phosphate buffer for purification by reverse-phase HPLC.

HPLC was carried out using an Agilent 1100 series G1311A pump with an Agilent model 7725i injector fitted with a 1-mL injection loop. The chromatogram was monitored by an Agilent 1100 series G1315B DAD detector at 210, 240, 270, 300, and 330 nm wavelengths.

HPLC conditions: Phenomonex Prodigy C18 (2) 250 x 10.00 mm 5 µ micron semi-preparatory column, 2 mL/min; buffer A = 20 mM K_2HPO_4, 0.5 mM EDTA, pH = 7.4 with HCl, buffer B = acetonitrile. Method 1, t = 0 min 1.5% B, t = 15 min 1.5% B, t = 30 min 30% B, t = 35 min 30% B, t = 40 min 1.5% B, t = 55 min 1.5% B.

For the hydroxamate assay, a stock solution (100 µL) of hydroxylamine hydrochloride (50 mM) in phosphate buffer (pH 7.4) was added to the crude antibiotic-containing solution (900 µL), and was incubated for 1 h at room temperature before it was injected for HPLC analysis using the method described above. The fractions containing a peak in the control that was absent when treated with hydroxylamine were collected and employed for bioassay on *E. coli* ESS.

To prepare samples for NMR analysis, the crude antibiotic-containing solution (50 mL) was HPLC purified using method described above and the peak that reacted with hydroxylamine was collected for all runs. The biologically active peak was collected and lyophilized. In order to remove excess salts from the resulting powder for NMR experimentation, the entire mixture was purified by one run of HPLC. The peak was collected in 1 mL fractions and lyophilized. Samples taken for NMR were dissolved in D_2O (333 µL, 100%) and placed in a 5 mm D_2O Shigemi tube.

^1H NMR (600 MHz, D_2O using Shigemi advanced NMR microtube, Bruker

Avance II 600 spectrometer at 298 K, processed using the ACD labs software from Advanced Chemistry Development, Inc.): 7.60 (d, *J* = 13.7 Hz, 1H), 6.41 (d, *J* = 14.7 Hz, 1H), 4.94 (qd, *J* = 5.9, 14.7 Hz, 1H), 4.49 (dt, *J* = 3.9, 5.9 Hz, 1H), 3.98 (dd, *J* = 5.9, 8.8 Hz, 1H), 3.52 (dd, *J* = 8.8, 17.6 Hz, 1H), 3.12 (dd, *J* = 10.8, 17.6 Hz, 1H), 2.14 (s, 3H), 1.54 (d, *J* = 6.8 Hz, 3H). ^{1}H NMR and UV-Vis spectrum matched the data reported in the literature for MM 4550[29,30].

ESI Mass spec of MM 4550: $C_{13}H_{15}N_2O_9S_2^-$ calc: 407.0224 found: 407.0226 . The analysis was run on a PerkinElmer AxIon TOF in the negative mode.

For mass-spectroscopic analysis of carbapenem intermediates in mutants, cultures grown in ISP4^{++} were directly injected onto the UPLC-MS. UPLC-MS was carried out using a Waters Acquity H-Class UPLC system with a multi-wavelength UV-Vis diode array detector in tandem with high-resolution MS analysis by a Waters Xevo-G2 Q-ToF ESI mass spectrometer.

UPLC conditions: Waters Acquity BEH UPLC column packed with ethylene bridged hybrid C-18 2.1 mm X 50 mm, 1.7 micron, 0.3 mL/min; solvent A = H_2O, solvent B = acetonitrile. Method: t=0 min 0% B, t= 1 min 0% B. t = 7.5 min 80% B, t = 8.4 min 80% B, t = 10 min 0% B. Samples were run in the negative mode with a 1 min solvent purge after injection.

Synthesis of carbapenems:

(3*SR*,4*RS*)-4-allyl-1-*tert*-butyldimethylsilyl-3-(1,2-dihydroxy-2-propyl)-2-azetidinone (3a and 3b). The title compound was prepared as by Ona[23]. A solution of 2 M LDA

(12.4 mL, 24.8 mmol, 1.4 eq) in THF (60 mL) at -78 ºC was added a solution of 4-allyl-1-*tert*-butyldimethylslyl-azetidinone **2** (4.0 g, 17.7 mmol, 1.0 eq) in THF (10 mL). This solution was stirred at -78 ºC for 40 min. Then a solution of trimethylsilyloxyacetone (5.3 mL, 40.71 mmol, 2.3 eq) in THF (6 mL) was added and stirred at -78 ºC for 30 min. The reaction mixture was then diluted with brine and extracted with ethyl acetate (2 × 130 mL). The organic layer was dried with anhydrous sodium sulfate, filtered and concentrated *in vacuo*. The oily residue was dissolved in methanol containing 1% acetic acid and stirred overnight at room temperature then concentrated. The residue was purified by silica gel chromatography using (1:1) benzene:ethyl acetate to give **3a** (1.84 g, 35%) and **3b** (1.0 g, 18.9%). ^{1}H-NMR (400 MHz,$CDCl_3$): **3a** δ 5.0-6.2 (m, 3H), 3.0-4.7 (m, 5H), 2.85 (d, J = 2 Hz, 1H), 2.0-2.8 (m, 2H), 1.08 (s, 3H), 1.00 (s, 9H), 0.30 (s, 3H), 0.23 (s, 3H) **3b:** δ 4.9-6.2 (m, 3H), 1.9-4.0 (m, 8H), 1.30 (s, 3H), 1.00 (s, 9H), 0.27 (s, 3H), 0.23 (s, 3H) ppm. ^{1}H-NMR confirmed the spectrum reported for this compound in the literature[23].

(3*SR*,4*RS*)-4-Allyl-3-(4-methyl-2-oxo-1,3-dioxolan-4-yl)-2-azetidinone. (4a, b). The title compound was prepared as by Ona[23]. Triphosgene (286.9 mg, 0.96 mmol, 0.4 eq) was added to the diol **3b** (0.72 g, 2.4 mmol, 1.0 eq) in dichloromethane containing pyridine (424.8 uL, 417.2 mg, 5.3 mmol, 2.2 eq) at 0 ºC, and the mixture was stirred for 30 min, then diluted with ethyl acetate (53 mL) and washed successively with water (21.6 mL) and brine (20 mL). The organic layer was dried with anhydrous sodium sulfate, filtered and concentrated to give crude carbonate **4b** (727.7 mg, 93%). A solution of crude carbonate **4b** (2.28 g, 7.0 mmol, 1.0 eq) in THF (37.4 mL) and acetic acid (873.4 uL, 2.0 eq) was treated with (n-Bu)$_4$NF (TBAF) (2.98 g, 9.4 mmol, 1.4 eq), and the

mixture was stirred at room temperature for 1 h, then diluted with ethyl acetate (230 mL) washed with brine (100 mL). The organic layer was dried with anhydrous sodium sulfate, filtered, and concentrated. The residue was purified by silica gel chromatography using (1:1) benzene:ethyl acetate to give **4b** (1.09 g, 82%) %) ^{1}H NMR (400 MHz, $CDCl_3$): δ 6.25 (bs, 1H), 5.0-5.3 and 5.5-6.1 (m, 3H), 4.18 and 4.39 (ABq, J = 9 Hz, 2H), 3.69 (ddd, J = 3, J = 6, J = 6 Hz, 1H), 3.14 (d, J = 3 Hz, 1H), 2.48 (bd, J = 6 Hz, 1H), 2.41 (bd, J = 6 Hz, 1H), 1.64 (s, 3H) ppm.

Under the same conditions **3a** was reacted to form **4a** (1.02 g, 63%). ^{1}H NMR (400 MHz, $CDCl_3$): δ 6.6 (br. s, 1H), 4.9-6.1 (m, 3H), 4.14 and 4.68 (ABq, J_{AB} = 8 Hz, 2H), 3.6-3.8 (m, 1H), 3.07 (d, J = 2 Hz, 1H), 2.3-2.6 (m, 2H), 1.53 (s, 3H) ppm. ^{1}H-NMR confirmed the spectrum reported for this compound in the literature[23].

(3*S*, 4*R*)-3-(4-Methyl-2-oxo-1,3-dioxolan-4-yl)-4-carboxymethyl-2-azetidinone (5a). The title compound was prepared from a modified procedure as by Ona[23]. Ozone was bubbled through a solution of **4a** (6.02 g, 28.5 mmol) in a mixture of CH_2Cl_2 (200 mL) and methanol (135 mL) at -78 °C until a blue color persisted. Excess ozone was removed by bubbling with nitrogen. Dimethyl sulfide (28 mL) was added, and the reaction mixture was stirred for 1 h, then washed with water, dried with Na_2SO_4, and concentrated *in vacuo*. The residue was dissolved in *tert*-butyl alcohol (150 mL) and treated with 2-methyl-2-butene (66 mL, 0.62 mol) followed by a solution of NaH_2PO_4 (11.8 g, 85.5 mmol) and $NaClO_2$ (7.73 g, 85.5 mmol) in water (150 mL). The resulting mixture was stirred at RT for 16 h, concentrated in vacuo to 200 mL, diluted with water (400 mL) and at 0 °C, acidified to pH = 2 with HCl (aq 1 M), saturated with NaCl, and extracted with methyl ethyl ketone (5 x 100 mL). The combined organic phases were dried over

anhydrous Na_2SO_4 and concentrated *in vacuo* to give a white solid, which was recrystallized from ethyl acetate / ether to give 3.08 g pure **5a** (47% yield). ^{1}H-NMR (400 MHz, CD_3CN + DMSO-d_6) δ: 1.51 (s, 3H), 2.6-2.7 (m, 2H), 3.24 (d, J = 2.5 Hz, 1H), 3.87 (m, 2H), 4.21 and 4.56 (ABq, J_{AB} = 8 Hz, 2H), 7.4 (br, s, 2H). ^{1}H-NMR confirmed the spectrum reported for this compound in the literature[23].

(3*S*, 4*R*)-3-(4-Methyl-2-oxo-1,3-dioxolan-4-yl)-4-(3-*p*-methoxybenzyloxycarbonyl-2-oxopropyl)-2-azetidinone (6a). The title compound was prepared as by Ona[23]. *N*,*N'*-Carbonyldiimidazole (0.83 g, 1.2 eq) was added to a solution of **5a** (0.98 g, 4.28 mmol) in acetonitrile (25 mL), and the mixture was stirred at room temperature for 2 h. Then a solution of malonic acid mono-*p*-methoxybenzyl ester monomagnesium salt (2.42 g, 1.2 eq) in acetonitrile (30 mL) [prepared from the malonic acid mono-PMB ester and $MgCl_2$] was added. The reaction mixture was stirred for 16 h at 45 °C, diluted with EtOAc, washed with 1 N HCl (3 x 25 mL) and brine (50 mL), dried with Na_2SO_4 and concentrated *in vacuo*. The residue was chromatographed on a SiO_2 column (EtOAc:hexanes gradient 30:70 → 70:30) to yield **6a** (0.96 g, 57%) as a yellow foam. ^{1}H-NMR (400 MHz, $CDCl_3$) δ: 1.48 (s, 3H), 2.7-3.2 (m, 2H), 3.02 (d, J = 2.5 Hz, 1H), 3.49 (s, 2H), 3.77 (s, 3H), 3.7-4.2 (m, 1H), 4.09 and 4.60 (ABq, J_{AB} = 9 Hz, 2H), 5.06 (s, 2H), 6.8 (br. s, 1H), 6.88 and 7.28 (ABq, J = 9 Hz, 4H). ^{1}H-NMR confirmed the spectrum reported for this compound in the literature[23].

(3*S*, 4*R*)-3-(4-Methyl-2-oxo-1,3-dioxolan-4-yl)-4-(3-*p*-methoxybenzyloxycarbonyl-2-oxopropyl)-2-azetidinone (7a). The title compound was prepared as by Ona[23]. A solution of **6a** (0.91 g, 2.32 mmol) in acetonitrile (25 mL) containing triethylamine (422 μL, 1.3 eq) was treated with methanesulfonyl azide (255 mg, 1.3 eq) at 0 °C for 30

minutes. The mixture was diluted with EtOAc, washed with water, dried with Na_2SO_4 and concentrated *in vacuo*. The residue was chromatographed on a SiO_2 column (EtOAc/hexane 60:40) to give **7a** (540 mg, 56%)**.** ^{1}H-NMR (400 MHz, $CDCl_3$) δ: 1.24 (s, 3H), 2.81 (dd, J = 17.0 Hz, J = 8.0 Hz, 1H), 2.94 (d, J = 2.0 Hz, 1H), 3.05 (dd, J = 17.0, 5.0 Hz, 1H), 3.51 (s, 3H), 3.67 (dt, J = 8.0, 2.0 Hz, 1H), 3.91 and 4.32 (ABq, J_{AB} = 9.0 Hz, 2H), 4.91 (s, 2H), 6.36 (br. s, 1H), 6.64 and 7.06 (ABq, J_{AB} = 9.0 Hz, 4H). ^{1}H-NMR confirmed the spectrum reported for this compound in the literature[23].

***p*-Methoxybenzyl (5*R*,6*S*)-2-(*E*)-(2-Acetamidoethenyl)thio-6-(4-methyl-2-oxo-1,3-dioxolan-4-yl)carbapen-2-em-3-carboxylate (9a).** The title compound was prepared as by Ona[23]. **7a** was dissolved in benzene (113 mL) and heated to reflux before a small scoop of Rh_2OAc_4 (5 % w/w, 24 mg) was added in one portion. After 15 min, the reaction mixture was cooled, filtered through Celite and concentrated *in vacuo* to provide **8a** as a foam (360 mg, 82%), which was used without further purification. A mixture of **8a** (360 mg, 0.937 mmol), diphenylchlorophosphate (214 µL, 1.03 mmol), and diisopropylethylamine (179 µL, 1.03 mmol) in acetonitrile (25 mL) was stirred for 10 minutes at 0 ºC, and then silver (*E*)-2-acetamido-1-ethenethiolate (524 mg, 2.34 mmol) and sodium iodide (351 mg, 2.34 mmol) were added. The mixture was allowed to warm to room temperature and was stirred for 50 min. The mixture was diluted with ethyl acetate, washed with water, dried with sodium sulfate and concentrated *in vacuo*. The residue was chromatographed on silica gel (hexane-dichloromethane-ethyl acetate-acetonitrile 1:1:1:1) to give **9a** (257 mg, 56%). ^{1}H-NMR (400 MHz, DMSO): **9a** δ 1.48 (s, 3H), 1.93 (s, 3H), 3.17 (ABq, J_{AB} = 4.6, 8.8 Hz, 2H), 3.74 (s, 3H), 3.97 (d, J = 2.8 Hz, 1H), 4.18 (dt, J = 9.2, 3.2 Hz, 1H), 4.40 (ABq, J_{AB} = 4.4, 8.4 Hz, 2H), 5.14 (q, J = 12.4

Hz, 2H), 5.85 (d, J = 14 Hz, 1H), 6.91 (d, J = 8.4 Hz, 2H), 7.08 (ABq, J_1 = 14 Hz, J_2 = 10.4 Hz, 1H), 7.34 (d, J = 8.4 Hz, 2H), 10.38 (d, J = 10 Hz, 1H). ^{1}H-NMR confirmed the spectrum reported for this compound in the literature[23].

***p*-Methoxybenzyl 2-(*E*)-(2-Acetamidoethenyl)thio-6-[(*E*)-1-(hydroxymethyl)ethylidene] carbapen-2-em-3-carboxylate (10).** The title compound was prepared as by Ona[23]. DBU (78.6 µL, 0.526 mmol) was added to a solution of **9a** in benzene (4.38 mL) and dichloromethane (21.9 mL). The mixture was stirred at room temperature for 30 min. Upon completion of the reaction the mixture was diluted with ethyl acetate and was washed with water, dried with sodium sulfite and concentrated *in vacuo*. The crude oil was purified by silica gel chromatography (hexane-dichloromethane-ethyl acetate-acetonitrile 1:1:1:1) to give **10**. The semi-crude oil contaminated with the 1-em isomer was used for the next reaction without further purification.

Sodium 2-(*E*)-(2-Acetamidoetheynyl)thio-6-[(*E*)-1-(hydroxymethyl)ethylidene] carbapen-2-em-3-carboxylate ((±)-asparenomycin C) (11). The title compound was prepared as by Ona[23]. A crude solution of **10** (obtained from **9a** without purification) in acetonitrile was added to a solution of aluminum(III) trichloride (175 mg, 1.315 mmol) in anisole (2.5 mL) and dichloromethane (2.5 mL) at -60 ºC and was stirred for 10 min. After the reaction is complete, a solution of sodium bicarbonate in water was added, and the reaction mixture was allowed to warm to room temperature. After stirring vigorously for 30 min, the mixture was filtered through a 0.2 µm membrane filter and washed with dichloromethane. The crude mixture was immediately subject to preparative HPLC (Phenomonex Luna C18, 20 x 250 mm, 9:1 0.01 M pH 7 ammonium bicarbonate buffer /

acetonitrile). The product was collected and lyophilized to yield (±)-asparenomycin C **11** (30 mg, 15% from **9a**) as a white powder. ^{1}H-NMR (400 MHz, H_2O): **11** δ 1.96 (s, 3H), 2.05 (s, 3H), 3.09 (ABq, J_{AB} = 8 Hz, 2H), 4.2 (s, 2H), 4.83 (t, J = 8 Hz, 1H), 6.01 (d, J = 14 Hz, 1H), 7.12 (d, J = 14 Hz, 1H). HRMS (ESI, H_2O) *m/z*: (MH+) calc: 325.0853 found: 325.0855. ^{1}H-NMR confirmed the spectrum reported for this compound in the literature[23].

Synthesis of Sodium 2-(*E*)-(2-Acetamidoetheynyl)sulfinyl-6-[(*E*)-1-(hydroxymethyl)ethylidene] carbapen-2-em-3-carboxylate [(±)-asparenomycin A]. The title compound was prepared as by Ona[23]. The crude powder was purified by preparative HPLC (Phenomonex Luna C18, 20 x 250 mm, 9:1 0.01 M pH 7 ammonium bicarbonate buffer / acetonitrile). The sulfoxide (*S*)-diastereomer (t_R^2 = 9 min), which eluted first, was cleanly separated from the desired (*R*)-diastereomer (t_R^2 = 12 min). The peaks were separately collected and lyophilized to yield (±)-asparenomycin A (2 mg) as a white powder. ^{1}H-NMR (400 MHz, H_2O): δ 1.98 (s, 3H), 2.11 (s, 3H), 2.82 (d, J = 14.8 Hz, 1H), 3.17 (d, J = 10.8 Hz, 1H), 3.50 (t, J = 6.4 Hz, 1H), 4.26 (d, J = 3.6 Hz, 2H), 6.34 (d, J = 14 Hz, 1H), 7.55 (d, J = 14 Hz, 1H). HRMS (ESI, H_2O) *m/z*: (MH+) calc: 341.0849 found: 341.0778. ^{1}H NMR matched the data reported in the literature[20,23,26].

NMR Spectral Data for MM4550:

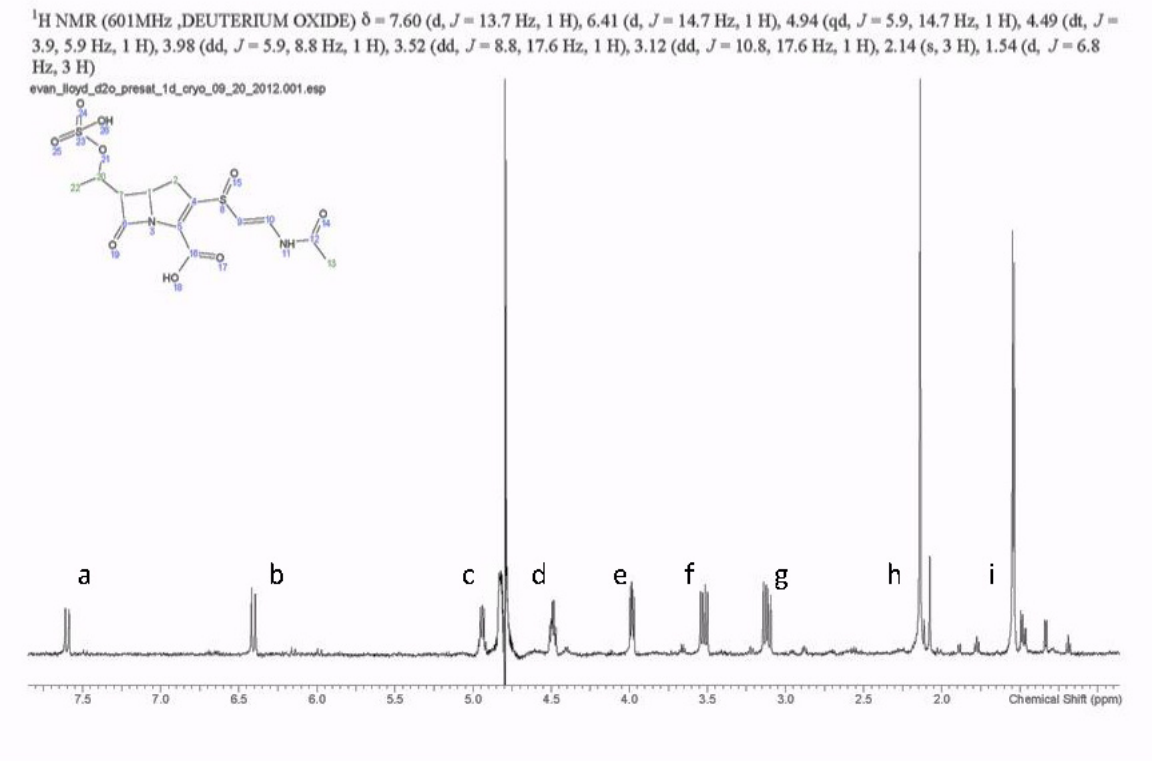

^{1}H NMR of MM4550

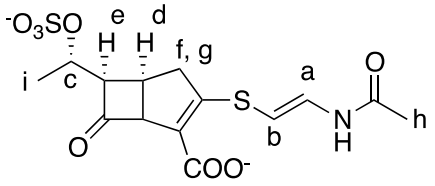

MM4550

^{1}H NMR (600 MHz, D_2O using Shigemi advanced NMR microtube, Bruker Avance II 600 spectrometer at 298 K, processed using the ACD labs software from Advanced Chemistry Development, Inc.): 7.60 (d, J = 13.7 Hz, H_a), 6.41 (d, J = 14.7 Hz, H_b), 4.94 (qd, J = 5.9, 14.7 Hz, H_c), 4.49 (dt, J = 3.9, 5.9 Hz, H_d), 3.98 (dd, J = 5.9, 8.8 Hz, H_e), 3.52 (dd, J = 8.8, 17.6 Hz, H_f), 3.12 (dd, J = 10.8, 17.6 Hz, H_g), 2.14 (s, 3H_h), 1.54 (d, J = 6.8 Hz, 3H_i). ^{1}H NMR matched the data reported in the literature[29,30].

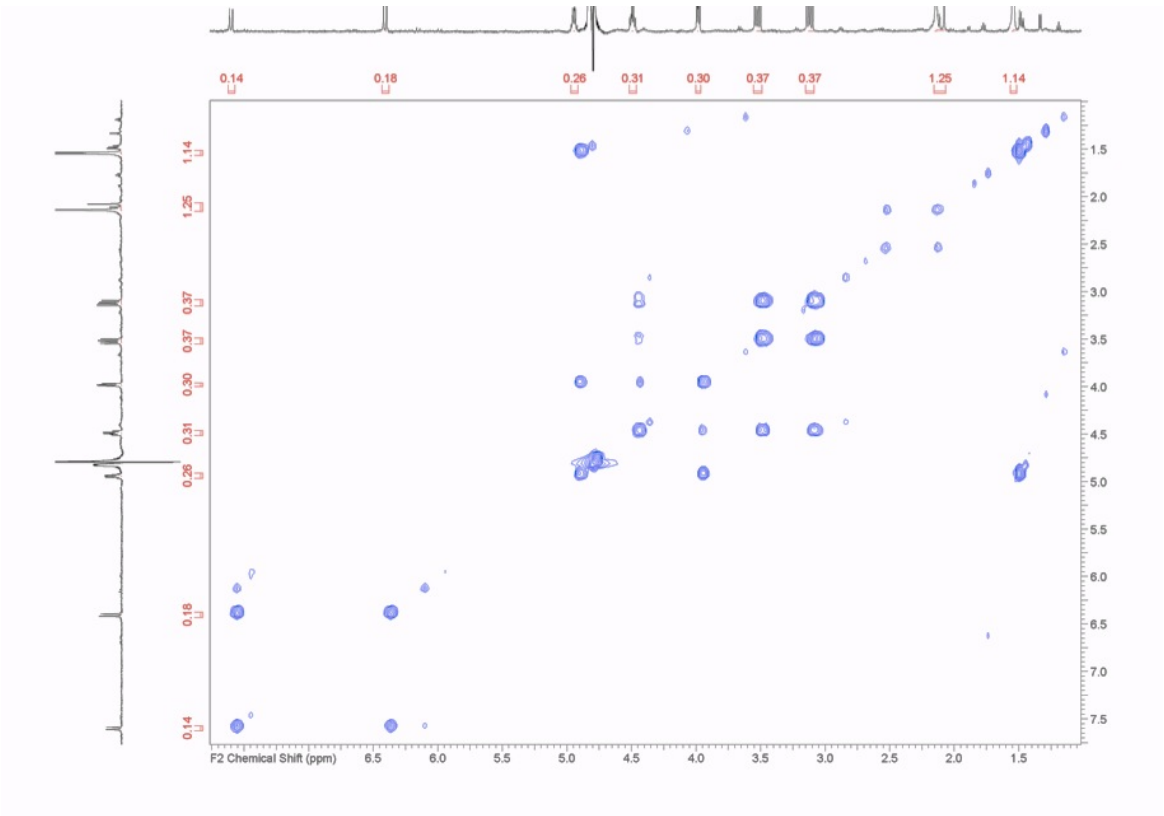

^{1}H-^{1}H COSY of MM4550

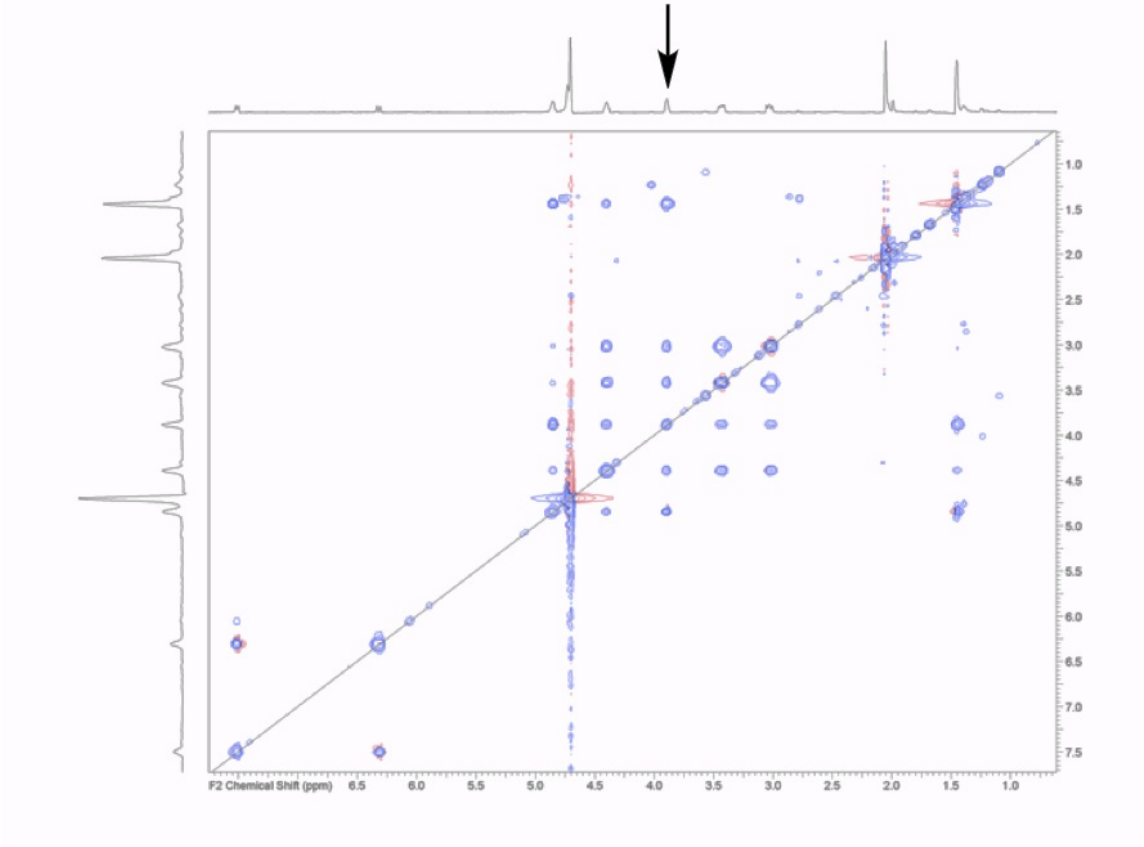

^{1}H-^{1}H TOCSY of MM4550

Full spin system observed for protons $H_{c\text{-}g}$, H_i (arrow)

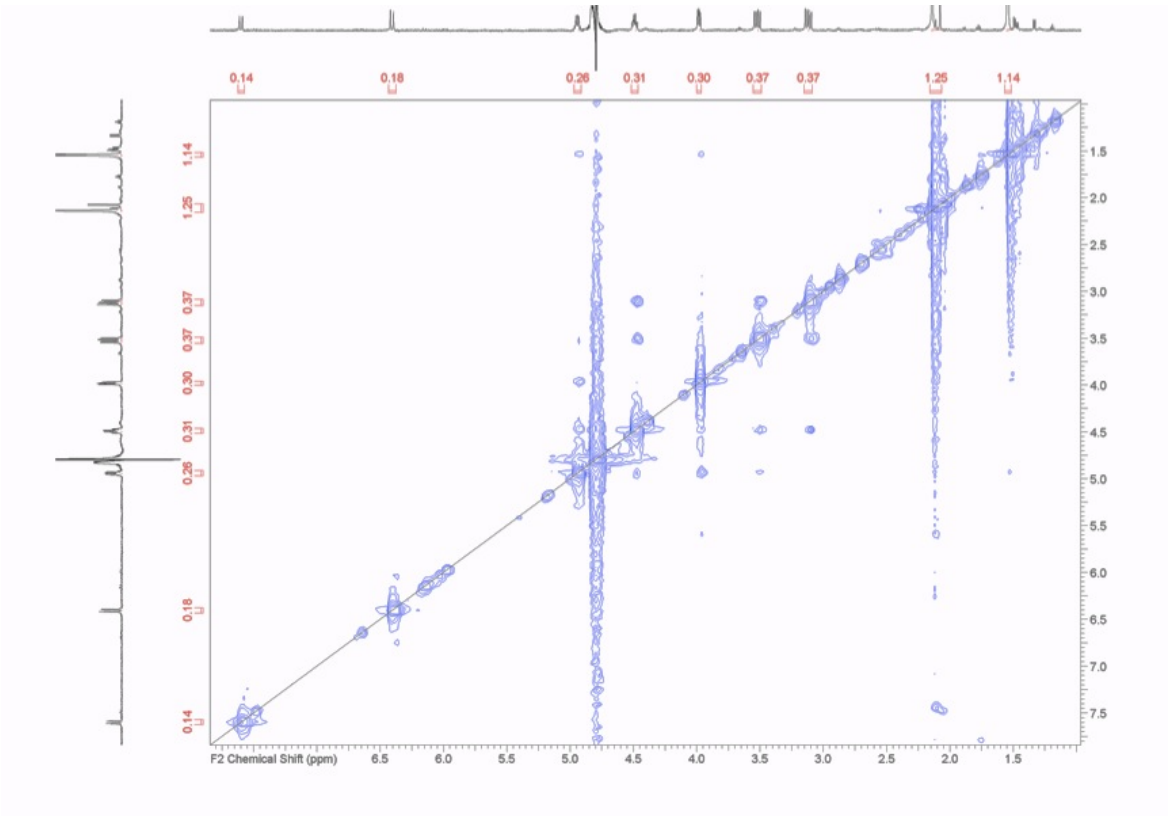

^{1}H-^{1}H ROESY of MM4550

References

1. Suárez, C., Lolans, K., Villegas, M. & Quinn, J. Mechanisms of resistance to β-lactams in some common Gram-negative bacteria causing nosocomial infections. *Expert Rev. Anti. Infect. Ther.* **3,** 915–922 (2005).

2. Sleeman, M. & Schofield, C. Carboxymethylproline synthase (CarB), an unusual carbon-carbon bond-forming enzyme of the crotonase superfamily involved in carbapenem biosynthesis. *J. Biol. Chem.* **279,** 6730–6736 (2004).

3. Miller, M., Gerratana, B., Stapon, A., Townsend, C. & Rosenzweig, A. Crystal structure of carbapenam synthetase (CarA). *J. Biol. Chem.* **278,** 40996–41002 (2003).

4. Li, R., Stapon, A., Blanchfield, J. T. & Townsend, C. A. Three Unusual Reactions Mediate Carbapenem and Carbapenam Biosynthesis. *J. Am. Chem. Soc.* **122,** 9296–9297 (2000).

5. Stapon, A. *et al.* Carbapenem Biosynthesis: Confirmation of Stereochemical Assignments and the Role of CarC in the Ring Stereoinversion Process from l-Proline. *J. Am. Chem. Soc.* **125,** 8486–8493 (2003).

6. Clifton, I. *et al.* Crystal structure of carbapenem synthase (CarC). *J. Biol. Chem.* **278,** 20843–20850 (2003).

7. Núñez, L. E., Méndez, C., Braña, A. F., Blanco, G. & Salas, J. A. The Biosynthetic Gene Cluster for the β-Lactam Carbapenem Thienamycin in Streptomyces cattleya. *Chem. Biol.* **10,** 301–311 (2003).

8. Bodner, M. J. *et al.* Definition of the Common and Divergent Steps in Carbapenem β-Lactam Antibiotic Biosynthesis. *ChemBioChem* **12,** 2159–2165 (2011).

9. Bodner, M. J., Phelan, R. M., Freeman, M. F., Li, R. & Townsend, C. A. Non-Heme Iron Oxygenases Generate Natural Structural Diversity in Carbapenem Antibiotics. *J. Am. Chem. Soc.* **132,** 12–13 (2010).

10. Hamed, R. B. *et al.* The enzymes of β-lactam biosynthesis. *Nat. Prod. Rep.* **30,** 21 (2012).

11. Freeman, M. F., Moshos, K. A., Bodner, M. J., Li, R. & Townsend, C. A. Four enzymes define the incorporation of coenzyme A in thienamycin biosynthesis. *Proc. Natl. Acad. Sci. U. S. A.* **105,** 11128–11133 (2008).

12. Rodriguez, M. *et al.* Mutational Analysis of the Thienamycin Biosynthetic Gene Cluster from Streptomyces cattleya. *Antimicrob. Agents Chemother.* **55,** 1638–1649 (2011).

13. Rodriguez, M. *et al.* Identification of transcriptional activators for thienamycin and cephamycin C biosynthetic genes within the thienamycin gene cluster from Streptomyces cattleya. *Mol. Microbiol.* **69,** 633–645 (2008).

14. Okamura, K. *et al.* PS-5, a new beta-lactam antibiotic from Streptomyces. *J. Antibiot. (Tokyo).* **31,** 480–482 (1978).

15. Tsuji, N. *et al.* Asparenomycins A, B and C, new carbapenem antibiotics. III. Structures. *J. Antibiot. (Tokyo).* **35,** 24–31 (1982).

16. Butterworth, D., Cole, M., Hanscomb, G. & Rolinson, G. Olivanic acids, a family of beta-lactam antibiotics with beta-lactamase inhibitory properties produced by Streptomyces species, I. Detection, properties and fermentation studies . *J. Antibiot.* **32,** 287–294 (1979).

17. Stapley, E. *et al.* Epithienamycins-novel beta-lactams related to thienamycin. I. productin and antibacterial activity. *J. Antibiot.* **34,** 628–636 (1981).

18. Tsuji, N. *et al.* Pluracidomycin-a2, a new carbapenem bearing a sulfinic acid, and other minor pluracidomycins. *J. Antibiot.* **38,** 270–274 (1985).

19. Nakayama, M. *et al.* Structures and absolute configurations of carpetimycins A and B. *J. Antibiot. (Tokyo).* **34,** 818–823 (1981).

20. Tanaka, K. *et al.* Asparenomycin A, a new carbapenem antibiotic. *J. Antibiot. (Tokyo).* **34,** 909–911 (1981).

21. Kawamura, Y., Yasuda, Y., Mayama, M. & Tanaka, K. Asparenomycins A, B and

C, new carbapenem antibiotics. I. Taxonomic studies on the producing microorganisms. *J. Antibiot. (Tokyo).* **35,** 10–14 (1982).

22. Haneishi, T. *et al.* A new carbapenam No. 17927 D substance. *J. Antibiot.* **36,** 1581–1584 (1983).

23. Ona, H., Uyeo, S., Motokawa, K. & Yoshida, T. Carbapenem and penem antibiotics. I. Total synthesis and antibacterial activity of dl-asparenomycins A, B and C and related carbapenem antibiotics. *Chem. Pharm. Bull.* **33,** 4346–4360 (1985).

24. Bal, B. S., Childers, W. E. & Pinnick, H. W. Oxidation of α,β-un saturated aldehydes. *Tetrahedron* **37,** 2091–2096 (1981).

25. Imuta, M. Carbapenem and Penem Antibiotics. V. Synthesis and Antibacterial Activity of 2-Functionalized-methyl-1-Methylcarbapenems Related to Asparenomycins. *Chem. Pharm. Bull.* **39,** 658–662 (1991).

26. Ona, H. & Uyeo, S. Total synthesis of dl-asparenomycins A, B and C, novel carbapenem antibiotics. *Tetrahedron Lett.* **25,** 2237–2240 (1984).

27. Ohtani, M., Watanabe, F. & Narisada, M. Mild deprotection of carbapenem esters with aluminum trichloride. *J. Org. Chem.* **49,** 5271–5272 (1984).

28. Tsuji, T. *et al.* Synthetic studies on β-lactam antibiotics. VII. Mild removal of the benzyl ester protecting group with aluminum trichloride. *Tetrahedron Lett.* **20,** 2793–2796 (1979).

29. Brown, A. G., Corbett, D. F., Eglington, A. J. & Howarth, T. T. Structures of olivanic acid derivatives MM 4550 and MM 13902; two new, fused ?-lactams isolated from Streptomyces olivaceus. *J. Chem. Soc. Chem. Commun.* 523 (1977).

30. Hood, J. D., Box, S. J. & Verrall, M. S. Olivanic acids, a family of beta-lactam antibiotics with beta-lactamase inhibitory properties produced by Streptomyces species. II. Isolation and characterisation of the olivanic acids MM 4550, MM 13902 and MM 17880 from Streptomyces olivaceus. *J. Antibiot. (Tokyo).* **32,** 295–304 (1979).

31. Nakamura Ono, E., Kohda, T., Shibai, H., Y. Highly targeted screening system for carbapenem antibiotics. *J. Antibiot.* **42,** 73–83 (1989).

32. Rose Schultz, E. R., Henikoff, J. G., Pietrokovski, S., McCallum, C. M., Henikoff, S., T. M. Consensus-degenerated hybrid oligonucleotide primers for amplification of distantly related sequences. *Nucleic Acid Res.* **26,** 1628–1635 (1998).

33. Blanco, G. Comparative analysis of a cryptic thienamycin-like gene cluster identified in Streptomyces flavogriseus by genome mining. *Arch. Microbiol.* **194,** 549–555 (2011).

34. Hamed, R., Batchelar, E., Clifton, I. & Schofield, C. Mechanisms and structures of crotonase superfamily enzymes - How nature controls enolate and oxyanion reactivity. *Cell. Mol. Life Sci.* **65,** 2507–2527 (2008).

35. Yan, Y. *et al.* Biosynthetic Pathway for High Structural Diversity of a Common Dilactone Core in Antimycin Production. *Org. Lett.* **14,** 4142–4145 (2012).

36. Negishi, M. *et al.* Structure and Function of Sulfotransferases. *Arch. Biochem. Biophys.* **390,** 149–157 (2001).

37. Shi, R. *et al.* Crystal structure of StaL, a glycopeptide antibiotic sulfotransferase from Streptomyces toyocaensis. *J. Biol. Chem.* **282,** 13073–13086 (2007).

38. Hamed, R. B., Batchelar, E. T., Mecinović, J., Claridge, T. D. W. & Schofield, C. J. Evidence that Thienamycin Biosynthesis Proceeds via C-5 Epimerization: ThnE Catalyzes the Formation of (2 S,5 S)- trans-Carboxymethylproline. *ChemBioChem* **10,** 246–250 (2009).

39. Kakuta, Y., Pedersen, L. C. L. G. C. G., Pedersen, L. C. L. G. C. G. & Negishi, M. Conserved structural motifs in the sulfotransferase family. *Trends Biochem. Sci.* **23,** 129–130 (1998).

40. Paradkar, A., Aidoo, K. & Jensen, S. A pathway-specific transcriptional activator regulates late steps of clavulanic acid biosynthesis in Streptomyces clavuligerus. *Mol Microbiol* **27,** 831–843 (1998).

41. Perez-Redondo, R., Rodriguez-Garcia, A., Martin, J. & Liras, P. The claR gene of Streptomyces clavuligerus, encoding a LysR-type regulatory protein controlling clavulanic acid biosynthesis, is linked to the clavulanate-9-aldehyde reductase (car) gene. *Gene* **211,** 311–321 (1998).

42. Stock, J., Ninfa, A. & Stock, A. Protein-Phosphorylation and Regulation of Adaptive Responses in Bacteria. *Microbiol Rev* **53,** 450–490 (1989).

43. Hutchings, M., Hoskisson, P., Chandra, G. & Buttner, M. Sensing and responding to diverse extracellular signals? Analysis of the sensor kinases and response regulators of Streptomyces coelicolor A3(2). *Microbiology* **150,** 2795–2806 (2004).

44. Hwang, Y. S., Lee, J. Y., Kim, E. S. & Choi, C. Y. Optimization of transformation procedures in avermectin high-producing Streptomyces avermitilis. *Biotechnol. Lett.* **23,** 457–462 (2001).

45. Claros, M. G. & von Heijne, G. TopPred II: an improved software for membrane protein structure predictions. *Comput. Appl. Biosci.* **10,** 685–686 (1994).

46. Agnihotri, G. & Liu, H. Enoyl-CoA hydratase: Reaction, mechanism, and inhibition. *Bioorg. Med. Chem.* **11,** 9–20 (2003).

47. Christianson, D. Arginase: Structure, mechanism, and physiological role in male and female sexual arousal. *Acc. Chem. Res.* **38,** 191–201 (2005).

48. Tabor, C. & Tabor, H. Polyamines. *Annu. Rev. Biochem.* **53,** 749–790 (1984).

49. Nobary, S. & Jensen, S. A comparison of the clavam biosynthetic gene clusters in Streptomyces antibioticus Tu1718 and Streptomyces clavuligerus. *Can. J.*

Microbiol. **58,** 413–425 (2012).

50. Wu, T. K. *et al.* Identification, cloning, sequencing, and overexpression of the gene encoding proclavaminate amidino hydrolase and characterization of protein function in clavulanic acid biosynthesis. *J. Bacteriol.* **177,** 3714–3720 (1995).

51. Elkins, J. M. *et al.* Oligomeric structure of proclavaminic acid amidino hydrolase: evolution of a hydrolytic enzyme in clavulanic acid biosynthesis. *Biochem. J.* **366,** 423–434 (2002).

52. Gust, B., Challis, G. L., Fowler, K., Kieser, T. & Chater, K. F. PCR-targeted Streptomyces gene replacement identifies a protein domain needed for biosynthesis of the sesquiterpene soil odor geosmin. *Proc. Natl. Acad. Sci. U. S. A.* **100,** 1541–6 (2003).

53. Sykes, R. & Wells, J. Screening for beta-lactam antibiotics in nature. *J. Antibiot.* **38,** 119–121 (1985).

54. Corbett, D., Eglington, A. & Howarth, T. Structure Elucidation of Mm-17880, a New Fused Beta-Lactam Antibiotic Isolated from Streptomyces-Olivaceus - Mild Beta-Lactam Degradation Reaction. *J. Chem. Soc. Chem. Comm.* 953–954 (1977).

55. Ishizuka, H., Horinouchi, S., Kieser, H., Hopwood, D. & Beppu, T. A putative two-component regulatory system involved in secondary metabolism in Streptomyces spp. *J. Bacteriol.* **174,** 7585–7594 (1992).

56. Lu, Y. *et al.* Characterization of a novel two-component regulatory system involved in the regulation of both actinorhodin and a type I polyketide in Streptomyces coelicolor. *Appl. Microbiol. Biotechnol.* **77,** 625–635 (2007).

57. Kojima, I., Fukagawa, Y., Okabe, M., Ishikura, T. & Shibamoto, N. Mutagenesis of oa-6129 carbapenem-producing blocked mutants and the biosynthesis of carbapenems. *J. Antibiot.* **41,** 899–907 (1988).

58. Okabe, M. *et al.* Studies on the OA-6129 group of antibiotics, new carbapenem compounds. I. Taxonomy, isolation and physical properties. *J. Antibiot. (Tokyo).* **35,** 1255–63 (1982).

59. Wise, R. In vitro and pharmacokinetic properties of the carbapenems. *Antimicrob. Agents Chemother.* **30,** 343–349 (1986).

60. Williams, S. T. *Actinomycetes*. *Methods in Microbiology* **4,** (Academic Press, 1971).

Chapter 3

Total synthesis of epithienamycins and exploration into the roles of CmmSu, Cmm17 and CmmPah in epithienamycin biosynthesis

We chose an *in vitro* enzymatic approach to study the biosynthetic mechanism of C-6 and C-8 inversion in MM 4550 biosynthesis. Currently the enzymes of interest are the presumed sulfotransferase CmmSu, the putative enoyl-CoA hydratase Cmm17, and the hypothesized enzyme CmmPah[1,2]. We proposed that these enzymes are involved in the epimerization of the C-6 and C-8 stereocenters as the point of divergence from the thienamycin biosynthetic pathway to that of the epithienamycins[3]. One such biosynthetic transformation is shown in Scheme 3.1.

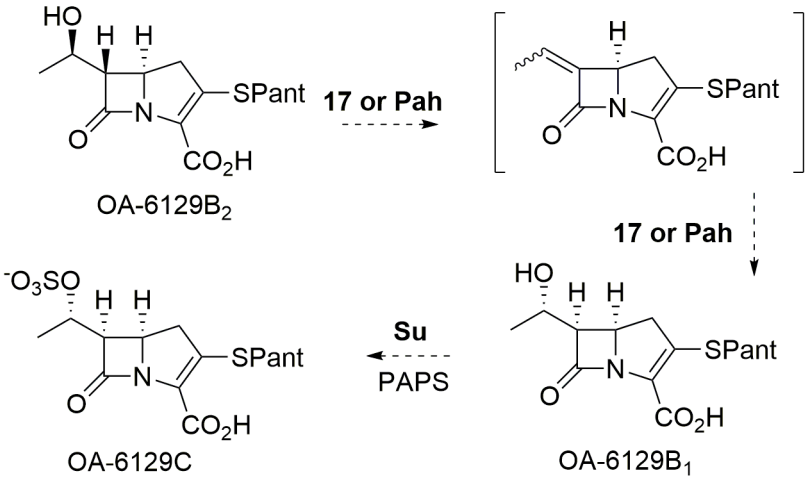

Scheme 3.1: Proposed epimerization of the C-6/8 stereocenters that lead to epithienamycins[1]

Epimerization of the C-6/8 positions is thermodynamically unfavorable. There is no energetic reason why equilibration would favor formation of a sterically crowded product. Mechanistically, it would make better sense if the C-8 hydroxyl were oxidized and then reduced selectively from the less hindered face for epimerization to occur. However, no reductases or uncharacterized oxygenases exist within the MM 4550 gene

cluster. We presume that the enoyl-CoA hydratase Cmm17 and the protein CmmPah can perform the acid-base chemistry for either the elimination or addition of water the epimerize these stereocenters and hope that the steric control by the enzyme active site(s) would be enough to favor this chemistry.

Isolation of carbapenems from *S. argenteolus ΔcmmSu*

To identify target substrates for total synthesis we sought to identify the major antibiotic produced in the CmmSu knockout of *S. argenteolus* (Δ*cmmSu*) by isolation of the presumed substrate for sulfuryl transfer from the mutant strain. An initial attempt at isolation using Aliquat 336, as done for MM 4550 isolation, was inefficient. These results, in combination with the likelihood that the intermediate is lacks a sulfate at C-8, led to the abandonment of the phase transfer strategy. A different mode of extraction using similar principles was executed. The published procedure for epithienamycin isolation from *Streptomyces flavogriseus* MB 4638 was used as a guide for isolation[3].

Dowex® 1x2 anion-exchange resin was suspended in filtered *S. argenteolus* Δ*cmmSu* medium to draw antibiotic out of the medium, and the antibiotically-active portion of the saline eluate was purified through a column of Amberlite® XAD polystyrene resin. The carbapenem was further purified by adsorption on activated charcoal followed by elution with 10% aqueous *n*-butanol before it was concentrated *in vacuo*. It was critical that all chromatography, adsorption and elution were performed in the shortest time possible and at 4 °C as degradation proved to be accelerated for this compound *vs.* MM 4550. HPLC purification and analysis by UPLC-HRMS revealed a compound that matched the mass and λ_{max} (300 nm) of epithienamycin A and *N*-acetyl

thienamycin, although the UV spectrum has an apparent second λ_{max} at 240 nm which is typical for 2-ethylidenethiol derivatives[3] (Figure 3.1). At -80 °C in K_2HPO_4 buffer (pH = 7, 20 mM) the isolated compound degraded rapidly and after 1 week the compound was completely degraded. Syntheses of multiple carbapenems for CmmSu activity assays would provide additional evidence for the stereochemical preferences of the enzyme.

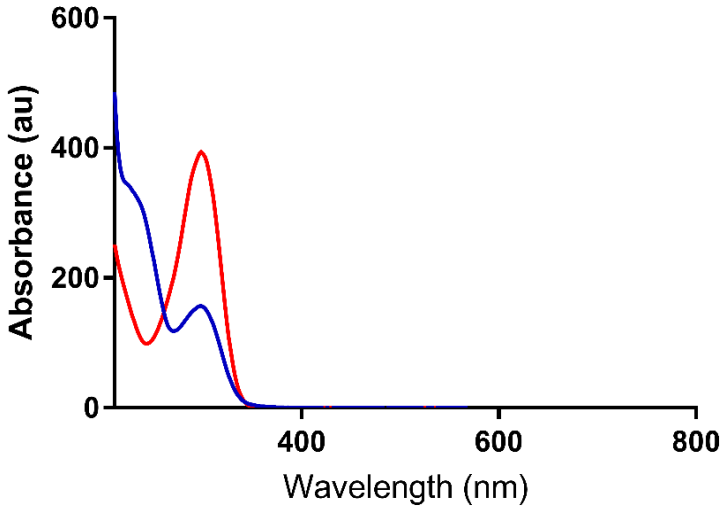

Figure 3.1: UV Spectrum of Epithienamycin A (red) and Δ*cmmSu* Product (blue)

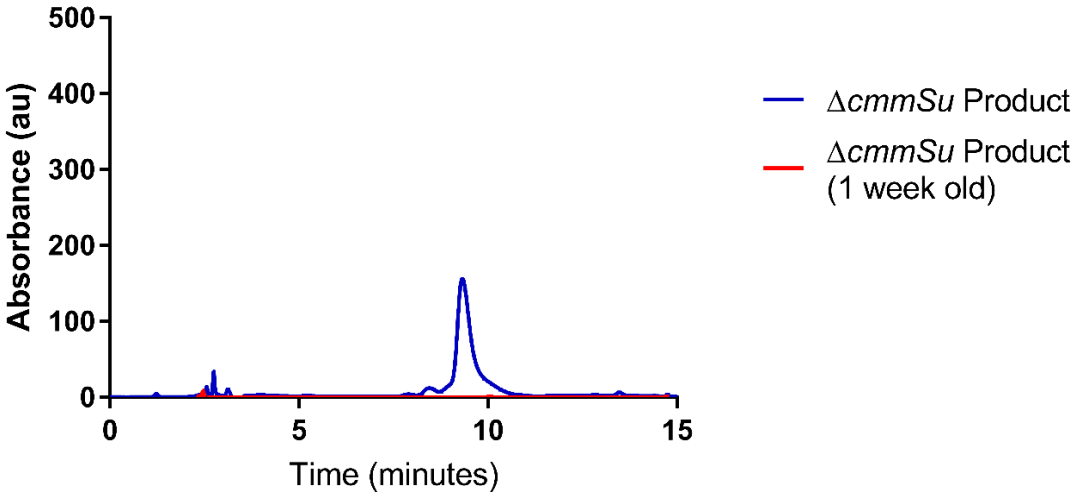

Figure 3.2: HPLC chromatogram for purified Δ*cmmSu* Product

Synthesis of thienamycins and epithienamycins for CmmSu activity assays

The synthesis of epithienamycin A and OA6129-B_1 required the construction of a 5,6-*cis*-relationship on the carbapenem bicycle core. In the literature, there exist many routes to "5,6-*cis*-carbapenems"[4–8], with the most efficient published by Micah Bodner and Ryan Phelan[9]. That synthesis, although elegant, relies on an early deprotection step that uses three equivalents of expensive samarium iodide and an unreliable Arndt-Eistert[10] homologation late in the synthesis that requires the use of a high-pressure mercury UV lamp. Different routes were utilized to generate the kinetic product 3,4-*cis*-azetidinone from *N*-*tert*-butyldimethylsilyl 4-allyl-2-azetidinone and acetaldehyde[7]. It was found that after the preparation of the initial 3,4-*cis*-azetidinone, all remaining steps were easily and repeatedly performed in good yield. The synthetic route to 2-oxocarbapenam **8** is shown in Scheme 3.2.

The chiral synthesis of *N*-*tert*-butyldimethylsilyl 4-allyl-2-azetidinone **1** has been repeated using the efforts outlined by Ueda *et al*.[11,12] and described in further detail by Dr. Kristos Moshos and Daniel Marous[13,14]. Azetidinone **1** was reacted with lithium diisopropylamide (LDA) and acetaldehyde to produce **2**, **2a** and **2b** with an average combined yield of 35%. The optimal ratio of 3,4-*cis*-(**2**) to 3,4-*trans*-products (**2a**, **2b**) was achieved (1:2) when quenched with acetic acid at -78 °C. Although this overall yield of **2** from **1** was very low yielding (15% or less), being the first step in the synthesis allowed large scale to overcome this limitation. The remaining synthetic sequence was reliable to stereopure 5,6-*cis*-carbapenems after chromatography, where 5g of **1** could eventually yield 100 mg or more prior to the final deprotection of the PNB esters. Protection of **2a** with *p*-nitrobenzyl chloroformate in the presence of

dimethylaminopyridine (DMAP) provided the carbonate **3** in 80% yield. Compound **3** was deprotected under HF/pyridine; conditions that provide an improved yield versus tetrabutylammonium fluoride (TBAF) to give the free amide **4**. Where TBAF allows for reliable deprotection, HF/pyridine excels not only in yield, but in shortened reaction time (<15 min) and ease of purification. HF/pyridine was easily removed from the crude reaction by workup with saturate ammonium chloride and brine, however it was found that silica gel chromatography immediately after workup ensured the removal of all residual HF, which could cause degradation in long-term storage. It is reccomended to use a plastic flask when working with HF, to avoid etching of Pyrex during the course of the reaction and potentially contaminating the product.

Ozonolysis followed by dimethyl sulfide reduction of the subsequent ozonide and further oxidation of the resulting aldehyde using Pinnick oxidation conditions[15,16] provided the acid **5** in 56% yield, although occasionally yields were much higher depending on the purity of the starting material. Direct oxidation of the ozonide with H_2O_2 was attempted but resulted in unrecoverable product material. For ease of purification, keeping the ozonide and product aldehyde anhydrous before Pinnick oxidation provided a very clean product **5,** which was crystallized from ethyl acetate/hexanes after acidic organic extraction. Addition of *p*-nitrobenzyl magnesium malonate to the imidazole-activated acid at 65 °C gave the β-keto ester **6,** which was then reacted with methanesulfonyl azide and diisopropylethylamine (DIPEA) to provide the diazo compound **7**. Rhodium(IV) acetate-mediated carbene insertion into the β-lactam N-H bond yielded the 2-oxopenam **8** quantitatively. From **8,** the enol phosphate was produced *in situ* from diphenylphosphoryl chloride and DIPEA. The intermediate was

then reacted with the thiol of choice; in this case either *N*-acetylcysteamine (SNAC) or *O,O*-1,3-bistriethylsilyl-pantetheine in 66% and 47% yield, respectively. The SNAC derivative **9** was directly deprotected to produce epithienamycin A **12**. Yields of TES deprotection were poor when the pantetheine derivative **10** was stirred with TBAF, but preferable to complete degradation from the use of HF/pyridine. It was found that the low-yielding TES deprotection step could be avoided by the direct addition of pantetheine itself to the enol phosphate, as developed using the methods described for conjugate addition of thiols to carbapenems[17,13]. Hydrogenolysis of the *p*-nitrobenzyl esters provided OA6129-B_1 (**13**) after purification by preparative HPLC (Scheme 3.3).

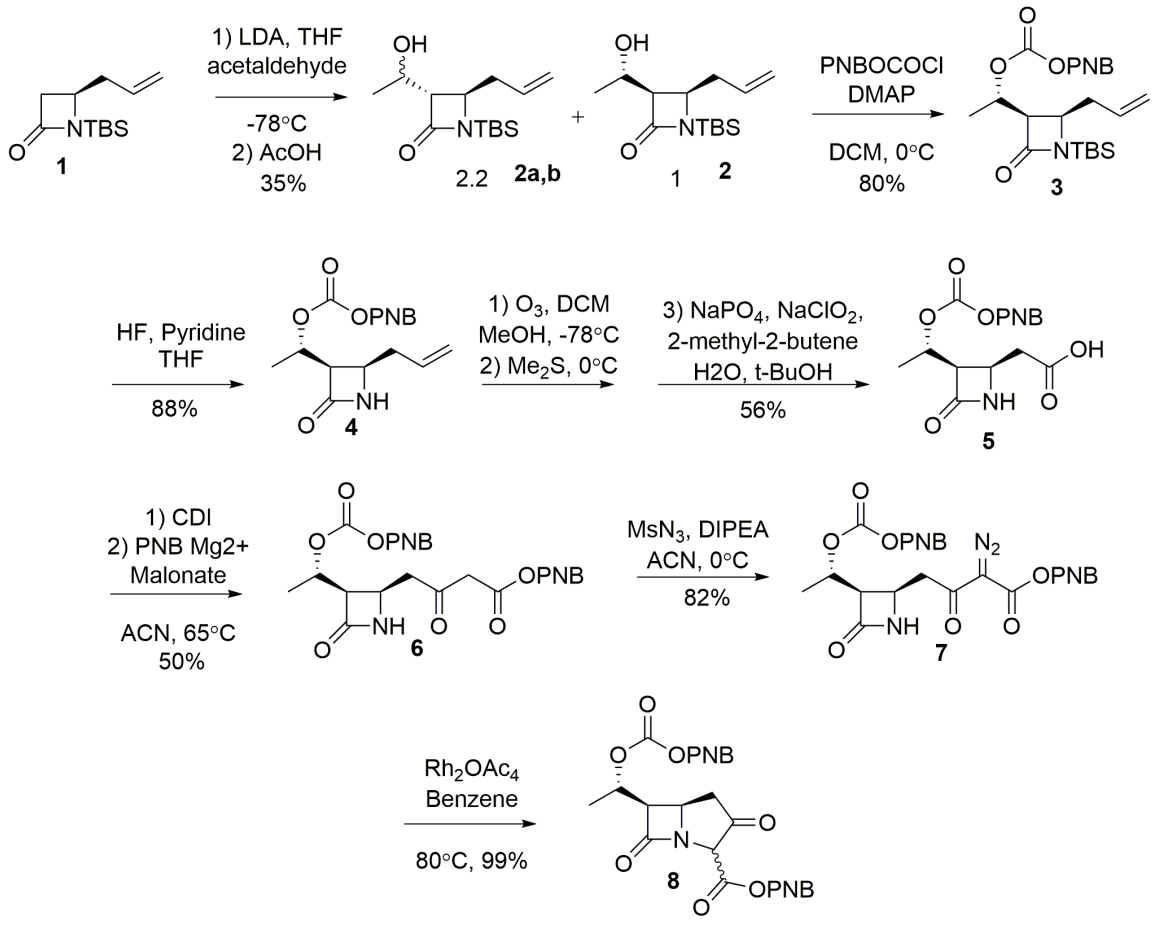

Scheme 3.2: Synthesis of 5,6-*cis*-carbapenam **8**

The synthesis of 5,6-*trans*-carbapenams was performed in parallel using intermediate **2b**. Conveniently, the 2-oxocarbapenam **14** (Scheme 3.4), an intermediate of imipenem synthesis, was purchased for $60/g from Ark Pharm, Inc. The purchased intermediate was used to produce *N*-acetyl thienamycin (**18**) and OA6129-B_2 (**19**) as shown in Scheme 3.4.

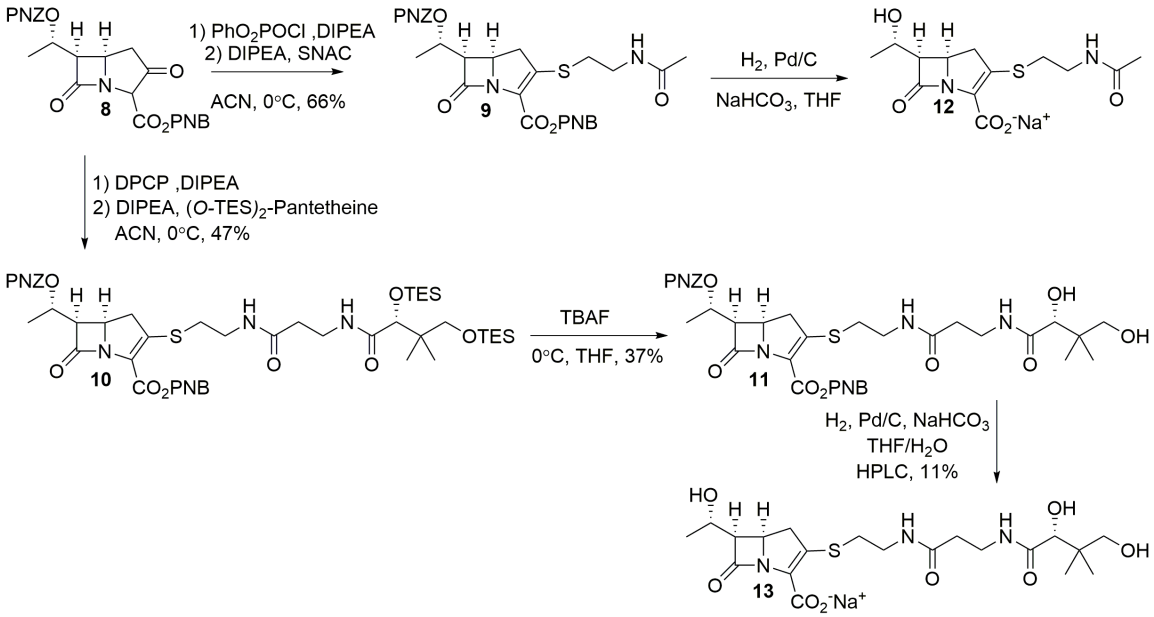

Scheme 3.3: Synthesis of epithienamycin A and OA6129-B_1 from 5,6-*cis*-carbapenam **8**

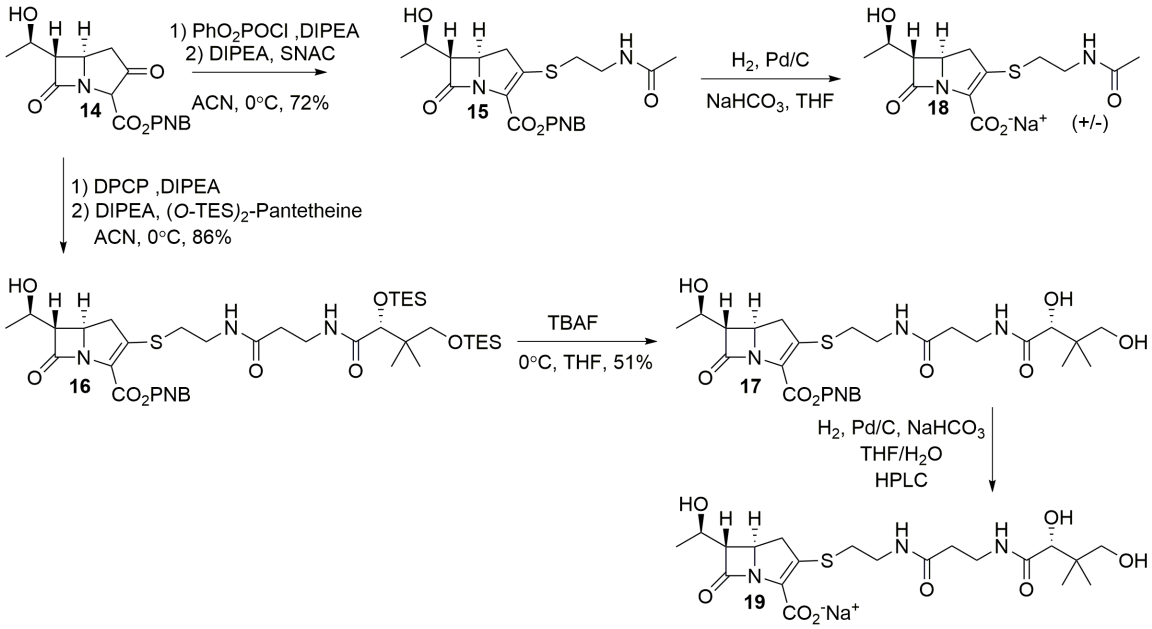

Scheme 3.4: Synthesis of *N*-acetylthienamycin and OA6129-B_2 from 2-oxocarbapenam **14**

New strategies for the total synthesis of epithienamycins

The current route to 5,6-*cis*-carbapenems employed in Scheme 3.2 as well as those reported the literature[4–8] are highly inefficient and not currently amenable to industrial scale up[18]. Should 5,6-*cis*-carbapenems be found of clinical value, it would be advantageous to choose a synthetic route which could account for addition of the necessary 1β-methyl substituent on the carbapenem bicycle; providing carbapenem resistance to degradation by dehydropeptidase 1 (DHP-1). Current methods incorporate the 1β-methyl substituent by chiral addition into a 4-acetoxyazetidin-2-one by methods like the example shown in Scheme 3.5[19].

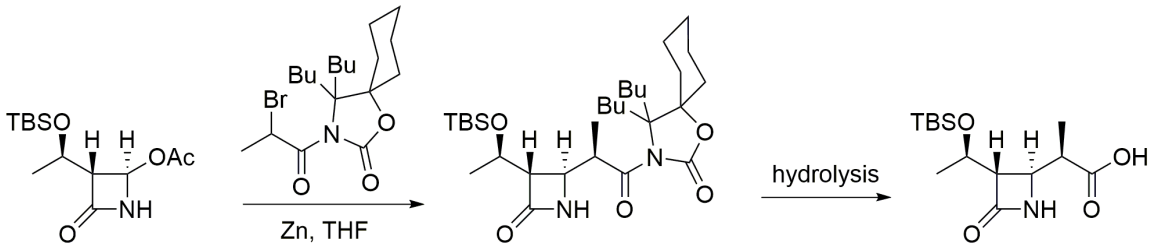

Scheme 3.5: Reformatsky-Mediated Addition of a Chiral Enolate to 4-acetoxy-2-azetidinones

It would be optimal to follow a similar strategy for the generation of 5,6-*cis*-carbapenems. Intermolecular nucleophilic addition to an *N*-acyliminium intermediate generated from 4-acetoxy-2-azetidinones solely produce *trans*-azetidinones; therefore, a new strategy is proposed that involves intramolecular ring closure (Scheme 3.6) to force nucleophilic attack from the more hindered face. This approach will not preclude 1β-methyl group installation, as the required stereochemistry would be set by steric limitations. Favorable 6-membered ring formation would render insertion from the other side to form a *trans*-azetidinone geometrically impossible. Once the methodology was implemented, the synthesis would be modified to converge to the current route to carbapenems as proposed in Scheme 3.6.

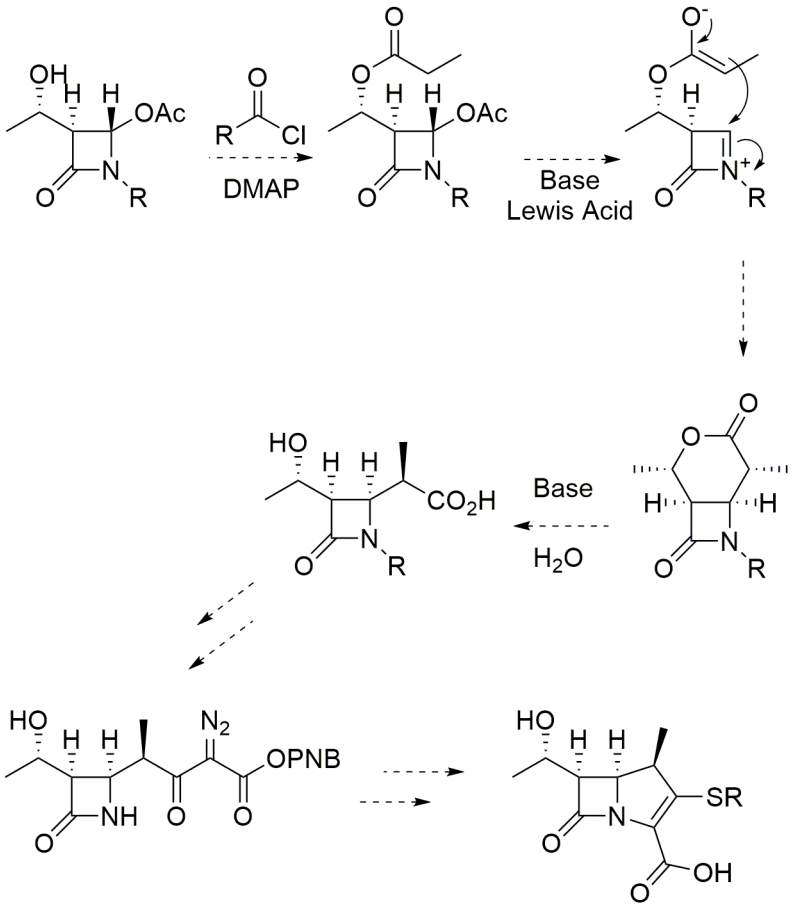

Scheme 3.6: An ideal route to 5,6-*cis*-carbapenems

First, the 4-acetoxy-3-hydroxyethyl-2-azetidinone **24** was desired. Using D-aspartic acid, the synthesis of 4-acetoxy azetidinone **25** was possible through chemistry established by Merck for the synthesis of the enantiomer acetoxyazetidinone used in the production of imipenem[20] (Scheme 3.7).

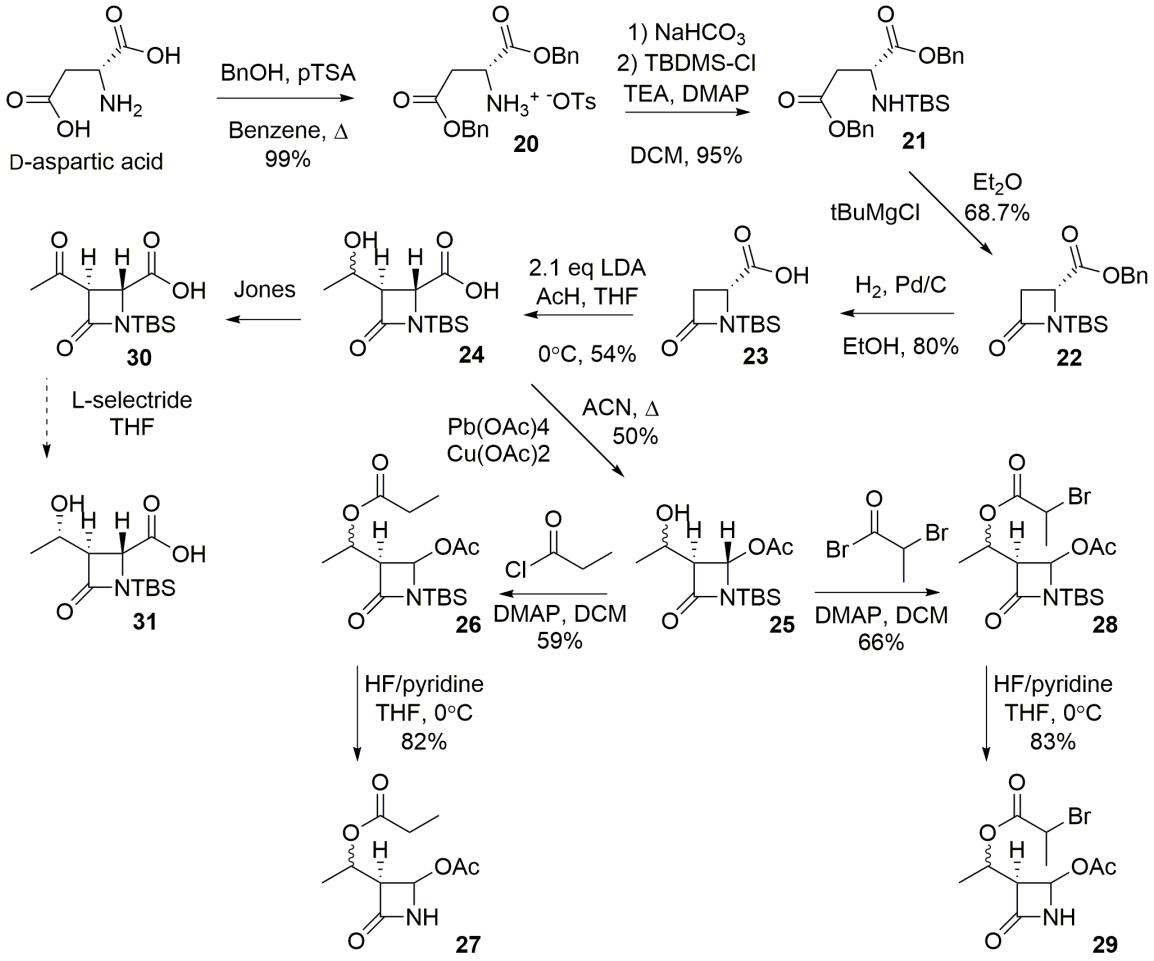

Scheme 3.7: Synthesis of 4-acetoxy-2-azetidinones

Following established chemistry[20], Fisher esterification[21] of D-aspartic acid with benzyl alcohol under dehydrating Dean-Stark conditions[22] provided the tosyl salt **20** in near quantitative yield after crystallization from cyclohexane. A primary amine was generated through deprotonation by sodium bicarbonate and was then reacted with *tert*-butyldimethylsilyl chloride to provide the secondary amine **21**. Deprotonation of the amine was facilitated by *tert*-butyl magnesium chloride and the resulting anion was reacted with the benzyl ester to yield the azetidinone **22** in a yield of 69%. Hydrogenolysis of the remaining benzyl ester followed by recrystallization from diethyl ether provided the acid **23**. A dianion was generated using two equivalents of lithium

diisiopropylamide (LDA). The enolate at the 3 position was reacted with acetaldehyde to give 3,4-*trans*-azetidinone diastereomeric alcohols. Literature procedures exist for the oxidation of the secondary alcohol with sodium dichromate in sulfuric acid (Jones reagent), and the reduction of the product ketone to generate the stereopure alcohol[23]. Resolution of diasteromers was avoided, however, as our first goal was to solve the chemistry of cyclization. Meanwhile, the diastereomeric alcohols **24** were carried forward. The acid was oxidized with lead (IV) tetraacetate under mild heating in the presence of a catalytic amount of copper acetate to provide the 4-acetoxy azetidinone **25** without the deprotection of the *N*-*tert*-butyldimethylsilyl group in 50% yield[24]. The resulting alcohols were acylated with either propionyl chloride or 2-bromopropionyl bromide in 59% and 66% yields respectively. The silyl group was cleaved with 60% hydrofluoric acid in pyridine. The propionyl esters **26** and **28** were necessary for enolate generation and the 2-bromopropionyl esters **27** and **29** were primed for generation of an α-anion through a Reformatsky or Grignard mechanism[25].

The azetidinones **26**-**29** could not undergo ring closure. The screening of Lewis acids, bases, and various highly activated metals, such as Reike zinc or freshly ground magnesium did not produce the desired transformation. It was hoped that formal deprotonation of the azetidinone nitrogen and would allow formation of the *N*-acyl iminium species when Lewis acid methods failed; however, no intramolecular addition occurred. To explore other routes, closure of a five-membered ring as described by Gallucci and coworkers[26] was investigated (Scheme 3.8). The crucial step of epimerization of the aldehyde **33** at the 4-position of the azetidinone transiently provided the desired 3,4-*cis*-stereochemistry, which was preserved after spontaneous ring closure

to a hemiacetal. Scheme 3.8 illustrates the synthesis of **42**.

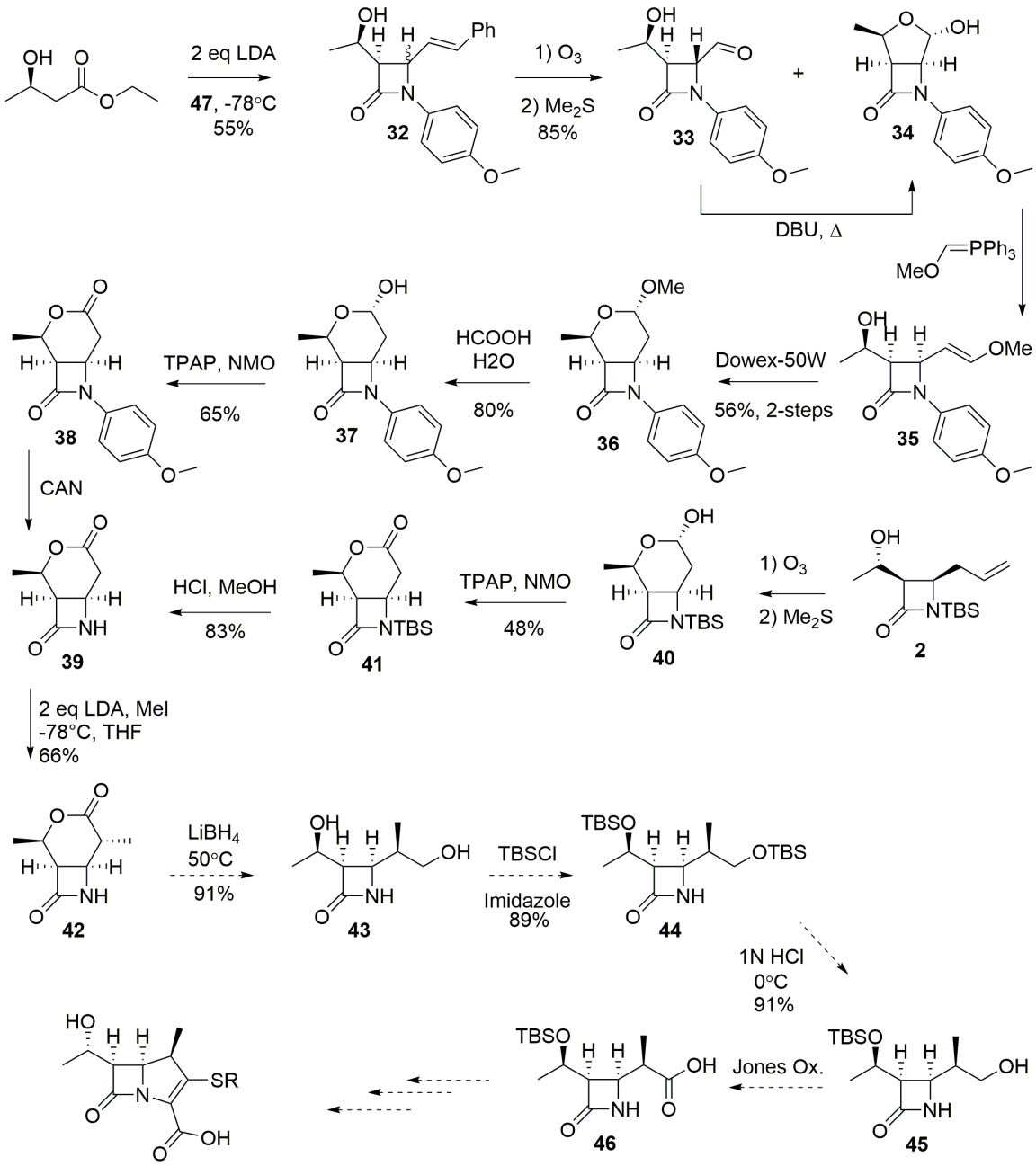

Scheme 3.8: Synthesis of 1-β-methyl-epithienamycins through **42**

The 2-hydroxytetrahydrofuran **34** was expanded to a 6-membered cyclic methyl acetal by reaction with a methoxymethyl triphenylphosphine ylid followed by ring closure in acidic conditions. The methyl acetal **36** was converted to the hemiacetal **37** and oxidized to the lactone **38** with *N*-methylmorpholine *N*-oxide (NMO) in the presence

of catalytic tetrapropylammonium perruthenate (TPAP). For this step, Pinnick oxidation conditions[15,16] were insufficient to oxidize the hemiacetal where pyridine dichromate was successful; however, TPAP/NMO was preferable due to the cleanliness of the reaction and higher yield. Oxidative removal of the *N*-methoxyphenyl group with ceric ammonium nitrate (CAN) provided the free amide **39**. With **42** in hand, the remainder of the synthetic sequence followed the precedent of Kaga *et al*.[27]. Through these methods, a route to 1-β-methyl epithienamycin would be possible when using the established methods of Galluci, Kaga and coworkers. For convenience, it was also possible to ozonolyze the intermediate **2** to form the [4.2.0] ring system directly, and is preferred for the racemic synthesis of epithienamycins owing to the wide availability of (±)-4-allylazetidin-2-one.

Biosynthetic Studies of the MM 4550 producing gene cluster in *S. argenteolus* ATCC 11009

We believe the point of biosynthetic divergence from thienamycin to MM 4550 occurs prior to truncation of the C-2 pantetheine sidechain by ThnT/CmmT because of the isolation of the OA-6129 carbapenems from a single strain of *Streptomyces fulvuviridis*[28]. Comparison of the MM 4550 and thienamycin gene clusters revealed three enzymes unique to the MM 4550 cluster, which are thought to account for the structural differences between MM 4550 and thienamycin. The sulfotransferase is likely involved in sulfonation of the C-8 hydroxyl position, leaving Cmm17 and CmmPah to alter the stereochemistry of the C-6 side chain.

Dr. Rongfeng Li cloned out of *S. argenteolus* and into a pET29 vector *cmmSu*

with a *C*-terminal His_6-tag. Test expressions encountered low solubility; however, optimization of conditions by utilizing a 1 h cold shock before induction with IPTG and fermentation at 15 °C for 24 h resulted in a high quantity of soluble protein. Typical procedures using a nickel column for purification of the protein were followed, and the purified CmmSu was buffer-exchanged into pH 7.0 potassium phosphate. The protein was found to be unstable with these conditions, and, therefore, buffer screening was performed to optimize stability. The most stable buffer conditions found were 50 mM MOPS pH = 7.8 with 10% glycerol, in which the protein would remain soluble for many hours at ambient temperature.

Epithienamycin A, *N*-acetyl thienamycin or derivatives thereof are produced by *S. argenteolus ΔcmmSu* and these substrates were synthesized for the profiling of CmmSu *in vitro*. Carbapenems have been isolated from *Streptomyces* that are functionalized at C-2 with pantetheine, and at C8 as a sulfate[29–31], so testing of compounds with *N*-acetylcysteamine and pantetheine at C-2 are necessary. C-5/6-*trans* carbapenems have never been isolated from *Streptomyces* that contain a sulfate at C-8; however, these are likely intermediates in the biosynthetic pathway and may be substrates for CmmSu *in vitro*.

As a negative control, a mutant of CmmSu was generated to knockout the key catalytic arginine residue. Quik-change® PCR allowed for the generation of CmmSu-R18A, which was expressed and purified in the same manner as for the wild-type enzyme.

CmmSu *in vitro* assays

Each of *N*-acetyl thienamycin, epithienamycin A, OA6129-B_1 and OA6129-B_2 were separately incubated with CmmSu and 3'-phosphoadenosine 5'-phosphosulfate (PAPS) in MOPS buffer. The enzyme was functional at 30-37 °C, but due to increased precipitation of CmmSu at elevated temperatures, we chose to run the majority of assays at room temperature. Analyses of the reactions by HPLC (Figure 3.3) found the conversion of each compound to its respective sulfate. Conversion seemed highest with the reaction of CmmSu with 5,6-*cis*-carbapenem OA-6129B_1. UPLC ESI-MS confirmed the presence of a sulfonate in the products (Figure 3.4). Repetition of the experiment with the R18A mutant resulted in the abolishment of *O*-sulfotransferase activity vs. the wild-type enzyme (Figure 3.3).

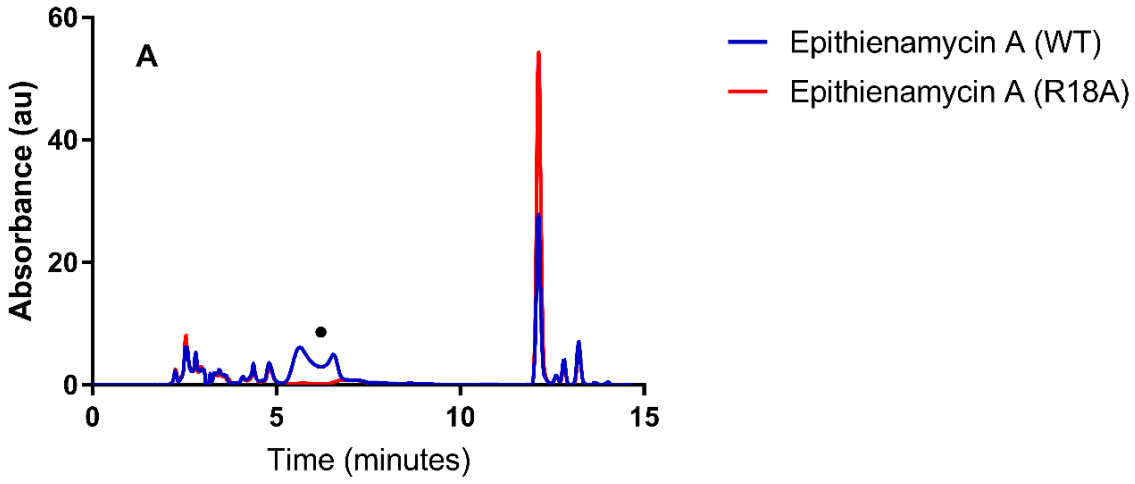

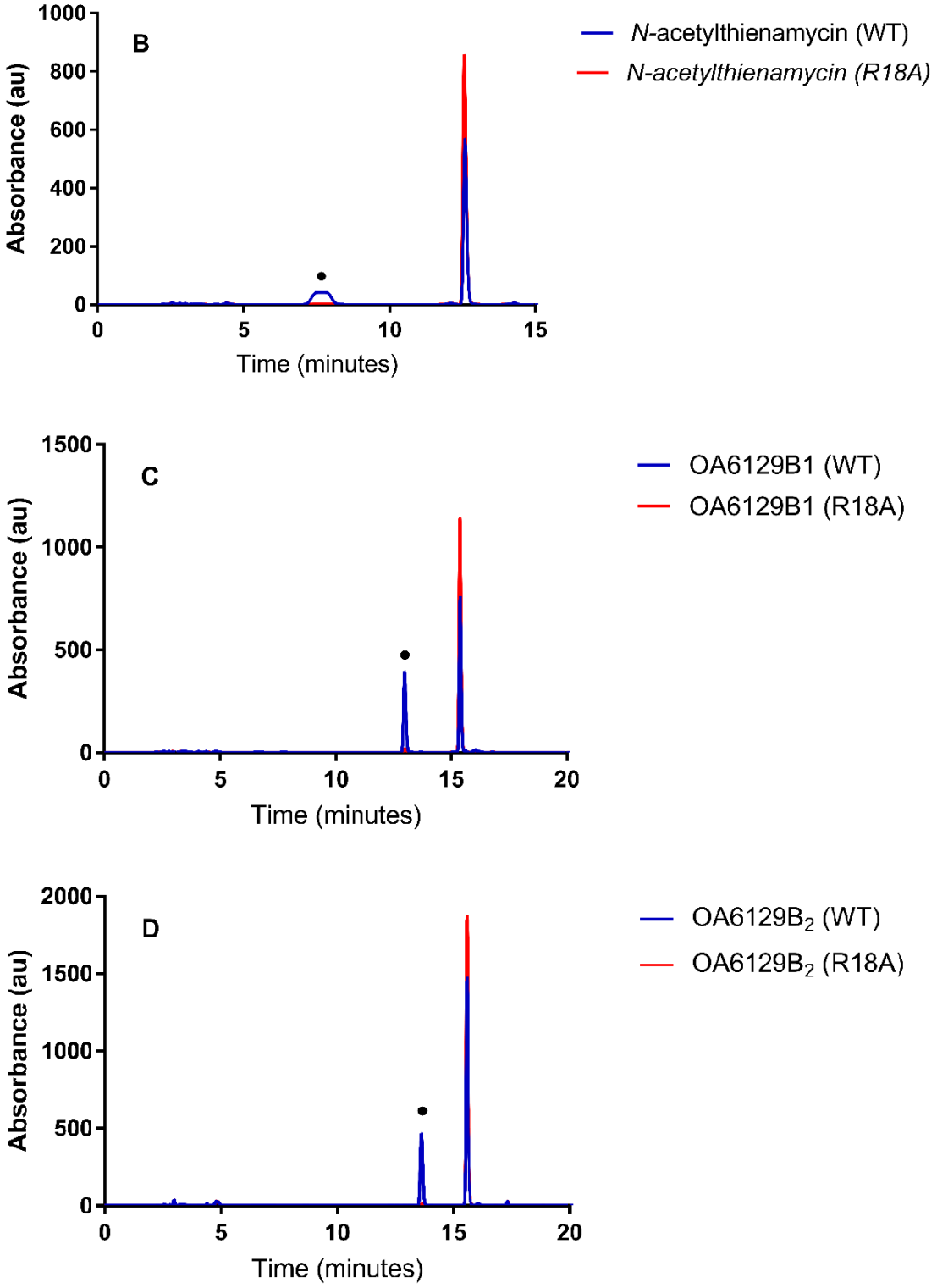

Figure 3.3: HPLC analyses of CmmSu products when incubated with (a) Epithienamycin A (b) *N*-acetylthienamycin (c) $OA6129B_1$ (d) $OA6129B_2$. Peaks labeled with a heavy dot (●) indicate sulfonated product, as confirmed by UPLC-HRMS.

Retention times and good separation of substrates and products showed that direct analysis of sulfated product was the best course of action. The carbapenem does have a significant chromophore, and the C-2 pantetheine carbapenem alcohols and their products give resolved peaks by HPLC. In the future, a standard curve should be made from these synthetic compounds so a time course experiment would provide comparative data by monitoring rates of substrate consumption and product formation.

Cmm17 and CmmPah *in vitro* assays

Dr. Rongfeng Li was able to express soluble constructs of Cmm17 and CmmPah in *E. coli*. CmmPah proved the more difficult to express as soluble protein was only isolated from the expression using a pET41 vector that adds a glutathione *S*-transferase (GST) tag at the *N*-terminus. Once purified, the GST/CmmPah construct was very stable with no precipitation after 24 hours or after freezing in liquid nitrogen and thawing to room temperature. The buffer used was 50 mM MOPS, pH = 7.8. Cmm17 is not as stable in any of the buffers previously tested, so it must be purified from cells on the same day as experimentation, and used within hours of buffer exchange.

In the hope that the Cmm17/Pah paired enzyme system alone is necessary for stereochemical inversion of the C-6/8 positions, assays were developed that included CmmPah, Cmm17, and both CmmPah and Cmm17 together. Each of these scenarios was incubated with the synthetic carbapenem substrates OA6129B_1 and OA6129B_2. The homologue of CmmPah in the clavulanic acid producer[32] and the similar arginases studied in the literature use manganese as the Lewis acidic metal involved in the hydrolysis of a guanidinyl group[2,33]. We theorized that CmmPah may use a similar

acid/base driven mechanism, and so 0.5mM manganese chloride was added to the assays.

Incubations of OA6129B$_1$, OA6129B$_2$, epithienamycin A and *N*-acetyl thienamycin with CmmPah or Cmm17 separately or together did not produce any new products detectable by UV Vis in the HPLC or a new mass in the UPLC ESI-MS. These negative results led to a hypothesis that carbapenems must to be *o*-sulfonated prior toward reaction with either CmmPah or Cmm17. To test this, enzyme assays including CmmSu were performed, with CmmSu, CmmPah, Cmm17 and PAPS in the same reaction (Figure 3.4). Each of the carbapenems previously tested was used as substrate in the incubations. The results were again disappointing. The only new products were sulfated derivatives of OA6129B$_1$, OA6129B$_2$, epithienamycin A and *N*-acetyl thienamycin, which had been seen before in the CmmSu experiments.

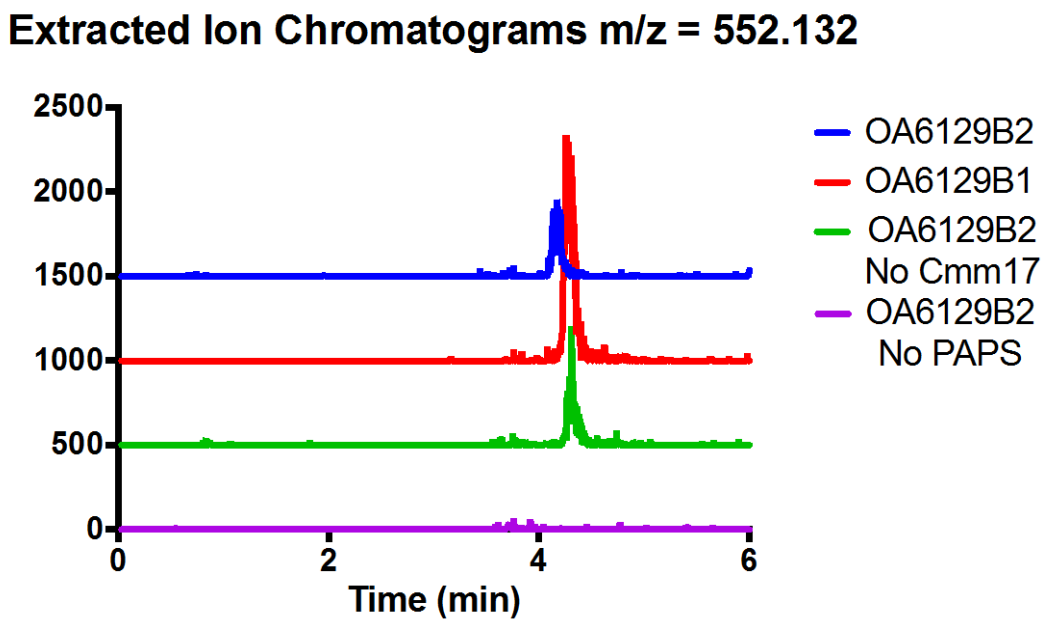

Figure 3.4: Extracted ion chromatogram for sulfonated pantetheinyl carbapenem products in dual enzyme assays of CmmSu and Cmm17, incubated with OA-6129B$_1$ (red) or OA-6129B$_2$ (blue). No Cmm17 control for the reaction with OA-6129B$_2$ is in green. The no PAPS control is shown in purple. The calculated mass for sulfonated carbapenems (negative mode) $C_{20}H_{30}N_3O_{11}S_2^-$ = 552.132 da.

Discussion

Analysis of all isolated carbapenem structures revealed that only 5,6*cis* carbapenems contain a sulfate at C-8. It is possible that stereochemical inversion can only occur with a sulfate present (Scheme 3.9), or conversely that it can occur with a free hydroxyl. It was hoped that CmmSu would be a stereoselective gatekeeper for sulfonation as observed with other enzymes in thienamycin biosynthesis, such as ThnM, ThnQ, or ThnK, and that conclusive preference for one substrate over another would give insight into the order of the inversion process. Unfortunately, sulfonation by CmmSu was successful with all substrates, so little insight was gained. CmmPah and Cmm17 were unable to alter the stereochemistry of the C-6/8 positions alone; however, these enzymes may not function *in vitro* without the proper substrates or cofactors. Possible substrates may include 2-ethylidene carbapenems, which are proposed as intermediates after desaturation (Scheme 3.1). Possible cofactors may be metal ions, such as Mn^{+2} for Pah. Alternatively, identification of the β-lactamase-inducing intermediate that accumulates in the Cmm17 gene-disruption mutant, as seen by nitrocefin assay with incubation of *S. argenteolus* Δ*cmm17* medium with *S. aureus*, would give comprehension to the function of Cmm17. Isolation could be performed in the future using previous techniques following β-lactamase induction activity to easily monitor small quantities of the compound.

Conclusion

The syntheses of epithienamycins were possible following established chemistry. Modification of synthetic routes by Gallucci, Kaga and coworkers[26,27] provided a new,

reliable route to epithienamycins, which could incorporate a 1β-methyl group on the carbapenem core if desired. The early synthetic steps followed by Galluci and coworkers[26] could be avoided if the chiral synthesis of 4-allylazetidin-2-one could be performed economically and on large scale.

CmmSu was found to sulfate a variety of carbapenems, with seemingly little preference for a particular C-6 or C-8 stereochemical orientation. C-2 pantetheinyl carbapenems provided greater enzymatic turnover when compared to their *N*-acetylcysteamine counterparts. When 6-hydroxyethyl carbapenems or their sulfonated products are incubated with CmmPah and/or Cmm17, no apparent stereochemical inversion is observed from analysis by HPLC (Figure 3.4). Further experiments which could uncover the mysteries of divergence from thienamycin to epithienamycins are the isolation of bioactive intermediates from Δ*cmm17*, and repetition of the isolation of the carbapenem from Δ*cmmSu* with synthetic standards in hand to determine the stereochemistry of that compound. If the Δ*cmmSu* isolate is a C-5/6-*trans*-carbapenem, that would indicate sulfonation is a necessary step prior to C-6/8 inversion. If the isolate is 5,6-*cis*, then sulfonation is only a modification after the fact and the historical isolation of only 5,6-*cis*-carbapenems with a C-8 sulfonate from natural producers is merely coincidental.

Experimental

General methods:

Restriction enzymes, DNA modifying enzymes, and PCR reagents were obtained from New England Biolabs (Ipswich, MA). Plasmid kits were from Thermo Scientific

(Waltham, MA). *E. coli* DH5α (Invitrogen) was usually used for DNA cloning and ThnK expression was done in *E. coli Rosetta 2*(DE3) (Novagen). Plasmid DNA was sequenced by the Synthesis and Sequencing Facility of the Johns Hopkins University. Solvents and reagents were purchased from Sigma Aldrich or Fisher Scientific in purity of ≥98%. Silica gel chromatography was performed using 60Å silica gel from Sorbtech. Thin layer chromatography (TLC) was performed using 250 μm Analtech GHLF silica plates. A Bruker Avance (Billerica, MA) 300 or 400 MHz spectrometer was utilized for all ^{1}H and ^{13}C NMR spectra, which are reported in parts per million (δ) referenced against a TMS standard or residual solvent peak. The JHU Chemistry Department Mass Spectrometry Facility determined exact masses by fast atom bombardment (FAB) or electrospray ionization (ESI).

Purification of Epithienamycin A from *S. argenteolus ΔcmmSu*:

15 liters of 96-h fermentation of *S. argenteolus* Δ*CmmSu* in ISP4^{+} medium was filtered through cheesecloth and 18.5 cm fast flow filter paper, and the eluate was stirred with 400 mL 20-50 mesh Dowex 1x2 resin for 2.5 h at 4 °C. The resin was loaded to a column and the remaining media was discarded. The carbapenem was eluted from the resin with 2 L 5% sodium chloride in 20 mM K_2HPO_4 buffer, pH = 7 at 4 °C. The eluate was loaded to 400 mL Amberlite XAD-4. The antibiotic was eluted with 4 L deionized water, and the remainder was eluted with 2 L 3% NaCl in 1:1 methanol/water at 4 °C. The eluate was incubated with 195 mL activated charcoal by stirring for 1 h at 4 °C. The charcoal was filtered through 7.5 cm fast flow filter paper, and the carbon cake was suspended in 540 mL 10% sec-butanol in water at 4 °C. The carbon cake was again

removed by filtration and the eluate was lyophilized and the resulting solids suspended in a minimum amount of water (50 mL). The crude antibiotic-containing solution was twice filtered through a 0.2 μ nylon filter before injection onto preparatory C18 high pressure liquid chromatography (HPLC) (decribed in chromatographic techniques below, preparatory method 1). Bioassay using extra-sensitive *E. coli* (ESS) verified the presence of antibiotic after lyophilization. Antibiotic containing solution was injected onto a Phenomonex Luna® semi-preparatory C18(2) column 10 x 250 mm 5 μ, and each 2 mL fraction from 7 min to 24 min elution time was collected for bioassay. Min 13 through 24 were bioactive and the remainder of the crude solution was injected and collected for lyophilization.

The fractions collected from semi-preparatory HPLC were suspended in a minimum amount of water and injected onto an analytical Phenomonex Polar-RP® column, 4.6 x 250 mm 5 μ (described in the chromatographic techniques section, analytical HPLC method 3). 2 mL fractions every minute from 2-16 min were collected for ESS bioassay and min 10-12 indicated the highest level of antibiotic. The remainder of the sample was purified on a polar-RP column (Method 4), and then was subject to the same column with a different mobile phase that contained 5% ammonium bicarbonate, a volatile buffer. The peak at 4.2 min was found to be potently bioactive and was collected for analysis. UPLC-HRMS revealed the compound to have a mass consistent with that of epithienamycin A.

Chromatographic techniques:

Analytical HPLC was carried out using an Agilent 1200 series G1311A pump with an Agilent model G1329A injector. The chromatograms were monitored by an Agilent 1200 series G1315D DAD detector at 210, 240, 270, 300, and 330 nm wavelengths.

UPLC conditions: Waters Acquity BEH UPLC column packed with ethylene bridged hybrid C-18 2.1 mm X 50 mm, 1.7 micron, 0.3 mL/min; solvent A = H_2O, solvent B = acetonitrile. Method: t=0 min 0% B, t= 1 min 0% B. t = 7.5 min 80% B, t = 8.4 min 80% B, t = 10 min 0% B. Samples were run in the negative mode with a 1 min solvent purge after injection.

Preparative HPLC was carried out using an Agilent 1100 series G1311A pump with an Agilent model 7725i injector fitted with a 1-mL injection loop. The chromatogram was monitored by an Agilent 1100 series G1315B DAD detector at 210, 240, 270, 300, and 330 nm wavelengths.

Preparatory HPLC conditions: Phenomonex Prodigy C18 (2) 250 x 10.00 mm 5 µ semi-preparatory column, 2 mL/min; buffer A = 20 mM K_2HPO_4, 0.5 mM EDTA, pH = 7.4 with HCl, buffer B = acetonitrile, buffer C = 5 mM ammonium bicarbonate. Method 1: t = 0 min, 98.5% A 1.5% B; t = 15 min, 98.5% A 1.5% B; t = 30 min, 65% A 35% B; t = 35 min, 65% A 35% B; t = 40 min, 98.5% A 1.5% B; t = 55 min, 98.5% A 1.5% B. Method 2: t = 0 min, 10% C, 90% B; t = 25 min, 10% C, 90% B.

Analytical HPLC conditions: Phenomonex Synergi Polar-RP 250 x 4.6 mm 3 µ analytical column, 1 mL/min; buffer A = 20 mM K_2HPO_4, 0.5 mM EDTA, pH = 7.4 with HCl, buffer B = acetonitrile, buffer C = 5 mM ammonium bicarbonate. Method 3: t = 0 min, 100% A 0% B; t = 3 min, 100% A 0% B; t = 10 min, 85% A 15% B; t = 14 min, 85% A 15% B; t = 16 min, 100% A 0% B; t = 25 min, 100% A 0% B. Method 4: t = 0

min, 100% C 0% B; t = 6 min, 100% C 0% B; t = 10 min, 85% C 15% B; t = 14 min, 85% C 15% B; t = 16 min, 100% C 0% B; t = 25 min, 100% C 0% B. Method 5: t = 0 min, 100% A 0% B; t = 5 min, 100% A 0% B; t = 15 min, 85% A 15% B; t = 30 min, 60% A 40% B; t = 35 min, 60% A 40% B; t = 45 min, 100% A 0% B; t = 55, 100% A 0% B.

Quik-Change PCR of *cmmSu*, Restriction digest of PCR products with DpnI, and transformation into *E. coli*:

Forward (5') and reverse (3') primers were designed and ordered from Sigma Aldrich. Forward primer (c52g_g53c-F): TCTGGGTACGGGAGCCTGTGGGTCGACG. Reverse primer (c52g_g53c-R): CGTCGACCCACAGGCTCCCGTACCCAGA. Two identical 100 µL reactions were prepared for PCR. The reactions consisted of G/C buffer (20 µL, 5x); dNTPs (2 µL, 10 mM); 5'-primer (2 µL, 20 mM); 3'-primer (2 µL, 20 mM); pBS/cmmSu (50 ng/µL); Phusion® DNA polymerase (1 µL); DMSO (5 µL); ddH_2O (60 µL). The reactions were placed in an Eppendorf® PCR thermocycler with the following sequence: Initial denaturation: 2 min, 98 °C; 20x [Denaturation: 20 s, 98 °C; Annealing: 20 s, 60 °C; Extension: 2.5 min, 72 °C]; Final extention: 10 min, 72 °C; Hold temp: 4 °C.

DNA PCR products were recovered in 300 µL ddH_2O and suspended in 500 µL phenol before the solution was vortexed for 10-20 s to precipitate proteins. The sample was centrifuged for 2 min at 14,000 RPM a RT. The aqueous phase of the supernatant was recovered to which was added 50 µL sodium acetate (3 M, pH = 5.2), then 1 mL ethanol before cooled to -20 °C over 20 min. DNA was precipitated by centrifugation at

14,000 RPM for 35 min at 4 °C. The pellet was recovered and washed with 1 mL 70% ethanol and centrifuged at 14,000 RMP at RT for 10 min. The pellet was resuspended in 25 µL ddH_2O to which was added 3 µL NEB buffer 4 and 2 µL Dpn1 and mixed gently. The restriction digestion was incubated at 37 °C for 1 h.

Digested PCR product (10 µL) was added to 100 µL super-competent *E. coli* DH5α (Dr. Rongfeng Li) and agitated gently with a pipette tip before incubation on ice for 30 min. The transformation mixture was heat-shocked at 42 °C for 30 s and cold-shocked for 2 min at 0 °C. 900 µL LB was added to the cells and the transformation mixture was shaken at 37 °C for 1 h. The transformed *E. coli* was pelleted by centrifugation at 14,000 RPM at RT for 10 min, and the pellet was resuspended in 100 µL LB by gentle agitation with a pipette tip. 50 µL of the transformed cell mixture was plated on each of 2 LB plates with ampicillin (100 µg/mL) and incubated for 4 h at 27 °C, then 14 h at 37 °C after which time a multitude of colonies was visible. Ten colonies were picked and each shaken in 6 mL LB overnight at 37 °C containing ampicillin (100 µg/mL). A mini-prep was used to purify the DNA for each sample using the following protocol (mini-prep kit and protocol by Fisher Scientific): 2 mL of each of 10 samples in 2 mL Eppendorf® tubes were centrifuged for 1 min and the supernatant discarded. This step was repeated two more times to recover all 6 mL of culture. The cell pellet was suspended in buffer A (250 µL) to which was added lysis buffer (250 µL) and shaken by hand immediately 20x. Neutralization buffer was then added (350 µL) and shaken hard 20x, after which the mixture was centrifuged at 14,000 RPM to pellet cell debris. The supernatant was recovered and added to 1 mL spin columns (Fisher scientific) and centrifuged for 1 min at 14,000 RPM. The spin columns were washed with washing

buffer (Fisher scientific, 2x, 450 µL) and centrifuged for 1 min at 14,000 RPM, the flow-through was discarded. The spin columns were eluted with 100 µL ddH_2O. Concentration of DNA was found to be 250 ng/µL from analysis by UV absorbance at 260 nm. Each of the ten samples was confirmed by sequencing analysis to ensure the integrity of the PCR products was conserved during amplification, as well as confirmation of the correct mutations, c52g_g53c.

The plasmid was transformed into electro-competent Rosetta 2 *E. coli*. 20 µL of a Rosetta2 competent cells cell stock (Dr. Rongfeng Li) was added to a 1.5 mL Eppendorf® tube to which 1 µL pET28/cmmSu-R18A was added at 0 °C. The mixture was added to an electroporation chamber and placed into a cell porator at 0 °C. The power supply and voltage booster were set to the following parameters: Capacitance = 330, kΩ = 4, Volts = low Ω DC. Once triggered from 300 volts charge, the transformed cells were removed and added to a clean 2 mL Eppendorf® tube and shaken in 1 mL LB for 1 h at 37 °C. The cells were pelleted by centrifugation at 14,000 RPM for 10 min, resuspended in 100 µL LB, and 50 µL were streaked onto each of 2 LB/agar plates with chloroamphenicol (25 µg/mL) and kanamycin (50 µg/mL). Colonies were used for inoculation of starter cultures used for protein expression. A sample of starter culture was suspended in glycerol to a final concentration of 20% and stored long term at -80 °C.

Expression and Purification of CmmSu and CmmSuR18A:

Stock culture of Rosetta2 (pET29/cmmSu or pET29/CmmSuR18A) cells were streaked onto LB agar with kanamycin (50 µg/mL) and chloroamphenicol (25 µg/mL) and grown for 16 h at 30 °C. A single colony was picked and used for the inoculation of

50 mL LB with kanamycin and chloroamphenicol. The seed culture was shaken for 15 h at 30 °C and used to inoculate 5 L LB medium with 100 mg chloroamphenicol (final concentration 20 μg/mL) and 200 mg kanamycin (40 μg/mL). The culture was shaken at 37 °C for 195 min when the optical density at 600 nm (OD_{600}) reached 0.6 absorbance units (AU). The culture was cooled to 0 °C and cold-shocked at this temperature for 2 h. At this time 1.07 g isopropyl β-D-1-thiogalactopyranoside (IPTG) was added and the culture was grown for 24 h at 16 °C. At this time the cell paste was harvested by centrifugation at 4000 g for 12 min at 4 °C and frozen by liquid nitrogen suspension to recover 23 g Rosetta2 (pET29/cmmSu) cells or 28 g Rosetta2 (pET29/cmmSuR18A) cells. To 20 g each of Rosetta2 (pET29/cmmSu) cells and Rosetta2 (pET29/cmmSuR18A) cells was added 80 mL lysis buffer (300 mM NaCl, 50 mM NaH_2PO_4, 10 mM imidazole, 10% v/v glycerol, pH = 8.0) and 160 mg lysozyme. The cells were suspended and incubated on ice for 30 min before sonication for 3 min (6s on 9s off) at 60% amplitude with the large tip. The cell debris was removed by centrifugation at 16,000 rpm for 20 min at 4° C. To the supernatant was added 4 mL Ni resin and incubated for 1 h at 4 °C. The Ni resin was pelleted by centrifugation at 800 g for 10 min at 4 °C. The Ni resin was suspended in 6 mL lysis buffer and loaded into a glass column. The column was washed with 4 mL lysis buffer, then 10 mL wash buffer (300 mM NaCl, 50 mM NaH_2PO_4, 20 mM imidazole, 10% v/v glycerol, pH = 8.0) before elution of the protein with 4 mL elution buffer (300 mM NaCl, 50 mM NaH_2PO_4, 250 mM imidazole, 10% v/v glycerol, pH = 8.0). The eluted protein was loaded to a Bio-Rad P10 column (5 mL) that was pre-washed with 20 mL reaction buffer (50 mM MOPS pH = 7.8 with 10% v/v glycerol). The protein was buffer exchanged by elution from the P10

column with 3 mL reaction buffer. A protein concentration of 103 μM for CmmSu and 146 μM for CmmSuR18A was determined by Bradford assay.

CmmSu Reaction Conditions: 30 μM CmmSu or CmmSuR18A, 800 μM carbapenem substrate, 5 mM $MgCl_2$, 7 mM PAPS, 0.1 mM DTT, 50 mM MOPS, 10% v/v glycerol, pH = 7.8. Reactions were incubated for 2 h at 30 °C before the protein was removed by centrifugation through a 10 kD Amicon filter at 14,000 rpm for 20 min at 4 °C. HPLC samples were taken directly from the filtered reaction media.

Expression and Purification of CmmPah and Cmm17:

Stock of Rosetta2 (pET41/cmmPah or pET29/cmm17) cells were streaked onto LB agar with kanamycin and chloroamphenicol and grown for 16 h at 30 °C. A single colony was picked and used for the inoculation of 50 mL LB with kanamycin (50 μg/mL) and chloroamphenicol (25 μg/mL). The seed culture was grown for 15 h at 30 °C and used to inoculate 5 L LB medium with 100 mg chloroamphenicol (final concentration 20 μg/mL and 200 mg kanamycin (final concentration 40 μg/mL). The culture was shaken at 37 °C for 195 min when the optical density at 600 nm (OD_{600}) reached 0.6 absorbance units (AU). The culture was cooled to 0 °C on ice and cold-shocked at this temperature for 2 h. At this time 1.04 g isopropyl β-D-1-thiogalactopyranoside (IPTG) was added and the culture was shaken for 24 h at 15 °C. At this time the cell paste was harvested by centrifugation at 4000 g for 12 min at 4 °C and frozen by liquid nitrogen suspension to recover 14 g Rosetta2 (pET41/cmmPah) cells and 19 g Rosetta2 (pET29/cmm17) cells. To 7 g each of Rosetta2 (pET41/cmmPah) cells and Rosetta2 (pET29/cmm17) cells was added 35 mL lysis buffer (300 mM NaCl, 50 mM NaH_2PO_4, 10 mM imidazole, 10% v/v

glycerol, pH = 8.0) and 70 mg lysozyme. The cells were suspended and incubated on ice for 30 min before sonication for 3 min (6s on 9s off) at 60% amplitude with a large tip. The cell debris was removed by centrifugation at 16,000 rpm for 20 min at 4 °C. To the supernatant was added 2 mL Ni resin and incubated for 1 h at 4 °C. The Ni resin was pelleted by centrifugation at 1000 g for 10 min at 4 °C. The pellet was suspended in 6 mL lysis buffer and loaded to a column. The column was washed with 15 mL lysis buffer (as above) before elution of the protein with 4 mL elution buffer (300 mM NaCl, 50 mM NaH_2PO_4, 250 mM imidazole, 10% v/v glycerol, pH = 8.0). The eluted protein was loaded to a Bio-Rad P10 column that was pre-washed with 20 mL reaction buffer (50 mM MOPS pH = 7.8 with 10% v/v glycerol). The protein was buffer exchanged by elution from the P10 column with 3 mL reaction buffer. Protein concentrations were determined by Bradford assay.

CmmPah, Cmm17 Dual Assay Conditions: 10 μM CmmPah, 10 μM Cmm17, 900 μM carbapenem substrate, 0.5 mM $MgCl_2$, 0.5 mM $MnCl_2$, 250 μM PAPS, 30 mM MOPS, pH = 7.8. Reactions were incubated for 1 h at ambient temperature before the protein was removed by centrifugation through a 10 kD Amicon filter at 14,000 rpm for 20 min at 4 °C. HPLC samples were taken directly from the filtered reaction medium.

CmmPah, Cmm17, and CmmSu Triple Assay Conditions: 10 μM CmmSu, 10 μM Cmm17, 10 μM CmmPah, 900 μM carbapenem substrate, 0.5 mM $MgCl_2$, 0.5 mM $MnCl_2$, 250 μM PAPS, 30 mM MOPS, pH = 7.8. Reactions were incubated for 1 h at room temperature before the protein was removed by centrifugation through a 10 kD Amicon filter at 14,000 rpm for 20 min at 4 °C. HPLC samples were taken directly from the filtered reaction media.

Synthesis of carbapenems:

***N-tert*-butyldimethylsilyl-(4*R*)-allyl-2-azetidinone (1)**: *N-tert*-butyldimethylsilyl-4(*R*)-allyl-2-azetidinone **1** was prepared from *N-tert*-butyldimethylsilyl-4(*R*)-3-carbomenthyloxy-2-propen-1-yl)-2-azetidinone as described by Ueda *et al.*.[34]. Ozone was passed through a solution of *N-tert*-buyldimethylsilyl-4(*R*)-3-carbomenthyloxy-2-propen-1-yl)-2-azetidinone (12.96, 31.7 mmol) in dichloromethane (300 mL) at -78 °C until the blue color persisted. Argon was then passed through the solution at -78 °C until colorless. The solution was warmed to 0 °C to which was added dimethylsulfide (35 mL) and stirred for 70 min at 0 °C. The solution was washed twice with H_2O and then with brine. The organic extract was dried with anhydrous sodium sulfate, filtered, and concentrated *in vacuo*. In a separate flask, *n*-butyllithium in hexane (45 mL, 2.2 M, 100 mmol) was added to diisopropylamine (13.95 mL, 100 mmol) in tetrahydrofuran (775 mL) at 0 °C and stirred for 20 min at which time was added methyltriphenylphosphonium bromide (35.5 g, 100 mmol). The mixture was stirred for 1 h at ambient temperature. The ylid solution was cooled at 0 °C to which was slowly added the ozonolysis product crude oil and upon completion was stirred for 2 h at ambient temperature. Diethyl ether (300 mL) was added to the reaction mixture and it was quenched with saturated ammonium bicarbonate (120 mL). The phases were separated and the aqueous layer was extracted twice with diethyl ether (100 mL). The combined organic extracts were washed with brine (150 mL), dried with anhydrous sodium sulfate, filtered and concentrated *in vacuo*. The crude oil was purified by silica gel chromatography (hexanes:Et_2O, 9:1) to afford **1** (3.28g, 52%). ^{1}H-NMR (400 MHz, $CDCl_3$): δ 5.78-5.68 (m, 1H), 5.14-5.08 (m, 2H), 3.58 (ddt, J = 9.2, 5.9, 3.1 Hz, 1H), 3.41 (td, J = 10.4, 4.3 Hz, 1H), 3.09 (dd, J =

15.4, 5.4 Hz, 1H) 2.66 (dd, *J* = 15.4, 2.7 Hz, 1H), 2.62-2.56 (m, 1H), 2.21-2.13 (m, 1H), 0.971 (s, 9H), 0.250 (s, 3H), 0.226 (s, 3H). ^{1}H NMR data matched the spectrum reported in the literature[34].

***N-tert*-butyldimethylsilyl-(3*S*)-((1*R*)-hydroxyethyl)-(4*R*)-allyl-2-azetidinone (2a), *N-tert*-butyldimethylsilyl-(3*S*)-((1*S*)-hydroxyethyl)-(4*R*)-allyl-2-azetidinone (2b), *N-tert*-butyldimethylsilyl-(3*R*)-((1*S*)-hydroxyethyl)-(4*R*)-allyl-2-azetidinone (2)**: The synthesis of **2a**, **2b**, and **2c** from **1** was modified from the procedure of Bateson *et al.*.[35]. A solution of *n*-butyllithium in hexanes (11.6 mL, 2.11 M, 24.4 mmol) was added to a solution of diisopropylamine (3.44 mL, 24.4 mmol) in THF (60 mL) at -78 ºC and stirred for 30 min. A solution of **1** (2.5 g, 11.1 mmol) in THF (20 mL) was slowly added to the LDA mixture by addition funnel over 30 min during which time the solution became red. This solution was stirred at -78 ºC for an additional 30 min. Then a solution of acetaldehyde (5 mL, 89.7 mmol) in THF (5 mL) was cooled to -78 ºC and then added slowly by addition funnel and stirred at -78 ºC for 30 min during which time the solution became colorless. At this temperature the reaction was then quenched with acetic acid (5 mL) in THF (20 mL) and the mixture was stirred for 15 min at room temperature. The solution was then diluted with brine and extracted with ethyl acetate (3 × 100 mL). The organic layer was dried with anhydrous sodium sulfate, filtered and concentrated *in vacuo*. The oily residue was purified by silica gel chromatography (hexanes:EtOAc, 8:2) to give the diastereomers **2a** (320 mg, 11%), **2b** (480 mg, 17%), and **2** (344.8 mg, 12%). ^{1}H-NMR (400 MHz, $CDCl_3$) **2a**: δ 5.83-5.66 (m, 1H), 5.18-5.12 (m, 2H), 3.75 (ddd, *J* = 11.2, 6.2, 2.4 Hz, 1H), 3.61 (ddd, *J* = 9.5, 3.4, 2.6 Hz, 1H), 2.88 (dd, *J* = 5.2, 2.5, 1H), 2.62 (dtd, *J* = 5.1, 3.4, 1.6, 1H), 2.35-2.34 (m, 1H), 2.22-2.15 (m, 1H), 1.38 (d, *J* = 5.1

Hz, 3H), 0.96 (s, 9H), 0.27 (s, 3H), 0.22 (s, 3H).**2b**: δ 5.83-5.66 (m, 1H), 5.18-5.12 (m, 2H), 3.98 (td, *J* = 6.6, 3.3 Hz, 1H), 3.41 (ddd, *J* = 9.7, *3*.6, 2.5 Hz, 1H), 2.84 (dd, *J* = 7.1, 2.5 Hz, 1H), 2.57 (dddt, *J* = 6.7, 4.0, 2.8, 1.4 Hz, 1H), 2.34 (d, *J* = 3.7 Hz, 1H), 2.27-2.21 (m, 1H), 1.29 (d, *J* = 5.2 Hz, 3H), 0.96 (s, 9H), 0.26 (s, 3H), 0.21 (s, 3H). **2**: δ 5.69 (dq, *J* = 17.2, 8.6 Hz, 1H), 5.13-5.07 (m, 2H), 3.95 (quintet, *J* = 6.4 Hz, 1H), 3.39 (d, *J* = 9.5 Hz, 1H), 2.81 (dd, *J* = 6.7, 2.3 Hz, 1H), 2.53 (dd, *J* = 6.6, 6.0 Hz, 1H), 2.17 (dt, *J* = 14.0, 8.1 Hz, 1H), 1.21 (d, *J* = 6.3 Hz, 3H), 0.92 (s, 9H), 0.2166 (s, 3H), 0.17 (s, 3H). ^{1}H NMR data matched the spectrum reported in the literature[35].

***N-tert*-butyldimethylsilyl-(3*S*)-[(1*R*)-*p*-nitrobenzyloxycarbonyloxyethyl)-(4*R*)-allyl-2-azetidinone (3a), *N-tert*-butyldimethylsilyl-(3*S*)-((1*S*)-*p*-nitro-benzyl-oxy-carbonyl-oxyethyl)-(4*R*)-allyl-2-azetidinone (3b):** Dimethylaminopyridine (DMAP) was added to the diasteromeric alcohols **2a** and **2b** (720 mg, 2.97 mmol) in dichloromethane (3 mL) at 0 °C. A solution of *p*-nitrobenzylchloroformate (768 mg, 3.56 mmol) in dichloromethane (3 mL) was added to the reaction mixture at 0 °C and was allowed to stir for 1 h at this temperature. The reaction was diluted with dichloromethane (50 mL) and water (10 mL). The phases were separated and the aqueous layer was extracted with dichloromethane (10 mL). The combined organic fractions were washed with brine (20 mL) and dried with anhydrous sodium sulfate, filtered, and concentrated *in vacuo*. The crude oil was purified by silica gel chromatography (hexanes:EtOAc, 8:2) to yield **3a** and **3b** as a mixture of diastereomers (799 mg, 67%). ^{1}H-NMR (400 MHz, $CDCl_3$) **3a**: δ 8.23 (d, *J* = 8.7 Hz, 2H), 7.53 (d, *J* = 8.8 Hz, 2H), 5.77-5.65 (m, 1H), 5.28 (s, 1H), 5.23 (s, 2H), 5.16-5.08 (m, 1H), 5.03 (dd, *J* = 6.5, 4.6 Hz, 2H), 3.61 (dt, *J* = 9.4, 3.0 Hz, 1H), 3.01 (dd, *J* = 6.3, 2.6 Hz, 1H), 2.62-2.56 (m, 1H), 2.20 (td, *J* = 15.1, 8.2 Hz, 1H), 1.38 (d, *J* =

6.4 Hz, 3H), 0.96 (s, 9H), 0.27 (s, 3H), 0.20 (s, 3H). **3b**: δ 8.23 (d, *J* = 8.7 Hz, 2H), 7.53 (d, *J* = 8.8 Hz, 2H), 5.77-5.65 (m, 1H), 5.28 (s, 1H), 5.23 (s, 2H), 5.16-5.08 (m, 1H), 5.03 (dd, *J* = 6.5, 4.6 Hz, 1H), 3.46 (dt, *J* = 9.4, 3.0 Hz, 1H), 3.11 (dd, *J* = 4.5, 2.7 Hz, 1H), 2.62-2.56 (m, 1H), 2.20 (td, *J* = 15.1, 8.2 Hz, 1H), 1.43 (d, *J* = 6.5 Hz, 3H), 0.96 (s, 9H), 0.27 (s, 3H), 0.20 (s, 3H).

***N*-*tert*-butyldimethylsilyl-3(*R*)-[1(*S*)-*p*-nitro-benzyl-oxy-carbonyloxy-ethyl]-4(*R*)-allyl-2-azetidinone (3). 3** was synthesized from **2** following the procedure described above for **3a** and **3b**. The crude oil was purified by silica gel chromatography (hexanes:EtOAc, 8:2) to yield **3** as a colorless oil (760 mg, 43%). ^{1}H-NMR (400 MHz, $CDCl_3$) **3**: δ 8.23 (d, *J* = 8.7 Hz, 2H), 7.54 (d, *J* = 8.7 Hz, 2H), 5.76-5.66 (m, 1H), 5.26 (q, *J* = 16.0 Hz, 2H), 5.13-5.08 (m, 2H), 5.02 (dd, *J* = 17.2, 1.5 Hz, 1H), 3.77 (dt, *J* = 10.7, 5.1 Hz, 1H), 3.39 (dd, *J* = 5.7, 3.2 Hz, 1H), 2.47 (qd, *J* = 16.7, 7.9 Hz, 2H), 1.48 (d, *J* = 6.4, 3H), 0.97 (s, 9H), 0.27 (s, 3H), 0.22 (s, 3H).

(3*S*)-[(1*R*)-*p*-nitro-benzyl-oxy-carbonyl-oxy-ethyl]-(4*R*)-allyl-2-azetidinone (4a), (3*S*)-[(1*S*)-*p*-nitro-benzyl-oxy-carbonyl-oxy-ethyl]-hydroxyethyl)-(4*R*)-allyl-2-azetidinone (4b): A solution of HF/pyridine (6 mL) in pyridine (2 mL) was added to a solution of **3a** and **3b** (2.00 g, 4.46 mmol) in THF (50 mL) at 0 °C. The reaction mixture was stirred for 10 min before it was quenched with saturated ammonium chloride. The reaction was diluted with ethyl acetate and the organic layer was washed with saturated ammonium chloride. The combined aqueous fractions were washed with ethyl acetate. The combined organic phase was washed with brine and dried with anhydrous sodium sulfate, filtered, and concentrated *in vacuo*. The crude oil was purified by silica gel chromatography (hexanes:EtOAc, 7:3) to yield **4a** and **4b** as a mixture of inseparable

diastereomers (990 mg, 66%). Further purification can be achieved by crystallization from ethyl acetate and hexanes. Melting point = 119-122 °C. ^{1}H-NMR (400 MHz, $CDCl_3$) **4a**: δ 8.21 (d, *J* = 8.8 Hz, 2H), 7.52 (d, *J* = 8.9 Hz, 2H), 6.26-6.20 (br s, 1H), 5.7 (ddt, *J* = 17.1, 10.0, 7.1 Hz, 1H), 5.23 (s, 2H), 5.15-5.05 (m, 3H), 3.67 (td, *J* = 6.6, 2.2 Hz, 1H), 2.98 (ddd, *J* = 7.2, 2.3, 0.9 Hz, 1H), 2.39-2.33 (m, 2H), 1.41 (d, *J* = 6.3 Hz, 3H). **4b**: δ 8.21 (d, *J* = 8.8 Hz, 2H), 7.54 (d, *J* = 8.9 Hz, 2H), 6.26-6.20 (br s, 1H), 5.7 (ddt, *J* = 17.1, 10.0, 7.1 Hz, 1H), 5.23 (s, 2H), 5.15-5.05 (m, 3H), 3.55 (td, *J* = 6.6, 2.4 Hz, 1H), 3.09 (ddd, *J* = 5.1, 2.3, 1.0 Hz, 1H), 2.39-2.33 (m, 2H), 1.43 (d, *J* = 6.4 Hz, 3H). ^{13}C-NMR (101 MHz, $CDCl_3$) **4a**: δ 166.4, 154.1, 147.8, 142.3, 132.7, 128.3, 123.8, 118.6, 72.9, 67.9, 60.7, 51.4, 39.1, 18.5. **4b**: δ 166.4, 154.2, 147.8, 142.3, 132.7, 128.3, 123.8, 118.6, 72.1, 67.9, 59.6, 49.8, 38.8, 17.4. FAB MS: MH^+: calc = 335.1238, found = 335.1251.

3(*R*)-[1(*S*)-(*p*-nitrobenzyloxycarbonyloxy)ethyl]-4(*R*)-allyl-2-azetidinone (4): **4** was synthesized from **3** following the procedure described above for **4a** and **4b**.The crude oil was purified by silica gel chromatography with (hexanes:EtOAc, 7:3) to yield **4** (500 mg, 88%). Further purification can be achieved by recrystallization from ethyl acetate and hexanes. Melting point = 93-95 ºC. ^{1}H-NMR (400 MHz, $CDCl_3$) **4**: δ 8.21 (d, *J* = 8.8 Hz, 2H), 7.52 (d, *J* = 8.9 Hz, 2H), 6.26-6.20 (br s, 1H), 5.7 (ddt, *J* = 17.1, 10.0, J_3 = 7.1 Hz, 1H), 5.23 (s, 2H), 5.15-5.05 (m, 3H), 3.67 (td, *J* = 6.6, 2.2 Hz, 1H), 2.98 (ddd, *J* = 7.2, 2.3, 0.9 Hz, 1H), 2.39-2.33 (m, 2H), 1.41 (d, *J* = 6.3 Hz, 3H). ^{13}C-NMR (101 MHz, $CDCl_3$) **4**: δ 166.7, 154.1, 142.5, 133.2, 128.2, 123.7, 118.2, 71.0, 67.9, 56.6, 50.4, 35.0, 19.8. FAB MS: MH^+: calc = 335.1238, found = 335.1248.

(3*S*)-[(1*R*)-(*p*-nitrobenzyloxycarbonyloxy)ethyl]-(4*R*)-carboxymethyl-2-azetidinone

(5a), (3*S*)-[(1*S*)-(*p*-nitrobenzyloxycarbonyloxy)ethyl]-(4*R*)-carboxymethyl-2-azetidinone (5b): Ozone was passed through a solution of **4a** and **4b** (280 mg, 0.838 mmol) in dichloromethane (6.03 mL) and methanol (4.02 mL) at -78 ºC until blue. Nitrogen was bubbled through the solution until it turned colorless, at which point the temperature was raised to 0 ºC and dimethylsulfide (838 µL) was added. After stirring for 1 h at 0 ºC, the solution was washed with H_2O and the organic layer was dried with anhydrous sodium sulfate, filtered and concentrated *in vacuo*. The crude foam was dissolved in *tert*-butyl alcohol (7 mL) to which was then added 2-methyl-2-butene (3 mL) and a solution of monosodium phosphate (347 mg, 2.51 mmol) and sodium chlorite (227 mg, 2.51 mmol) in H_2O (7 mL) at ambient temperature. After 1 h the reaction was concentrated *in vacuo* to remove the *tert*-butyl alcohol, diluted with water, and acidified to pH = 2 with 1 M HCl in saturated sodium chloride. The aqueous mixture was extracted 5 times with ethyl acetate (5 mL) and the combined organic fractions were dried with anhydrous sodium sulfite, filtered, and concentrated *in vacuo*. **5a** and **5b** were purified by crystallization from ethyl acetate and diethyl ether to yield white crystals (306 mg, 99%). ^{1}H-NMR (400 MHz, $CDCl_3$) **5a**: δ 8.24 (d, *J* = 8.8 Hz, 2H), 7.54 (d, *J* = 8.7 Hz, 2H), 6.59 (br s, 1H), 5.25 (s, 2H), 5.14 (dt, 1H, *J* = 12.8, *J* = 6.2), 3.94 (ddd, *J* = 9.8, 3.7, 2.5 Hz, 1H), 3.04 (dd, *J* = 7.4, 2.3 Hz, 1H), 2.80 (t, *J* = 4.4, 1H), 2.57 (d, *J* = 10.8 Hz, 1H), 1.45 (d, *J* = 6.4 Hz, 3H). **5b**: δ 8.24 (d, *J* = 8.8 Hz, 2H), 7.55 (d, *J* = 8.7 Hz, 2H), 6.59 (br s, 1H), 5.25 (s, 2H), 5.14 (dt, *J* = 11.8, 6.2 Hz, 1H), 3.82 (ddd, *J* = 9.3, 4.1, 2.6 Hz, 1H), 3.14 (dd, *J* = 4.6, 2.3 Hz, 1H), 2.75 (t, *J* = 4.4 Hz, 1H), 2.63 (t, *J* = 10.2 Hz, 1H), 1.47 (d, *J* = 6.5 Hz, 3H). FAB MS MH^+ calc = 353.0979, found = 353.0983.

3(*R*)-[1(*S*)-(*p*-nitrobenzyloxycarbonyloxy)ethyl]-4(*R*)-carboxymethyl-2-azetidinone

(5): **5** was synthesized from **4** following the procedure described above for **5a** and **5b**. **5** were purified by crystallization from ethyl acetate and diethyl ether to yield white solid crystals (297 mg, 56%). ^{1}H-NMR (400 MHz, $CDCl_3$) **5**: δ 8.19 (d, *J* = 8.7 Hz, 2H), 7.54 (d, *J* = 8.8 Hz, 2H), 6.44 (br s, 1H), 5.26 (q, *J* = 19.2 Hz, 2H), 5.04 (quintet, *J* = 5.7 Hz, 2H), 4.06 (q, *J* = 6.3 Hz, 1H), 3.45 (t, *J* = 4.5 Hz, 1H), 2.64 (d, *J* = 7.1 Hz, 2H), 1.47 (d, *J* = 6.4 Hz, 3H). ^{13}C-NMR (101 MHz, $CDCl_3$) **5**: δ 174.7, 168.5, 153.9, 147.8, 142.4, 128.4, 123.8, 71.0, 68.1, 56.3, 47.7, 34.5, 19.5. FAB MS MH^+: calc = 353.0979, found = 353.0985.

(3*S*)-[(1*R*)-(*p*-nitrobenzyloxycarbonyloxy)ethyl]-(4*R*)-(3-*p*-nitrobenzyloxycarbonyl-2-oxopropyl)-2-azetidinone 6a and (3*S*)-[(1*S*)-(*p*-nitrobenzyloxycarbonyloxy)ethyl]-(4*R*)-(3-*p*-nitrobenzyloxycarbonyl-2-oxopropyl)-2-azetidinone 6b: **6a** and **6b** was synthesized from **5a** and **5b** following the procedures of Salzmann *et al.*[36]. Carbonyldiimidazole (169 mg, 1.042 mmol) was added to **5a** and **5b** (306 mg, 0.869 mmol) in a solution of acetonitrile (8.7 mL) at ambient temperature. After stirring for 1 h, the magnesium salt of the mono-*p*-nitrobenzyl ester of malonic acid (435 mg, 0.869 mmol) was added and the resulting mixture was stirred for 16 h at ambient temperature. The reaction mixture was diluted with ethyl acetate and washed three times with 1N HCl (25 mL). The organic layer was washed with brine (50 mL), dried with anhydrous sodium sulfate, filtered, and concentrated *in vacuo*. The crude oil was purified by silica gel chromatography (hexanes:EtOAc, 7:3 to 3:7) to yield **6a** and **6b** as a mixture of inseparable diastereomers (270 mg, 59%). ^{1}H-NMR (400 MHz, $CDCl_3$) **6a**: δ 8.20 (d *J* = 8.8 Hz, 4H), 7.52 (m, 4H), 6.27 (br s, 1H), 5.25 (s, 2H), 5.23 (s, 2H), 5.12 (quintet, *J* = 12.4 Hz, 1H), 3.95 (ddd, *J* = 9.0, 4.1, 2.4 Hz, 1H), 3.56 (s, 2H), 3.08-2.97 (m, 2H), 2.84

(dd, J =18.2, 8.9 Hz, 1H), 1.42 (d, J = 6.4 Hz, 1H). **6b**: δ 8.20 (d, J = 8.8 Hz, 4H), 7.54-7.49 (m, 4H), 6.24 (br s, 1H), 5.25 (s, 2H), 5.24 (s, 2H), 5.12 (quintet, J = 12.4 Hz, 1H), 3.84 (ddd, J = 8.4, 4.7, 2.6 Hz, 1H), 3.57 (s, 2H), 3.08-2.97 (m, 2H), 2.84 (dd, J = 18.2, 8.9 Hz, 1H), 1.44 (d, J = 6.5 Hz, 3H). FAB MS MH^+ calc = 530.1405, found = 530.1399. ^{1}H NMR data matched the spectrum reported in the literature[36].

(3*R*)-((1*S*)-*p*-nitrobenzyloxycarbonyloxyethyl)-(4*R*)-[3-(*p*-nitrobenzyloxycarbonyl-2-oxo)propyl]-2-azetidinone 6: **6** was synthesized from **5** following the procedure described above for **6a** and **6b**[5]. 1,1-Carbonyldiimidazole (169 mg, 1.042 mmol) was added to **5** (306 mg, 0.869 mmol) in a solution of acetonitrile (8.7 mL) at ambient temperature. After stirring for 1 h, the magnesium salt of the malonic acid mono-*p*-nitrobenzyl ester (435 mg, 0.869 mmol) was added and the resulting mixture was stirred for 16 h at ambient temperature. The reaction mixture was diluted with ethyl acetate and washed three times with 1 N HCl (25 mL). The organic layer was washed with brine (50 mL), dried with anhydrous sodium sulfate, filtered and concentrated *in vacuo*. The crude oil was purified by silica gel chromatography (hexanes:EtOAc, 7:3 to 3:7) to yield **6** (270 mg, 59%). ^{1}H-NMR (400 MHz, $CDCl_3$) **6**: δ 8.18 (d, J = 8.8 Hz, 2H), 8.16 (d, J = 8.8 Hz, 2H), 7.52 (d, J = 8.8 Hz, 2H), 7.48 (d, J = 8.8 Hz, 2H), 6.49 (br s, 1H), 5.27 (s, 2H), 5.22 (s, 2H), 5.01-4.95 (m, 1H), 4.10 (dt, J = 13.8, 6.7 Hz, 1H), 3.50 (s, 2H), 3.44 (t, J = 4.3 Hz, 1H), 2.97-2.91 (m, 2H), 1.44 (d, J = 6.4 Hz, 3H). ^{1}H NMR data matched the spectrum reported in the literature[5].

(4*R*)-(3-Diazo-3-*p*-nitro-benzyl-oxy-carbonyl-2-oxopropyl)-(3*S*)-[(1*R*)-*p*-nitro-benzyl-oxy-carbonyl-oxy-ethyl]-2-azetidinone 7a and (4*R*)-(3-Diazo-3-*p*-nitro-benzyl-oxy-carbonyl-2-oxopropyl)-(3*S*)-[(1*S*)-*p*-nitro-benzyl-oxy-carbonyl-oxy-

ethyl]-2-azetidinone 7b: **7a** and **7b** was synthesized from **6a** and **6b** following the procedures of Kametani *et al.*[5]. Methanesulfonylazide (69 mg, 0.57 mmol) was added to **6a** and **6b** (270 mg, 0.51 mmol) in a solution of acetonitrile (10.8 mL) at ambient temperature. A solution of diisopropylethylamine (319 μL, 1.84 mmol) in acetonitrile (3 mL) was added and the reaction mixture was stirred for 1.5 h. The reaction mixture was concentrated *in vacuo* and the resulting crude oil was purified by silica gel chromatography (hexanes:EtOAc, 1:1 to 8:2) to yield **7a** and **7b** as a mixture of inseparable diastereomers (188 mg, 66%). ^{1}H-NMR (400 MHz, $CDCl_3$) **7a**: δ 8.25-8.21 (m, 4H), 7.55 (d, *J* = 8.7 Hz, 4H), 6.03 (br s, 1H), 5.36 (s, 2H), 5.24 (d, *J* = 2.8 Hz, 2H), 5.16 (q, *J* = 11.6 Hz, 1H), 4.00 (ddd, *J* = 9.3, 4.0, 2.1 Hz, 1H), 3.25 (t, *J* = 5.0 Hz, 2H), 3.14-2.96 (m, 2H), 1.45 (d, *J* = 7.2 Hz, 3H). **7b**: δ 8.26 (d, *J* = 8.6 Hz, 2H), 8.24 (d, *J* = 8.4 Hz, 2H), 7.54 (d, *J* = 8.8 Hz, 4H), 6.00 (br s, 1H), 5.36 (s, 2H), 5.25 (d, *J* = 2.9 Hz, 2H), 5.16 (dt, *J* = 12.9, 6.6 Hz, 1H), 3.85 (ddd, *J* = 8.7, 4.2, 2.7 Hz, 1H), 3.30 (t, *J* = 5.0 Hz, 1H), 3.17 (dd, *J* = 4.6, 2.4 Hz, 1H), 3.11-3.04 (m, 1H), 1.47 (d, *J* = 6.6 Hz, 3H). ^{1}H NMR data matched the spectrum reported in the literature[5].

(4*R*)-(3-Diazo-3-*p*-nitrobenzyloxycarbonyl-2-oxopropyl)-(3*R*)-[(1*S*)-(*p*-nitro-benzyl-oxy-carbonyl-oxy)ethyl]-2-azetidinone 7: **7** was synthesized from **6** following the procedure described above for **7a** and **7b**. The resulting crude oil was purified by silica gel chromatography (hexanes:EtOAc, 1:1 to 8:2) to yield **7** (270 mg, 61%). ^{1}H-NMR (400 MHz, $CDCl_3$) **7**: δ 8.24 (d, *J* = 8.8 Hz, 2H), 8.22 (d, *J* = 8.7 Hz, 2H), 7.54 (d, *J* = 8.8 Hz, 2H) 7.50 (d, *J* = 8.8 Hz, 2H), 6.00 (br s, 1H), 5.30 (d, *J* = 5.8 Hz, 2H), 5.26 (s, 2H), 5.09 (qd, $_1$ = 6.2, 4.5 Hz, 1H), 4.17 (ddd, *J* = 9.5, 5.4, 3.9 Hz, 1H), 3.47 (td, *J* = 5.1, 1.7 Hz, 1H), 3.27 (dd, *J* = 18.2, 3.9 Hz, 1H), 3.15 (dd, *J* = 18.2, 9.4 Hz, 1H), 1.50 (d, *J* = 6.4

Hz, 3H). ^{1}H NMR data matched the spectrum reported in the literature[5].

***p*-Nitrobenzyl (5*R*), (6*S*)-[(1*S*)-(*p*-nitro-benzyl-oxy-carbonyl-oxy)ethyl]-3,7-dioxo-1-azabicyclo[3.2.0]heptane-2-carboxylate 8.** **8** was synthesized from **7c** following the procedures of Kametani *et al.*[5]. A catalytic amount of rhodium (II) acetate was added to **7c** (78 mg, 0.140 mmol) in a solution of benzene (6 mL) at 80 ºC and was stirred for 30 min. The reaction mixture was filtered through Celite and concentrated *in vacuo* to yield **8** as a white foam (75 mg, 99%). ^{1}H-NMR (400 MHz, $CDCl_3$) **8**: δ 8.25 (d, J = 7.3 Hz, 4H), 7.54 (d, J = 8.6 Hz, 4H), 5.31 (q, J = 11.3 Hz, 2H), 5.24 (s, 2H), 5.12 (dt, J = 12.8, 6.5 Hz, 2H), 4.74 (s, 1H), 4.30 (dd, J = 13.1, 7.6 Hz, 1H), 3.85 (t, J = 6.0 Hz, 1H), 2.72 (dd, J = 18.6, 8.0 Hz, 1H), 2.61 (dd, J = 19.1, 7.8 Hz, 1H), 1.47 (d, J = 6.3 Hz, 3H). ^{1}H NMR data matched the spectrum reported in the literature[5].

***p*-Nitrobenzyl (5*R*)-(2-Acetamidoethylthio)-(6*R*)-[(1*S*)-1-(*p*-nitro-benzyl-oxy-carbonyl-oxy)ethyl]-7-oxo-1-azabicyclo-[3.2.0]hept-2-ene-2-carboxylate 9.** **9** was synthesized from **8** following the procedures of Kametani *et al.*[5]. Diisopropylethylamine (37 µL, 0.213 mmol) was added to **8** (75 mg, 0.142 mmol) in acetonitrile (1.23 mL) at 0 ºC. Diphenylchlorophosphate (36 µL, 0.174 mmol) was added, and after stirring for 1 h at 0 ºC solutions of diisopropylethylamine (37 µL, 0.213 mmol) in acetonitrile (1 mL) and *N*-acetylcysteamine (21 µL, 0.198 mmol) in acetonitrile (1 mL) were added. After 1 h of stirring at 0 ºC, the reaction was diluted with ethyl acetate (20 mL) and washed three times with 100 mmol K_2HPO_4 pH = 7.0 (20 mL). The organic layer was washed with brine and dried with anhydrous sodium sulfite, filtered, and concentrated *in vacuo*. The crude oil was purified by silica gel chromatography (DCM:MeOH, 97:3) to give **9** (51 mg, 57%) as a yellow oil. ^{1}H-NMR (400 MHz, $CDCl_3$) **9**: δ 8.19 (d, J = 8.4 Hz, 2H), 8.18

(d, J = 8.5 Hz, 2H), 7.62 (d, J = 8.5 Hz, 2H), 7.53 (d, J = 8.7 Hz, 2H), 5.94 (br t, J = 5.6 Hz, 1H), 5.35 (q, J = 13.7 Hz, 2H), 5.22 (dd, J = 9.2, 4.8 Hz, 2H), 5.15 (dt, J = 13.5, 6.7 Hz, 1H), 4.32 (td, J = 9.4, 6.1 Hz, 1H), 3.77 (dd, J = 7.5, 6.3 Hz, 1H), 3.31 (dd, J = 17.9, 9.7 Hz, 1H), 3.14 (dd, J = 18.1, Hz, 1H), 3.00 (dt, J_1 = 13.3, J_2 = 6.8 Hz, 2H), 2.88-2.80 (m, 1H), 2.65 (q, J = 7.4 Hz, 2H), 1.95 (s, 3H), 1.43 (d, J = 6.3 Hz, 3H). ^{1}H NMR data matched the spectrum reported in the literature[5].

***p*-Nitrobenzyl (5*R*)-[2-(*N*-(3-amino-3-oxopropyl)-3,3-dimethyl-(2*R*),4-bis((triethylsilyl)oxy)butanamide)ethylthio]-(6*R*)-[(1*S*)-1-(*p*-nitro-benzyl-oxy-carbonyl-oxy)ethyl]-7-oxo-1-azabicyclo-[3.2.0]hept-2-ene-2-carboxylate 10:** **10** was synthesized from **8** following the procedure described above for **9**[5]. The crude oil was purified by silica gel chromatography (DCM:MeOH, 97:3) to give **10** (108 mg, 47%) as a colorless oil. ^{1}H-NMR (400 MHz, $CDCl_3$) **10**: δ 8.27-8.20 (m, 4H), 7.66-7.50 (m, 4H), 6.74 (br s, 1H), 6.26 (br s, 1H), 5.39 (q, J = 13.9 Hz, 2H), 5.28-5.22 (m, 3H), 4.37-4.10 (m, 1H), 4.01 (s, 1H), 3.62-3.42 (m, 6H), 2.81 (t, J = 6.4 Hz, 2H), 2.5 (t, J = 6.0 Hz, 2H), 1.44 (d, J = 6.3 Hz, 3H), 1.02-0.94 (m, 18H), 0.67-0.59 (m, 12H). HRMS (ESI), $C_{34}H_{39}N_5O_{14}S$ [M+H$^+$] calculated: 1002.4022; found: 1002.4089.

***p*-Nitrobenzyl (5*R*)-[2-(*N*-(3-amino-3-oxopropyl)-3,3-dimethyl-(2*R*),4-butanamide)ethylthio]-(6*R*)-[(1*S*)-1-(*p*-nitrobenzyloxycarbonyloxy)ethyl]-7-oxo-1-azabicyclo-[3.2.0]hept-2-ene-2-carboxylate 11.** Acetic acid (24 µL, 0.426 mmol) was added to **10** (108 mg, 0.106 mmol) in tetrahydrofuran (3 mL) at 0 ºC. A solution of tetrabutylammonium fluoride in tetrahydrofuran (234 µL, 1M, 0.234 mmol) was added, and after stirring for 1 h at 0 ºC the reaction was diluted with ethyl acetate (20 mL) and washed two times with water (10 mL). The organic layer was washed with brine and

dried with anhydrous sodium sulfate, filtered, and concentrated *in vacuo*. The crude oil was purified by silica gel chromatography (DCM:MeOH, 95:5) to give **11** (29 mg, 37%) as a colorless oil. ^{1}H-NMR (400 MHz, MeOD) **11**: δ 8.11 (d, J = 8.8 Hz, 2H), 8.11 (d, J = 8.9 Hz, 2H), 7.61 (d, J = 8.8 Hz, 2H), 7.52 (d, J = 8.8 Hz, 2H), 5.21 (s, 2H), 5.20 (ABq, J_{AB} = 13.8 Hz, 2H), 5.17-5.10 (m, 1H), 4.29 (td, J = 9.4, 6.0 Hz, 1H), 3.82-3.79 (m, 2H), 3.79 (s, 1H), 3.44-3.33 (m, 4H), 3.32 (ABq, J_{AB} = 11.0 Hz, 2H), 2.92 (dt, J = 13.5, 6.7 Hz, 1H), 2.82 (dt, J = 13.7, 7.0 Hz, 2H), 2.32 (t, J = 6.6 Hz, 1H), 1.36 (d, J = 6.3 Hz, 3H). ^{13}C-NMR (101 MHz, MeOD) **11**: 175.7, 174.6, 172.6, 160.7, 147.5, 143.7, 142.9, 128.2, 127.8, 123.2, 123.1, 75.9, 71.8, 68.9, 67.8, 64.7, 60.1, 56.8, 52.4, 39.4, 39.0, 35.4, 35.0, 34.9, 19.9, 19.5, 19.4, 17.9, 13.0. HRMS (ESI), $C_{34}H_{39}N_5O_{14}S$ [M+H$^+$] calculated: 774.2292; found: 774.2291.

(5*R*)-(2-Acetamidoethylthio)-(6*R*)-[(1*S*)-1-hydroxyethyl]-7-oxo-1-azabicyclo-[3.2.0]hept-2-ene-2-carboxylate (epithienamycin A) 12: 12 was synthesized from **9** following the procedures of Kametani *et al.*[5]. A small scoop of palladium hydroxide (50 mg, 50% suspension in water) was added to a solution of **11** in tetrahydrofuran (5 mL) and aqueous sodium bicarbonate (5 mL, 0.0319M) in a bomb flask. The flask was fitted to a Parr-shaker apparatus to which hydrogen was added to 40 psi. The reaction mixture was shaken for 1 h and the mixture was filtered through Celite and washed with diethyl ether (10 mL). The aqueous layer was collected and purified immediately by HPLC (semi preparatory C18, method 2). The desired peak eluted at 10 min and was collected and lyophilized to yield **12** as a white powder. ^{1}H NMR (400 MHz, D_2O) δ ppm 4.22-4.35 (m, 1H), 4.18 (dd, J = 8.3, 6.4 Hz, 1H), 3.61 (dd, J = 8.4, 5.7 Hz, 1H), 3.40 (t, J = 6.6 Hz, 2H), 3.12 (quin, J = 8.6 Hz, 1H), 3.02 (ddd, J = 13.4, 8.6, 6.5, 1H), 2.89 (ddd, J =

13.9, 11.8, 6.8, 1H), 2.66-2.82 (m, 1H), 1.99 (s, 3H), 1.25 (d, *J* = 6.3 Hz, 3H). ^{1}H NMR matched the spectrum reported in the literature[5].

(5*R*)-[2-(*N*-(3-amino-3-oxopropyl)-3,3-dimethyl-(2*R*),4-butanamide)ethylthio]-(6*R*)-[(1*S*)-1-(hydroxy)ethyl]-7-oxo-1-azabicyclo-[3.2.0]hept-2-ene-2-carboxylate (OA6129-B$_1$) 13: **13** was synthesized from **11** following the procedure described above for **12**[5]. The peak eluted at 10 min (method 2), was collected and lyophilized to yield 1.9 mg **13** as a white powder. ^{1}H-NMR (400 MHz, D_2O) **13**: δ 4.20 (dt, *J* = 12.3, 6.6 Hz, 2H), 3.49 (s, 1H), 3.50-3.47 (m, 2H), 3.40-3.30 (m, 2H), 3.27 (dd, *J* = 17.6, 9.8 Hz, 2H), 3.11 (dd, *J* = 17.3, 9.0 Hz, 1H), 2.99 (dt, *J* = 13.4, 6.5 Hz, 1H), 2.89 (dt, *J* = 13.3, 6.6 Hz, 1H), 2.49 (t, *J* = 5.7, 2H), 1.27 (d, *J* = 6.2, 3H), 0.90 (s, 3H), 0.086 (s, 3H). ^{13}C-NMR (101 MHz, MeOD) **13**: 179.5, 175.1, 174.0, 168.3, 160.9, 145.6, 139.5, 130.0, 75.7, 68.3, 64.9, 52.4, 39.3, 38.6, 35.4, 35.3, 30.7, 20.5, 20.5, 20.0. ^{1}H NMR matched the spectrum reported in the literature[28].

***p*-Nitrobenzyl (5*R*), (6*S*)-[(1*R*)-(*p*-nitrobenzyloxycarbonyloxy)ethyl]-3,7-dioxo-1-azabicyclo[3.2.0]heptane-2-carboxylate 14a and *p*-Nitrobenzyl (5*R*), (6*S*)-[(1*S*)-(*p*-nitrobenzyloxycarbonyloxy)ethyl]-3,7-dioxo-1-azabicyclo[3.2.0]heptane-2-carboxylate 14b.** **14a** and **14b** was synthesized from **7a** and **7b** following the procedure described above for **8**[36]. **14a** and **14b** were obtained as a mixture of diastereomers (179 mg, 99%). ^{1}H-NMR (400 MHz, $CDCl_3$) **14a**: δ 8.24 (d, *J* = 8.9 Hz, 4H), 7.55 (d, *J* = 8.9 Hz, 2H), 7.55 (d, *J* = 8.9 Hz, 2H), 5.31 (q, *J* = 14.2 Hz, 2H), 5.39-5.22 (m, 3H), 4.78 (s, 1H), 4.07 (td, *J* = 7.3, 1.9 Hz, 1H), 3.48 (dd, *J* = 4.8, 2.0 Hz, 1H), 2.90 (ddd, *J* = 6.9, 3.8, 0.6 Hz, 1H), 2.47 (dd, *J* = 19.2, 7.5 Hz, 1H), 1.53 (d, *J* = 6.5 Hz, 3H). **14b**: δ 8.24 (d, *J* = 8.9 Hz, 2H), 7.55 (d, *J* = 8.9 Hz, 2H), 7.55 (d, *J* = 8.9 Hz, 2H), 5.31 (q, *J* = 14.2 Hz, 2H),

5.39-5.22 (m, 3H), 4.77 (s, 1H), 4.14 (td, *J* = 7.3, 2.3, 1H), 3.38 (dd, *J* = 8.0, 2.0 Hz, 1H), 2.96 (ddd, *J* = 6.9, 3.9, 0.7 Hz, 1H), 2.47 (dd, *J* = 18.8, 7.8 Hz, 1H), 1.51 (d, *J* = 6.4 Hz, 3H). ^{1}H NMR matched the spectra reported in the literature[36].

***p*-Nitrobenzyl (5*R*)-(2-Acetamidoethylthio)-(6*S*)-[(1*R*)-1-*p*-nitro-benzyl-oxy-carbonyl-oxy-ethyl]-7-oxo-1-azabicyclo-[3.2.0]hept-2-ene-2-carboxylate 15a and *p*-Nitrobenzyl (5*R*)-(2-Acetamidoethylthio)-(6*S*)-[(1*S*)-1-*p*-nitro-benzyl-oxy-carbonyl-oxy-ethyl]-7-oxo-1-azabicyclo-[3.2.0]hept-2-ene-2-carboxylate 15b.** **15a** and **15b** was synthesized from **14** following the procedure described above for **9**. The crude diastereomers were purified by silica gel chromatography (DCM:MeOH, 95:5) to give **15a** and **15b** (178 mg, 80%) as a mixture of diastereomers. 4.22-4.44 (m, 2H), 3.35-3.6 (m, 2H), 3.12 (dd, *J* = 17.5, 8.0 Hz, 1H), 2.81-3.22 (m, 2H), 2.66-2.82 (m, 2H), 1.99 (s, 3H), 1.41 (d, *J* = 6.0 Hz, 3H). ^{1}H NMR matched the spectra reported in the literature[37].

***p*-Nitrobenzyl (5*R*)-[2-(*N*-(3-amino-3-oxopropyl)-3,3-dimethyl-(2*R*),4-bis((triethylsilyl)oxy)butanamide)ethylthio]-(6*S*)-[(1*R*)-1-(hydroxyl)ethyl]-7-oxo-1-azabicyclo-[3.2.0]hept-2-ene-2-carboxylate 16:** **16** was synthesized from **14** following the procedure described above for **9**. The crude oil was purified by silica gel chromatography using (DCM:MeOH, 97:3) to give **16** (380 mg, 86%) as a colorless oil. ^{1}H NMR (300 MHz, $CDCl_3$) δ ppm 8.18-8.27 (m, 2H), 7.60-7.68 (m, 2H), 6.90 (s, 1H), 6.72 (d, *J* = 0.4 Hz, 1H), 5.45-5.53 (m, 1H), 4.18-4.32 (m, 1H), 4.06 (s, 1H), 3.48-3.57 (m, 2H), 3.37-3.47 (m, 3H), 3.27-3.34 (m, 1H), 3.19-3.24 (m, 1H), 3.06-3.17 (m, 1H), 2.94-3.06 (m, 1H), 2.90 (s, 1H), 2.35-2.49 (m, 2H), 1.30-1.40 (m, 3H), 0.85-1.01 (m, 18H), 0.80 (s, 3H), 0.77-0.82 (m, 3H), 0.51-0.68 (m, 12H). HRMS (ESI), $C_{34}H_{39}N_5O_{14}S$ [$M+H^+$] calculated: 1002.4022; found: 1002.3948.

***p*-Nitrobenzyl (5*R*)-[2-(*N*-(3-amino-3-oxopropyl)-3,3-dimethyl-(2*R*),4-butanamide)ethylthio]-(6*S*)-(1*R*)-1-hydroxyethyl-7-oxo-1-azabicyclo-[3.2.0]hept-2-ene-2-carboxylate 17.** **17** was synthesized from **16** following the procedure described above for **11**. The crude oil was purified by silica gel chromatography using 5% methanol in dichloromethane to give **17** (89.5 mg, 51%) as a colorless oil. ^{1}H NMR (400 MHz, MeOD) δ ppm 8.13 (d, *J* = 8.8 Hz, 2H), 7.6 (d, *J* = 19.6 Hz, 2H), 5.3 (dd, *J* = 1.0 Hz, 2H), 4.1-4.2 (m, 1H), 4.01 (t, *J* = 6.44 Hz, 1H), 3.79 (s, 1H), 3.29-3.41 (m, 7H), 3.27 (d, *J* = 6.44 Hz, 1H), 3.11-3.20 (m, 1H), 2.95 (d, *J* = 6.9 Hz, 1H), 2.88 (d, *J* = 7.0 Hz, 1H), 2.3 (t, *J* = 6.7 Hz, 2H), 1.20 (d, 3H, *J* = 6.3 Hz), 0.94 (t, *J* = 7.3 Hz, 2H), 0.82 (s, 6H). HRMS (ESI), $C_{34}H_{39}N_5O_{14}S$ [M+H$^+$] calculated: 774.2292; found: 774.2301.

(5*R*)-[2-(*N*-(3-amino-3-oxopropyl)-3,3-dimethyl-(2*R*),4-butanamide)ethylthio]-(6*S*)-(1*R*)-1-hydroxyethyl-7-oxo-1-azabicyclo-[3.2.0]hept-2-ene-2-carboxylate (OA6129-B$_2$) 19: **19** was synthesized from **17** following the procedure described above for **12**[5]. The aqueous layer was collected and purified immediately by HPLC (semi preparatory C18, method 2). The peak eluted at 9 min was collected and lyophilized to yield 5.2 mg **19** as a white powder. ^{1}H NMR (400 MHz, D_2O) δ ppm 4.19 (spt, *J* = 1.0 Hz, 2H), 3.96 (s, 1H), 3.52-3.52 (m, 3H), 3.45-3.56 (m, 3H), 3.33-3.43 (m, 3H), 3.26 (dd, *J* = 1.0 Hz, 1H), 3.11 (dd, *J* = 1.0 Hz, 1H), 3.00 (dd, *J* = 1.0 Hz), 2.89 (dd, *J*=1.0 Hz, 1H), 2.49 (br s, 2H), 1.27 (d, *J* = 6.2 Hz, 1H), 0.90 (s, 4H), 0.86 (s, 3H). ^{1}H NMR matched the spectrum reported in the literature[28].

Synthesis of 3,4-*cis*-azetidinones:

D-aspartic acid dibenzyl ester *p*-toluenesulfonic acid salt 20: *p*-toluenesulfonic acid

(145.6 g) was added to D-aspartic acid (50 g) in benzyl alcohol (300 mL) and benzene (150 mL) and was heated to reflux in a 1 L round-bottom flask fitted with a Dean-Stark trap and a reflux condenser. The reaction mixture was stirred for 16 h ,then allowed to cool before it was diluted with benzene (600 mL) and diethyl ether (1.2 L). The resulting white crystals were filtered and rinsed with diethyl ether to yield **20** (384 g, 99%).[1]H NMR (400 MHz, $CDCl_3$) δ ppm 7.13 - 7.55 (m, 14H). 5.19 (br. s, 3H) 4.46 (t, J = 6.00 Hz, 1H) 3.01 (m, 2H), 2.28 (s, 3H). [1]H NMR results matched the spectrum reported in the literature[38].

***N-tert*-butyldimethylsilyl-D-aspartic acid dibenzyl ester 21:** A solution of **20** (150 g, 309 mmol) in dichloromethane (1 L) was washed twice with 500 mL saturated sodium bicarbonate. Once the evolution of carbon dioxide ceased, the phases were separated and the organic layer was washed with water (500 mL), dried with anhydrous magnesium sulfate and filtered. *tert*-Butyldimethylsilyl chloride (51.24 g, 339.99 mmol), dimethylaminopyridine (1.89 g, 15.45 mmol), and triethylamine (108 mL, 772.5 mmol) were added sequentially to the free amine in dichloromethane and the reaction mixture was stirred for 16 h. The reaction mixture was washed with saturated ammonium chloride (1 L), with saturated sodium bicarbonate (500 mL), water (500 mL), brine (500 mL) and was dried with anhydrous magnesium sulfate, filtered, and concentrated *in vacuo* to give **21** (123.4 g, 93%), which was used without purification. [1]H NMR (400 MHz, $CDCl_3$) δ ppm 7.27 - 7.50 (m, 10H). 5.18 (br. s, 1H) 4.07 (dd, J = 6.00, 2.84 Hz, 1H) 3.33 (dd, J = 15.2, 6.0 Hz, 1H), 3.07 (dd, J = 15.2, 2.8 Hz, 1H), 0.92 (s, 18H), 0.24 (s, 3H), 0.08 - 0.11 (m, 3H). [1]H NMR results matched the spectrum reported in the literature[20].

***N-tert*-butyldimethylsilyl 4(*R*)-carboxy-2-azetidinone benzyl ester 22:** *tert*-Butylmagnesium chloride in diethylether (194 mL, 1.7 M, 300 mmol) was added to a solution of **21** in diethylether (1.2 L) dropwise at 0 °C and was stirred overnight. The reaction mixture was cooled to 0 °C and quenched with saturated ammonium chloride (200 mL), the phases were separated and the organic layer was washed with water (500 mL). The combined aqueous layers were extracted twice with diethyl ether (200 mL). The combined organic fractions were dried with anhydrous sodium sulfate, concentrated, and immediately purified by silica gel (800 mL) chromatography using a gradient of 100% hexanes to 30% ethyl acetate in hexanes to yield **22** (63 g, 69%) as a yellow oil. ^{1}H NMR (300 MHz, $CDCl_3$) δ ppm 7.29 - 7.42 (m, 5H), 4.07 (dd, *J* = 6.0, 2.9 Hz, 1H), 3.33 (dd, *J* = 15.1, 6.0 Hz, 1H) 3.07 (dd, *J* = 15.16, 2.87 Hz, 1H) 0.92 - 0.94 (m, 9H) 0.24 (s, 3H) 0.10 (s, 3H). ^{1}H NMR results matched the spectrum reported in the literature[20].

***N-tert*-butyldimethylsilyl 4(*R*)-carboxy-2-azetidinone 23:** A catalytic amount of palladium on carbon (1 g, 2% w/w) was carefully added to a solution of **22** (68.7 g, 215 mmol) in ethanol (100 mL) in a bomb flask that was pressurized to 40 psi with hydrogen gas in a Parr-shaker apparatus. The reaction mixture was shaken for 1 h before it was filtered through Celite and concentrated *in vacuo*. The crude oil was purified by crystallization in a minimum amount of hot diethyl ether. The remaining of the product can be crystallized from the mother liquor by the addition of petroleum ether to yield **23** (37 g, 75%). ^{1}H NMR (400 MHz, $CDCl_3$) δ ppm 4.07 (t, *J* = 1.0 Hz, 1H), 3.39 (dd, *J* = 15.3, 6.1 Hz, 1H) 3.12 (d, *J* = 15.7 Hz, 1H), 0.89 (s, 9H) 0.30 (s, 3H), 0.11 (s, 3H). ^{1}H NMR results matched the spectrum reported in the literature[20].

***N-tert*-butyldimethylsilyl 4(*R*)-carboxy-3(*R*)-(1(*R*)-hydroxy)ethyl-2-azetidinone 24a**

and *N-tert*-butyldimethylsilyl 4(*R*)-carboxy-3(*R*)-(1(*S*)-hydroxy)ethyl-2-azetidinone 24b: A solution of *n*-butyllithium in hexanes (22.8 mL, 2.1 M, 48 mmol) was added to diisopropylamine (6.7 mL, 48 mmol) tetrahydrofuran (50 mL) dropwise at 0 °C. After stirring for 15 min, a solution of **23** (5.0 g, 21.8 mmol) in tetrahydrofuran (50 mL) was added over 5 min and then stirred vigorously for 15 min at 0 °C. Acetaldehyde (3.7 mL, 65.4 mmol) was added to the reaction mixture and then it was stirred for 1 h at 0 °C before allowing to warm to ambient temperature over an additional hour. The reaction mixture was diluted with ethyl acetate (100 mL) and quenched with saturated monobasic potassium sulfate (100 mL). The phases were separated and the aqueous layer was extracted twice with ethyl acetate (125 mL). The combined organic layers were washed with water (125 mL), brine (125 mL), dried with anhydrous sodium sulfate and concentrated *in vacuo*. The crude red oil was used for the next reaction without purification.

***N-tert*-butyldimethylsilyl 4(*S*)-acetoxy-3(*R*)-(1(*R*)-hydroxy)ethyl-2-azetidinone 25a and *N-tert*-butyldimethylsilyl 4(*S*)-acetoxy-3(*R*)-(1(*S*)-hydroxy)ethyl-2-azetidinone 25b: 25a** and **25b** were synthesized from **24a** and **24b** following the procedures of Ito *et al.*[24]. Dried lead (IV) tetraacetate and copper (II) acetate was added to **24a** and **24b** (10.8 g, 39.5 mmol) in acetonitrile (198 mL). A constant stream of nitrogen was bubbled through the reaction mixture while it was heated to 65 °C and stirred for 2 h. The reaction mixture was filtered through Celite, and the Celite plug was washed with ethyl acetate. The combined eluate was concentrated *in vacuo*. The residue was redissolved in ethyl acetate (100 mL) and saturated sodium bicarbonate (100 mL) was added. The pH of the aqueous phase was adjusted to 7 and the phases were separated. The organic layer

was washed with brine, dried with anhydrous sodium sulfate and concentrated *in vacuo*. The crude oil was purified by silica gel chromatography with 50% diethyl ether in hexanes to give **25a** and **25b** as a mixture of diastereomers (3.06 g, 48%). **25a:** ^{1}H NMR (400 MHz, $CDCl_3$) δ ppm) 5.81 (d, J = 0.9 Hz, 1H). 4.04 - 4.17 (m, 1H) 3.20 (dd, J = 4.5, 1.0 Hz, 1H), 2.10 (s, 3H), 1.35 (d, J = 6.6 Hz, 2H) 0.97 (s, 9H), 0.31 (s, 3H), 0.24 (s, 3H). **25b:** ^{1}H NMR (400 MHz, $CDCl_3$) δ ppm 5.80 (s, 1H), 4.17 - 4.26 (m, 1H), 3.88 - 4.00 (m, 1H), 3.08 - 3.16 (m, 1H), 2.12 (s, 3H), 1.33 (d, J = 6.4 Hz, 3H), 0.96 (s., 9H), 0.31 (s, 3H), 0.24 (s, 3H). ^{1}H NMR results matched those reported in the literature[24].

***N-tert*-butyldimethylsilyl 4(*S*)-acetoxy-3(*R*)-(1(*R*)-ethylcarbonyloxy)ethyl-2-azetidinone 26a and *N-tert*-butyldimethylsilyl 4(*S*)-acetoxy-3(*R*)-(1(*S*)-ethylcarbonyloxy)ethyl-2-azetidinone 26b:** Dimethylaminopyridine (425 mg, 3.48 mmol) was added to **25a** and **25b (**500 mg, 1.74 mmol) in dichloromethane (15 mL) at 0 °C. Propionyl chloride (313 µL, 3.48 mmol) was added to the reaction mixture and was allowed to stir for 16 h at 0 °C. The reaction was quenched with saturated ammonium chloride (10 mL) and the phases were separated. The aqueous layer was extracted with dichloromethane (10 mL) and the combined organic layers were washed with brine (20 mL), filtered and concentrated *in vacuo*. The crude oil was purified by silica gel chromatography to yield **26a** and **26b** as a mixture of diastereomers (351 mg, 59%). **26a:** 1H NMR (400 MHz, $CDCl_3$) δ ppm = 5.76 (s, 1H), 5.24 (q, J = 6.4 Hz, 1H) 3.28 (d, J = 3.5 Hz, 1H) 2.31 (q, J = 7.5 Hz, 2H) 1.40 (d, J = 6.51 Hz, 1H) 1.13 (t, J = 7.52 Hz, 3H) 0.97 (s, 9H) 0.26 (s, 3H) 0.22 (s, 3H). **26b:** 1H NMR (400 MHz, $CDCl_3$) δ ppm = 6.05 (s, 1H), 5.30 (qd, J_1 = 6.5, J_2 = 3.2 Hz, 1H), 3.24 (d, J = 6.3 Hz, 1H), 2.31 (s, 3H), 2.08 (q, J = 7.54 Hz, 2H), 1.36 (d, J = 6.38 Hz, 3H), 1.13 (t, J = 7.52 Hz, 3H), 0.97 (s, 9H)

0.25 (s, 3H), 0.21 (s, 3H).

4(*S*)-acetoxy-3(*R*)-(1(*R*)-ethylcarbonyloxy)ethyl-2-azetidinone 27a and 4(*S*)-acetoxy-3(*R*)-(1(*S*)-ethylcarbonyloxy)ethyl-2-azetidinone 27b: A solution of hydrogen fluoride in pyridine (200 µL, 30% w/v) was added to **26a** and **26b** (65 mg, 0.189 mmol) in tetrahydrofuran (1.89 mL) at 0 °C and was stirred for 10 min. The reaction mixture was diluted with ethyl acetate (20 mL) and washed twice with saturated ammonium chloride (10 mL). The combined aqueous layers were extracted with ethyl acetate (10 mL) and the combine organic fractions were washed with brine (10 mL), dried with anhydrous sodium sulfate, filtered and concentrated *in vacuo*. The crude oil was purified by silica gel chromatography using 30% ethyl acetate in hexanes to give **27a** and **27b** as a mixture of diastereomers (36 mg, 83%). **27a:** ^{1}H NMR (300 MHz, $CDCl_3$) δ ppm 6.62 (br. s., 1H), 5.58 (d, *J* = 1.3 Hz, 1H), 5.25 (q, *J* = 13.0 Hz, 1H), 3.39 (dd, *J* = 3.8, 1.4 Hz, 1H), 2.35 (t, *J* = 1.0 Hz, 2H), 2.10 (s, 3H), 1.41 (d, *J* = 1.0 Hz, 3H), 1.14 (t, *J* = 1.0 Hz, 3H). **27b:** ^{1}H NMR (300 MHz, $CDCl_3$) δ ppm 6.64 (br. s., 1H), 5.79 (d, *J* = 1.3 Hz, 1H), 5.30 (dq, *J* = 6.6, 3.3 Hz, 1H), 3.33 (dd, *J* = 6.3, 1.3 Hz, 1H), 2.30 (t, *J* = 1.0 Hz, 2H), 2.11 (s, 3H), 1.37 (d, *J* = 6.4 Hz, 3H), 1.11 (q, *J* = 1.0 Hz, 3H).

***N-tert*-butyldimethylsilyl 4(*S*)-acetoxy-3(*R*)-[1(*R*)-(1-bromoethylcarbonyl)oxy]ethyl-2-azetidinone 28a and *N-tert*-butyldimethylsilyl 4(*S*)-acetoxy-3(*R*)-[1(*S*)-(1-bromoethylcarbonyl)oxy]ethyl-2-azetidinone 28b:** Dimethylaminopyridine (170 mg, 1.392 mmol) was added to **25a** and **25b (**200 mg, 0.696 mmol) in dichloromethane (5 mL) at 0 °C. 2-bromopropionyl bromide (147 µL, 1.392 mmol) was added to the reaction mixture and was allowed to stir for 2 h at 0 °C. The reaction was quenched with saturated ammonium chloride (10 mL) and the phases were separated. The aqueous layer

was extracted with dichloromethane (10 mL) and the combined organic layers were washed with brine (20 mL), filtered and concentrated *in vacuo*. The crude oil was purified by silica gel chromatography to yield **28a** and **28b** as a mixture of diastereomers (194 mg, 66%) and was carried forward without further purification.

4(*S*)-acetoxy-3(*R*)-[1(*R*)-(1-bromoethylcarbonyl)oxy]ethyl-2-azetidinone 29a and 4(*S*)-acetoxy-3(*R*)-[1(*S*)-(1-bromoethylcarbonyl)oxy]ethyl-2-azetidinone 29b: A solution of hydrogen fluoride in pyridine (600 μL, 30%w/v) was added to **28a** and **28b** (194 mg, 0.459 mmol) in tetrahydrofuran (4.6 mL) at 0 °C and was stirred for 10 min. The reaction mixture was diluted with ethyl acetate (20 mL) and washed twice with saturated ammonium chloride (20 mL). The combined aqueous layers were extracted with ethyl acetate (20 mL) and the combine organic fractions were washed with brine (20 mL), dried with anhydrous sodium sulfate, filtered and concentrated *in vacuo*. The crude oil was purified by silica gel chromatography using 30% ethyl acetate in hexanes to give **29a** and **29b** as a mixture of diastereomers (116 mg, 82%). **29a:** ^{1}H NMR (300 MHz, $CDCl_3$) δ ppm 5.81 (d, J = 1.4 Hz, 1H), 5.21 - 5.40 (m, 1H), 4.27 - 4.48 (m, 1H), 3.43 (dd, J = 3.5, 1.4 Hz, 1H), 2.12 (s, 3H) 1.83 (t, J = 2.9 Hz, 3H) 1.47 (d, J = 3.4 Hz, 3H). **29b:** ^{1}H NMR (300 MHz, $CDCl_3$) δ ppm 5.81 (d, J = 1.4 Hz, 1H), 5.24 - 5.42 (m, 1H), 4.30 - 4.44 (m, 1H), 3.38 (ddd, J = 6.7, 3.9, 1.3 Hz, 1H), 2.11 (s, 3H) 1.80 (t, J = 2.9 Hz, 3H), 1.45 (d, J = 3.4 Hz, 3H).

(3*R*,4*R*)-*N*-(4-methoxyphenyl)-3-((*R*)-1-hydroxyethyl)-4-[(*E*)-styryl]-2-azetidinone (32a) and (3*R*,4*S*)-*N*-(4-methoxyphenyl)-3-((*R*)-1-hydroxyethyl)-4-[(*E*)-styryl]-2-azetidinone (32b). 32a and **32b** was synthesized following the procedures of Gallucci *et al*[26]. A solution of (3*R*)-hydroxybutyric acid ethyl ester (5.00g, 37.8 mmol) in

tetrahydrofuran (25 mL) was added dropwise to a solution of lithium bis(trimethylsilyl)amide in tetrahydrofuran (96.8 mL, 0.809M, 78.3 mmol) at -78 °C and stirred for 1h. A solution of **47** (8.98 g, 37.8 mmol) in tetrahydrofuran (75 mL) was added dropwise to the solution at -78 °C and was allowed to warm to room temperature while stirring over 20 h. The reaction mixture was diluted with dichloromethane (500 mL) and washed with saturated aqueous ammonium chloride (500 mL). The aqueous layer was extracted twice with dichloromethane (400 mL). The combined organic layers were dried with anhydrous magnesium sulfate, filtered and concentrated *in vacuo*. The crude oil was purified by silica gel chromatography (hexanes:ethyl acetate, 7:3) to yield **26a** and **26b** as a mixture of diastereomers (6.85 g, 53%). TLC (hexanes:ethyl acetate, 7:3) = 0.35. **32a:** ^{1}H-NMR (300 MHz, $CDCl_3$) δ. 7.37-7.41 (m, 5H), 7.27 (d, J = 8.4 Hz, 2H), 6.84 (d, J = 7.6 Hz, 2H), 6.30 (dd, J = 15.7, 10.5 Hz, 1H), 4.49 (d, J = 8.3 Hz, 1H), 4.21 (tt, J = 10.9, 5.5 Hz, 1H), 3.76 (s, 3H), 3.14 (d, J = 6.2 Hz, 1H), 1.41 (d, J = 6.3 Hz, 3H). HRMS (FAB), $C_{20}H_{22}NO_3$ [M+H$^+$] calculated: 324.15997; found: 324.16013; Δ 0.5 ppm. **32b:** ^{1}H-NMR (300 MHz, $CDCl_3$) δ 7.37-7.41 (m, 5H), 7.27 (d, J = 8.4 Hz, 2H), 6.84 (d, J = 7.6 Hz, 2H), 6.4 (dd, J = 16.2, 9.0 Hz, 1H), 4.75 (t, J = 7.4 Hz, 1H), 4.22 (tt, J = 11.4, 5.7 Hz, 1H), 3.76 (s, 3H), 3.45 (t, J = 6.3 Hz, 1H), 1.33 (d, J = 6.3 Hz, 3H). HRMS (FAB), $C_{20}H_{22}NO_3$ [M+H$^+$] calculated: 324.15997; found: 324.1601. ^{1}H NMR results matched those reported in the literature[26].

(1*S*,2*R*,4*S*,5*R*)-4-Hydroxy-6-(4-methoxyphenyl)-2-methyl-3-oxa-6-azabicyclo[3.2.0]heptan-7-one (33). **33** was synthesized following the procedures of Gallucci *et al*[26]. Ozone was passed through a solution containing a mixture of **32a** and **32b** (8.61g, 26.6 mmol) in dichloromethane (270mL) at -78 °C until the color of solution

changed from yellow to near colorless. The bubbling of ozone must cease before the solution becomes blue or green as over-oxidation by degradation of the 4-methoxyhenyl group occurred. The reaction can also be monitored by TLC. Once complete, dimethyl sulfide (45 mL) is added and stirred at room temperature. The crude solution was concentrated directly *in vacuo* to provide **33** as a pale yellow oil. Silica chromatography (hexanes:ethyl acetate, 3:2) provides **33** and the *trans* aldehyde **34,** which are purified as a mixture (4.02 g, 16.1 mmol, 85%). **34** and **33** in dichloromethane (100 mL) were subjected to 1,8-diazobicyclo[5.4.0]undec-7-ene (0.6 mL, 4.0 mmol) and the reaction mixture was refluxed for 70 min. The product solution was diluted with dichloromethane (300 mL), washed with 0.2 N HCl (300 mL), and the aqueous layer was extracted twice with dichloromethane (200 mL). The combined organic layers were dried over anhydrous sodium sulfate, filtered, and concentrated *in vacuo*. Purification by silica gel chromatography (hexanes:ethyl acetate, 1:1) provided **33** as a white solid (2.53 g, 10.15 mmol, 63% from **34**, 38% from **32a** and **32b**). **33:** TLC (hexanes:ethyl acetate, 3:2) = 0.25. ^{1}H NMR (400 MHz, $CDCl_3$) δ 7.30 (d, J = 8.8 Hz, 2H), 6.86 (d, J = 9.0 Hz, 2H), 5.55 (s, 1H), 4.42 (t, J = 6.1 Hz, 2H), 4.39 (d, J = 4.0 Hz, 1H), 3.77 (s, 3H), 3.73 (q, J = 3.2 Hz, 1H), 1.51 (d, J = 6.4 Hz, 3H). ^{13}C NMR (101 MHz, $CDCl_3$) δ 162.45, 156.21, 130.89, 117.61, 114.51, 94.96, 71.30, 61.18, 60.42, 56.59, 55.48, 21.02, 15.67, 14.15. HRMS (FAB), $C_{13}H_{16}NO_4$ [M+H$^+$] calculated: 250.10793; found: 250.1079. ^{1}H and ^{13}C NMR results matched those reported in the literature[26].

[3*R*,4*R*(*E*)]-3-[1(*R*)-Hydroxyethyl]-4-(2-methoxyethenyl)-1-(4-methoxyphenyl)-2-azetidinone (35) and (1*R*,2*R*,4*S*,6*R*)-4-Methoxy-7-(4-methoxyphenyl)-2-methyl-3-oxa-7-azabicyclo[4.2.0]octan-8-one (36). **36** was synthesized following the procedures

of Gallucci *et al*[26]. A solution of *n*-butyllithium (2.0 M, 40.6 mmol, 20.3 mL) in hexanes was added to a solution of diisopropylamine (5.73 mL, 40.6 mmol) in tetrahydrofuran (100 mL) at -78 °C and stirred for 20 min at this temperature. (Methoxymethyl)-triphenylphosphonium chloride (10.4 g, 30.45 mmol) was added in one portion and the slurry was stirred for 10 min at -78 °C before it was allowed to warm to 0 °C in an ice bath and stirred for another 10 min. The ylid was then cooled to -78 °C and a solution of **33** (2.53 g, 10.15 mmol) in tetrahydrofuran (100 mL) was added over 5 min. Once addition was complete, the dry ice/acetone bath was removed and the reaction mixture allowed to warm to room temperature and then stirred for 20 h. If desired, the reaction can be concentrated and chromatographed (hexanes:ethyl acetate 3:2) at this stage to give **35** as a white solid. However, it is much more efficient to proceed directly to **36** without purification. The crude reaction was cooled to 0 °C before it was quenched with 1 N HCl (100 mL) over 5 min and then stirred for 5 h. The solution was diluted with dichloromethane (400 mL) and washed with saturated sodium bicarbonate (500 mL). The aqueous layer was extracted twice with dichloromethane (200 mL). The combined organic extracts were dried with anhydrous sodium sulfate, filtered and concentrated *in vacuo*. The crude oil was purified by silica gel chromatography (hexanes:ethyl acetate, 3:2) to provide **36** as a white solid (1.58 g, 56%). **35:** TLC (hexanes:ethyl acetate, 3:2) = 0.20. MP = 187-188 °C. ^{1}H NMR (400 MHz, $CDCl_3$) δ 7.38 (d, *J* = 9.1 Hz, 2H), 6.85 (d, *J* = 9.1 Hz, 2H), 6.74 (d, *J* = 12.8 Hz, 1H), 4.95 (q, *J* = 7.5 Hz, 2H), 4.55 (q, *J* = 5.2 Hz, 1H), 4.16 (m, 1H), 3.78 (s, 3H), 3.58 (s, 3H), 3.33 (q, *J* = 4.1 Hz, 1H), 1.34 (d, *J* = 6.3 Hz, 3H). ^{13}C NMR (101 MHz, CD_3CN_SPE) δ 165.76, 155.99, 152.50, 131.35, 118.55, 114.21, 97.69, 65.07, 59.67, 56.36, 55.44, 54.73, 22.08. HRMS (FAB),

$C_{15}H_{19}NO_4$ [M^+] calculated: 277.13141; found: 277.1315. **36:** TLC (hexanes:ethyl acetate, 3:2) = 0.40. MP = 120-123 °C. ^{1}H NMR (400 MHz, $CDCl_3$) δ 7.34 (q, *J* = 3.0 Hz, 1H), 6.88 (d, *J* = 9.1 Hz, 1H), 4.73 (q, *J* = 4.7 Hz, 1H), 4.29 (m, *J* = 1.9 Hz, 1H), 4.24 (m, *J* = 3.1 Hz, 1H), 3.79 (s, 1H), 3.34 (s, 1H), 3.27 (q, *J* = 2.7 Hz, 1H), 2.60 (m, *J* = 3.5 Hz, 1H), 1.82 (m, *J* = 3.9 Hz, 1H), 1.49 (d, *J* = 6.5 Hz, 1H). HRMS (FAB), $C_{15}H_{19}NO_4$ [M^+] calculated: 277.13141; found: 277.1315. ^{1}H NMR results matched those reported in the literature[26].

(1*R*,2*R*,4*S*,6*R*)-4-Methoxy-7-(4-methoxyphenyl)-2-methyl-3-oxa-7-azabicyclo-[4.2.0]-octan-8-one (36). **36** was synthesized following the procedure of Gallucci *et al*[26]. Dowex 50WX8-100 hydrogen-form resin was added to a solution of **35** (400 mg, 1.4 mmol) in methanol (25 mL) and the suspension was stirred for 5 h. The resin was filtered and washed with dichloromethane (25 mL) and the filtrate was concentrated *in vacuo*. The product was purified by silica gel chromatography (hexanes:ethyl acetate, 3:1) to provide 5 as a white solid (122.5 mg, 31%).

(1*R*,2*R*,4*S*,6*R*)-4-Hydroxy-7-(4-methoxyphenyl)-2-methyl-3-oxa-7-azabicyclo[4.2.0]octan-8-one (37). **36** was synthesized following the procedure of Gallucci *et al*[26]. **36** (830 mg, 2.99 mmol) was dissolved in 70% formic acid in water (25 mL) and was stirred for 8 h. The product was extracted with ethyl acetate, dried with anhydrous sodium sulfate, filtered, concentrated, and crystallized from dichloromethane and hexanes to provide **37** as white crystals (628 mg, 80%). **37:** TLC (hexanes:ethyl acetate, 3:2) = 0.20. MP = 155-158 °C. ^{1}H NMR (400 MHz, $CDCl_3$) δ 7.33 (d, *J* = 9.0 Hz, 2H), 6.88 (d, *J* = 9.0 Hz, 2H), 5.25 (q, *J* = 4.7 Hz, 2H), 4.37 (m, *J* = 2.7 Hz, 1H), 4.31 (m, *J* = 3.0 Hz, 1H), 3.79 (s, 1H), 3.27 (q, *J* = 2.7 Hz, 1H), 2.64 (m, *J* = 3.4 Hz, 1H), 1.86

(m, J = 3.9 Hz, 1H), 1.48 (d, J = 6.5 Hz, 3H). ^{13}C NMR (101 MHz, $CDCl_3$) δ 171.16, 164.08, 156.13, 130.93, 118.16, 114.55, 90.16, 63.60, 60.39, 55.50, 52.71, 47.87, 28.05, 21.04, 18.46, 14.18. HRMS (FAB), $C_{14}H_{17}NO_4$ [M^+] calculated: 263.11576; found: 263.1153. ^{1}H and ^{13}C NMR results matched those reported in the literature[26].

(1*R*,2*R*,6*R*)-7-(4-methoxyphenyl)-2-methyl-3-oxa-7-azabicyclo[4.2.0]octan-4-8-dione (38). Tetra-*n*-propylammonium perruthenate (6.2 mg, 0.018 mmol) was added to a solution of **37** (93 mg, 0.35 mmol), *N*-methylmorpholine-*N*-oxide (61.5 mg, 0.525 mmol) and 3 Å molecular sieves (10 mg) in dichloromethane (4 mL) and the reaction mixture was shielded from light and stirred for 1 h. The solution was filtered, concentrated and purified directly by silica gel chromatography (ethyl acetate) to provide the product as a pure solid (59 mg, 65%). **38:** TLC (hexanes:ethyl acetate, 1:4) = 0.20. MP = 207-207.5°C. ^{1}H NMR (400 MHz, $CDCl_3$) δ 7.26 (d, J = 8.9 Hz, 2H), 6.87 (d, J = 9.0 Hz, 2H), 4.63 (d, J = 3.2 Hz, 1H), 4.53 (d, J = 2.2 Hz, 1H), 3.79 (s, 3H), 3.59 (q, J = 2.8 Hz, 1H), 3.25 (q, J = 6.1 Hz, 1H), 2.76 (q, J = 6.7 Hz, 1H), 1.69 (d, J = 6.5 Hz, 3H). ^{13}C NMR (101 MHz, $CDCl_3$) δ 168.24, 161.11, 156.78, 129.56, 118.78, 114.68, 71.80, 55.51, 51.90, 48.28, 32.28, 17.90. HRMS (FAB), $C_{14}H_{15}NO_4$ [M^+] calculated: 261.10011; found: 261.0998. ^{1}H and ^{13}C NMR results matched those reported in the literature[26].

(1*R*,2*R*,6*R*)-2-methyl-3-oxa-7-azabicyclo[4.2.0]octan-4-8-dione (39). HCl (12.1 N, 2 mL) was added dropwise to a solution of **41** (900 mg, 3.34 mmol) in methanol (10 mL) and was stirred while carefully monitoring by TLC. Once complete, the solution was concentrated *in vacuo* and purified by silica gel chromatography (ethyl acetate) to provide **39** as a white solid (429 mg, 83%). **39:** TLC (ethyl acetate) = 0.20. ^{1}H NMR (300 MHz, $CDCl_3$) δ 6.01 (br. s, 1H), 4.76 (qd, J = 6.5, 3.3, 1H), 3.92 (dd, J = 3.3, 1.7,

1H), 3.52 (ddd, *J* = 5.3, 3.2, 2.2, 1H), 3.04 (m, 2H). ^{1}H NMR matched those reported in the literature[27].

(1*R*,2*R*,4*S*,6*R*)-4-Hydroxy-7-(tertbutyldimethylsilyl)-2-methyl-3-oxa-7-azabicyclo[4.2.0]octan-8-one (40). Ozone was passed through a solution of **2** (2.3 g, 8.5 mmol) in dichloromethane (128 mL) at -78 °C until a blue color persisted. The ozonide was quenched with dimethylsulfide (21.3 mL) and the reaction mixture was stirred for 2 h while warming to room temperature. The solution was concentrated *in vacuo* and directly purified by silica gel chromatography (hexanes:ethyl acetate, 7:3) to provide **40** (1.9 g, 82%). **40:** TLC (hexanes:ethyl acetate, 7:3) = 0.20. ^{1}H NMR (300 MHz, $CDCl_3$) δ 5.43 (q, *J* = 4.7 Hz, 1H), 4.25 (m, *J* = 3.1 Hz, 1H), 3.84 (m, *J* = 2.9 Hz, 1H), 3.22 (q, *J* = 2.8 Hz, 1H), 2.33 (m, *J* = 3.5 Hz, 1H), 1.77 (m, *J* = 3.9 Hz, 1H), 1.40 (d, *J* = 6.5 Hz, 3H), 0.97 (s, 9H), 0.28 (s, 3H), 0.21 (s, 3H). HRMS (FAB), $C_{13}H_{26}NO_3Si$ [M+H$^+$] calculated: 272.16820; found: 272.1677.

(1*R*,2*R*,4*S*,6*R*)-4-Hydroxy-7-(tertbutyldimethylsilyl)-2-methyl-3-oxa-7-azabicyclo[4.2.0]octan-8-one (41). A solution of **10** (450 mg, 1.66 mmol) in dichloromethane (3.3 mL) was added to a solution of pyridinium chlorochromate (716 mg, 3.3 mmol) in dichloromethane (6.6 mL). The solution was stirred for 3 h and filtered through Celite. The filter cake was washed twice with ethyl acetate (5 mL) and the filtrate was dried with anhydrous sodium sulfate, filtered and concentrated *in vacuo*. The crude product was purified by silica gel chromatography (hexanes:ethyl acetate, 1:1) to provide **41** (270 mg, 60%). **41:** TLC (hexanes:ethyl acetate, 3:2) = 0.20. MP = 82-84°C ^{1}H NMR (400 MHz, $CDCl_3$) δ 4.49 (m, 1H), 4.05 (m, 1H), 3.53 (q, *J* = 2.8 Hz, 1H), 2.90 (q, *J* = 6.1 Hz, 1H), 2.67 (q, *J* = 6.5 Hz, 1H), 1.58 (d, *J* = 6.5 Hz, 3H), 0.95 (s, 9H), 0.26

(s, 3H), 0.22 (s, 3H). ^{13}C NMR (101 MHz, CD_3CN_SPE) δ 169.56, 169.19, 71.81, 53.88, 46.55, 35.15, 26.02, 18.29, 17.61, -5.58, -5.76. HRMS (FAB), $C_{13}H_{24}NO_3Si$ [M+H$^+$] calculated: 270.15255; found: 270.1529.

(1*R*,2*R*,5*R*,6*R*)-2,5-dimethyl-3-oxa-7-azabicyclo[4.2.0]octan-4-8-dione (42). **42** was synthesized from **39** following the procedures of Kaga *et al*[27]. A solution of *n*-butyllithium in hexanes (2.29 M, 6.09 mmol, 2.66 mL) was added to a solution of diisopropylamine (860 µL, 6.09 mmol) in tetrahydrofuran (14 mL) at -78 °C and stirred at this temperature for 30 min. A solution was **39** (429 mg, 2.77 mmol) in tetrahydrofuran (7 mL) was added to the LDA solution at -78 °C and stirred at this temperature for 40 min. A solution of methyl iodide (379 µL, 6.09 mmol) was added to the reaction mixture at -78 °C and stirred for 1 h. The reaction mixture was quenched at -78 °C with saturated ammonium chloride and allowed to warm to room temperature. The organic layer was separated, and the aqueous layer was washed with ethyl acetate. The combined organic layers were dried with anhydrous sodium sulfate, filtered and concentrated *in vacuo*. The crude oil was purified by silica gel chromatography (ethyl acetate) and the purified product is recrystallized with ethyl acetate and hexanes to provide **42** as white needles (310 mg, 66%). **42:** TLC (ethyl acetate) = 0.25. ^{1}H-NMR (300 MHz, $CDCl_3$) ^{1}H NMR (300 MHz, $CDCl_3$) δ 6.00 (s, 1H), 4.75 (m, *J* = 3.2 Hz, 1H), 3.92 (q, *J* = 2.3 Hz, 1H), 3.52 (m, *J* = 1.8 Hz, 1H), 3.05 (m, *J* = 3.6 Hz, 1H), 1.62 (d, *J* = 6.5 Hz, 1H), 1.32 (d, *J* = 7.8 Hz, 3H). ^{1}H NMR matched those reported in the literature[27].

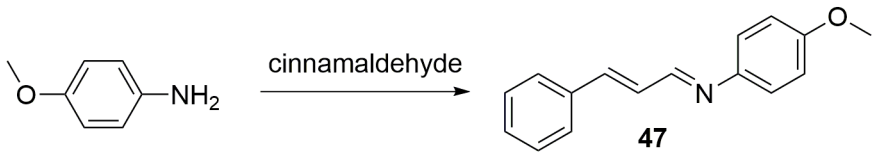

47

(1*E*,2*E*)-*N*-(4-methoxyphenyl)-3-phenylprop-2-en-1-imine (47). (*trans*)-cinnamaldehyde (6.61 g, 50 mmol) was added to a solution of *p*-anisidine (6.78 g, 55 mmol) in ethanol (100 mL) dropwise at room temperature. After 30 min, yellow crystals began to form in the reaction solution. The crystals were filtered and washed with ethanol to yield 25 as yellow needles (9.79 g, 83%). **47:** TLC (hexanes:ethyl acetate, 7:3) = 0.70. ^{1}H-NMR (300 MHz, $CDCl_3$) δ 8.30 (t, J = 4.2 Hz, 1H), 7.53 (dd, J_1 = 8.1, J_2 = 1.5 Hz, 2H), 7.38 (q, J = 7.5 Hz, 3H), 7.21 (d, J = 9.0 Hz, 2H), 7.12 (d, J = 4.6 Hz, 2H), 6.92 (d, J = 9.0 Hz, 2H), 3.83 (s, 3H). ^{1}H NMR results matched those reported in the literature[26].

References

1. Li, R., Lloyd, E. P., Moshos, K. A. & Townsend, C. A. Identification and characterization of the carbapenem MM 4550 and its gene cluster in streptomyces argenteolus ATCC 11009. *ChemBioChem* **15,** 320–331 (2014).
2. Wu, T. K. *et al.* Identification, cloning, sequencing, and overexpression of the gene encoding proclavaminate amidino hydrolase and characterization of protein function in clavulanic acid biosynthesis. *J. Bacteriol.* **177,** 3714–3720 (1995).
3. Cassidy, P. J. *et al.* Epithienamycins. II. Isolation and structure assignment. *J. Antibiot. (Tokyo).* **34,** 637–648 (1980).
4. Knierzinger, A. & Vasella, A. Synthesis of 6-epithienamycin. *J. Chem. Soc. Chem. Commun.* 9 (1984).
5. Kametani, T., Huang, S.-P., Nagahara, T. & Ihara, M. Total synthesis of (+/-)-epithienamycins A and B [(+/-)-olivanic acids MM22380 and MM22382] and derivatives. *J. Chem. Soc. Perkin Trans. 1* 2282 (1981).
6. Kametani, T., Nagahara, T. & Ihara, M. An asymmetric synthesis of synthetic intermediates to thienamycin and epithienamycins A and B. *J. Chem. Soc. Perkin Trans. 1* 3048 (1981).
7. Bateson, J. H., Robins, A. M. & Southgate, R. Olivanic acid analogues. Part 8. Halogenation and sulphenylation reactions leading selectively to cis-carbapenem precursors; stereospecific synthesis of (+)-6-epithienamycin. *J. Chem. Soc. Perkin Trans. 1* **0,** 29–35 (1991).
8. Bateson, J. H., Quinn, A. M. & Southgate, R. Sulphenylation and halogenation

reactions leading selectively to cis-carbapenem precursors; stereospecific synthesis of (+/-)-6-epithienamycin. *J. Chem. Soc.* 1151 (1986).

9. Bodner, M. J., Phelan, R. M. & Townsend, C. A. A Catalytic Asymmetric Route to Carbapenems. *Org. Lett.* **11,** 3606–3609 (2009).

10. Arndt, F. & Eistert, B. Ein Verfahren zur Überführung von Carbonsäuren in ihre höheren Homologen bzw. deren Derivate. *Berichte der Dtsch. Chem. Gesellschaft (A B Ser.* **68,** 200–208 (1935).

11. Ueda, Y., Damas, C. E. & Vinet, V. Nuclear analogs of β-lactam antibiotics. XIX. Syntheses of racemic and enantiomeric p-nitrobenzyl carbapen-2-em-3-carboxylates. *Can. J. Chem.* **61,** 2257–2263 (1983).

12. Ueda, Y., Damas, C. E. & Vinet, V. Nuclear analogs of β-lactam antibiotics. XIX. Syntheses of racemic and enantiomeric p-nitrobenzyl carbapen-2-em-3-carboxylates. *Can. J. Chem.* **61,** 2257–2263 (1983).

13. Moshos, K. A. Design and Synthesis of Substrates and Standards Used to Elucidate Activities of Enzymes in Carbapenem Gene Clusters. (Johns Hopkins University, 2011).

14. Marous, D. R. Radical SAM Enzymes in Thienamycin Biosynthesis. (Johns Hopkins University, 2015).

15. Lindgren, B. O. *et al.* Preparation of Carboxylic Acids from Aldehydes (Including Hydroxylated Benzaldehydes) by Oxidation with Chlorite. *Acta Chem. Scand.* **27,** 888–890 (1973).

16. Bal, B. S., Childers, W. E. & Pinnick, H. W. Oxidation of α,β-unsaturated aldehydes. *Tetrahedron* **37,** 2091–2096 (1981).

17. Marous, D. R. *et al.* Consecutive radical S-adenosylmethionine methylations form the ethyl side chain in thienamycin biosynthesis. *Proc. Natl. Acad. Sci. U. S. A.* **112,** 10354–10358 (2015).

18. Grabowski, E. J. J. Enantiopure drug synthesis: From methyldopa to imipenem to efavirenz. *Chirality* **17,** S249–S259 (2005).

19. Prashad, A. S., Vlahos, N., Fabio, P. & Feigelson, G. B. A highly refined version of the α-keto ester based carbapenem synthesis: The total synthesis of meropenem. *Tetrahedron Lett.* **39,** 7035–7038 (1998).

20. Reider, P. J. & Grabowski, E. J. J. Total synthesis of thienamycin: a new approach from aspartic acid. *Tetrahedron Lett.* **23,** 2293–2296 (1982).

21. Fischer, E. & Speier, A. Darstellung der Ester. *Berichte der Dtsch. Chem. Gesellschaft* **28,** 3252–3258 (1895).

22. Dean, E. W. & Stark, D. D. A Convenient Method for the Determination of Water in Petroleum and Other Organic Emulsions. *J. Ind. Eng. Chem.* **12,** 486–490 (1920).

23. Cainelli, G., Contento, M., Giacomini, D. & Panunzio, M. Stereocontrolled total synthesis of the chiral building block (3S, 4R)-3-[(R)-1-hydroxyethyl]-4-acetyloxy-azetidin-2-one: a useful synthon for the synthesis of (+)-thienamycin, carbapenems and penems. *Tetrahedron Lett.* **26,** 937–940 (1985).

24. Sunagawa, M., Matsumura, H., Enomoto, M., Inoue, T. & Sasaki, A. Synthetic studies of carbapenem and penem antibiotics. I: Facile synthesis of a key intermediate: 4-acetoxy-3-(1-hydroxyethyl)-2-azetidinone. *Chem. Pharm. Bull. (Tokyo).* **39,** 1931–1938 (2004).

25. Molander, G. A. & Etter, J. B. 1,3-Asymmetric induction in intramolecular Reformatsky-type reactions promoted by samarium diiodide. *J. Am. Chem. Soc.* **109,** 6556–6558 (1987).

26. Gallucci, J. C., Ha, D.-C. & Hart, D. J. Preparation of aminosaccharides using ester-imine condensations: syntheses of methyl -benzoylacosaminide and methyl -[oxo(phenylmethoxy) acetyl)daunosaminide from (S)-ethyl 3-hydroxybutyrate. *Tetrahedron* **45,** 1283–1292 (1989).

27. kaga, H., Kobayashi, S. & M, O. A Stereoselective Route to the Key Intermediate of 1-Beta-Methylcarbapenems by Chemicoenzymatic Approach. *Tetrahedron Lett.* **30,** 113–116 (1989).

28. Yoshioka, T. *et al.* Structures of OA-6129A, B1, B2 and C, new carbapenem antibiotics produced by Streptomyces sp. OA-6129. *J. Antibiot. (Tokyo).* **36,** 1473–1482 (1983).

29. Kubo, K., Ishikura, T. & Fukagawa, Y. Studies on the biosynthesis of carbapenem antibiotics. II. Isolation and functions of a specific acylase involved in the depantothenylation of the OA-6129 compounds. *J. Antibiot. (Tokyo).* **37,** 1394–1402 (1984).

30. Harada, S., Nozaki, Y., Shinagawa, S. & Kitano, K. C-19393 E5, a new carbapenem antibiotic. Fermentation, isolation and structure. *J. Antibiot. (Tokyo).* **35,** 957–962 (1982).

31. Box, S. J., Corbett, D. F., Robins, K. G., Spear, S. R. & Verrall, M. S. A new olivanic acid derivative produced by Streptomyces olivaceus: isolation and structural studies. *J. Antibiot. (Tokyo).* **35,** 1394–1396 (1982).

32. Hodgson, J. E. *et al.* Clavulanic acid biosynthesis in Streptomyces clavuligerus: gene cloning and characterization. *Gene* **166,** 49–55 (1995).

33. Elkins, J. M. *et al.* Oligomeric structure of proclavaminic acid amidino hydrolase: evolution of a hydrolytic enzyme in clavulanic acid biosynthesis. *Biochem. J.* **366,** 423–434 (2002).

34. Ueda, Y., Roberge, G. & Vinet, V. A simple method of preparing trimethylsilyl- and tert -butyldimethylsilyl-enol ethers of α-diazoacetoacetates and their use in the synthesis of a chiral precursor to thienamycin analogs. *Can. J. Chem.* **62,** 2936–2940 (1984).

35. Bateson, J. H., Quinn, A. M. & Smale, T. C. Olivanic acid analogues. Part 2. Total synthesis of some C (6)-substituted 7-oxo-1-azabicyclo [3.2.0] hept-2-ene-2-carboxylates. *J. Chem. Soc. Perkin Trans. 1* 2219 (1985).

36. Salzmann, T. N., Ratcliffe, R. W., Christensen, B. G. & Bouffard, F. A. A stereocontrolled synthesis of (+)-thienamycin. *J. Am. Chem. Soc.* **102,** 6161–6163 (1980).

37. Corbett, D. F., Brown, N. D. P. & Ponsford, R. J. Process for the preparation of azabicyclo(3.2.0)-hept-2-ene derivatives. 87 (1982).

38. Deng, G. *et al.* Tryptophan-containing dipeptide derivatives as potent PPARγ antagonists: Design, synthesis, biological evaluation, and molecular modeling. *Eur. J. Med. Chem.* **43,** 2699–2716 (2008).

Chapter 4

Consecutive radical *S*-adenosylmethionine methylations form the ethyl side chain in thienamycin biosynthesis and attachment of extended, CoA-derived thiols in complex carbapenem biosynthesis

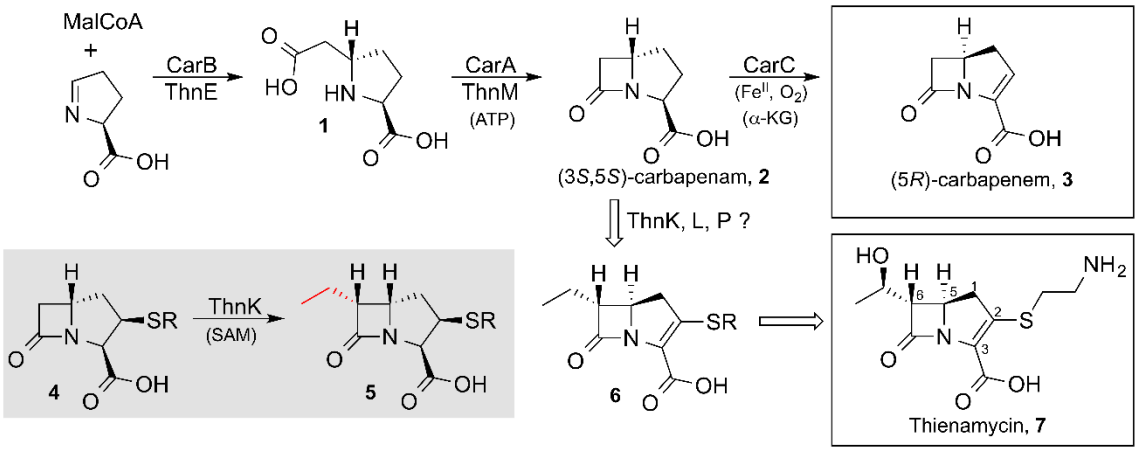

Figure 4.1: Biosynthesis of thienamycin and activity of ThnK. Two enzymes ThnE and ThnM form the (3*S,*5*S*)-carbapenam **2**, which is then acted upon by other enzymes, likely including ThnK, ThnL, and ThnP to form thienamycin. Correspondingly, CarB and CarA can also form **2** that CarC can convert to the simple carbapenem **3**. The demonstrated activity of ThnK is highlighted in gray.

Bacterial resistance to penicillin and cephalosporin has placed increased clinical reliance on the carbapenem class of β-lactam antibiotics, notably synthetic variants of the naturally-occurring thienamycin (Figure 4.1)[1]. Approximately 50 "complex" carbapenems are known, which are distinguished by a vinylthio substituent at C-2 and a short alkyl chain at C-6. These natural products have been isolated from actinomyces while the lone "simple" carbapenem-3-carboxylic acid **3** is known from an enterobacterium, *Pectobacterium carotovorum*[1]. Despite their evolutionary distance, the first two biosynthetic steps to each are shared[2]. Thus, CarB encoded in the latter and ThnE from *Streptomyces cattleya*, and correspondingly CarA and ThnM give (3*S*,5*S*)-carbapenam **2** as shown in Figure 4.1. At this point the two pathways diverge in a striking

manner where the simple carbapenem **3** is produced by both configurational inversion at the bridgehead and C-2/3-desaturation mediated by CarC[3]. In contrast, the path to thienamycin **7**, and likely all complex carbapenems, involves an entirely separate sequence of transformations. Apart from the identification of ThnR, ThnH, and ThnT in the stepwise truncation of coenzyme A (CoASH) to the C-2-cysteamine side chain of thienamycin[4], the timing of these tailoring events with respect to the introduction of the C-2-substituent onto the carbapenam(em) nucleus, alkylation at C-6, ring inversion and desaturation remain shrouded in mystery, although compound **6** is hypothesized to be an intermediate. Unique to the complex carbapenems are three apparent cobalamin-dependent radical *S*-adenosylmethionine (RS) enzymes ThnK, ThnL, and ThnP (all annotated as Class B RS methylases)[5], which we now demonstrate likely play critical roles in the central undefined steps of thienamycin biosynthesis.

RS enzymes are commonly identified by a conserved Cx_3Cx_2C motif, typically responsible for coordinating a [4Fe-4S] cluster[6], which enables this protein family to perform more than 40 so-far-identified biochemical transformations including sulfur insertion and methylation relevant to thienamycin biosynthesis[7]. The three thienamycin RS enzymes also contain *N*-terminal extensions thought to be cobalamin (B_{12})-binding domains, which would appear in keeping with early observations that Co^{II} and cobalamin increased carbapenem titers in cultures of producing strains[8]. Indeed the low turnover of RS enzymes may account for why thienamycin could not be produced by cost-effective fermentation methods, and as a consequence all clinically–used carbapenems are manufactured synthetically[1].

While probable that the carbapenem RS enzymes perform several intermediate biosynthetic steps and potentially use unprecedented chemistry, the challenge of deciphering their activities is exacerbated by their intrinsic instability, unknown substrates, and multiple possible reactions. Fellow graduate student Daniel Marous and I took the first step in illuminating the obscure center of the thienamycin biosynthetic pathway by identifying substrates for ThnK and establishing that this enzyme performs two consecutive methylations to generate the C-6-ethyl side chain stereospecifically (Figure 1). While other RS cobalamin-dependent enzymes that act on carbon have been investigated[9–12], this is the first *in vitro* characterization of a RS methylase acting sequentially to form a side chain.

Construction of an initial synthetic library for ThnK activity assays

Daniel Marous and I collaborated very closely on the synthesis of a library of candidate substrates the preparation of product standards, including the simple (3*S,*5*S*)-carbapenam **2** and related C-2 and C-6-substituted derivatives **12**-**15**, **38** and **39** as shown in Scheme 4.1. Often times we performed the same reactions separately, and in some instances either he or I performed a certain reaction, many of which followed the thesis work of Dr. Kristos Moshos, who made many similar carbapenams for his studies with ThnR, T, H and F. Our library was biased toward structures with the (3*S,*5*S*)-stereochemistry, matching that of the ThnM product **2**, and those bearing the 6*R*-configuration (**38**, 3**9**) matching that of thienamycin (Figure 4.4A). A pantetheinyl moiety was selected for the side chain at C-2 (**12**-**15**) in keeping with the OA-6129 series of metabolites that has been isolated from carbapenem producers[13,14].

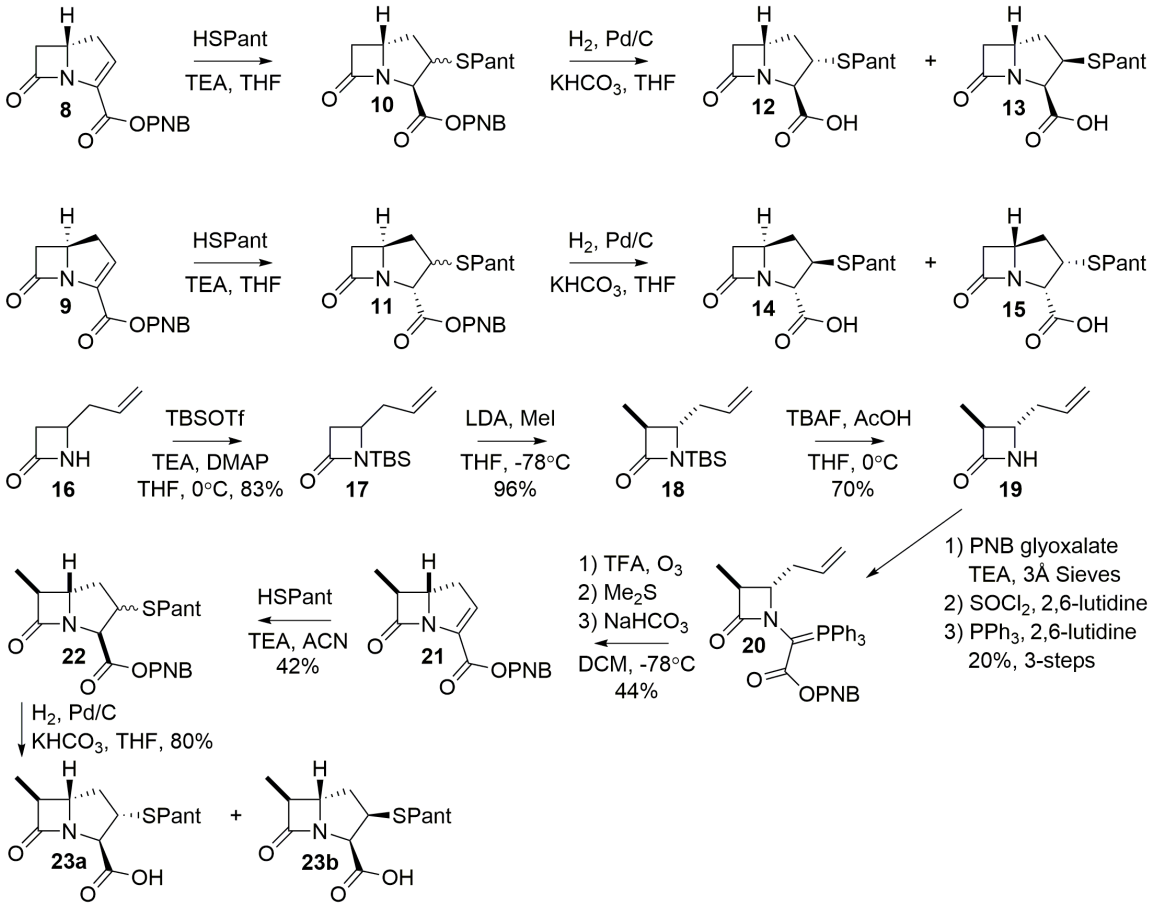

Scheme 4.1: Synthesis of an initial library for ThnK substrates

Synthesis of carbapenam PNB esters **10** and **11** proceeded easily through conjugate addition of pantetheine thiol in the presence of trimethylamine. Hydrogenolysis of the PNB esters followed by HPLC purification afforded the pure diastereomers **12**, **13**, **14** and **15**. To produce initial C-6 methyl carbapenams as substrates or product standards, racemic 4-allylazetidinone was used as an easily accessible starting material. TBS protection of the amide followed by enolate addition to methyl iodide and subsequent TBS removal provided the 4-allyl-3-methylazetidinone **18**. Reaction of the resulting amide with PNB glyoxalate using 3Å molecular sieves was followed by conversion of the resulting aminal with thionyl chloride to provide a reactive

intermediate for the production of the triphenylphosphine ylid **20**. The carbapenem **21** was produced in one step after ozonolysis and reduction of the ozonide to an aldehyde. The product aldehyde is not recovered, as spontaneous Wittig closure of the ylid and aldehyde occurs upon quenching with sodium bicarbonate. The presence of trifluoroacetic acid was necessary during the addition of ozone to protonate the ylid, making it unreactive until basic workup. With carbapenem **21** in hand, facile conjugate addition of pantetheine thiol and hydrolysis of the 3-PNB ester affords the methyl carbapenam **23** as a mixture of C-2 diastereomers.

Expression, purification, and analysis of ThnK

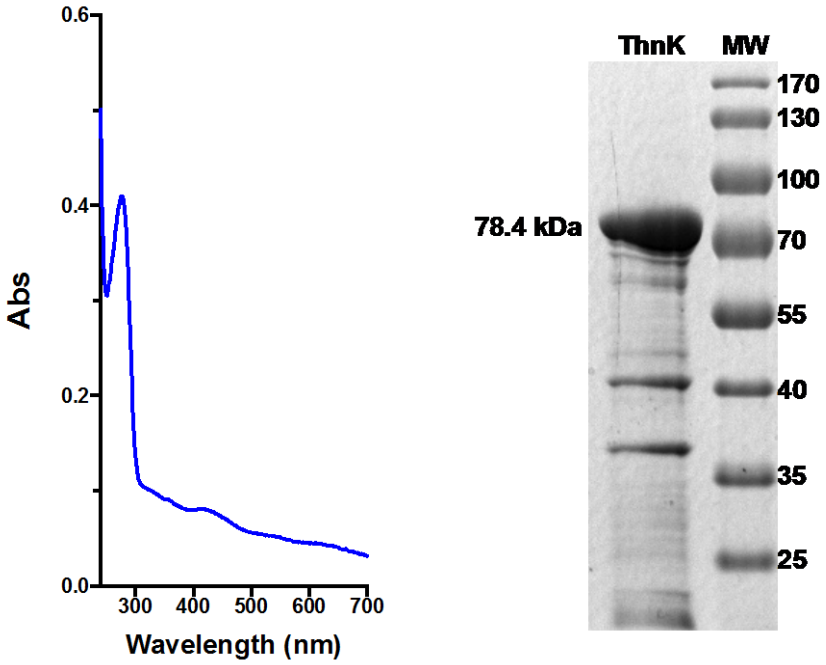

Figure 4.2: UV-Visible spectrum and SDS PAGE of ThnK**.** The UV-visible spectrum of ThnK shows a 420 nm shoulder, indicative of a bound iron sulfur cluster.

The best behaved of the three RS enzymes, ThnK, was cloned from *Streptomyces cattleya* by Dr. Rongfeng Li, where Andrew Buller originally found experimental conditions that gave moderate levels of soluble protein when expressed with a C-terminal His_6-tag in *E. coli* Rosetta 2(DE3). Because ThnK was expected to utilize both an iron-sulfur (Fe/S) cluster and cobalamin, protein production was conducted in ethanolamine-M9 medium due to the suggestion of Tyler Grove in the laboratory of Squire Booker. Ethanolamine-M9 facilitates uptake of externally supplied hydroxocobalamin into *E. coli*, and with concurrent expression of the *Azotobacter vinelandii isc* operon, encoded on plasmid pDB1282. Daniel Marous and I purified ThnK under strictly anaerobic conditions. The UV-visible spectrum of purified ThnK revealed a 420 nm shoulder (Figure 4.2) typical of a bound iron-sulfur cluster. The relative stoichiometry of iron and sulfide bound by the as-isolated protein was determined to be 7.4 ± 1.4 and 3.7 ± 0.8 per polypeptide, respectively, consistent with the presence of a [4Fe-4S] cluster. Excess iron has been observed with other RS enzymes[11,15], and was similarly seen in an alanine variant control (Figure 4.7).

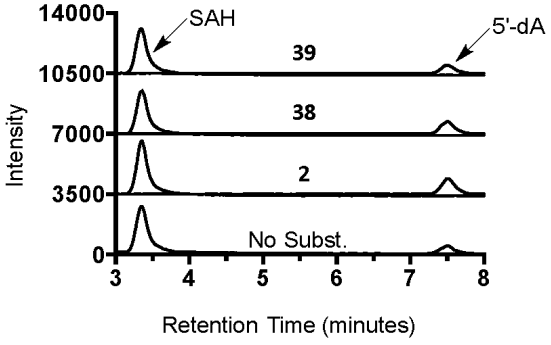

Figure 4.3: Detection of SAM-derived products of ThnK with compounds **2, 38,** and **39.** LC-MS/MS was used to detect SAM-derived coproducts, SAH (385.4 -> 136 *m/z*) and 5'-dA (252.1 -> 136 *m/z*). The extracted-ion chromatograms (EICs) for the transitions of SAH and 5'-dA are overlaid for each reaction. The reactions with compounds **2**, **38**, and **39** show about the same level of turnover as the reaction without substrate. Reactions were run for approximately 2 hours at room temperature.

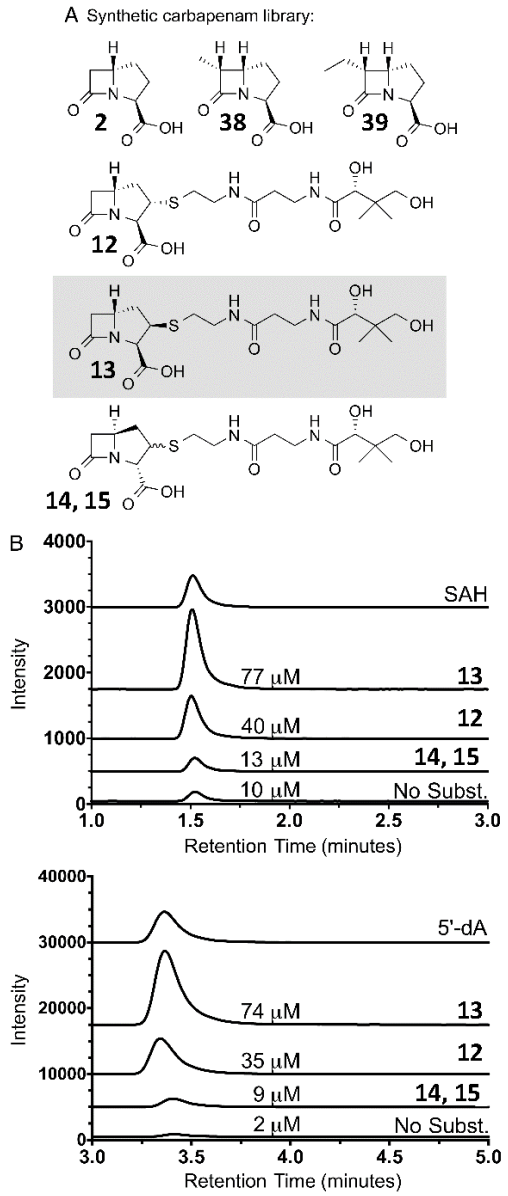

Figure 4.4: Carbapenam synthetic library and detection and quantification of SAM products of ThnK. (*A*) Compounds synthesized to probe ThnK activity. (B) LC-MS/MS detection of enzymatic SAM co-products, SAH (385.4 -> 136 *m/z*) and 5'-dA (252.1 -> 136 *m/z*). The extracted-ion chromatograms (EICs) for the transitions of SAH and 5'-dA are shown for each reaction. The reaction with compound **13** gave the highest levels of these SAM co-products. Quantified levels of SAH and 5'dA are shown for each reaction.

Analysis of SAH and 5'da produced from ThnK turnover

To determine whether any of our library compounds was a substrate for ThnK, Tyler Grove and Anthony Blaszczykk, graduate students in the Booker lab, helped develop a LC-MS analytical screen whereby enzymatic reactions were monitored for appearance of the expected RS methylase co-products, *S*-adenosylhomocysteine (SAH) and 5'-deoxyadenosine (5'-dA)[16,17]. Initial screens were conducted with ThnK, SAM, and potential carbapenam substrates in the presence of methyl viologen and NADPH as Fe/S cluster reductants[10]. The (3*S,*5*S*)-carbapenam and related C-6-methyl and ethyl derivatives (**2**, **38**, and **39**) gave nearly background (no-substrate control) levels of SAH and 5'-dA (Figure 4.3). In contrast, SAM co-products accumulated when ThnK was incubated with C-2-substituted carbapenams, suggesting that the full methyl transfer reaction(s) had occurred (Figure 2B). Alternate Fe/S cluster reductants, including dithionite and the flavodoxin/flavodoxin reductase/NADPH reducing system were also examined, but did not give improved activity (Figure 4.5). To assess enzymatic turnover, the amounts of SAH and 5'-dA were quantified by LC-MS/MS (Figure 2B). Compounds bearing the now (3*R,*5*R*)-stereochemistry with a pantetheine side chain at C-2 gave the greatest levels of turnover of the pantetheinyl carbapenams. Therefore, each C-2 diastereomer (compound **12** or **13**) was tested individually. The (2*R*,3*R*,5*R*)-carbapenam **13** yielded ~2-fold higher amounts of SAM co-products. These stereochemical preferences were found to be reproducible (Figure 4.6) and SAH and 5'dA were present in approximately equimolar amounts in each reaction.

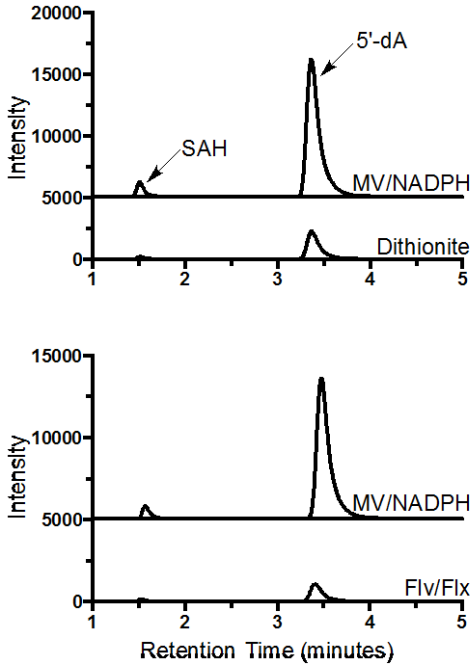

Figure 4.5: LC-MS/MS comparison of enzymatic turnover using different iron-sulfur cluster reductants. The extracted-ion chromatograms (EICs) for the transitions of SAH (385.4 -> 136 *m/z*) and 5'-dA (252.1 -> 136 *m/z*) are overlaid for each reaction. Methyl viologen with NADPH gave higher turnover than dithionite or flavodoxin with flavodoxin reductase and NADPH. Reactions were run for approximately 2 hours at room temperature with substrate **13**.

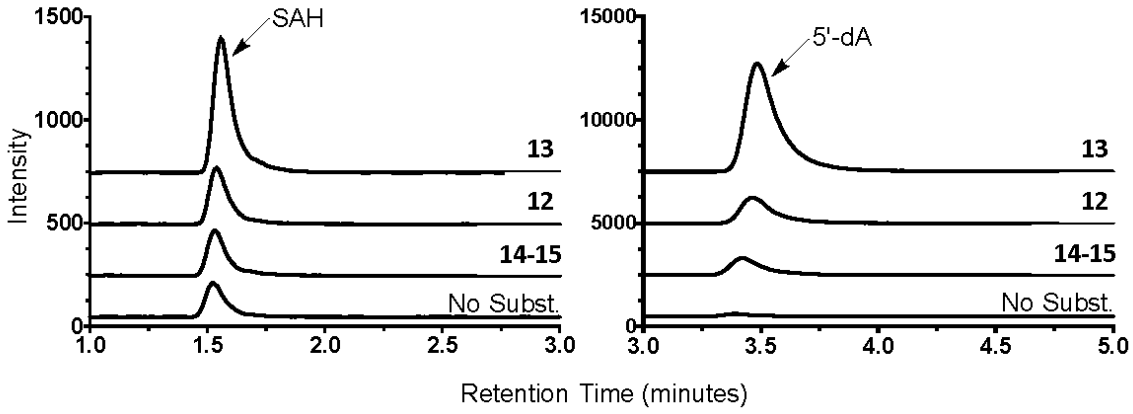

Figure 4.6: Reproducibilty of SAM-derived products of ThnK. LC-MS/MS was used to detect SAM-derived coproducts, SAH (385.4 -> 136 *m/z*) and 5'-dA (252.1 -> 136 *m/z*). The extracted-ion chromatograms (EICs) for the transitions of SAH and 5'-dA are overlaid for each reaction. The reaction with compound **13** gave the highest levels of these SAM-derived coproducts. Reactions with ThnK (~80 μM) were run for 1.5 hours at room temperature and included 1 mM HOCbl, though added cobalamin was determined not to be required for activity.

Analysis of the [4Fe-4S] cluster

To test the role of the [4Fe-4S] cluster in catalysis, Daniel Marous generated a variant of ThnK where the conserved cluster binding motif Cx_3Cx_2C was changed from three cysteine to three alanine residues. The variant protein was prepared as described for wild-type ThnK and incubated with substrate **13**. The inactivated enzyme did produce low levels of SAH, but no detectable 5'-dA (Figure 4.7), consistent with reliance of the wild-type enzyme on a functional Fe/S cluster. WT ThnK was also expressed in M9 medium lacking hydroxocobalamin for another control experiment. The purified protein with substrate **13** did not produce SAH or 5'dA; however, enzymatic activity could be rescued if cobalamin was added to the reaction mixture (Figure 4.8).

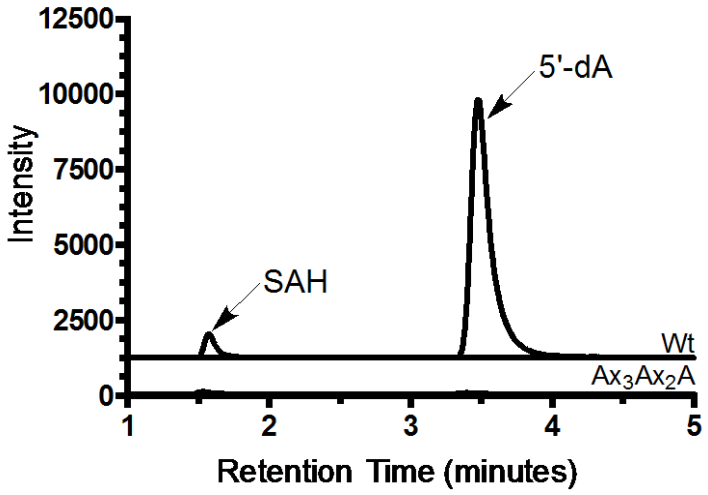

Figure 4.7: Fe/S cluster required for ThnK activity. LC-MS/MS was used to detect SAM-derived coproducts, SAH (385.4 -> 136 *m/z*) and 5'-dA (252.1 -> 136 *m/z*). The extracted-ion chromatograms (EICs) for the transitions of SAH and 5'-dA are overlaid for each reaction. Alteration of the Cx_3Cx_2C motif to Ax_3Ax_2A resulted in little SAH production and no 5'-dA production. Reactions were run for approximately 2 hours at room temperature with substrate **13**.

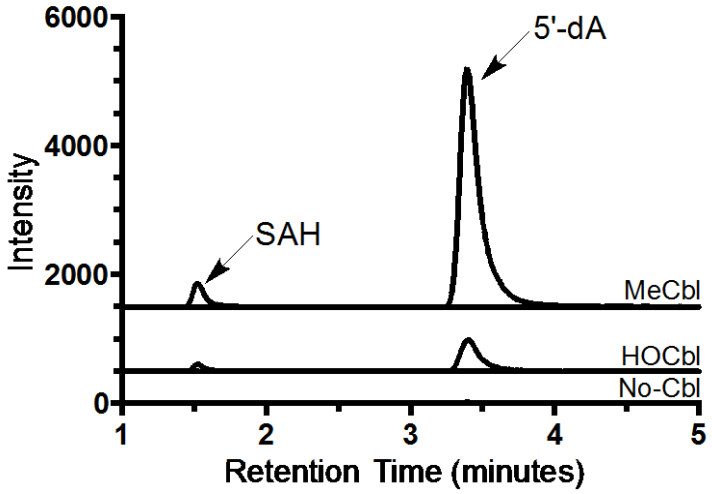

Figure 4.8: Cobalamin required for ThnK activity. LC-MS/MS was used to detect SAM-derived coproducts, SAH (385.4 -> 136 *m/z*) and 5'-dA (252.1 -> 136 *m/z*). The extracted-ion chromatograms (EICs) for the transitions of SAH and 5'-dA are overlaid for each reaction. ThnK, expressed in and isolated from *E. coli* cultured in the absence of cobalamin, was either given no cobalamin, HOCbl, or MeCbl. Added cobalamin was able to rescue ThnK activity with MeCbl yielding higher levels of SAH and 5'-dA than HOCbl. Reactions were run for 1 hour and 10 minutes at room temperature with substrate **13**.

Chemo- and stereoselectivity of methyl transfer by ThnK

We next sought to determine how the substrate was transformed during the reaction with ThnK. Assays with **13** were analyzed by UPLC-HRMS. Exact masses were obtained matching methylated (calc: *m/z* 446.1961, found: 446.1954) and twice-methylated (calc: *m/z* 460.2117, found: 460.2104) modifications of the substrate. The extracted-ion chromatograms for these masses showed retention times that were consistent with increasing hydrophobicity relative to the substrate (Figure 4.9). The highly diagnostic β-lactam mass fragment (calc: *m/z* 390.1699) corresponding to the loss of a ketene from cleavage of the β-lactam ring[18] was observed (found: *m/z* 390.1701) (Figure 4.10), which was further consistent with methylation at C-6. To establish SAM as

the methyl donor, additional ThnK reactions were performed in vollaboration with the Booker lab using biosynthesized *S*-adenosyl-L-[*methyl*-d_3]methionine (d_3-SAM) that they provided us. The corresponding M+3 *m/z* shift was observed for the methylated product and an M+5 *m/z* shift was seen for the twice-methylated product (Figure 4.10), fully in accordance with formation of the ethyl side chain at C-6 in thienamycin by successive methyl transfers.

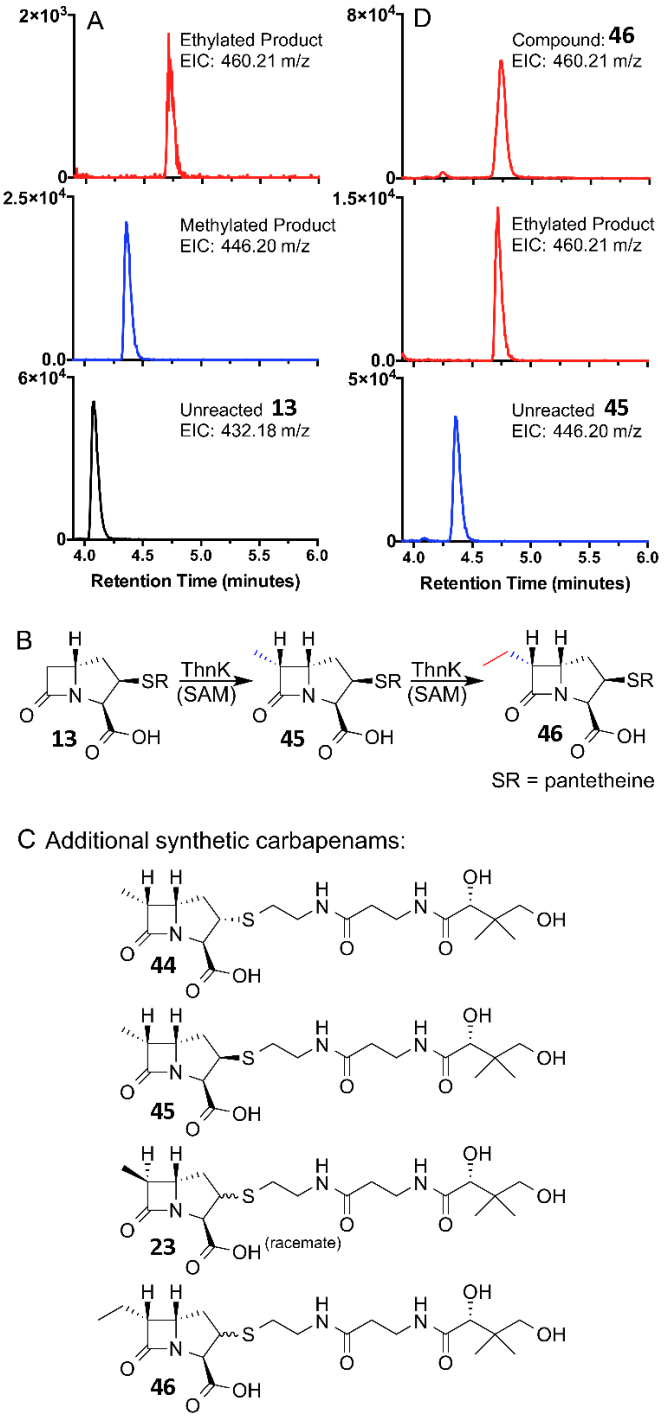

Figure 4.9: Carbapenam synthetic library and detection and quantification of SAM products of ThnK. (a) Compounds synthesized to probe ThnK activity. (b) LC-MS/MS detection of enzymatic SAM co-products, SAH (385.4 -> 136 *m/z*) and 5'-dA (252.1 -> 136 *m/z*). The extracted-ion chromatograms (EICs) for the transitions of SAH and 5'-dA are shown for each reaction. The reaction with compound **13** gave the highest levels of these SAM co-products. Quantified levels of SAH and 5'dA are shown for each reaction.

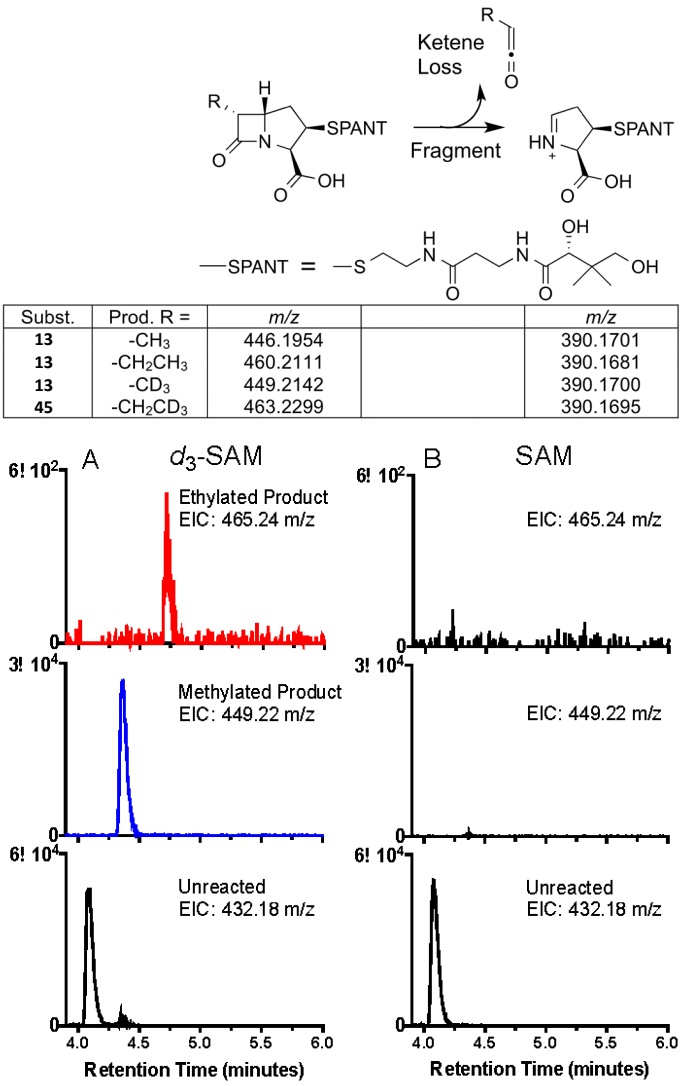

Subst.	Prod. R =	*m/z*		*m/z*
13	$-CH_3$	446.1954		390.1701
13	$-CH_2CH_3$	460.2111		390.1681
13	$-CD_3$	449.2142		390.1700
45	$-CH_2CD_3$	463.2299		390.1695

Figure 4.10: Product detection of ThnK assays with d_3-SAM. (a) UPLC-HRMS detection of carbapenams from ThnK reaction with compound **13** and d_3-SAM. The bottom, middle, and top traces show the extracted-ion chromatograms (EICs, $m/z \pm 0.05$) for unreacted substrate (432.18 *m/z*), methylated product (449.22 *m/z*), and ethylated product (465.24 *m/z*), respectively. The middle and top traces show a +3 m/z and a +5 *m/z* shift, respectively, from Figure 4.9A. (b) UPLC-HRMS detection of carbapenams from ThnK reaction with compound **13** and natural abundance SAM. The shifted masses observed in A are not present in B.

To secure the stereochemistry of the first methylation, synthesis of a set of C-6-methylcarbapenams (**23**, **44**, **45**, Figure 4.9, Scheme 4.2) was carried out by both Daniel

Marous and myself before assaying with ThnK. While compounds **44** and **23** displayed trace or no measurable activity, respectively, **45** afforded unequivocal production of SAH and 5'-dA (Figure 4.11). This result underscored the importance of the stereochemical relationship between the C-3-carboxylate and the pantetheinyl side chain and confirmed that the C-6-methyl is attached in the *R*-configuration, as occurs in thienamycin. By UPLC-ESI/MS analysis, the ethylated product of **45** (resulting from a single methyl transfer) matched the exact mass and retention time of the ethylated product of compound **13** (Figure 4.9A and 4.9D). In further support, the (6*R*)-ethyl standard **46** was synthesized and determined to match the retention time, exact mass, and fragmentation pattern for the aforementioned products, as expected (Figure 4.9A and 4.9D). The observed activity of ThnK is summarized in Figure 4.9B.

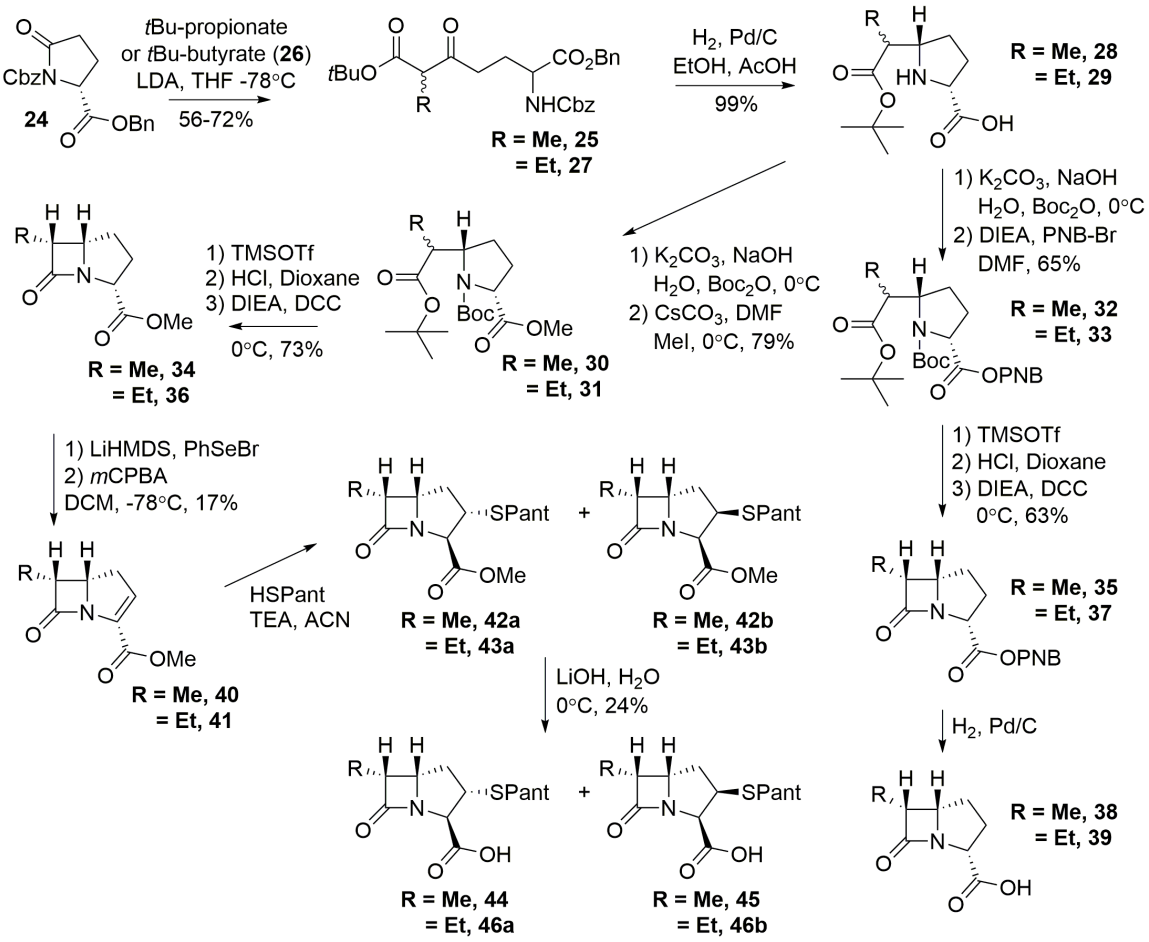

Scheme 4.2: Synthesis of 5,6-*cis*-carbapenams

In order to obtain *cis*-6-alkylcarbapenams, a different synthetic strategy was implemented to set the appropriate stereochemistry of the C-6 alkyl substituent[19]. Reaction of the lithium enolate of either *tert*-butylpropionate or *tert*-butylbutyrate with the amide carbonyl of *N*-carboxybenzylpyroglutamic acid benzyl ester opened the pyrrolidin-2-one to provide the β-ketoesters **25** and **26** as a mixture of α-diastereomers. Hydrogenolysis of the *N*-carboxybenzyl group liberates the primary amine so that imine condensation occurs *in situ*, followed by reductive amination to produce the pyrrolidines **28** and **29**. Protection of the secondary amine with Boc anhydride followed by esterification to the PNB ester allowed for its hydrolytic removal later in the production

of non-2-substituted carbapenams **38** and **39**. To our surprise, we found through attempts to deprotonate the C-3 position with LiHMDS later in the synthesis that the acidic benzyl protons of the PNB ester were incompatible. Since our goal was to synthesize 2-pantetheinyl carbapenams, formation of a methyl ester was necessary to avoid this pitfall. To close the β-lactam ring, deprotection of the *tert*-butyl ester and carbamate was possible using anhydrous conditions, which were necessary for a good yield during *N*,*N*-dicyclohexylcarbodiimide coupling. After the carbapenam was made, epimerization of the C-3 position with DBU in acetonitrile at 60 °C for 72 h provided diastereomers which were separable by flash chromatography. With enantiopure **34** and **36** in hand, production of the lithium enolate allows for addition into phenylselenyl bromide. The selenium adducts rapidly eliminated upon oxidation with *m*-CPBA at -30 °C to provide the carbapenems **40** and **41**, although in poor yield due to unstable reaction conditions that degrade the carbapenem. Recovery could be improved with careful monitoring of reaction progress by TLC, but a yield of 30% over two steps was typical. Conjugate addition of pantetheine to the carbapenems **42**-**43** followed by saponification of the methyl esters and separation of the diastereomers by HPLC provided the desired *cis*-carbapenams **44**-**46**. It is a lengthy synthesis without stereochemical control, but divergence to separable diasteromers was used to our advantage for the testing of each stereoisomer against ThnK in enzyme activity assays.

ThnK Substrate Profiling with C-2-Thioether Variants

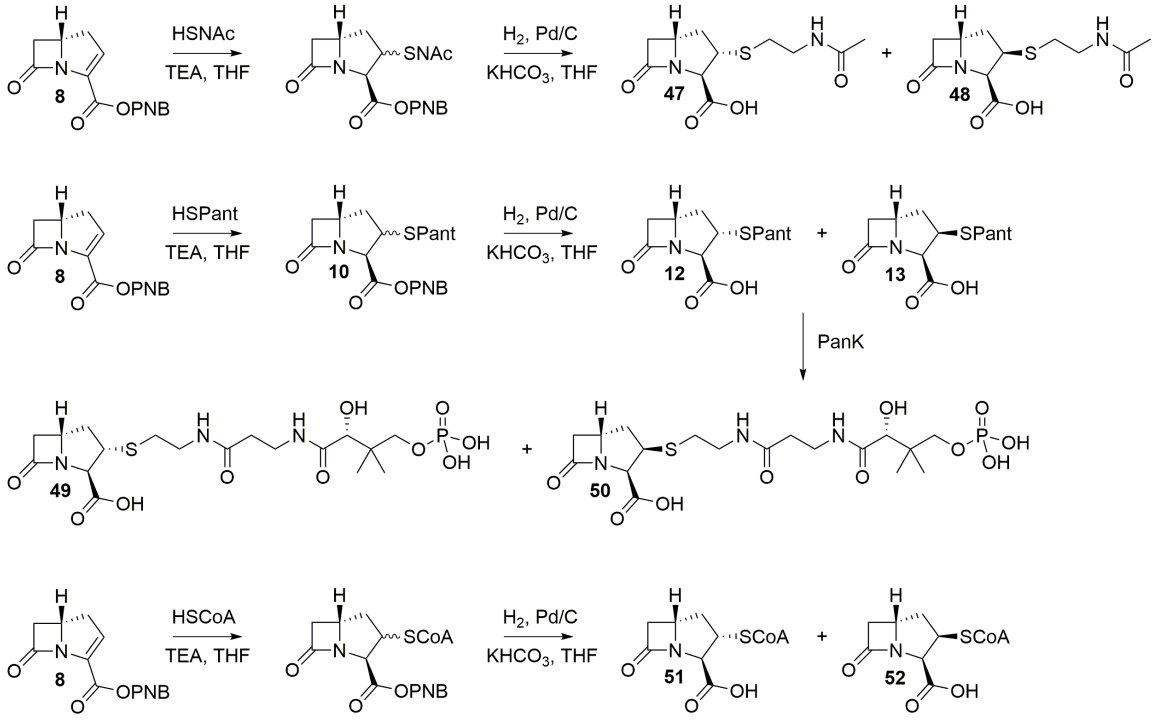

Scheme 4.3: Overview of the Synthesis of C-2-Substituted Carbapenams to Test with ThnK. The enzyme PanK was used to install the terminal phosphate on the phosphopantetheinyl side chain

Once the function of ThnK was established, it was anticipated that the substrate specificity of ThnK could be leveraged to provide insight into which thiol is added to the bicyclic core. That is, it could be possible to deduce the function of ThnL. Beginning with CoA, three enzymes in the thienamycin cluster, ThnR, ThnH, and ThnT, successively cleave to yield 4-phosphopantetheine, pantetheine, and cysteamine, respectively[4]. Knowing this sequence, four thiols are potentially available for attachment. As possible substrates for ThnK, carbapenams with C-2-substituents representing all the truncation states were desired, although the cysteamine side chain was replaced with the more chemically inert *N*-acetylcysteamine (SNAC). The

carbapenem **8** was synthesized using previously established methods[20] to facilitate the generation of these compounds (Scheme 4.3). From the common intermediate **8**, pantetheine or SNAC could be inserted by β-addition been demonstrated[4,21,22]. Additionally, it was found that CoA itself could be added into the carbapenem, enabling a direct route to the CoA-substituted compounds. High-performance liquid chromatography (HPLC) was utilized to separate the resulting C-2-diastereomers, giving compounds **47**, **48**, **49**, **50**, **51** and **52** (Scheme 4.3). To address the synthetic challenge of generating the phosphopantetheinyl carbapenams, we employed a chemoenzymatic strategy. The pantetheinyl compounds **12** and **13** were converted into their corresponding phosphopantetheinyl analogs **49** and **50** using the enzyme pantothenate kinase as done previously (PanK, CoA)[23].

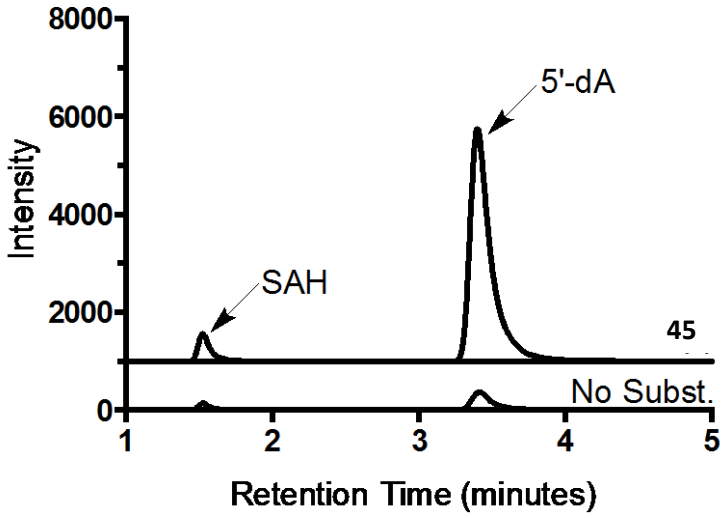

Figure 4.11: Detection of SAM-derived products of ThnK with compound **45**. LC-MS/MS was used to detect SAM-derived coproducts. The fragmentation patterns of SAH (385.4 -> 136 *m/z*) and 5'-dA (252.1 -> 136 *m/z*) were specifically measured to generate an extracted ion chromatogram (EIC). The EICs for the transitions of SAH and 5'-dA are overlaid for each reaction. The reaction with compound **45** shows increased turnover compared to the no substrate control. Reactions were run for 2 hours and ten minutes at room temperature.

With the synthetic targets in hand, ThnK was expressed and purified anaerobically as previously described[22]. To evaluate the synthetic substrates, each compound (1 mM) was incubated with ThnK along with [4Fe-4S] cluster reductants (methyl viologen, 1 mM and NADPH, 2 mM), and SAM (1 mM). ThnK was confirmed to perform consecutive methylations at C-6, as expected (Figure 4.13).

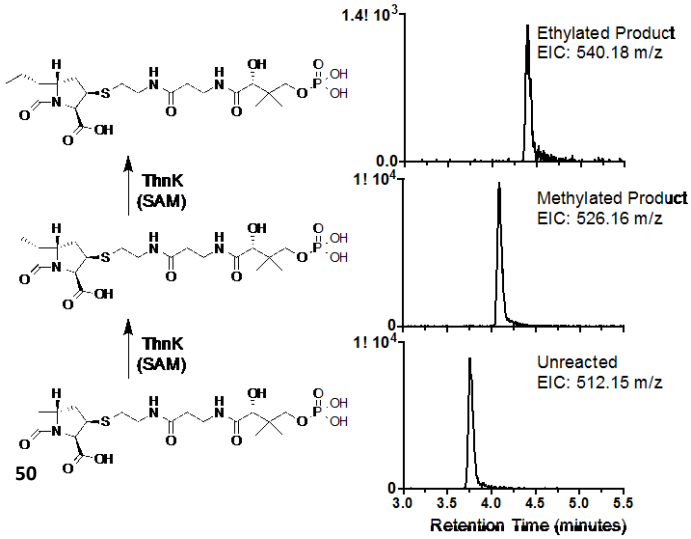

Figure 4.12: Sequential Methylations by ThnK. UPLC-HRMS detection of carbapenams from the ThnK reaction with compound **15**. The bottom, middle, and top traces show the extracted-ion chromatograms (EICs) (*m/z* ± 0.05) for unreacted substrate **50** (512.15 *m/z*), methylated product (526.16 *m/z*), and ethylated product (540.18 *m/z*), respectively.

For assessment of the relative turnover with the various substrates, the RS methylase SAM-derived coproducts *S*-adenosylhomocysteine (SAH) and 5′-deoxyadenosine (5′-dA)[17] were again monitored by LC-MS/MS. Several trends were apparent from sampling the levels of accumulated 5′-dA (Figure 4.14A). Three compounds consistently gave the lowest turnover: both C-2-SNAC molecules (**47** and **48**) and the (2*S*)-pantetheine-substituted **12**. The (2*R*)-carbapenam **13** gave higher levels of 5’-dA than its diastereomer **12**, as had been observed previously[22]. With the (2*R*)-series

(**13**, **48**, **50**, **52**), extending the side chain to phosphopantetheine **50** or CoA **52** did not hinder turnover, but rather led to modest gains. Strikingly, with the (2*S*)-series (**12**, **47**, **49**, **51**), the phosphopantetheine **49** and CoA **51** analogs gave significantly improved activity compared to the pantetheine compound **12**. In fact, CoA-functionalized **51** produced the greatest amounts of 5'-dA of all the substrates tested. Correspondingly, these trends with 5'-dA levels mirrored those of SAH accumulation (Figure 4.14B). Overall, the compounds with longer C-2 side chains were better substrates than their shorter side chain counterparts.

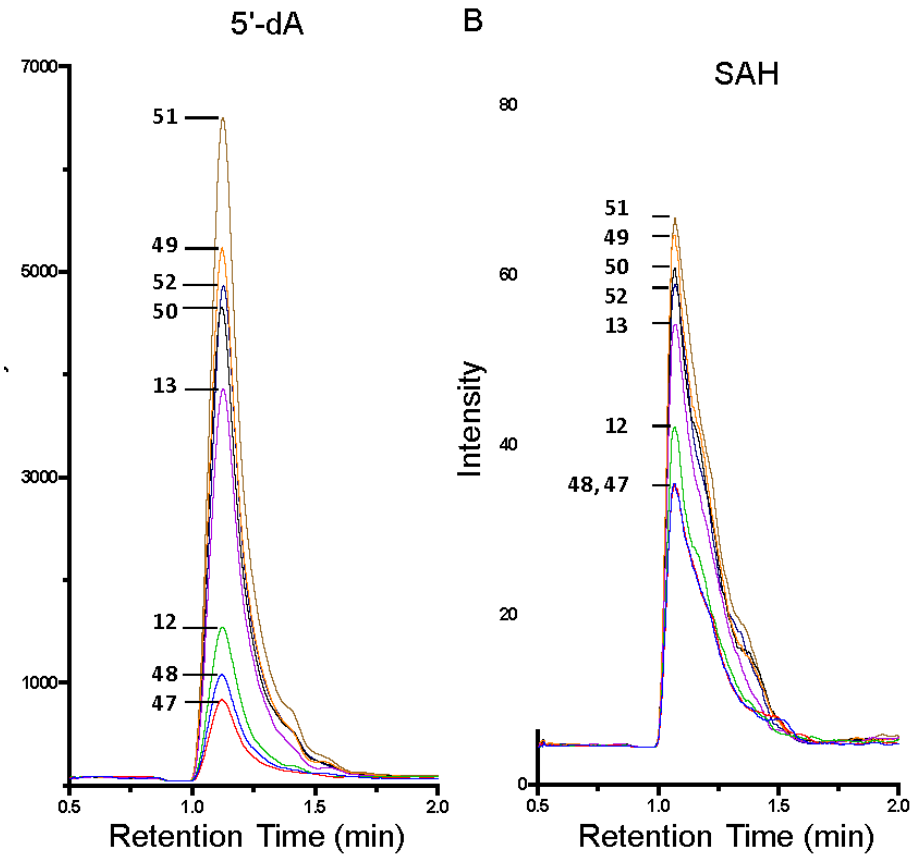

Figure 4.13: LC-MS/MS Detection of Enzymatic SAM-Derived Coproducts 5'-dA and SAH from Assays with Compounds 10-17. (a) The extracted-ion chromatograms (EICs) for the transition of 5′-dA (252.1→136 *m/z*). (b) The EICs for the transition of SAH (385.4 → 136 *m/z*).

Discussion

Mechanistically, ThnK resembles GenK, a cobalamin-dependent RS *C*-methylase in gentamicin biosynthesis[10], as both produce near equimolar amounts of SAH and 5'-dA during catalysis. Early labeling experiments established that the C-6-ethyl side chain of thienamycin was derived from methionine[24]. A labeled carbon was also found in the C-6-hydroxymethyl side chain of northienamycin, a minor co-metabolite of thienamycin, suggesting a singly-methylated intermediate in the formation of the ethyl side chain[24]. The present *in vitro* analysis of ThnK agrees with these early experiments. An experiment incorporating chiral [^{1}H, ^{2}H, ^{3}H-*methyl*]-L-methionine demonstrated that the absolute configuration of the terminal methyl in the C-6-side chain was largely retained, consistent with an overall methyl transfer process involving two inversions and a methylcobalamin intermediate[25]. The B_{12}-dependence of ThnK reactions established above supports the role of a methylcobalamin intermediate, as has been implicated in other methyltransferases including TsrM[9] and GenK[10]. While the tryptophan methylase TsrM may utilize a similar intermediate, the enzyme is likely mechanistically distinct from ThnK and GenK because it does not produce detectable levels of 5'-dA[9].

The catalysis of consecutive methylations observed for ThnK likely occurs elsewhere in nature. Within the carbapenem family, the carpetimycins have three carbons in their C-6 side chain[8] suggesting that a ThnK ortholog may be responsible for three methyl transfers. The natural product pactamycin has traditionally been compared to thienamycin because both possess a hydroxyethyl side chain[24]. A recent genetic knockout study suggests, however, that more than one enzyme takes part in attaching the ethyl group[26]. While sequential methylations appear not to occur by a single enzyme in

pactamycin biosynthesis, other RS enzymes including Swb9[27] and PoyB or PoyC[28] in quinomycin and polytheonamide biosynthesis, respectively, have been implicated in multiple methylations of a single substrate chain.

The preference for long C-2 sidechains is a critical topic in terms of the placement of the activity by ThnK in thienamycin biosynthesis. Increased turnover of ThnK with carbapenams that have either CoA or phosphopantetheine at C-2 implies that adenosyl or phosphoryl cleavage occurs after methylation at C-6. The stereochemical preference of C-2 thioalkyl substituents changes in CoA or phosphopantetheinyl carbapenams when compared to pantetheinyl carbapenams. It is possible that with either less room or different charge interactions in active site binding of the larger substrates, the stereochemical preferences change. However, without a reliable crystal structure of ThnK with substrates bound, these specific binding interactions are only speculative.

Conclusion

The data reported here establish notable catalytic roles for ThnK. It methylates in two distinct chemical environments (alpha to the β-lactam ring and on an unactivated methyl group). The second methyl transfer presumably involves a primary radical intermediate, a particularly high-energy species. The substrates that exhibit the highest efficiency for ThnK methylation are those that contain 2(*S*)-SCoA or 2(*S*)-phosphopantetheine substituents. By identifying favorable substrates for ThnK and elucidating its activity, we have gained additional clues about the unknown central steps in thienamycin biosynthesis as well. With formation of the ethyl side chain accounted for,

ThnL and ThnP can provisionally be assigned non-methyltransferase functions, potentially distinct chemistry for the RS-cobalamin family, as both proteins are essential for carbapenem production[29,30]. Since ThnK activity was only observed when a C-2-side chain was present (compounds **12**-**15**, **46-52** vs. **2**, **38**, and **39**), we deduce that C-2-thioether formation likely mediated by ThnL or ThnP precedes C-6-methylation in the pathway. The stereochemical preference for (2*R*)-pantetheinyl carbapenams **13** and **45** indicates that the thiol is likely introduced in the 2-*exo*-configuration, however is contradicted by CoA or phosphopantetheinyl carbapenams, where the (2*S*) configuration is favored. Furthermore, the observation of activity with substrates matching the (3*S,*5*S*)-carbapenam **2** at C-5 (compounds **12**, **13**, and **45**) suggests that bridgehead epimerization occurs after C-6-methylation (ethylation). Consequently, C-2-thiol attachment, C-6-alkylation, and C-5-epimerization likely occur in that order. The orchestration of these biosynthetic events with C-2/3-desaturation and maturation of the C-2-cysteamine will be addressed in due course.

Experimental

General methods and abbreviations:

Hydroxocobalamin (HOCbl), 4-(2-hydroxyethyl)-1-piperazineethane- sulfonic acid (HEPES), isopropyl β-D-1-thiogalactopyranoside (IPTG), 2-mercaptoethanol (BME), methylcobalamin (MeCbl), methyl viologen (MV), nicotinamide adenine dinucleotide, phosphate hydrate (NADPH), phenylmethysulfonyl fluoride (PMSF).

Restriction enzymes, DNA modifying enzymes, and PCR reagents were obtained from

New England Biolabs (Ipswich, MA). Plasmid kits were from Thermo Scientific (Waltham, MA). *E. coli* DH5α (Invitrogen) was usually used for DNA cloning and ThnK expression was done in *E. coli Rosetta 2*(DE3) (Novagen). The plasmid pDB1282 was utilized for Fe/S cluster expression[10]. SAM and *S*-adenosyl-L-[*methyl*-d_3]methionine (d_3-SAM) were synthesized as described previously[22]. Recombinant flavodoxin (Flv) and flavodoxin reductase (Flx) were over-produced in *E. coli* as previously described[31]. Plasmid DNA was sequenced by the Synthesis and Sequencing Facility of the Johns Hopkins University. Solvents and reagents were purchased from Sigma Aldrich or Fisher Scientific in purity of ≥98%. Silica gel chromatography was performed using 60Å silica gel from Sorbtech. Thin layer chromatography (TLC) was performed using 250 μm Analtech GHLF silica plates. A Bruker Avance (Billerica, MA) 300 or 400 MHz spectrometer was utilized for all ^{1}H and ^{13}C NMR spectra, which are reported in parts per million (δ) referenced against a TMS standard or residual solvent peak. The JHU Chemistry Department Mass Spectrometry Facility determined exact masses by fast atom bombardment (FAB) or electrospray ionization (ESI).

Cloning and Expression of *Streptomyces cattleya* ThnK. The *thnK* gene was PCR amplified from genomic DNA of *Streptomyces cattleya* (NRRL8057) using the following primers: 5' – CAAGACATATGACCGTCCCCGCCGCGC – 3',
5' TATCTCGAGCCGCTGCTCGGTCAGGACGGG – 3'. The *thnK* PCR product was digested using *NdeI* and *XhoI* and ligated into the vector pET29b (Novagen) to obtain the *C*-terminal 6-His construct of *thnK*. The plasmid was sequence-verified. The pET29b:t*hnK* was transformed into *E. coli* Rosetta DE3 for expression of ThnK as a *C*-

terminal His_6 construct. The *thnK* Rosetta strain was also transformed with the vector pDB1282, containing the ISC operon with arabinose induction[32]. The resulting strain was grown in 4 x 3.5 L of Ethanolamine-M9 medium[33], which included hydroxocobalamin (HOCbl), and was supplemented with $FeCl_3$ (~0.14 mM) at 37 °C and shaken at 180 rpm. When the optical density of the cultures reached 0.3 at 600 nm, 25 μM $FeCl_3$, 150 μM cysteine, and 0.1% arabinose were added. When the optical density of the fermentation reached 0.4-0.6 (8-10 h), the cultures were chilled on ice (~45 min) and an additional 25 μM $FeCl_3$, 150 μM cysteine, and 0.1% arabinose were added. ThnK expression was induced with 1 mM IPTG and the cultures were shaken at 180 rpm overnight at 19 °C. Cells were collected by centrifugation (4,000*g*, 12 min), which were then frozen on liquid nitrogen and stored for later use.

Anaerobic Purification of ThnK. Enzyme purification was performed in an anaerobic chamber (Coy). Frozen cells were resuspended in lysis buffer (10% glycerol, 300 mM KCl, 50 mM HEPES pH 8.0, 10 mM BME, 2-5 mM imidazole) along with lysozyme (1 mg/mL final volume), PMSF (1 mM), DNAse (~ 0.1 mg/mL final volume), and optional HOCbl (~0.4 mg/g cell paste). Cells were lysed by sonication and insoluble material was removed by centrifugation (50,000 × g for 1 h at 4 °C). Soluble ThnK was allowed to bind to pre-equilibrated TALON Co^{II} resin (Clontech) and purified by immobilized metal affinity chromatography. The resin was washed with 5 mM and 10 mM imidazole in lysis buffer. The protein was eluted using 250 mM imidazole in the lysis buffer. The enzyme was concentrated using Amicon centrifugal filter devices (Millipore) with a 10 kDA molecular weight limit. Using a PD-10 column (GE Biosciences), the protein was

transferred into assay buffer (10% glycerol, 300 mM KCl, 50 mM HEPES pH 7.5, 10 mM BME).

ThnK Protein Analysis. The concentration of ThnK was determined by the Bradford assay[34] (Varian Cary 50 Bio UV/ Visible Spectrophotometer) using Coomassie Protein Assay Reagent (Thermo Scientific). A concentration correction factor was obtained using amino acid analysis (Molecular Structure Facility, UC Davis). The amount of iron bound by ThnK was determined by established methods[35], and the amount of sulfide was determined as reported[36].

ThnK Activity Assays. ThnK was mixed with 50-100 mM HEPES pH 7.5, 200 mM KCl, 1 mM SAM or d_3-SAM, 1 mM methyl viologen, 4 mM NADPH, and 1 mM substrate. Initial activity screens also included 0.5 mM HOCbl and 0.5 mM MeCbl, though it was later determined not to be necessary to add cobalamin for activity. Assays of potential substrates lacking a C-2-substituent also included 1 mM cysteine and 1 mM coenzyme A. When utilized, dithionite (3 mM) or flavodoxin (90 μM), flavodoxin reductase (9 μM), and NADPH (1 mM) were supplemented at the indicated concentrations in place of methyl viologen and NADPH (default reductant unless otherwise noted). Assays were conducted anaerobically at room temperature and were typically run for 1-2 h.

ThnK SAH and 5'-dA Quantification Assays. ThnK (50 μM, final concentration) was mixed with 100 mM HEPES pH 7.5, 200 mM KCl, 1 mM SAM or d_3-SAM, 1 mM

methyl viologen, 4 mM NADPH, and 1 mM substrate. Assays were run anaerobically for 2 h and 10 min at room temperature.

No-cobalamin ThnK Expression, Purification, and Activity. The ThnK wt Rosetta strain was grown in standard M9 medium lacking cobalamin, but supplemented with $FeCl_3$ (~0.14 mM) and thiamine (0.074 mM). Expression and purification of the no-cobalamin ThnK was conducted as described for the wild-type protein, but no HOCbl was added during purification. Assays were conducted with 50 μM ThnK and 1 mM HOCbl or 1mM MeCbl when utilized and were otherwise as described for ThnK from ethanolamine medium.

Knockout of CX_3CX_2C Motif in ThnK and Mutant Protein Expression, Purification, and Activity. The pET29b:*thnK* plasmid was used as a template for a two-step PCR method that utilized the following primers: 5'-CGC GGC GCC CCC TAC TCG GCT GCC TTC GCC GAC TGG-3' and 5'-CCA GTC GGC GAA GGC AGC CGA GTA GGG GGC GCC GCG-3'. The C206A C210A C213A PCR product was digested with *NdeI* and *XhoI* and ligated into the pET29b vector. The resulting plasmid was sequenced and found to be without error. The mutant *thnK* vector was transformed into an *E. coli* Rosetta DE3 strain containing the pDB1282 plasmid. Expression, purification, and assays of the mutant ThnK (85 μM final concentration) were conducted as described for the wild type protein.

LC-MS Analysis of Carbapenams. UPLC-MS detection of carbapenams was conducted on a Waters Acquity H-Class UPLC system equipped with a Waters Acquity BEH UPLC column packed with an ethylene bridged hybrid C18 stationary phase (2.1 mm x 50 mm, 1.7 um) followed by a multi-wavelength UV-Vis diode array detector coupled with accurate mass analysis by a Waters Xevo-G2 Q-ToF ESI mass spectrometer. Mobile phase: 0-1 min 100% water + 0.1% formic acid, 1-7.5 min up to 80% acetonitrile + 0.1% formic acid, 7.5 – 8.5 min isocratic 80% acetonitrile + 0.1% formic acid, 8.5-10 min 100% water + formic acid. The flow rate was 0.3 mL/min. The first min of eluant was discarded prior to MS analysis.

LC-MS Analysis of SAH and 5'-dA. LC-MS detection of *S*-adenosyl-homocysteine (SAH) and 5'-deoxyadenosine (5'-dA) was carried out on an Agilent Technologies (Santa Clara, CA) 1200 system equipped with an autosampler and an Agilent Technologies Zorbax Rapid Resolution Extended-C18 column (4.6 mm × 50 mm, 1.8 μm particle size) and coupled to an Agilent Technologies 6410 QQQ mass spectrometer. Assay mixtures were quenched with H_2SO_4 and insoluble material was pelleted prior to analysis. Method 1 (Compounds **2, 8, 9**): method is similar to that reported previously[31]. Mobile phase: The initial conditions included 95% solvent A (40 mM aqueous ammonium acetate, pH 6.0 with glacial acetic acid, and 5% methanol) and 5% solvent B (methanol), 0.5-5 min up to 13% B, 5-6.5 min up to 27% B, 6.5-7.0 min up to 53% B, 7.0-7.5 min isocratic 53% B, 7.5-8 min down to 5% B, 8.0-10.0 min re-equilibrate at 5% B. Method 2 (Compounds **10-15**): Mobile phase: The initial conditions included 90.5% solvent A (0.1% formic acid, pH 2.6) and 9.5% solvent B (methanol), 0-0.2 min 9.5% B, 0.2-3.3 min up to 9.8%

B, 3.3-4.1 min up to 30% B, 4.1-4.7 min up to 60% B, 4.7-5.1 min isocratic 60% B, 5.1-5.5 min down to 9.5% B, 5.5-8.7 min isocratic 9.5% B. Data collection and analysis were conducted with the associated MassHunter software package. Detection of SAH and 5'-dA was performed using electrospray ionization in the positive mode (ESI+) with multiple reaction monitoring (MRM). The masses used for the detection of SAH and 5'-dA are shown in Table 4.1. Quantification of SAH and 5'd-A levels was conducted using the MassHunter software with appropriate standard curves and utilized a tyrosine internal standard. The mass transition from the parent ion to product ion 1 was used for quantification.

Table 4.1: LC-MS mass fragments for detection of SAH and 5'd-A

	Parent Ion	Product Ion 1	Product Ion 2
SAH	385.4	136	134
5'-dA	252.1	136	119
Tyrosine	182.0	165	123

Table 4.1: Detection of SAH and 5'-dA was performed using electrospray ionization in the positive mode (ESI+) with multiple reaction monitoring (MRM). The masses used for the detection of SAH and 5'-dA are shown. The mass transition from the parent ion to product ion 1 was used for quantification.

Synthesis of Substrates.

Compounds 10-12, 15:

The *p*-nitrobenzyl (5*R*)-carbapenem-3-carboxylate (**9**) and the *p*-nitrobenzyl (5*S*)-carbapenem-3-carboxylate (**8**) were prepared as previously described[37].

General procedure for pantetheine 1,4-addition:

***p*-Nitrobenzyl (2*R*,3*R*,5*R*)-2-pantetheinyl-carbapenam-3-carboxylate (10b).** To pantetheine acetonide (563.6 mg, 1.77 mmol) was added tetrahydrofuran (1.7 mL) and 1 M HCl (1.7 mL) and the solution was stirred for about 30 min or until the reaction was complete by TLC (10% ethanol/chloroform). Then 1 M NaOH (1.7 mL) was added followed by triethylamine (149.4 μL). This solution was added to a separate flask containing *p*-nitrobenzyl (5*S*)-carbapenem-3-carboxylate **8** [2,4] (340 mg, 1.18 mmol) [or *p*-nitrobenzyl (5*R*)-carbapenem-3-carboxylate **9** and acetonitrile (4.8 mL)]. The reaction mixture was stirred at room temperature for 40 min, then diluted with ethyl acetate (75 mL) and washed with saturated ammonium chloride (8 mL) and brine (20 mL). The aqueous layer was extracted with ethyl acetate (25 mL). The organic layers were combined, dried over anhydrous sodium sulfate, filtered, and concentrated *in vacuo* to yield a yellow oil. The oil was purified by silica gel chromatography using 5% ethanol/chloroform to provide a mixture of the two isomers **10a** and **10b** (398 mg, 55%) oil; TLC (ethanol:chloroform, 1:9 v/v) major isomer $R_f = 0.33$, minor isomer $R_f = 0.29$. Repeated chromatography enriched each isomer for characterization.

***p*-Nitrobenzyl (2*S*,3*R*,5*R*)-2-pantetheinyl-carbapenam-3-carboxylate (10a).** major isomer $[\alpha]^{24.0\ °C} = -60.6°$ (c = 1.020, $CHCl_3$); IR 3408, 1769, 1667, 1644, 1530, and, 1348 cm^{-1}; **^{1}H NMR** (400 MHz, $CDCl_3$): δ 8.22 (d, *J* = 8.8 Hz, 2H), 7.54 (d, *J* = 8.3 Hz, 2H), 7.40 (bt, *J* = 5.8 Hz, 1H), 6.61 (bt, *J* = 5.4 Hz, 1H), 5.29 (s, 2H), 4.41 (d, *J* = 5.8 Hz, 1H), 3.97 (s, 1H), 3.86-3.93 (m, 1H), 3.78-3.85 (m,1H), 3.54 (q, *J* = 5.5 Hz, 1H), 3.46 (s, 2H), 3.36-4.44 (m, 2H), 3.35 (dd, *J* = 15.9, 5.1 Hz, 1H), 2.86 (dd, *J* = 16.0, 1.6 Hz, 1H),

2.74-2.82 (m, 1H), 2.58-2.70 (m, 2H), 2.44 (t, *J* = 5.5 Hz, 1H), 1.64-1.74 (m, 1H), 0.98 (s, 3H), 0.89 (s, 1H) ppm; **^{13}C NMR** (100 MHz, $CDCl_3$): δ 175.8, 173.9, 171.7, 169.4, 147.6, 142.2, 128.3, 123.7, 77.2, 70.5, 65.7, 60.3, 52.5, 51.7, 44.1, 39.1, 38.5, 38.3, 35.6, 35.1, 31.7, 21.1, 20.4 ppm; **HRMS** *m/z*: $[M+H]^+$ calcd. for $C_{25}H_{34}N_4O_9S$ 567.2125; found 567.2126. The assignment of stereochemistry of the C-2 and C-3 -positions were based on Nuclear Overhauser Effect (n.O.e.) NMR experiments performed and described in the thesis of Kristos Moshos[37].

***p*-Nitrobenzyl (2*R*,3*R*,5*R*)-2-pantetheinyl-carbapenam-3-carboxylate (10b).** minor isomer $[\alpha]^{22.5\ °C}$ = -23.0° (c = 0.90, $CHCl_3$); IR 3396, 1769, 1660, 1650, 1608, 1522, and, 1347 cm^{-1}; **^{1}H NMR** (400 MHz, $CDCl_3$): δ ^{1}H NMR (400 MHz, $CDCl_3$): δ 8.25 (d, *J* = 8.8 Hz, 2H), 7.56 (d, *J* = 8.3 Hz, 2H), 7.32 (bt, *J* = 5.0 Hz, 1H), 6.33 (bt, *J* = 5.8 Hz, 1H), 5.29 (s, 2H), 4.80 (d, *J* = 7.1 Hz, 1H), 4.08-4.14 (m, 1H), 4.00 (s, 1H), 3.60-3.68 (q, *J* = 8.0 Hz, 1H), 3.58 (t, *J* = 5.9 Hz, 2H), 3.49 (s, 2H), 3.33-3.45 (m, 3H), 2.81 (dd, *J* = 16.5, 2.8 Hz, 1H), 2.60-2.80 (m, 2H), 2.41 (t, *J* = 5.1 Hz, 2H), 2.23-2.32 (m, 1H), 2.12-2.22 (m, 1H), 1.02 (s, 3H), 0.91 (s, 3H) ppm; **^{13}C NMR** (100 MHz, $CDCl_3$): δ 176.5, 174.0, 171.7, 168.0, 147.7, 142.2, 128.7, 124.7, 77.2, 70.5, 65.4, 60.3, 52.1, 48.8, 44.2, 42.5, 39.2, 35.6, 35.2, 32.3, 24.1, 21.0, 20.4 ppm; **HRMS** *m/z*: $[M+H]^+$ calcd. for $C_{25}H_{34}N_4O_9S$ 567.21248; found 567.212229. The assignment of stereochemistry of the C-2 and C-3 -positions were based on Nuclear Overhauser Effect (n.O.e.) NMR experiments performed and described in the thesis of Kristos Moshos[37].

***p*-Nitrobenzyl (2*R*,3*S*,5*S*)-2-pantetheinyl-carbapenam-3-carboxylate (11a).** major isomer $[\alpha]^{24.8\ °C}$ = +29.3° (c = 1.55, CH_2Cl_2); IR 3408, 1769, 1667, 1644, 1609, 1530, and, 1348 cm^{-1}; **^{1}H NMR** (400 MHz, $CDCl_3$): δ 8.22 (d, *J* = 8.8 Hz, 2H), 7.54 (d, *J* = 8.3

Hz, 2H), 7.40 (bt, *J* = 5.8 Hz, 1H), 6.61 (bt, *J* = 5.4 Hz, 1H), 5.29 (s, 2H), 4.41 (d, *J* = 5.8 Hz, 1H), 3.97 (s, 1H), 3.86-3.93 (m, 1H), 3.78-3.85 (m, 1H), 3.54 (q, *J* = 5.5 Hz, 1H), 3.46 (s, 2H), 3.36-4.44 (m, 2H), 3.35 (dd, *J* = 15.9, 5.1 Hz, 1H), 2.86 (dd, *J* = 16.0, 1.6 Hz, 1H), 2.74-2.82 (m, 1H), 2.58-2.70 (m, 2H), 2.44 (t, *J* = 5.5 Hz, 1H), 1.64-1.74 (m, 1H), 0.98 (s, 3H), 0.89 (s, 1H) ppm; **^{13}C NMR** (100 MHz, $CDCl_3$): δ 175.9, 173.7, 171.7, 169.5, 147.8, 142.2, 128.4, 123.9, 77.2, 70.7, 65.9, 65.6, 52.6, 51.8, 44.2, 39.3, 38.6, 38.3, 35.7, 35.2, 31.8, 21.3, 20.4 ppm; **HRMS** *m/z*: $[M+H]^+$ calcd. for $C_{25}H_{34}N_4O_9S$ 567.2125; found 567.2124. The assignment of stereochemistry of the C-2 and C-3 -positions were based on Nuclear Overhauser Effect (n.O.e.) NMR experiments performed and described in the thesis of Kristos Moshos[37].

***p*-Nitrobenzyl (2*S*,3*S*,5*S*)-2-pantetheinyl-carbapenam-3-carboxylate (11b).** minor isomer $[\alpha]^{22.5\ °C}$ = +44.3° (c = 0.970, $CHCl_3$); IR 3373, 1749, 1650, 1523, and, 1347 cm^{-1}; **^{1}H NMR** (400 MHz, $CDCl_3$): δ 8.25 (d, *J* = 8.8 Hz, 2H), 7.56 (d, *J* = 8.3 Hz, 2H), 7.32 (bt, *J* = 5.0 Hz, 1H), 6.33 (bt, *J* = 5.8 Hz, 1H), 5.29 (s, 2H), 4.80 (d, *J* = 7.1 Hz, 1H), 4.08-4.14 (m, 1H), 4.00 (s, 1H), 3.60-3.68 (q, *J* = 8.0 Hz, 1H), 3.58 (t, *J* = 5.9 Hz, 2H), 3.49 (s, 2H), 3.33-3.45 (m, 3H), 2.81 (dd, *J* = 16.5, 2.8 Hz, 1H), 2.60-2.80 (m, 2H), 2.41 (t, *J* = 5.1 Hz, 2H), 2.23-2.32 (m, 1H), 2.12-2.22 (m, 1H), 1.02 (s, 3H), 0.91 (s, 3H) ppm; **^{13}C NMR** (100 MHz, $CDCl_3$): δ 176.5, 174.0, 171.7, 168.0, 147.7, 142.2, 128.7, 124.7, 77.2, 70.5, 65.4, 60.3, 52.1, 48.8, 44.2, 42.5, 39.2, 35.6, 35.2, 32.3, 24.1, 21.0, 20.4 ppm; **HRMS** *m/z*: $[M+H]^+$ calcd. for $C_{25}H_{34}N_4O_9S$ 567.2125; found 567.2124. The assignment of stereochemistry of the C-2 and C-3 -positions were based on Nuclear Overhauser Effect (n.O.e.) NMR experiments performed and described in the thesis of Kristos Moshos[37].

General procedure for deprotection of *p*-nitrobenzyl esters:

The *p*-nitrobenzyl ester (310 mg, 0.76 mmol) was dissolved in tetrahydrofuran (10 mL) and potassium bicarbonate (76.09 mg, 0.76 mmol) in water (5 mL) was added followed by 10% Pd on carbon (36 mg). Hydrogen (40 psi) was admitted to the reaction mixture in a pressure tube and shaken on a Parr apparatus for 2 h. The catalyst was removed by filtration on Celite. The filtrate was washed twice with ethyl acetate (15 mL). The aqueous layer was filtered through 0.2 µm nylon filter and lyophilized to give an amorphous solid. The solid was dissolved in a minimum amount of water and applied to a bed of Diaion® HP-20 resin and eluted with distilled water. After any excess salt was removed, 10% ethanol/water was used to elute the product. The presence of salt was detected using silver nitrate solution and the presence of desired compound was detected using potassium permanganate solution. Fractions that contained product and were salt free were pooled and lyophilized.

Potassium (2*S*,3*R*,5*R*)-2-pantetheinyl-carbapenam-3-carboxylate (12). major isomer $[\alpha]^{22.4\,^\circ C}$ = -36.1° (c = 1.050, H_2O); **^{1}H NMR** (400 MHz, D_2O): δ 4.17 (d, *J* = 5.3 Hz, 1H), 3.97 (s, 1H), 3.94-4.00 (m, 1H), 3.78 (dd, *J* = 12.6, 6.6 Hz, 1H), 3.20-3.60 (m, 7H), 2.90 (dd, *J* = 16.6, 2.3 Hz), 2.74-2.95 (m, 3H), 2.60 (td, *J* = 13.6, 6.8 Hz, 1H), 2.50 (t, *J* = 6.4 Hz, 2H), 1.70 (td, *J* = 13.7, 6.8 Hz, 1H), 0.92 (s, 3H), 0.88 (s, 3H) ppm; **^{13}C NMR** (100 MHz, D_2O): δ 181.2, 177.4, 175.7, 174.5, 76.4, 69.4, 69.0, 53.1, 53.1, 43.6, 39.2, 39.2, 37.6, 36.1, 35.8, 31.5, 21.2, 19.8 ppm; **HRMS** *m/z*: $[M-H]^-$ calcd. for $C_{18}H_{29}N_3O_7S$ 430.1653; found 430.1665.

Potassium (2*R*,3*R*,5*R*)-2-pantetheinyl-carbapenam-3-carboxylate (13). minor isomer $[\alpha]^{23.1\ °C}$ = -59.0° (c = 0.7300, H_2O); **^{1}H NMR** (400 MHz, D_2O): δ 4.52 (d, *J* = 6.6 Hz, 1H), 4.05-4.14 (m, 1H), 3.99 (s, 1H), 3.90-3.97 (m, 1H), 3.35-3.55 (m, 6H), 3.31 (dd, *J* = 16.9, 4.5 Hz), 2.75-2.93 (m, 3H), 2.51 (t, *J* = 6.2 Hz, 2H), 2.30-2.37 (m, 1H), 2.07 (td, *J* = 13.4, 6.6 Hz, 1H), 0.92 (s, 3H), 0.88 (s, 3H) ppm; **^{13}C NMR** (100 MHz, D_2O): δ 181.7, 176.0, 175.7, 174.4, 76.3, 69.0, 67.5, 53.1, 51.7, 41.6, 39.2, 38.5, 37.7, 36.1, 35.9, 32.2, 21.2, 19.8 ppm; **HRMS** *m/z*: $[M+H]^+$ calcd. for $C_{18}H_{29}N_3O_7S$ 432.1805; found 432.1797. The diastereomers **13** and **14** were separated and purified using an Agilent model 1100 HPLC equipped with a multi-wavelength ultraviolet–visible detector in conjunction with a reverse-phase Phenomenex Luna 10µ C18(2) 100 Å preparatory column (250 x 21.20 mm ID). The mobile phase was 25% methanol and 75% buffer (10 mM potassium phosphate, pH 6.65) at a flow rate of 5 ml per min. Compound **13** eluted at 29 min and compound **14** eluted at 22 min.

Potassium (2*R*,3*S*,5*S*)-2-pantetheinyl-carbapenam-3-carboxylate (14). major isomer **^{1}H NMR** (400 MHz, D_2O): δ 4.17 (d, *J* = 5.0 Hz, 1H), 3.97 (s, 1H), 3.94-4.00 (m, 1H), 3.78 (dd, *J* = 12.8, 6.0 Hz, 1H), 3.20-3.60 (m, 7H), 2.90 (dd, *J* = 16.6, 2.4 Hz), 2.74-2.95 (m, 3H), 2.60 (td, *J* = 13.4, 6.8 Hz, 1H), 2.50 (t, *J* = 6.2 Hz, 2H), 1.70 (td, *J* = 13.7, 6.9 Hz, 1H), 0.92 (s, 3H), 0.88 (s, 3H) ppm; **^{13}C NMR** (100 MHz, D_2O): δ 181.2, 177.4, 175.7, 174.5, 76.3, 69.4, 69.0, 53.1, 53.1, 43.6, 39.2, 39.2, 37.6, 36.1, 35.9, 31.5, 21.2, 19.8 ppm; **HRMS** *m/z*: $[M+H]^+$ calcd. for $C_{18}H_{29}N_3O_7S$ 432.1799; found 432.1808.

Potassium (2*S*,3*S*,5*S*)-2-pantetheinyl-carbapenam-3-carboxylate (15). minor isomer **^{1}H NMR** (400 MHz, D_2O): δ 4.52 (d, *J* = 6.6 Hz, 1H), 4.05-4.14 (m, 1H), 3.98 (s, 1H),

3.90-3.97 (m, 1H), 3.35-3.55 (m, 6H), 3.31 (dd, *J* = 17.0, 4.8 Hz), 2.75-2.93 (m, 3H), 2.51 (t, *J* = 6.2 Hz, 2H), 2.33 (td, *J* = 13.1, 5.0 Hz, 1H), 2.06 (td, *J* = 13.6, 6.8 Hz, 1H), 0.91 (s, 3H), 0.87 (s, 3H) ppm; **^{13}C NMR** (100 MHz, D_2O): δ 181.8, 176.1, 175.7, 174.5, 76.3, 69.0, 67.5, 53.1, 51.7, 41.5, 39.2, 38.5, 37.6, 36.1, 36.0, 32.2, 21.2, 19.7 ppm; **HRMS** *m/z*: $[M+H]^+$ calcd. for $C_{18}H_{29}N_3O_7S$ 432.1799; found 432.1780. C-2 and C-3 stereochemical assignments were established by Nuclear Overhauser Effect (n.O.e.) NMR experiments and confirmed previous stereochemical analyses[38].

(±)-4-Allylazetidin-2-one (16). The procedure was carried out as described previously[38]. To 1,4-pentadiene (6.6 g, 96.9 mmol), chlorosulfonyl isocyanate (7.79 ml, 12.7 g) was added at 0 °C, then stirred at room temperature for 3 days in a pressure bottle. The reaction mixture was diluted with dichloromethane (110 mL) and was then add slowly to a solution of sodium sulfite (14.5 g) and dibasic potassium phosphate (8.51 g) in water (52.5 ml) at 0 °C. Then aqueous sodium hydroxide (1 M) was added to maintain pH = 7.0 - 8.0. After the addition, the reaction mixture was stirred at room temperature for 2 h, then extracted with ethyl acetate (3 × 100 ml). The organic layers were combined, dried with anhydrous sodium sulfate, filtered, and concentrated to give **16** as a light yellow oil, which was used crude in the next reaction (5.57g, 52%). TLC (ethyl acetate:hexanes, 3:7 v/v): R_f = 0.67; **^{1}H NMR** (400 MHz, $CDCl_3$): δ 6.67 (s, 1H), 5.64-5.78 (m, 1H), 5.00-5.10 (m, 2H), 3.58-3.66 (m, 1H), 2.97 (dd, *J* = 14.9, 5.1 Hz, 1H), 2.53 (dd, *J* = 14.9, 1.1 Hz, 1H), 2.24-2.36 (m, 2H); **^{13}C NMR** (100 MHz, $CDCl_3$): δ 168.1, 133.1, 117.8, 46.9, 42.7, 39.2 ppm. ^{1}H and ^{13}C NMR matched the data as previously reported in the literature[38].

(±)-4-Allyl-1-dimethyl-*t*-butylsilyl-azetidin-2-one (17). The procedure was carried out as described previously[38]. Triethylamine (16.15 ml, 115.8 mmol) and *N,N*-dimethylaminopyridine (1.1g, 9.26 mmol) were added to **16** (5.15g, 46.3 mmol) in tetrahydrofuran (173 ml) at 0 °C. *t*-Butyldimethylsilyl-methanesulfonate (12.8 ml, 55.56 mmol) was then added to the reaction mixture slowly. The solution was stirred at 0 °C for 20 min before it was allowed to warm to room temperature for 1 h. After concentration *in vacuo*, the mixture was dissolved in ethyl acetate (200 ml) and washed with saturated ammonium chloride (80 ml) and brine (100 ml), dried with anhydrous sodium sulfate, filtered, and concentrated *in vacuo*. The crude oil was purified by silica gel chromatography (diethyl ether:hexanes, 1:9) to yield **17** as a light yellow oil (8.71 g, 83%); TLC (ethyl acetate:hexanes, 3:7 v/v): $R_f = 0.67$; **^{1}H NMR** (300 MHz, $CDCl_3$): δ 5.65-5.80 (m,1H), 5.50-5.15 (m, 2H), 3.54-3.63 (m, 1H), 3.09 (dd, *J* = 15.4, 5.5 Hz, 1H), 2.66 (dd, *J* = 15.3, 2.7 Hz, 1H), 2.52-2.62 (m, 1H), 2.10-2.24 (m, 1H), 0.96 (s, 9H), 0.25 (s, 3H), 0.22 (s, 3H) ppm. ^{1}H NMR matched the data as previously reported in the literature[38].

(±)-(3*S*,4*S*)-4-Allyl-1-dimethyl-*t*-butylsilyl-3-methylazetidin-2-one (18). The procedure was carried out as described previously[38]. A solution of **17** (7.0 g, 31.1 mmol) in tetrahydrofuran (77.8 mL) was added to lithium diisopropylamine (2 M, 34.21 mL, 68.4 mmol) in tetrahydrofuran (155 mL) at -78°C under a nitrogen atmosphere. After stirring for 30 min at -78 °C, methyl iodide (19.4 mL, 44.14g, 310.9 mmol) was added and the reaction mixture was stirred at -78 °C for 30 min before it was allowed to warm to room temperature for 1 h. Acetic acid (3.9 mL) was added to the solution, and the reaction mixture was concentrated *in vacuo*. The resulting oil was dissolved in ethyl

acetate (155 mL) and washed with brine (85.5 mL), dried with anhydrous sodium sulfate, filtered, and concentrated *in vacuo*. The resulting oil was purified by silica gel chromatography (diethyl ether:hexanes, 1:9) to provide **18** as a light yellow oil (7.13 g, 96%). TLC (ethyl acetate:hexanes, 2:8 v/v): R_f = 0.72; IR 2940, 2860, 1725, and, 1640 cm^{-1}; **^{1}H NMR** (400 MHz, $CDCl_3$): δ 5.65-5.80 (m, 1H), 4.91-5.21 (m, 2H), 3.15 (ddd, *J* = 9.0, 4.0, 3.0 Hz, 1H), 2.77 (qd, *J* = 8.0, 3.0 Hz, 1H), 1.9-2.6 (m, 2H), 1.21 (d, *J* = 8.0 Hz), 0.91 (s, 9H), 0.21 (s, 3H), 0.20 (s, 3H) ppm. ^{1}H NMR matched the data as previously reported in the literature[38].

(±)-(3*S*,4*S*)-4-Allyl-3-methylazetidin-2-one (19). The procedure was carried out as described previously[38]. Acetic acid (5.11 mL, 89.4 mmol) followed by tetra-*n*-butylammonium fluoride (13.2 g, 41.72 mmol) was added to a solution of **18** (7.13 g, 29.8 mmol) in anhydrous tetrahydrofuran (150 mL) at 0 °C. The reaction mixture was stirred at 0 °C for 30 min, diluted with ethyl acetate (500 mL) and washed with water (2 × 140 mL) and brine (150 mL). The organic layer was dried with anhydrous sodium sulfate, filtered and concentrated *in vacuo*. The resulting oil was purified by silica gel chromatography (ethyl acetate:hexanes, 3:7 to 4:6) to provide **19** as a colorless oil (1.18 g, 70%). TLC (ethyl acetate:hexanes, 2:3 v/v): R_f = 0.36; IR 3420, 1755, and, 1640 cm^{-1}; **^{1}H NMR** (400 MHz, $CDCl_3$): δ 6.5 (br s, 1H), 5.8 (m, 1H), 5.15-5.25 (m, 1H), 4.95-5.1 (m, 1H), 3.30 (td, *J* = 6.0, 2.0 Hz, 1H), 2.80 (qd, *J* = 7.0, 2.0, 1H), 2.36 (td, *J* = 6.0, 1.0 Hz, 2H), 1.30 (d, *J* =7.0 Hz, 3H), ppm. ^{1}H NMR matched the data as previously reported in the literature[38].

***p*-Nitrobenzyl (±)-2-(2-allyl-3-methyl-4-oxoazetidin-1-yl)-2-(triphenyl-λ$_5$-phosphanylidene)acetate (20).** The procedure was carried out as described previously[38].

p-Nitrobenzyl glyoxylate hydrate (6.03 g, 26.5 mmol), triethylamine (432.7 μL, 3.08 mmol), and 4.9 g 3Å molecular sieves were added sequentially to a solution of **19** (3.32 g, 26.5 mmol) in anhydrous tetrahydrofuran (93.2 mL) and stirred at room temperature for 16 h. The reaction mixture was filtered through Celite, washed with ethyl acetate, and concentrated *in vacuo*. The crude residue was dissolved in anhydrous tetrahydrofuran (82.2 mL), cooled to -15 °C to which was then added 2,6-lutidine (5.85 mL, 50.4 mmol) followed by thionyl chloride (2.70 mL, 37.1 mmol) dropwise. The reaction mixture was stirred for 1 h at -15 °C. The solution was filtered through Celite, and the filtrate was washed with ethyl acetate and concentrated *in vacuo*. The crude oil was dissolved in 1,4-dioxane (85.1 mL) and triphenylphosphine (9.02 g, 34.4 mmol) and 2,6-lutidine (3.38 mL, 39.2 mmol) were added. The resulting mixture was stirred at room temperature for 16 h, diluted with ethyl acetate (858.7 mL), and washed with water (244.4 mL) and brine (244.4 mL). The organic layer was dried with anhydrous sodium sulfate, filtered, and concentrated *in vacuo*. The resulting brown oil was purified by silica gel chromatography (ethyl acetate:hexanes, 1:1 to 7:3) to yield **20** as an orange foam (3.07g, 20 % yield). The product was characterized by subsequent transformation to the respective bicyclic β-lactams (*vide infra*). TLC (diethyl ether:ethyl acetate, 1:1 v/v): R_f = 0.52.

***p*-Nitrobenzyl (±)-(5*S*,6*S*)-6-methylcarbapenem-3-carboxylate (21).** The procedure was carried out as described previously[38]. Trifluoroacetic acid (7.17 mL) was added to a solution of **20** (3.07 g, 5.3 mmol) in dichloromethane (117 mL) at 0 °C. The reaction mixture was cooled to -78 °C and ozone was bubbled through the solution until a blue color persisted. The solution was stirred for 5 min at -78 °C, then a stream of nitrogen

was bubbled through the reaction mixture until the color changed from blue to yellow. Dimethyl sulfide (7.83 mL) was added to the solution at 0 °C and the solution was stirred for 1 h. The reaction mixture was diluted with dichloromethane (70 mL) and washed with saturated sodium bicarbonate (2 × 200 mL) and brine (201 mL). The organic layer was dried with anhydrous sodium sulfate, filtered, and concentrated *in vacuo*. The crude brown oil was purified by silica gel chromatography (ethyl acetate:hexanes, 3:7 to 6:4) to give a diastereomeric mixture of the *cis* and *trans* methyl isomers (1.24 g, 78%). Repeated purification gave the desired *trans* methyl isomer **21** (0.70 g, 44%). TLC (ethyl acetate:hexanes, 4:6 v/v): R_f = 0.45 **epi-21**, 0.37 **21**; IR 2970, 1778, 1730, 1608, 1521, and, 1348 cm^{-1}; **^{1}H NMR** (400 MHz, $CDCl_3$): δ 8.23 (d, *J* = 8.6 Hz, 2H), 7.62 (d, *J* = 8.3 Hz, 2H), 6.54 (t, *J* = 2.8 Hz, 1H), 5.45, 5.28 (ABq, J_{AB} = 16, 2H), 3.98 (ddd, *J* = 10.3, 7.8, 2.8 Hz, 1H), 3.23 (dq, *J* = 7.5, 2.8 Hz, 1H), 2.97 (ddd, *J* = 19.5, 9.7, 3.1 Hz, 1H), 2.80 (ddd, *J* = 19.4, 7.8, 2.5 Hz, 1H), 1.45 (d, *J* = 7.3 Hz, 3H), ppm; **^{13}C NMR** (100 MHz, $CDCl_3$): δ 180.1, 160.0, 147.6, 142.7, 134.5, 132.3, 128.1, 123.7, 65.3, 59.1, 54.5, 36.0, 13.9 ppm; **HRMS** *m/z*: $[M+H]^+$ calcd. for $C_{15}H_{14}N_2O_5$ 303.0981; found 303.0978. ^{1}H and ^{13}C NMR matched the data as previously reported in the literature[38].

***p*-Nitrobenzyl (±)-(3*R*,5*S*,6*S*)-6-methyl-2-pantetheinyl-carbapenam-3-carboxylate (22).** Pantetheine acetal (1.1 g, 3.45 mmol) in tetrahydrofuran (3.5 mL) was added 1 M HCl and stirred at room temperature for 30 min or until deprotection was determined to be complete by TLC. The reaction mixture was then neutralized by the addition of aqueous NaOH (3.5 mL, ~1 M) followed by triethylamine (297.5 µL). This was added to *p*-nitrobenzyl **21** (0.70 g, 2.3 mmol) in acetonitrile (9.4 mL). After stirring for 20 min at room temperature, the reaction mixture was diluted with ethyl acetate (125 mL) and

washed with saturated ammonium chloride (16 mL) and brine (35 mL). The aqueous layer was removed and extracted with ethyl acetate (40 mL). The combined organic layers were dried with anhydrous sodium sulfate, filtered, and concentrated in *vacuo*. The product was purified by silica gel chromatography (ethanol:chloroform, 1:9) to give **22** as inseparable C-2 stereoisomers (560 mg, 42%). ^{1}H NMR analysis of the crude mixture revealed the C-2 diastereomers in a ratio of 4:1. TLC (ethanol:chloroform, 1:9 v/v): major isomer **22a** R_f = 0.36, minor isomer **22b** R_f = 0.32; IR 3408, 2967, 2856, 1772, 1749, 1661, 1643, 1525, 1442, and, 1346 cm^{-1}; **22a: ^{1}H NMR** (400 MHz, $CDCl_3$): δ 8.24 (d, *J* = 8.6 Hz, 2H), 7.54 (d, *J* = 8.3 Hz, 2H), 7.36 (bt, *J* = 5.6 Hz, 1H), 6.44 (bt, *J* = 5.4 Hz, 1H), 5.28 (s, 2H), 4.45 (dd, *J* = 8.8, 4.9 Hz, 1H), 3.92-4.08 (m, 2H), 3.74-3.82 (m, 1H), 3.20-3.60 (m, 6H), 3.12 (dq, *J* = 7.5, 2.1 Hz, 1H), 2.40-2.80 (m, 5H), 1.68-1.78 (m, 1H), 1.40 (d, *J* = 7.6 Hz, 3H), 1.00 (s, 3H), 0.91 (s, 3H) ppm; **22b: ^{1}H NMR** (400 MHz, $CDCl_3$): δ 8.24 (d, *J* = 8.6 Hz, 2H), 7.54 (d, *J* = 8.3 Hz, 2H), 7.36 (bt, *J* = 5.6 Hz, 1H), 6.44 (bt, *J* = 5.4 Hz, 1H), 5.28 (s, 2H), 4.79 (dd, *J* = 7.1, 3.8 Hz, 1H), 3.92-4.08 (m, 2H), 3.74-3.82 (m, 1H), 3.20-3.60 (m, 6H), 3.01 (dq, *J* = 7.3, 2.8 Hz, 1H), 2.40-2.80 (m, 4H), 2.24-2.34 (m, 1H), 2.06-2.19 (m, 1H), 1.39 (d, *J* = 7.3 Hz, 3H), 1.00 (s, 3H), 0.91 (s, 3H) ppm; **^{13}C NMR** (100 MHz, $CDCl_3$): δ 179.2, 173.9, 171.8, 169.4, 147.8, 142.2, 128.4, 123.8, 70.7, 65.8, 65.3, 60.1, 53.1, 51.7, 39.2, 38.5, 37.3, 35.7, 31.9, 31.8, 21.3, 21.0, 20.4, 13.8 ppm; **HRMS** *m/z*: $[M+H]^+$ calcd. for $C_{26}H_{36}N_4O_9S$ 581.2281; found 581.2277.

Potassium (±)-(3*R*,5*S*,6*S*)-6-methyl-2-pantetheinyl-carbapenam-3-carboxylate (23). Water (4.9 mL) containing potassium bicarbonate (74.5 mg, 0.74 mmol) was added to a solution of **22** (360.0 mg, 0.62 mmol) in tetrahydrofuran (10.4 mL) in a pressure flask.

10% palladium on carbon (40 mg) was carefully added to the solution. The flask was fitted to a Parr apparatus to which hydrogen was added (40 PSI) and shaken for 2 h. The catalyst was removed by filtration of the reaction mixture through Celite and the filtered solids were washed with water (6 mL) followed by ethyl acetate (30 mL). The aqueous layer was separated from the filtrate and washed with ethyl acetate (25 mL). The washed aqueous layer was filtered through a 25 mm 0.2 µm nylon syringe filter and lyophilized. The resulting solids were dissolved and desalted by Diaion-HP resin chromatography (water). Fractions that contained **23** (visualized with potassium permanganate) that were free of salt (visualized by silver nitrate precipitation) were lyophilized to produce **23** (239.6 mg, 80%) as a white solid. ^{1}H NMR analysis of the crude mixture revealed the ratio of C-2 diastereomers in a ratio of 7:3 (**23a**:**23b**). **23a: ^{1}H NMR** (400 MHz, $CDCl_3$): δ 4.21 (d, *J* = 4.3 Hz, 1H), 4.00 (s, 1H), 3.75-3.95 (m, 2H), 3.35-3.60 (m, 6H), 3.18 (qd, *J* = 7.3, 1.1 Hz, 1H), 2.70-2.90 (m, 2H), 2.59 (dt, *J* = 13.9, 7.1 Hz, 1H), 2.52 (t, *J* = 6.4 Hz, 2H), 1.76 (dt, *J* = 13.9, 6.1 Hz, 1H), 1.36 (d, *J* = 7.6 Hz, 3H), 0.93 (s, 3H), 0.89 (s, 3H) ppm; **23b: ^{1}H NMR** (400 MHz, $CDCl_3$): δ 4.52 (d, *J* = 6.6 Hz, 1H), 4.00 (s, 1H), 3.70 (bt, *J* = 5.6 Hz, 2H), 3.35-3.60 (m, 6H), 3.07 (qd, *J* = 6.6, 1.1 Hz, 1H), 2.70-2.90 (m, 2H), 2.52 (t, *J* = 6.4 Hz, 2H), 2.25-2.35 (m, 1H), 2.08-2.18 (m, 1H), 1.36 (d, *J* = 7.6 Hz, 3H), 0.93 (s, 3H), 0.89 (s, 3H) ppm; **^{13}C NMR** (100 MHz, $CDCl_3$): δ 184.5, 177.1, 175.7, 174.5, 76.4, 69.2, 69.0, 60.6, 53.1, 52.6, 39.2, 39.1, 36.5, 36.1, 35.9, 31.5, 21.2, 19.8, 13.5 ppm; **HRMS** *m/z*: $[M+H]^+$ calcd. for $C_{19}H_{31}N_3O_7S$ 446.1956; found 446.1977.

Benzyl (2*R*)-1-carboxybenzyl-5-oxopyrrolidine-2-carboxylate (24).

Diisopropylethylamine (54 mL, 310 mmol was added to D-pyroglutamic acid (20 g, 155 mmol, TCI America/AK Scientific) in dichloromethane (500 mL). Benzyl bromide (22

ml, 185 mmol) was added and the solution was refluxed for 4h. The reaction mixture was concentrated *in vacuo* and the crude oil was redissolved in ethyl acetate (400 ml). The cloudy mixture was filtered through silica on top of Celite and the silica/Celite plug was washed twice with ethyl acetate (200 mL). The eluate was concentrated *in vacuo* and redissolved in tetrahydrofuran (600 mL) to which was added lithium bis(trimethylsilyl)amide (154.5 mL, 1.0 M, 155 mmol) at -78 ˚C and stirred for 10 min. Benzyl chloroformate (30.8 mL, 202 mmol) was added and the reaction mixture was allowed to stir for 10 min. The reaction was quenched with aqueous ammonium chloride (400 mL) and the solution was warmed to room temperature and the phases were separated. The aqueous layer was extracted 5× with ethyl acetate (400 mL) and the combined organic fractions were washed with brine, dried with anhydrous magnesium sulfate, filtered, and concentrated *in vacuo*. The solid crude product was recrystallized from hot ethyl acetate/hexanes to give **24** as white crystals (34.4 g, 63% yield). **^{1}H-NMR** (400 MHz; $CDCl_3$): δ 7.36-7.28 (m, 10H), 5.22 (d, *J* = 1.3 Hz, 2H), 5.13 (s, 2H), 4.72 (dd, *J* = 9.4, 2.7 Hz, 1H), 2.68-2.58 (m, 1H), 2.50 (ddd, *J* = 17.6, 9.3, 3.3 Hz, 1H), 2.34 (ddt, *J* = 13.4, 10.4, 9.4 Hz, 1H), 2.09-2.02 (m, 1H) ppm; **^{13}C NMR** (101 MHz; $CDCl_3$): δ 172.9, 170.9, 150.9, 135.10, 135.08, 128.80, 128.73, 128.69, 128.56, 128.41, 128.26, 68.5, 67.5, 58.9, 31.1, 21.9 ppm. **HRMS** (FAB) *m/z*: $[M+H]^+$ calcd. for $C_{20}H_{19}NO_5$ 354.13415; found 354.13342.

7-Benzyl 1-*tert*-butyl (6*R*)-6-(benzyloxycarbonylamino)-2-methyl-3-oxoheptanedioate (25). This synthesis was adapted from the procedures of Ohta *et al.*[19]. A solution of lithium diisopropylamide in tetrahydrofuran (17 mL, 2.0 M, 33.6 mmol) was added to a solution of *tert*-butyl propionate (4.26 ml, 28 mmol) in tetrahydrofuran

(300 mL) at -78 ˚C and allowed to stir for 30 min. A solution of **24** in tetrahydrofuran (40 mL) was added slowly to the reaction mixture. After stirring for 30-60 min at -78 ˚C, the reaction was quenched with saturated ammonium chloride and the phases were separated. The aqueous layer was extracted three times with dichloromethane (50 mL). The combined organic layers were washed with brine, dried with anhydrous magnesium sulfate, and concentrated *in vacuo*. The crude oil was purified by silica gel chromatography using 25% ethyl acetate in hexanes to give **25** (9.88 g, 72%) as a colorless oil, which solidified overnight at room temperature. TLC (ethyl acetate:hexanes, 2:3 v/v): R_f = 0.75; **^{1}H-NMR** (400 MHz; $CDCl_3$): δ 7.35 (s, 10H), 5.30-5.46 (m, 1H), 5.17 (s, 2H), 5.09 (s, 2H), 4.31-4.47 (m, 1H), 3.34-3.36 (m, 1H), 2.47-2.73 (m, 2H), 1.94-2.22 (m, 2H), 1.42 (s, 9H), 1.23 (bd, *J* = 6.8 Hz, 3H) ppm; **^{13}C NMR** (101 MHz; $CDCl_3$): δ 205.2, 171.8, 169.6, 156.0, 136.2, 135.3, 128.74, 128.62, 128.44, 128.29, 128.20, 82.0, 67.4, 67.2, 53.9, 53.6, 37.3, 28.0, 26.4, 12.8 ppm; **HRMS** (FAB) *m/z*: $[M\text{-}OH]^+$ calcd. for $C_{27}H_{33}NO_7$ 466.2230; found 466.2207. ^{1}H and ^{13}C NMR matched the data as previously reported in the literature[19].

***tert*-Butyl butyrate (26).** Conditions were modeled after a similar reaction (http://orgprepdaily.wordpress.com/2007/07/25/2-chloro-5-iodobenzoic-acid-tert-butyl-ester/. [Accessed 09 April 15]). Butyryl chloride (20 mL, 191 mmol) in tetrahydrofuran (40 mL) was added to a slurry of tetrahydrofuran (400 mL) and potassium *tert*-butoxide (23.4 g, 209 mmol) at 0 ˚C. Mixture was stirred for 90 min and then warmed to room temperature. Silica gel (76 g, 1.3 mol) and distilled water (1.14 mL, 62.6 mmol) were added and allowed to stir 20 min. Slurry was filtered through silica gel and concentrated. A yellow oil (18.1 g, 66%) was isolated. The crude product was purified by vacuum

distillation (heating at 35-40 ˚C, and collected over liquid nitrogen) to give a clear oil. **^{1}H-NMR** (400 MHz; $CDCl_3$): δ 2.18 (t, *J* = 7.4 Hz, 2H), 1.61 (sext, *J* = 7.4 Hz, 2H), 1.44 (s, 9H), 0.93 (t, *J* = 7.4 Hz, 3H) ppm; **^{13}C NMR** (101 MHz; $CDCl_3$): δ 173.3, 80.0, 37.6, 28.2, 18.7, 13.7 ppm. ^{1}H and ^{13}C NMR matched the data as previously reported in the literature[39].

7-Benzyl 1-*tert*-butyl (6*R*)-6-(benzyloxycarbonylamino)-2-ethyl-3-oxoheptanedioate (27). Reaction was conducted similarly to that for compound **25**, but utilized **26**. The oil was purified by silica gel chromatography using ethyl acetate/hexanes (3:20) to give the titled product (56%) as an oil, which solidified to a white solid. TLC (ethyl acetate:hexanes, 2:3 v/v): R_f = 0.69; **^{1}H-NMR** (400 MHz; $CDCl_3$): δ 7.34 (bs, 10H), 5.40-5.34 (m, 1H), 5.16 (s, 2H), 5.09 (s, 2H), 4.42-4.36 (m, 1H), 3.21-3.16 (m, 1H), 2.64-2.48 (m, 2H), 2.20-1.90 (m, 2H), 1.81-1.73 (m, 2H), 1.42 (s, 9H), 0.89-0.85 (m, 3H) ppm; **^{13}C NMR** (101 MHz; $CDCl_3$): δ 204.7, 171.87, 171.85, 168.9, 156.0, 136.2, 135.3, 128.75, 128.62, 128.43, 128.29, 128.19, 82.01, 81.97, 67.4, 67.2, 61.7, 53.57, 53.51, 37.71, 37.61, 28.0, 26.44, 26.31, 21.6, 12.0 ppm; **HRMS** (FAB) *m/z*: $[M+H]^+$ calcd. for $C_{28}H_{35}NO_7$ 498.24918; found 498.24837.

(2*R*,5*S*)-5-(1-(*tert*-Butoxy)-1-oxopropan-2-yl)pyrrolidine-2-carboxylic acid (28). This synthesis was adapted from the procedures of Ohta *et al.*[19]. Palladium on carbon (0.4 g, 8%w/w) was carefully added to a solution of **25** (5 g, 10 mmol) in acetic acid (1 mL) and ethanol (40 mL) in a bomb flask. The reaction mixture was pressurized to 50 psi with hydrogen gas in a Parr-shaker apparatus and shaken for 16 h. The reaction mixture was then filtered over Celite and concentrated *in vacuo*. The as-isolated product is a thick foam/oil (near quantitative yield). TLC (methanol:acetonitrile, 3:7 v/v): R_f = 0.19; **^{1}H-**

NMR (400 MHz; $CDCl_3$): δ 4.05 (t, *J* = 6.8 Hz, 1H), 3.77-3.59 (m, 1H), 2.85-2.74 (m, 1H), 2.30-2.21 (m, 2H), 2.12-2.00 (m, 1H), 1.66-1.57 (m, 1H), 1.46 (s, 9H), 1.33 (d, *J* = 7.1 Hz, 2H), 1.27 (d, *J* = 7.3 Hz, 1H) ppm; **^{13}C NMR** (101 MHz; $CDCl_3$): δ 173.56, 173.52, 172.6, 172.0, 82.33, 82.23, 62.3, 61.4, 60.8, 60.4, 42.5, 42.3, 29.2, 29.0, 28.3, 28.04, 28.01, 27.7, 15.4, 14.4 ppm; **HRMS** (ESI) *m/z*: $[M+H]^+$ calcd. for $C_{12}H_{21}NO_4$ 244.1549; found 244.1551. ^{1}H and ^{13}C NMR matched the data as previously reported in the literature[19].

(2*R*,5*S*)-5-(1-(*tert*-Butoxy)-1-oxobutan-2-yl)pyrrolidine-2-carboxylic acid (29). Reaction with compound **27** was conducted as described above for **28**. The product is a glas (near quantitative yield). TLC (methanol:acetonitrile, 3:7 v/v): R_f = 0.18; **^{1}H-NMR** (400 MHz; $CDCl_3$): δ 4.08 (t, *J* = 6.1 Hz, 1H), 3.82-3.63 (m, 1H), 2.64-2.53 (m, 1H), 2.31-2.20 (m, 2H), 2.05-2.00 (m, 1H), 1.86-1.69 (m, 2H), 1.69-1.57 (m, 1H), 1.51-1.43 (m, 9H), 0.97 (t, *J* = 7.2 Hz, 3H) ppm; **^{13}C NMR** (101 MHz; $CDCl_3$): δ 173.50, 173.47, 172.4, 171.5, 82.7, 82.2, 61.3, 60.76, 60.57, 50.7, 49.4, 29.06, 28.88, 28.3, 28.1, 23.7, 23.4, 11.61, 11.47 ppm; **HRMS** (ESI) *m/z*: $[M+H]^+$ calcd. for $C_{13}H_{23}NO_4$ 258.1705; found 258.1699. ^{1}H and ^{13}C NMR matched the data as previously reported in the literature[19].

The following protections (<u>30</u>-<u>33</u>) result in mixtures of diastereomers/rotamers, so NMR analyses were done at 50 °C:

Methyl (2*R*,5*S*)-1-(*tert*-butyloxycarbonyl)-5-(1-(*tert*-butoxy)-1-oxopropan-2-yl)pyrrolidine-2-carboxylate (30). This synthesis was adapted from the procedures of Ohta *et al.*[19]. Potassium carbonate (3.49 g, 25 mmol) and sodium hydroxide (0.49 g, 12.5

mmol) were added to a solution of **28** (2.05 g, 8.4 mmol) in water (25 mL) at 0 ˚C. A solution of di-*tert*-butyl dicarbonate (3.67g, 17 mmol) in tetrahydrofuran (33.8 mL) was added to the mixture at 0 ˚C over 15 min. The reaction mixture was stirred for 1 h at 0 ˚C and then allowed to warm to room temperature and stirred for 16 h. The reaction mixture was concentrated *in vacuo,* washed with diethyl ether, and acidified to pH = 2 with potassium bisulfate. The solution was then extracted twice with ethyl acetate and the combined organic layers were washed with brine, dried with anhydrous magnesium sulfate, and concentrated *in vacuo*. The crude residue was dissolved in dimethylformamide (84 mL) to which cesium carbonate (3.43 g, 10.5 mmol) was added and allowed to stir for 10 min. Methyl iodide (1.05 mL, 16.9 mmol) was added to the reaction mixture dropwise and the solution was stirred for 16 h. The reaction was quenched with saturated ammonium chloride, the phases separated, and the aqueous layer was extracted twice with diethyl ether. The combined organic fractions were dried with anhydrous magnesium sulfate and concentrated *in vacuo*. The crude oil was purified by silica gel chromatography using ethyl acetate:hexanes (1:3) to give **30** (2.39 g, 79%) as an oil, which became a waxy solid overnight. TLC (ethyl acetate:hexanes, 7:13 v/v): R_f = 0.77; (major isomer) **^{1}H-NMR** (400 MHz; $CDCl_3$): δ 4.20 (dd, *J* = 19.9, 8.4 Hz, 1H), 4.03 (app t, *J* = 8.2 Hz, 1H), 3.65 (s, 3H), 2.39-2.10 (m, 2H), 1.92-1.60 (m, 3H), 1.40 (s, 9H), 1.36 (s, 9H), 1.16 (d, *J* = 7.0 Hz, 3H) ppm; (minor isomer) **^{1}H-NMR** (400 MHz; $CDCl_3$): δ 4.24-4.16 (m, 1H), 4.13-4.08 (m, 1H), 3.65 (s, 3H), 2.39-2.10 (m, 2H), 1.92-1.60 (m, 3H), 1.40 (s, 9H), 1.36 (s, 9H), 1.03 (d, *J* = 7.2 Hz, 3H) ppm; (major isomer) **^{13}C NMR** (101 MHz; $CDCl_3$): δ 173.5, 173.0, 153.6, 79.6, 79.1, 59.3, 59.1, 51.5, 44.7, 27.7, 27.4, 25.3, 14.7 ppm; (minor isomer) **^{13}C NMR** (101 MHz; $CDCl_3$): δ 173.1, 172.8,

153.6, 79.4, 79.1, 59.8, 59.3, 51.3, 44.7, 27.7, 27.4, 23.3, 9.5 ppm; **HRMS** (FAB) *m/z*: $[M+H]^+$ calcd. for $C_{18}H_{31}NO_6$ 358.22296; found 358.22304. ^1H and ^{13}C NMR matched the data as previously reported in the literature[19].

Methyl (2*S*,5*S*)-1-(*tert*-butyloxycarbonyl)-5-(1-(*tert*-butoxy)-1-oxobutan-2-yl)pyrrolidine-2-carboxylate (31). Reaction with compound **29** was conducted as described above. The crude oil was purified by silica gel chromatography using 20% ethyl acetate in hexanes to give **31** (73%) as an oil. TLC (ethyl acetate:hexanes, 1:4 v/v): $R_f = 0.52$; (major isomer) **^{1}H-NMR** (400 MHz; $CDCl_3$): δ 4.20 (dd, *J* = 16.3, 7.9 Hz, 1H), 4.00 (m, 1H), 3.64 (s, 3H), 2.30-2.22 (m, 2H), 1.90-1.52 (m, 5H), 1.41 (s, 9H), 1.36 (s, 9H), 0.84 (t, *J* = 7.4 Hz, 3H) ppm; (minor isomer) **^{1}H-NMR** (400 MHz; $CDCl_3$): δ 4.18 (dd, *J* = 16.1, 7.6 Hz, 1H), 4.00 (m, 1H), 3.64 (s, 3H), 2.15-2.07 (m, 1H), 1.90-1.52 (m, 6H), 1.40 (s, 9H), 1.36 (s, 9H), 0.83 (t, *J* = 7.3 Hz, 3H) ppm; (major isomer) **^{13}C NMR** (101 MHz; $CDCl_3$): δ 173.0, 172.7, 153.5, 79.7, 79.1, 59.3, 59.0, 52.4, 51.4, 28.2, 27.6, 27.5, 25.4, 22.5, 11.5 ppm; (minor isomer) **^{13}C NMR** (101 MHz; $CDCl_3$): δ 172.4, 172.3, 153.5, 79.4, 59.8, 59.0, 52.4, 51.3, 28.2, 27.6, 27.5, 25.5, 22.5, 12.3 ppm; **HRMS** (FAB) *m/z*: $[M+H]^+$ calcd. for $C_{19}H_{33}NO_6$ 372.23727; found 372.23770.

***p*-Nitrobenzyl (2*R*,5*S*)-1-(*tert*-butyloxycarbonyl)-5-(1-(*tert*-butoxy)-1-oxopropan-2-yl)pyrrolidine-2-carboxylate (32).** The Boc protection of **28** was conducted as described above for **30**. The residue (0.2 g, 0.58 mmol) was redissolved in dimethylformamide (6 mL) and diisopropylethylamine (0.22 ml, 1.3 mmol) followed by the addition of *p*-nitrobenzyl bromide (0.14 g, 0.64 mmol) in dimethylformamide (3 mL). Solution was stirred 80 min. Saturated ammonium chloride was added to the solution and was extracted twice with ethyl acetate. The combined organic layers were washed

with brine, dried, and concentrated. Silica gel chromatography (ethyl acetate/hexanes, 1:4) was used to purify the oil (0.227 g, 65% over both steps). TLC (ethyl acetate:hexanes, 1:4 v/v): R_f = 0.21; (major isomer) **^{1}H-NMR** (400 MHz; $CDCl_3$): δ 8.22 (d, *J* = 8.7 Hz, 2H), 7.64 (d, *J* = 8.7 Hz, 2H), 5.34, 5.23 (ABq, J_{AB} = 14 Hz, 2H), 4.31 (q, *J* = 8.0 Hz, 1H), 4.07-4.02 (m, 1H), 2.39-2.28 (m, 2H), 1.98-1.84 (m, 2H), 1.64 (q, *J* = 5.7 Hz, 1H), 1.39 (s, (H), 1.33 (s, 9H), 1.11 (d, *J* = 7.0 Hz, 3H) ppm; (minor isomer) **^{1}H-NMR** (400 MHz; $CDCl_3$): δ 8.22 (d, *J* = 8.7 Hz, 2H), 7.64 (d, *J* = 8.7 Hz, 2H), 5.34, 5.23 (ABq, J_{AB} = 14 Hz, 2H), 4.31 (q, *J* = 8.0 Hz, 1H), 4.12 (dt, *J* = 8.0, 4.2 Hz, 1H), 2.39-2.28 (m, 1H), 2.21-2.14 (m, 1H), 1.98-1.84 (m, 2H), 1.79-1.73 (m, 1H), 1.39 (s, (H), 1.33 (s, 9H), 0.99 (d, *J* = 7.2 Hz, 3H) ppm; (major isomer) **^{13}C NMR** (101 MHz; $CDCl_3$): δ 173.3, 172.1, 153.6, 147.0, 143.4, 128.3, 123.1, 79.5, 79.2, 64.5, 59.4, 59.1, 44.7, 28.8, 27.6, 27.4, 25.0, 14.7 ppm; (minor isomer) **^{13}C NMR** (101 MHz; $CDCl_3$): δ 173.3, 172.7, 153.6, 147.0, 143.4, 128.3, 123.1, 79.3, 79.2, 64.5, 59.9, 59.4, 44.7, 28.8, 27.6, 27.4, 25.0, 9.4 ppm; **HRMS** (FAB) *m/z*: $[M+H]^+$ calcd. for $C_{24}H_{34}N_2O_8$ 479.23934; found 479.23938.

***p*-Nitrobenzyl (2*R*,5*S*)-1-(*tert*-butyloxycarbonyl)-5-(1-(*tert*-butoxy)-1-oxobutan-2-yl)pyrrolidine-2-carboxylate (33).** Reaction with **29** was conducted as described above. Multiple rounds of silica gel chromatography (ethyl acetate:hexanes, 1:19 to 3:7) were used to purify the product as an oil (51%). TLC (ethyl acetate:hexanes, 1:4 v/v): R_f = 0.35; (major isomer) **^{1}H-NMR** (400 MHz; $CDCl_3$): δ 8.22 (d, *J* = 8.4 Hz, 2H), 7.63 (d, *J* = 8.5 Hz, 2H), 5.34, 5.22 (ABq, J_{AB} = 13.6 Hz, 2H), 4.34-4.27 (m, 1H), 4.05-3.99 (m, 1H), 2.25-2.14 (m, 2H), 1.91-1.83 (m, 2H), 1.67-1.60 (m, 2H), 1.57-1.49 (m, 1H), 1.39 (s, (H), 1.34 (s, 9H), 0.74 (t, *J* = 8.2 Hz, 3H) ppm; (minor isomer) **^{1}H-NMR** (400 MHz;

$CDCl_3$): δ 8.22 (d, *J* = 8.4 Hz, 2H), 7.63 (d, *J* = 8.5 Hz, 2H), 5.28 (s, 2H), 4.34-4.27 (m, 1H), 4.05-3.99 (m, 1H), 2.35-2.29 (m, 1H), 1.91-1.83 (m, 3H), 1.67-1.60 (m, 2H), 1.57-1.49 (m, 1H), 1.39 (s, (H), 1.34 (s, 9H), 0.77 (t, *J* = 8.1 Hz, 3H) ppm; (major isomer) **^{13}C NMR** (101 MHz; $CDCl_3$): δ 172.6, 172.1, 153.4, 147.1, 143.4, 128.4, 123.2, 79.8, 79.3, 64.5, 59.5, 59.1, 52.4, 28.3, 27.6, 27.5, 25.5, 22.5, 11.4 ppm; (minor isomer) **^{13}C NMR** (101 MHz; $CDCl_3$): δ 172.2, 172.1, 153.7, 147.1, 143.4, 128.4, 123.2, 79.4, 79.3, 64.5, 60.0, 59.1, 52.4, 28.3, 27.6, 27.5, 25.5, 22.5, 12.2 ppm; **HRMS** (FAB) *m/z*: $[M+H]^+$ calcd. for $C_{25}H_{36}N_2O_8$ 493.25499; found 493.25445.

Methyl (3*S*,5*S*,6*R*)-6-methylcarbapenam-3-carboxylate (34). This synthesis was adapted from the procedures of Ohta *et al.*[19]. 2,6-Lutidine (1.44 mL, 12 mmol) and trimethylsilyl triflate (1.82 mL, 10 mmol) were added slowly to a solution of **30** (1.2 g, 3.3 mmol) in dichloromethane (35 mL) at 0 ˚C and the mixture stirred for 2 h. A solution of hydrochloric acid in dioxane (7.65 mL, 4M, 31 mmol) was added at 0 ˚C and stirred for 10 min. The reaction mixture was concentrated *in vacuo* to yield dark red oil. The crude oil was dissolved in dichloromethane (500 mL) to which diisopropylethylamine (2.63 mL, 15 mmol) followed by a solution of *N,N′*-dicyclohexylcarbodiimide (0.9 g, 4.4 mmol) in dichloromethane (10 mL) were added at 0 ˚C. The mixture was allowed to slowly warm to ambient temperature while stirring over 23 h. The reaction mixture was concentrated *in vacuo* and dissolved in dichloromethane and filtered through Celite. The eluate was washed 3 × with a cold solution of acetic acid in water (5%), dried with anhydrous sodium sulfate, and concentrated *in vacuo*. The crude oil was purified by silica gel chromatography using ethyl acetate:hexanes (1:2) to give a clear oil (0.452 g, 73%). TLC (ethyl acetate:hexanes, 2:3 v/v): R_f = 0.36. 1,8-Diazabicyclo[5.4.0]undec-7-

ene (1.13 mL, 7.6 mmol) was added to a solution of the mixture of diastereomers (1.38 g, 7.5 mmol) in acetonitrile (150 mL) and stirred at 50 ˚C for 5 d. The reaction mixture was concentrated *in vacuo* to give a brown oil. The crude product was purified from its diastereomer by silica gel chromatography using ethyl acetate:hexanes (3:17) to give the titled compound (eluted first) as an oil (0.59 g, 43%). TLC (ethyl acetate:hexanes, 2:3 v/v): R_f = 0.52; **^{1}H-NMR** (300 MHz; $CDCl_3$): δ 4.35 (t, *J* = 7.3 Hz, 1H), 3.96 (app q, *J* = 6.3 Hz, 1H), 3.73 (s, 3H), 3.50 (qd, *J* = 7.7, 5.5 Hz, 1H), 2.45-2.35 (m, 1H), 2.29-2.17 (m, 1H), 2.06-1.96 (m, 1H), 1.63 (app. ddt, *J* = 13.1, 9.0, 7.8 Hz, 1H), 1.13 (d, *J* = 7.7 Hz, 3H) ppm; **^{13}C NMR** (101 MHz; $CDCl_3$): δ 181.1, 172.0, 58.6, 57.7, 52.5, 45.3, 34.6, 25.2, 9.3 ppm; **HRMS** (ESI) *m/z*: $[M+H]^+$ calcd. for $C_9H_{13}NO_3$ 184.0974; found 184.0966. ^{1}H and ^{13}C NMR matched the data as previously reported in the literature.

***p*-Nitrobenzyl (3*S*,5*S*,6*R*)-6-methylcarbapenam-3-carboxylate (35)**. The coupling reaction was conducted as above using **32**, 63% yield overall. TLC (ethyl acetate:hexanes, 2:3 v/v): R_f = 0.31; **^{1}H-NMR** (400 MHz; $CDCl_3$): δ 8.23 (d, *J* = 8.8 Hz, 2H), 7.52 (d, *J* = 8.8 Hz, 2H), 5.25 (s, 2H), 4.43 (t, *J* = 7.3 Hz, 1H), 3.97 (app. dd, *J* = 12.9, 6.5 Hz, 1H), 3.52 (qd, *J* = 7.7, 5.6 Hz, 1H), 2.49-2.41 (m, 1H), 2.29-2.20 (m, 1H), 2.07-1.99 (m, 1H), 1.71-1.63 (m, 1H), 1.15 (d, *J* = 7.7 Hz, 3H) ppm; **HRMS** (FAB) *m/z*: $[M+H]^+$ calcd. for $C_{15}H_{16}N_2O_5$ 305.11375; found 305.11333. The product data matched previous characterization[40].

Methyl (3*S*,5*S*,6*R*)-6-ethylcarbapenam-3-carboxylate (36). The coupling reaction was conducted as above using **31,** 35% yield overall. TLC (ethyl acetate:hexanes, 2:3 v/v): R_f = 0.61; **^{1}H-NMR** (300 MHz; $CDCl_3$): δ 4.34 (t, *J* = 7.5 Hz, 1H), 3.95 (app dt, *J* = 7.5, 5.9 Hz, 1H), 3.73 (s, 3H), 3.33 (ddd, *J* = 9.6, 7.4, 5.4 Hz, 1H), 2.48-2.37 (m, 1H), 2.29-2.17

(m, 1H), 2.09-1.99 (m, 1H), 1.74-1.40 (m, 3H), 0.98 (t, J = 7.4 Hz, 3H) ppm; **^{13}C NMR** (101 MHz; $CDCl_3$): δ 180.3, 172.1, 58.4, 57.2, 52.52, 52.49, 34.6, 25.3, 18.4, 12.0 ppm; **HRMS** (ESI) *m/z*: $[M+H]^+$ calcd. for $C_{10}H_{15}NO_3$ 198.1130; found 198.1126.

***p*-Nitrobenzyl (3*S*,5*S*,6*R*)-6-ethylcarbapenam-3-carboxylate (37).** The coupling reaction was conducted as above using **33,** 29% yield overall. TLC (ethyl acetate:hexanes, 2:3 v/v): R_f = 0.38; **^{1}H-NMR** (400 MHz; $CDCl_3$): δ 8.23 (d, J = 8.7 Hz, 2H), 7.52 (d, J = 8.8 Hz, 2H), 5.25 (s, 2H), 4.41 (t, J = 7.5 Hz, 1H), 3.97-3.92 (m, 1H), 3.35 (ddd, J = 9.6, 7.4, 5.4 Hz, 1H), 2.52-2.39 (m, 1H), 2.31-2.17 (m, 1H), 2.13-1.99 (m, 1H), 1.75-1.57 (m, 2H), 1.55-1.42 (m, 1H), 0.99 (t, J = 7.4 Hz, 3H) ppm; **HRMS** (FAB) *m/z*: $[M+H]^+$ calcd. for $C_{16}H_{18}N_2O_5$ 319.12940; found 319.12849. ^{1}H and NMR matched the data as previously reported in the literature[38].

Potassium (3*S*,5*S*,6*R*)-6-methylcarbapenam-3-carboxylate (38). 35 (60 mg) was dissolved in tetrahydrofuran (4 mL) and potassium phosphate buffer (2 mL, 0.5M, pH 7.0). 10% palladium on carbon (1:1 w/w with compound **S25**) was added and placed under hydrogen (40 psi) for 1 h with shaking. The mixture was filtered through Celite and washed with water and diethyl ether. The aqueous solution was washed with diethyl ether, filtered (0.2 μm, nylon), and lyophilized. The resulting powder was desalted by passage through HP-20 diaion resin. **^{1}H-NMR** (400 MHz; D_2O): δ 4.14 (t, J = 7.8 Hz, 1H), 3.95 (dt, J = 8.1, 5.6 Hz, 1H), 3.50 (qd, J = 7.7, 5.1 Hz, 1H), 2.56-2.48 (m, 1H), 2.14-2.05 (m, 1H), 2.01-1.94 (m, 1H), 1.67-1.57 (m, 1H), 1.11 (d, J = 7.8 Hz, 3H) ppm; **HRMS** (ESI) *m/z*: $[M-H]^-$ calcd. for $C_8H_{11}NO_3$ 168.0661; found 168.0648. ^{1}H NMR matched the data as previously reported in the literature[38].

Potassium (3*S*,5*S*,6*R*)-6-ethylcarbapenam-3-carboxylate (39). **37** was deprotected in a similar fashion to the C-6-methyl analog **38**). **^{1}H-NMR** (400 MHz; D_2O): δ 4.12 (t, *J* = 7.8 Hz, 1H), 3.96-3.91 (m, 1H), 3.38-3.32 (m, 1H), 2.58-2.50 (m, 1H), 2.11-1.96 (m, 2H), 1.65-1.47 (m, 3H), 0.93 (t, *J* = 7.4 Hz, 3H) ppm; **^{13}C NMR** (101 MHz; D2O): δ 184.8, 180.4, 61.6, 57.9, 51.2, 36.1, 25.6, 18.3, 11.6 ppm; **HRMS** (ESI) *m/z*: $[M-H]^-$ calcd. for $C_9H_{13}NO_3$ 182.0817; found 182.0804.

Methyl (5*S*,6*R*)-6-methylcarbapenem-3-carboxylate (40). This synthesis was adapted from the procedures of Ohta *et al.*[19]. A solution of lithium hexamethyl-disilazane in tetrahydrofuran (3.576 mL, 1M, 3.58 mmol) was added to **34** (301 mg, 1.643 mMol) in tetrahydrofuran (16.4 mL) at -78 ˚C and stirred for 5 min. Phenylselenium bromide (1.16 g, 4.93 mmol) was added at -78 ˚C and allowed to warm to room temperature over 1h. The reaction mixture was diluted with ethyl acetate (20 mL) and washed with water (20 mL), brine (20 mL), dried with anhydrous sodium sulfate, filtered and concentrated *in vacuo*. The crude residue was run through a silica plug with 20% ethyl acetate in hexanes to remove excess phenyl selenium bromide and then concentrated. The resulting oil (257 mg, 0.760 mmol) was dissolved in dichloromethane (41 mL) to which was then added a solution of *m*-chloroperbenzoic acid (131 mg, 0.760 mmol) in dichloromethane (5 mL) at -30˚C. The reaction was stirred for 15 min at -30 ˚C before it was quenched with triethylamine (141 µL, 1.01 mmol) and diluted with dichloromethane (150 mL). The reaction mixture was washed twice with saturated ammonium bicarbonate (50 mL), brine (50 mL), dried with anhydrous sodium sulfate, filtered, and concentrated *in vacuo*. The crude residue was purified by silica gel chromatography using ethyl acetate:hexanes (3:7) to give **40** (52 mg, 17%) as a yellow oil. TLC (ethyl acetate:hexanes, 3:7 v/v): R_f=

0.32; **^{1}H-NMR** (300 MHz; $CDCl_3$): δ 6.52 (t, *J* = 2.8 Hz, 1H), 4.37 (ddd, *J* = 10.0, 8.7, 6.2 Hz, 1H), 3.83 (s, 3H), 3.74-3.66 (m, 1H), 2.76 (app. qdd, *J* = 19.4, 9.4, 2.8 Hz, 2H), 1.27 (d, *J* = 7.7 Hz, 3H) ppm; **^{13}C NMR** (101 MHz; $CDCl_3$): δ 180.8, 161.3, 135.9, 132.4, 56.1, 52.5, 47.4, 30.65, 9.9 ppm; **HRMS** (ESI) *m/z*: $[M+H]^+$ calcd. for $C_9H_{11}NO_3$ 182.0817; found 182.0809. ^{1}H and ^{13}C NMR matched the data as previously reported in the literature.

Methyl (5*S*,6*R*)-6-ethylcarbapenem-3-carboxylate (41). 36 was desaturated in a similar fashion to the C-6-methyl analog (**34**) to give **41** (40.8 mg, 9.4%). TLC (ethyl acetate:hexanes, 3:7 v/v): R_f = 0.60; **^{1}H-NMR** (400 MHz; $CDCl_3$): δ 6.51 (t, *J* = 2.6 Hz, 1H), 4.35 (ddd, *J* = 9.9, 8.9, 6.1 Hz, 1H), 3.82 (s, 3H), 3.53 (dt, *J* = 9.6, 6.6, 1H), 2.82-2.68 (m, 2H), 1.89-1.78 (m, 1H), 1.65-1.54 (m, 1H), 1.00 (t, *J* = 7.4 Hz, 3H) ppm; **^{13}C NMR** (101 MHz; $CDCl_3$): δ 180.1, 161.3, 135.7, 132.3, 55.7, 54.3, 52.5, 30.9, 18.9, 11.9 ppm; **HRMS** (ESI) *m/z*: $[M+H]^+$ calcd. for $C_{10}H_{13}NO_3$ 196.0974; found 196.0971.

Methyl (3*R*,5*S*,6*R*)-6-methyl-2-pantetheinyl-carbapenam-3-carboxylate (42). Hydrochloric acid (471 µL, 1M) was added to pantetheine acetonide (157 mg, 0.495 mmol, as described elsewhere[4]) in tetrahydrofuran (691 µL) and stirred for 30 min. Sodium hydroxide (471 µL, 1M) was then added to neutralize the reaction mixture. The product pantetheine diol was directly added to **40** (64 mg, 0.353 mmol) in acetonitrile (960 µL) to which was added triethylamine (25 µL, 0.177 mmol) and stirred for 30 min at ambient temperature. The reaction mixture was diluted with ethyl acetate (15 mL), washed with saturated ammonium chloride (4 mL), and brine (10 mL). The combined aqueous layers were extracted with ethyl acetate (15 mL) and the combined organic fractions were dried with anhydrous sodium sulfate, filtered, and concentrated *in vacuo.*

The crude oil was purified by silica gel chromatography using ethanol:chloroform (1:9) to give **42** (16 mg) as an inseparable mixture of C-2 diastereomers in a ratio of 7:5 (**42a**:**42b**) by ^{1}H-NMR. TLC (ethanol:chloroform, 1:9 v/v): R_f = 0.25; **42a: ^{1}H-NMR** (400 MHz; MeOD): δ 4.67 (d, *J* = 7.2 Hz, 1H), 4.2-4.14 (m, 2H), 3.89 (s, 1H), 3.74 (s, 3H), 3.58-3.53 (m, 3H), 3.50, 3.36 (ABq, J_{AB} = 14.4 Hz, 2H), 2.84-2.65 (m, 4H), 2.43 (t, *J* = 6.5 Hz, 2H), 2.28 (ddd, *J* = 14.0, 8.2, 3.5 Hz, 1H), 1.97 (ddd, *J* = 13.8, 10.1, 8.3 Hz, 1H), 1.15 (d, *J* = 7.8, 3H), 0.92 (s, 6H) ppm; **42b: ^{1}H-NMR** (400 MHz; MeOD): δ 4.17 (d, *J* = 6.1 Hz, 1H), 4.2-4.14 (m, 1H) 3.99 (ddd, *J* = 8.0, 6.5, 5.4 Hz, 1H), 3.85 (s, 1H), 3.76 (s, 3H), 3.58-3.53 (m, 3H), 3.43, 3.29 (ABq, J_{AB} = 11.2 Hz, 2H), 2.84-2.65 (m, 6H), 2.43 (t, *J* = 5.7 Hz, 2H), 1.19 (d, *J* = 7.7, 3H), 0.92 (s, 6H) ppm; **HRMS** (ESI) *m/z*: $[M+H]^+$ calcd. for $C_{20}H_{33}N_3O_7S$ 460.2117; found 460.2112.

Methyl (3*R*,5*S*,6*R*)-6-ethyl-2-pantetheinyl-carbapenam-3-carboxylate (43).

The carbapenem **41** was reacted with pantetheine in a similar fashion to the C-6-methyl analogue (carbapenem **40**) to give **43**(12 mg, 13%) as an inseparable mixture of C-2 diastereomers in a nearly equal ratio by ^{1}H-NMR. TLC (ethanol:chloroform, 1:9 v/v): R_f = 0.45; **43a: ^{1}H-NMR** (400 MHz; MeOD): δ 4.60 (d, *J* = 7.3 Hz, 1H), 4.15-3.98 (m, 1H), 3.83-3.78 (m, 1H), 3.81 (s, 1H), 3.71 (s, 3H), 3.48-3.26 (m, 4H), 3.43, 3.29 (ABq, J_{AB} = 10.8 Hz, 2H), 2.72 (dt, *J* = 13.0, 6.2, 1H), 2.64 (dt, *J* = 12.9, 6.5, 1H), 2.36 (t, *J* = 5.5 Hz, 2H), 2.31-2.13 (m, 2H), 1.61-1.41 (m, 2H), 0.94 (t, *J* = 7.8 Hz, 3H), 0.85 (s, 6H) ppm; **43b: ^{1}H-NMR** (400 MHz; MeOD): δ 4.08 (d, *J* = 6.5 Hz, 1H), 4.15-3.98 (m, 1H), 3.94-3.86 (m, 1H), 3.82 (s, 1H), 3.67 (s, 3H), 3.49-3.60 (m, 1H), 3.48-3.26 (m, 4H), 3.43, 3.29 (ABq, J_{AB} = 10.8 Hz, 2H), 3.08-2.79 (m, 2H), 2.55-2.39 (m, 1H), 2.36 (t, *J* = 5.5 Hz, 2H), 1.61-1.41 (m, 2H), 0.96 (t, *J* = 7.5 Hz, 3H), 0.85 (s, 6H) ppm; **43a and 43b: ^{13}C NMR**

(101 MHz; MeOD): δ 177.0, 175.2, 174.9, 173.1, 172.5, 80.5, 78.3, 71.4, 68.8, 68.4, 67.3, 67.2, 59.2, 55.4, 55.3, 54.6, 54.5, 54.2, 54.1, 53.4, 53.3, 41.4, 37.5, 37.4, 37.3, 34.1, 33.1, 22.4, 22.0, 20.7 20.3, 13.3, 13.0 ppm; **HRMS** (ESI) *m/z*: $[M+H]^+$ calcd. for $C_{21}H_{35}N_3O_7S$ 474.2274; found 474.2267.

Ammonium (3*R*,5*S*,6*R*)-6-methyl-2-pantetheinyl-carbapenam-3-carboxylate (44, 45). A solution of lithium hydroxide in water (1M, 20 µL) was added to **42** (8 mg, 0.0176 mmol) in tetrahydrofuran (500 µL) at 0 ˚C and stirred for 20 min, at which time TLC monitoring revealed incomplete reaction. A second batch of lithium hydroxide solution (1M, 20 µL) was then added and after 30 min at 0 ˚C the reaction was quenched with K_2HPO_4 (10 mM, pH = 7.0, 500 µL). The mixture was concentrated *in vacuo* to remove the organic solvent, and immediately injected onto a preparatory reverse-phase HPLC (Phenomonex Luna C18(2) 250 x 21.2 mm 10 micron 100 Å, 10:90 5 mM NH_4HCO_3 in water : acetonitrile, 5 mL/min) for purification. The C-2/3 "cis" diastereomer **45** eluted at 11 min and the C-2/3 "trans" diastereomer **44** eluted at 13 min, allowing for enrichment of each diastereomer. The compounds were collected and lyophilized to give carbapenams **44** (1.27 mg, 16%) and **45** (0.63 mg, 8%) as white powders. **44: ^{1}H-NMR** (400 MHz; D_2O): δ 4.06 (d, J = 5.4 Hz, 1H), 4.08-4.04 (m, 1H), 3.99 (s, 1H), 3.82-3.75 (m, 1H), 3.61 (dd, J = 8.2, 5.3 Hz, 1H), 3.53-3.38 (m, 4H), 3.58, 3.34 (ABq, J_{AB} = 11.0 Hz, 2H), 2.86 (td, J = 13.3, 6.5 Hz, 1H), 2.78 (td, J = 13.0, 6.3 Hz, 1H), 2.51 (t, J = 6.3, 2H), 2.45 (dt, J = 13.9, 6.8 Hz, 1H), 1.7 (dt, J = 14.3, 7.2 Hz, 1H), 1.20 (d, J = 7.9 Hz, 3H), 0.93 (s, 3H), 0.89 (s, 3H) ppm; **HRMS** (ESI) *m/z*: $[M+H]^+$ calcd. for $C_{19}H_{31}N_3O_7S$ 446.1961; found 446.1957; **45: ^{1}H-NMR** (400 MHz; D_2O): δ 4.34 (d, J = 7.3 Hz, 1H), 4.10 (dd, J = 13.5, 6.2, 1H), 3.90 (s, 1H), 3.71 (s, 1H), 3.67 (dd,

J = 12.3, 6.4 Hz, 1H), 3.56 (dd, *J* = 11.9, 4.7 Hz, 1H), 3.56-3.34 (m, 3H), 3.48, 3.24 (ABq, J_{AB} = 11.6 Hz, 2H), 2.41 (t, *J* = 6.6, 2H), 2.09 (dt, *J* = 13.5, 6.8 Hz, 1H), 2.00 (dt, *J* = 13.4, 6.7 Hz, 1H), 1.04 (d, *J* = 7.7 Hz, 3H), 0.83 (s, 3H), 0.80 (s, 3H) ppm; **HRMS** (ESI) *m/z*: $[M+H]^+$ calcd. for $C_{19}H_{31}N_3O_7S$ 446.1961; found 446.1952.

Sodium (3*R*,5*S*,6*R*)-6-ethyl-2-pantetheinyl-carbapenam-3-carboxylate (46). An analytical amount of the protected methyl ester **43** was dissolved in 1:1 acetonitrile:H_2O. The solution was adjusted to pH ≥ 10 with NaOH (~1 M) and allowed to react at room temperature for 10 min. The solution was then neutralized to pH = 7 with HCl (~1 M) and analyzed by UPLC-MS. **HRMS** (ESI) *m/z*: $[M+H]^+$ calcd. for $C_{20}H_{33}N_3O_7S$ 460.2117; found 460.2112.

Potassium (2*S*,3*R*,5*R*)-2-(2-acetamidoethylthiol)-carbapenam-3-carboxylate (47) and **potassium (2*R*,3*R*,5*R*)-2-(2-acetamidoethylthiol)-carbapenam-3-carboxylate (48).** The title compounds were synthesized using the carbapenem **8** as previously described and characterized. The final diastereomers **47** and **48** were purified and separated from each other using an Agilent model 1100 HPLC equipped with a multi-wavelength ultraviolet–visible detector (210 nm) in conjunction with a reverse-phase Phenomenex Luna 10µ C18(2) 100 Å preparatory column (250 x 21.20 mm ID). The mobile phase was 18% methanol and 82% buffer (10 mM potassium phosphate, pH 6.65) at a flow rate of 5 ml per min. Compound **47** eluted at 23 min and compound **48** eluted at 18 min. Excess phosphate buffer was removed using Diaion® HP-20 resin.

Potassium (2*S*,3*R*,5*R*)-2-(4-phosphopantetheinyl)-carbapenam-3-carboxylate (49) and **potassium (2*R*,3*R*,5*R*)-2-(4-phosphopantetheinyl)-carbapenam-3-carboxylate (50).** The C-2-phosphopantetheine carbapenams were generated from the C-2-pantetheine

analogs **49** and **50** using pantothenate kinase, PanK[23], provided by D.H. Long, Townsend Lab. Reactions included: ~ 0.40 mg/mL enzyme, 15 mM substrate (~18 mg), 15 mM ATP, 20 mM KCl, 10 mM $MgCl_2$, and 50 mM Tris, pH 7.5 and were run for at least 2 hours at RT. The protein was removed by centrifugal filtration (Amicon, 10 kDa MWCO). The titled compounds were purified using the 1100 HPLC as described for **47** and **48** (detection: 210 nm). The mobile phase was 15% methanol and 85% buffer (10 mM potassium phosphate, pH 6.65) for **50** and it eluted at approximately 17 min. The mobile phase was 20% methanol and 80% buffer for **49** and it eluted at approximately 17 min. Excess phosphate buffer was removed using Diaion® HP-20 resin.

Potassium (2*S*,3*R*,5*R*) 2-(4-phosphopantetheinylthio)-7-oxo-2-azabicyclo[3.2.0]heptane-3-carboxylate (49). ^{1}H NMR (300 MHz, D_2O): δ 4.15 (d, *J* = 5.5 Hz, 1H), 4.08 (s, 1H), 3.90-4.0 (m, 1H), 3.69-3.80 (m, 1H), 3.49 (t, *J* = 6.5 Hz, 2H), 3.35-3.44 (m, 4H), 3.32 (dd, *J* = 16.4, 4.9 Hz, 1H), 2.88 (dd, *J* = 16.3, 2.1 Hz, 1H), 2.70-2.84 (m, 2H), 2.52-2.64 (m, 1H), 2.49 (t, *J* = 6.5 Hz, 2H), 1.62-1.74 (m, 1H), 0.96 (s, 3H), 0.81 (s, 3H) ppm. ^{31}P NMR (121.5 MHz, D_2O): δ 2.40 (s); HRMS (ESI) *m/z*: $[M+H]^+$ calcd. for $C_{18}H_{30}N_3O_{10}PS$ 512.1468; found 512.1470.

Potassium (2*R*,3*R*,5*R*) 2-(4-phosphopantetheinylthio)-7-oxo-2-azabicyclo[3.2.0]heptane-3-carboxylatemajor (50). ^{1}H NMR (300 MHz, D_2O): δ 4.45 (d, *J* = 6.8 Hz, 1H), 4.03 (s, 1H), 3.81-3.90 (m, 1H), 3.62-3.70 (m, 1H), 3.42 (t, *J* = 6.4 Hz, 2H), 3.28-3.39 (m, 4H), 3.24 (dd, *J* = 16.4, 4.9 Hz, 1H), 2.74 (dd, *J* = 16.3, 2.0 Hz), 2.71 (t, *J* = 6.8 Hz, 2H), 2.44 (t, *J* = 6.4 Hz, 2H), 2.20-2.32 (m, 1H), 1.92-2.04 (m, 1H), 0.94 (s, 3H), 0.76 (s, 3H) ppm. ^{31}P NMR (121.5 MHz, D_2O): δ 2.43 (s); HRMS (ESI) *m/z*: $[M+H]^+$ calcd. for $C_{18}H_{30}N_3O_{10}PS$ 512.1468; found 512.1463.

Potassium (2*S*,3*R*,5*R*)-2-CoA-carbapenam-3-carboxylate (51) and **potassium (2*R*,3*R*,5*R*)-2-CoA-carbapenam-3-carboxylate (52).** A solution of Coenzyme A (49 mg, 0.064 mmol) and with triethylamine (6.3 µL, 0.045 mmol) in water was added to a solution of carbapenem **9** (31 mg, 0.11 mmol) in tetrahydrofuran (0.40 mL). The solution was stirred for 75 min. The reaction mixture was then transferred to a pressure tube along with a catalytic amound of 10% Pd on carbon, 0.5 mL 0.5 M potassium phosphate (pH 7), 1 mL water, and 1 mL tetrahydrofuran and shaken on a Parr apparatus for 1 h under hydrogen (20 psi). The catalyst was removed by filtration through Celite. The filtrate was washed with diethyl ether (15 mL) and extracted. The aqueous layer was filtered through a 0.2 µm nylon filter and lyophilized. Prior to HPLC injection, the sample was dissolved in water and filtered through a centrifugal device (Amicon, 10 kDa MWCO). The diastereomers **51** and **52** were separated from each other and purified using an Agilent 1100 HPLC (detection: 254 nm). The mobile phase was 13% methanol and 87% buffer (10 mM potassium phosphate, pH 6.65) at a flow rate of 5 ml per min. Compound **51** eluted at 22 min and compound **52** eluted at 17.5 min. Excess phosphate buffer was removed using Diaion® HP-20 resin. **51:** ^{1}H-NMR (300 MHz. D_2O) δ: 8.51 (s, 1H), 8.24 (s, 1H), 6.14 (d, *J* = 6.8 Hz, 1H), 4.52-4.55 (m, 1H), 4.19 (dd, *J* = 4.5, 3.4 Hz, 2H), 4.10 (d, *J* = 5.4 Hz, 1H), 3.95 (s, 1H), 3.90 (dd, *J* = 4.7. 2.2 Hz, 1H), 3.74 (ddd, *J* = 18.0, 11.5, 6.4 Hz, 2H), 3.50 (dd, *J* = 9.9, 5.0 Hz, 1H), 3.42 (td, *J* = 6.5, 2.4 Hz, 2H), 3.36-3.40 (m, 2H), 3.27 (d, *J* = 5.1 Hz, 1H), 2.84 (dd, *J* = 16.3, 2.0 Hz, 1H), 2.73 (q, *J* = 8.0 Hz, 2H), 2.53 (dt, *J* = 14.1, 6.6 Hz, 1H), 2.42 (t, *J* = 6.8 Hz, 2H), 1.62 (dt, *J* = 14.0, 7.0 Hz, 1H), 0.82 (s, 3H), 0.69 (s, 3H); **HRMS** (ESI) *m/z*: $[M+H]^+$ calcd. for $C_{28}H_{43}N_8O_{19}P_3S$ 921.1656; found 921.1636; **52:** ^{1}H-NMR (400 MHz. D_2O) δ: 8.51 (s, 1H), 8.25 (s, 1H),

6.14 (d, J = 6.8 Hz, 1H), 4.53-4.55 (m, 1H), 4.47 (d, J = 6.7 Hz, 1H), 4.19 (dd, J = 4.6, 3.4 Hz, 2H), 3.97-4.06 (m, 1H), 3.95 (s, 1H), 3.88 (td, J = 6.5. 3.6 Hz, 1H), 3.73-3.78 (m, 2H), 3.24-3.49 (m, 6H), 2.75 (dd, J = 16.6, 2.1 Hz, 1H), 2.70 (dd, J = 10.1, 6.8 Hz, 2H), 2.62-2.65 (m, 1H), 2.42 (t, J = 6.5 Hz, 2H), 2.20-2.29 (m, 2H), 1.95-2.02 (m, 1H), 0.81 (s, 3H), 0.68 (s, 3H); **HRMS** (ESI) *m/z*: $[M+H]^+$ calcd. for $C_{28}H_{43}N_8O_{19}P_3S$ 921.1656; found 921.1628.

References

1. Coulthurst, S. J., Barnard, A. M. L. & Salmond, G. P. C. Regulation and biosynthesis of carbapenem antibiotics in bacteria. *Nat. Rev. Microbiol.* **3,** 295–306 (2005).
2. Bodner, M. J. *et al.* Definition of the Common and Divergent Steps in Carbapenem β-Lactam Antibiotic Biosynthesis. *ChemBioChem* **12,** 2159–2165 (2011).
3. Li, R., Stapon, A., Blanchfield, J. T. & Townsend, C. A. Three Unusual Reactions Mediate Carbapenem and Carbapenam Biosynthesis. *J. Am. Chem. Soc.* **122,** 9296–9297 (2000).
4. Freeman, M. F., Moshos, K. A., Bodner, M. J., Li, R. & Townsend, C. A. Four enzymes define the incorporation of coenzyme A in thienamycin biosynthesis. *Proc. Natl. Acad. Sci. U. S. A.* **105,** 11128–11133 (2008).
5. Zhang, Q., van der Donk, W. A. & Liu, W. Radical-Mediated Enzymatic Methylation: A Tale of Two SAMS. *Acc. Chem. Res.* **45,** 555–564 (2012).
6. Broderick, J. B., Duffus, B. R., Duschene, K. S. & Shepard, E. M. Radical S-adenosylmethionine enzymes. *Chem. Rev.* **114,** 4229–4317 (2014).
7. Frey, P. A., Hegeman, A. D. & Ruzicka, F. J. The Radical SAM Superfamily. *Crit. Rev. Biochem. Mol. Biol.* **43,** 63–88 (2008).
8. Williamson, J. M. & Brown, G. M. The Biosynthesis of Thienamycin and Related Carbapenems. *Crit. Rev. Biotechnol.* **4,** 111–131 (1986).
9. Pierre, S. *et al.* Thiostrepton tryptophan methyltransferase expands the chemistry of radical SAM enzymes. *Nat. Chem. Biol.* **8,** 957–959 (2012).
10. Kim, H. J. *et al.* GenK-Catalyzed C-6′ Methylation in the Biosynthesis of Gentamicin: Isolation and Characterization of a Cobalamin-Dependent Radical SAM Enzyme. *J. Am. Chem. Soc.* **135,** 8093–8096 (2013).

11. Allen, K. D. & Wang, S. C. Initial characterization of Fom3 from Streptomyces wedmorensis: The methyltransferase in fosfomycin biosynthesis. *Arch. Biochem. Biophys.* **543,** 67–73 (2014).

12. Huang, C. *et al.* Delineating the biosynthesis of gentamicin X2, the common precursor of the gentamicin C antibiotic complex. *Chem. Biol.* **22,** 251–261 (2015).

13. Yoshioka, T. *et al.* Structures of OA-6129A, B1, B2 and C, new carbapenem antibiotics produced by Streptomyces sp. OA-6129. *J. Antibiot. (Tokyo).* **36,** 1473–1482 (1983).

14. Yoshioka, T. *et al.* Structures of OA-6129D and E, new carbapenam antibiotics. *J. Antibiot. (Tokyo).* **37,** 211–217 (1984).

15. Allen, K. D. & Wang, S. C. Spectroscopic characterization and mechanistic investigation of P-methyl transfer by a radical SAM enzyme from the marine bacterium Shewanella denitrificans OS217. *Biochim. Biophys. Acta - Proteins Proteomics* **1844,** 2135–2144 (2014).

16. Yan, F. *et al.* RlmN and Cfr are Radical SAM Enzymes Involved in Methylation of Ribosomal RNA. *J. Am. Chem. Soc.* **132,** 3953–3964 (2010).

17. Bauerle, M. R., Schwalm, E. L. & Booker, S. J. Mechanistic Diversity of Radical *S* -Adenosylmethionine (SAM)-dependent Methylation. *J. Biol. Chem.* **290,** 3995–4002 (2015).

18. Mitscher, L. A., Showalter, H. D., Shirahata, K. & Foltz, R. L. Chemical-ionization mass spectrometry of beta-lactam antibiotics. *J. Antibiot. (Tokyo).* **28,** 668–75 (1975).

19. Ohta, T., Sato, N., Kimura, T., Nozoe, S. & Izawa, K. Chirospecific synthesis of (+)-PS-5 from L-glutamic acid. *Tetrahedron Lett.* **29,** 4305–4308 (1988).

20. Ueda, Y., Damas, C. E. & Vinet, V. Nuclear analogs of $β$-lactam antibiotics. XIX. Syntheses of racemic and enantiomeric p-nitrobenzyl carbapen-2-em-3-carboxylates. *Can. J. Chem.* **61,** 2257–2263 (1983).

21. Bateson, J. H., Hickling, R. I., Roberts, P. M., Smale, T. C. & Southgate, R. Olivanic acids and related compounds: total synthesis of (+/-)-PS-5 and (+/-)-6-epi PS-5. *J. Chem. Soc. Chem. Commun.* 1084 (1980).

22. Marous, D. R. *et al.* Consecutive radical S-adenosylmethionine methylations form the ethyl side chain in thienamycin biosynthesis. *Proc. Natl. Acad. Sci. U. S. A.* **112,** 10354–10358 (2015).

23. Worthington, A. S. & Burkart, M. D. One-pot chemo-enzymatic synthesis of reporter-modified proteins. *Org. Biomol. Chem.* **4,** 44 (2006).

24. Williamson, J. M. *et al.* Biosynthesis of the beta-lactam antibiotic, thienamycin, by Streptomyces cattleya. *J. Biol. Chem.* **260,** 4637–47 (1985).

25. Houck, D. R., Kobayashi, K., Williamson, J. M. & Floss, H. G. Stereochemistry of

methylation in thienamycin biosynthesis: example of a methyl transfer from methionine with retention of configuration. *J. Am. Chem. Soc.* **108,** 5365–5366 (1986).

26. Lu, W., Roongsawang, N. & Mahmud, T. Biosynthetic Studies and Genetic Engineering of Pactamycin Analogs with Improved Selectivity toward Malarial Parasites. *Chem. Biol.* **18,** 425–431 (2011).

27. Watanabe, K. *et al. Escherichia coli* Allows Efficient Modular Incorporation of Newly Isolated Quinomycin Biosynthetic Enzyme into Echinomycin Biosynthetic Pathway for Rational Design and Synthesis of Potent Antibiotic Unnatural Natural Product. *J. Am. Chem. Soc.* **131,** 9347–9353 (2009).

28. Freeman, M. F. *et al.* Metagenome Mining Reveals Polytheonamides as Posttranslationally Modified Ribosomal Peptides. *Science.* **338,** 387-390 (2012).

29. Rodriguez, M. *et al.* Mutational Analysis of the Thienamycin Biosynthetic Gene Cluster from Streptomyces cattleya. *Antimicrob. Agents Chemother.* **55,** 1638–1649 (2011).

30. Li, R., Lloyd, E. P., Moshos, K. A. & Townsend, C. A. Identification and characterization of the carbapenem MM 4550 and its gene cluster in streptomyces argenteolus ATCC 11009. *ChemBioChem* **15,** 320–331 (2014).

31. Grove, T. L., Radle, M. I., Krebs, C. & Booker, S. J. Cfr and RlmN Contain a Single [4Fe-4S] Cluster, which Directs Two Distinct Reactivities for *S* -Adenosylmethionine: Methyl Transfer by S $_N$ 2 Displacement and Radical Generation. *J. Am. Chem. Soc.* **133,** 19586–19589 (2011).

32. Lanz, N. D. *et al.* in *Methods in enzymology* **516,** 125–152 (2012).

33. Bandarian, V. & Matthews, R. G. in *Methods in enzymology* **380,** 152–169 (2004).

34. Bradford, M. M. A rapid and sensitive method for the quantitation of microgram quantities of protein utilizing the principle of protein-dye binding. *Anal. Biochem.* **72,** 248–254 (1976).

35. Van De Bogart, M. & Beinert, H. Micro methods for the quantitative determination of iron and copper in biological material. *Anal. Biochem.* **20,** 325–334 (1967).

36. Kennedy, M. C. *et al.* Evidence for the formation of a linear [3Fe-4S] cluster in partially unfolded aconitase. *J. Biol. Chem.* **259,** 14463–71 (1984).

37. Moshos, K. A. Design and Synthesis of Substrates and Standards Used to Elucidate Activities of Enzymes in Carbapenem Gene Clusters. (Johns Hopkins University, 2011).

38. Bateson, J. H., Quinn, A. M., Smale, T. C. & Southgate, R. Olivanic acid analogues. Part 2. Total synthesis of some C(6)-substituted 7-oxo-1 -azabicyclo[3.2.0] hept-2-ene-2-carboxylates. *J. Chem. Soc. Perkin Trans. 1* 2219 (1985).

39. Ye, B. *et al.* Thiophene-Anthranilamides as Highly Potent and Orally Available Factor Xa Inhibitors [1]. *J. Med. Chem.* **50,** 2967–2980 (2007).

40. Bateson, J. H., Quinn, A. M., Smale, T. C. & Southgate, R. Olivanic acid analogues. Part 2. Total synthesis of some C(6)-substituted 7-oxo-1 - azabicyclo[3.2.0] hept-2-ene-2-carboxylates. *J. Chem. Soc. Perkin Trans. 1* 2219 (1985).

Chapter 5

Inhibitory activity of β-lactam antibiotics against L,D-transpeptidases in *Mycobacteria* and gram negative pathogenic bacteria

Peptidoglycan biosynthesis has been the drug target of choice for the treatment of bacterial infections, and inhibition of the enzymes involved has proved to be an excellent strategy in the development of some of the most potent antibiotics on the pharmaceutical market[1]. The final step in peptidoglycan biosynthesis was thought, until recently, to primarily be catalyzed by D,D-transpeptidases, commonly referred to as penicillin binding proteins (PBPs), catalyze the formation of classical 4→3 linkages between the fourth amino acid (D-ala) of one polypeptide stem and the third (often *meso*-diaminopimelic acid [*m*DAP]) of another[2]. In 2000, Mainardi and coworkers[3] found a novel linkage structure that connected the third amino acid of the first chain (*m*DAP) with *m*DAP thereby generating 3→3 linkages, as shown in Figure 5.1. In 2005, the same group found in *Enterococcus faecium* that these new cross-links were catalyzed by previously unknown enzymes, the L,D-transpeptidases (Ldts), which had no shared sequence homology to PBPs[4]. Ldts were shortly after found in *Mycobacterium tuberculosis*, as nearly two-thirds of peptidyl linkages are accounted for by 3→3 linkages[5,6].

Tuberculosis (TB), caused by the infection of *Mycobacterium tuberculosis*, is responsible for more deaths than any other infectious disease worldwide[7]. Its widespread proliferation, particularly in the third-world, has contributed to the development of drug-resistant TB, which is now a major problem in treatment of the disease. New anti-TB therapeutics are necessary to mitigate the symptoms and clear the disease in a shorter

time frame to alleviate the suffering of patients. Ldts provide a new target for antibacterial activity, and the study of Ldt inhibition may be an approach to solving this widespread problem.

Ldts have been discovered in a myriad of other bacterial pathogens besides *M. tuberculosis*, including Gram-positive and Gram-negative strains in the ESKAPE organisms. The ESKAPE group includes a collection of often drug-resistant bacteria responsible for severe nocosomial infections and includes; ***E****nterococcus faecium*, ***S****taphylococcus aureus*, ***K****lebsiella pneumoniae*, ***A****cinetobacter baumannii*, ***P****seudomonas aeruginosa* and ***E****nterobacter cloacae.* It is hypothesized that Ldts have evolved as possible resistance strategies against conventional transpeptidase inhibitors such as the widely prescribed penicillin and cephalosporin antibiotics, which are ineffective against these enzymes. Joint efforts of the Lamichhane lab at JHMI and the Townsend lab at JHU have been recently focused on the development of new drugs that are effective against organisms that express Ldts.

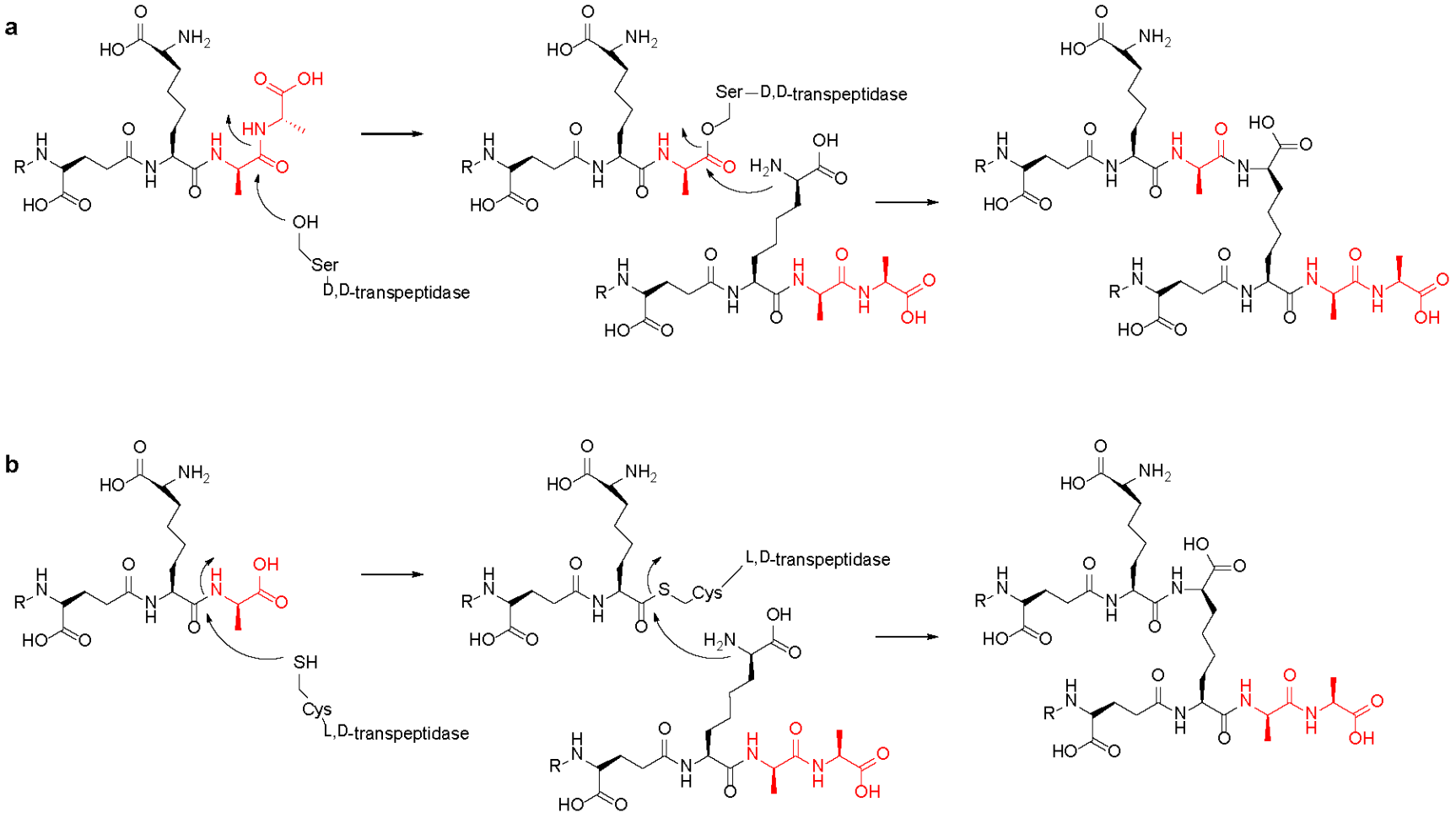

Figure 5.1: Typical 4→3 Crosslinking by D,D-transpeptidases (a) and 3→3 crosslinking by L,D-transpeptidases (b). D-alanine residues are highlighted in red[6].

The work of Gupta *et al.* showed that the loss of Ldt_{Mt2}, the major L,D-transpeptidase in *M. tuberculosis*, alters cell morphology rendering *M. tuberculosis* avirulent and susceptible to otherwise inactive subclasses of β-lactams[6]. This evidence provided the proof of principle that β-lactams in combination with an inhibitor of Ldt_{Mt2} would be lethal to *M. tuberculosis* (Figure 5.2, Table 5.1).

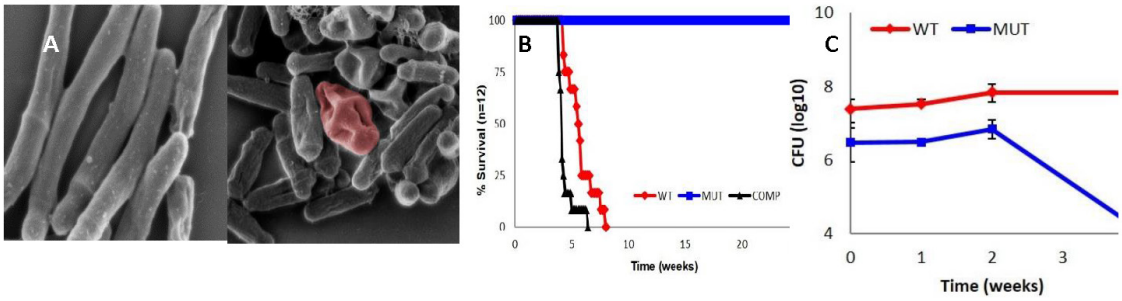

Figure 5.2: (**a**) Scanning electron micrographs of wild-type *M. tuberculosis* (left panel) and a mutant lacking ldt_{Mt2} (right panel). (**b**) Survival of BALB/c mice infected with *WT M. tuberculosis* (WT), ldt_{Mt2}*::Tn* (MUT) and the complemented strain (COMP). (**c**) Burden of *M. tuberculosis* infection (CFU) in the lungs of mice infected with either WT or MUT after four weeks of daily treatment with amoxicillin (200 mg/kg) and clavulanate (50 mg/kg)[6].

In this chapter, experiments for the inhibition of Ldts in *Mycobacteria* and other ESKAPE pathogens are described. My contribution to these studies was the analysis of β-lactam interactions with Ldts using intact protein mass spectrometry for the study of covalent inhibition. Our collaborators in the Lamichhane lab contributed all MIC_{90} data, the crystal structures for inhibitor-bound enzymes, as well as the cloning, expression and purification of Ldts for *in vitro* inhibition assays. In addition to the work summarized here, publications have been accepted and delve into further detail not discussed in this chapter, such as kinetics of inhibition through nitrocefin assay, isothermal calorimetry, data and methods for crystallization of Ldts, and *in vivo* mouse studies[8–10].

MIC_{90} data against *Mycobacteria*

To test the efficacy of drugs against Ldts in particular, our collaborators in the Lamichhane lab, namely Dr. Pankaj Kumar, collected minimum inhibitory concentrations (MICs) against *M. tuberculosis*. In particular, β-lactams were found to be the most successful family of antibiotics against drug-resistant *M. tuberculosis* as evidenced by their MIC_{90} values. Their established mode of action against PBPs makes candidates from this class of drugs likely to also inhibit Ldts, due to mechanistic similarities D,D- and L,D-transpeptidase function. Containing a catalytic cysteine residue, Ldts are susceptible to irreversible electrophilic inhibition by β-lactams whose core heterocycle closely mimics the polypeptide residues that the catalytic cysteine typically acylates, as shown in Figure 5.3. As a proposed double-edged sword, β-lactams already are highly effective against conventional PBPs, so finding effective β-lactam antibiotics against both PBPs and Ldts would be most desirable as inhibition of all transpeptidase activity make a much more efficient anti-infective strategy and eliminate one potential resistance mechanism.

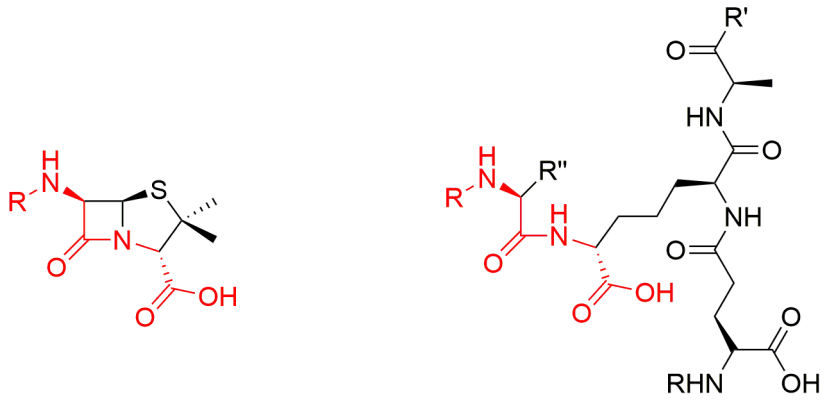

Figure 5.3: β-lactams mimic the natural substrate of cysteine proteases

The Lamichhane lab has collected MICs for 90% growth inhibition (MIC_{90}) for all commonly prescribed β-lactams across the penicillins, cephalosporins and carbapenems. While little activity was observed from penicillins and cephalosporins, carbapenems were found to be effective. A heavy focus was placed on carbapenem antibiotics inspired by Dr. Clifton Barry and coworkers at the National Institute of Allergy and Infectious Diseases (NIAID) who demonstrated that treatment of *M. tuberculosis in vivo* with a regiment of Meropenem and clavulanic acid was successful[11]. Partial results of our collaborators' whole-cell studies are summarized in Table 5.1, and the respective structures of compounds used are shown in Figure 5.4.

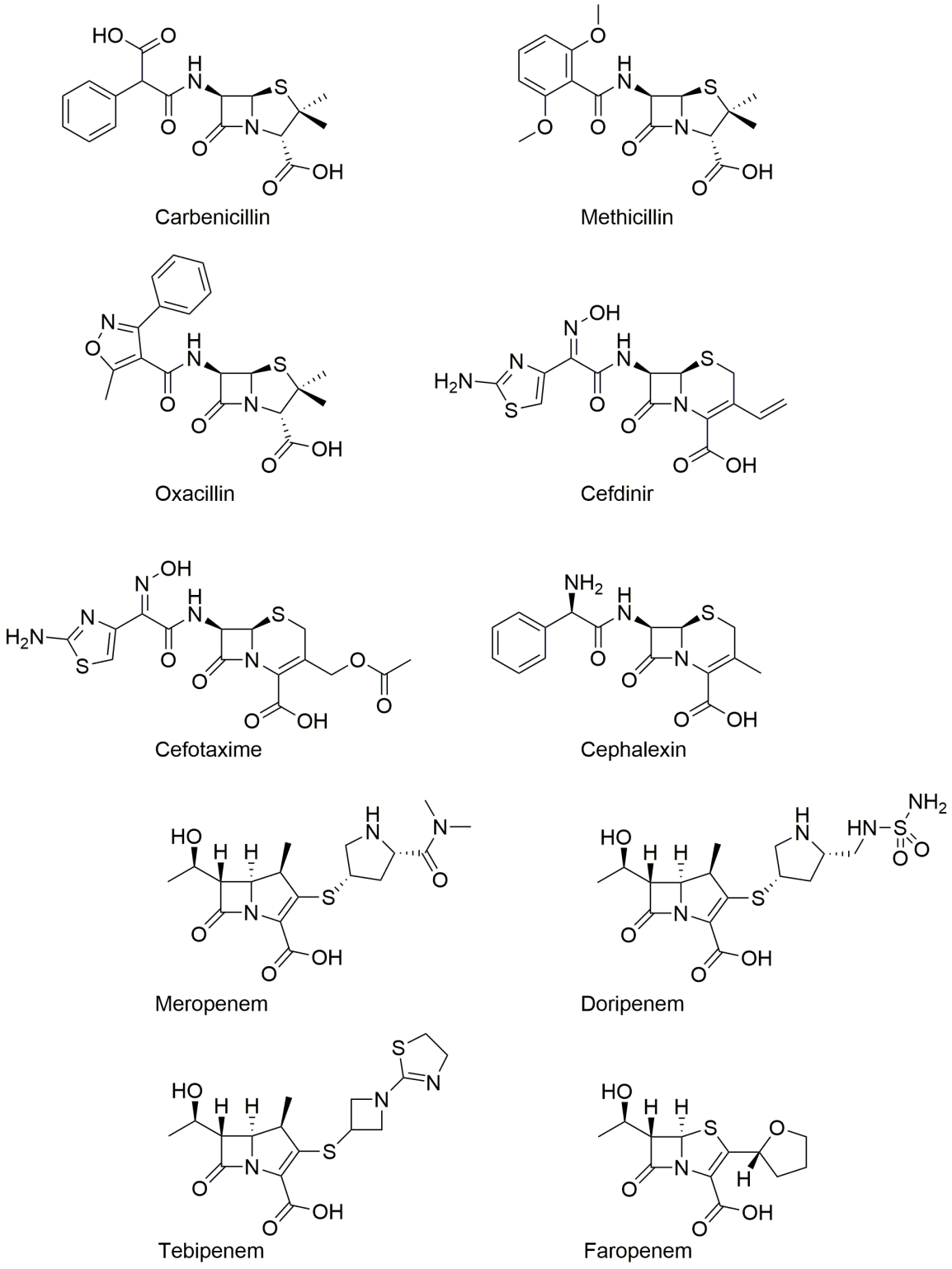

Figure 5.4. Representative β-lactams

Table 5.1. MIC values of various β-lactams against wild-type M. tuberculosis (H37Rv) and Ldt_{Mt2} knock-out strain

Drug	H37Rv	Ldt_{Mt2} knockout	Wild-type: Ldt_{Mt2} knockout
Carbenicillin	>64	2-4	>16
Methicillin	>64	2-4	>16
Oxacillin	>64	1-2	>32
Cefdinir	2-4	0.12-0.25	16
Cefotaxime	2-4	0.12-0.25	16
Cephalexin	4-8	0.12-0.25	32
Meropenem	4-8	0.5-1	8
Doripenem	4-8	0.5-1	8
Faropenem	0.5-1	0.25-0.50	2
Tebipenem	1-2	0.25-0.50	4

Acylation of Ldt_{Mt2} by β-lactams

To better understand the varying activities observed against *M. tuberculosis,* acylation of Ldts through an *in vitro* strategy was carried forward with the incubation of purified Ldts from *E. coli* overexpression against the carbapenems T103-T109. Initial studies from the Lamichhane group using a colorimetric Ninhydrin assay demonstrated that the carbapenems were able to inhibit the activity of Ldts[12]. To determine if inhibition was covalent, samples were prepared for ultraperformance liquid chromatography high-resolution mass-spectrometry (UPLC-HRMS), as it is the only technique sensitive enough to measure the mass difference between acylation adducts and uninhibited protein. A compilation of these data is shown in Table 5.2.

Table 5.2: UPLC-HRMS analysis of adducts formed between L,D-transpeptidases and β-lactams.

Enzyme	Amoxicillin	Cephalothin	Imipenem	Meropenem	Doripenem	Tebipenem	Biapenem	Faropenem	A-C-Z-F	D-B-F-Te
Ldt_{Mt1}	No adduct	No adduct	No adduct	No adduct	+376, +421	+338, +383	No adduct	+86	+86	+86
Ldt_{Mt2}	No adduct	+335	No adduct	No adduct	+123	+339, +384	+139	+86	+86	+86
Ldt_{Mt3}			+102, +150	No adduct	+376, +421	+339, +383	+127	+86		
Ldt_{Mt4}								+86		
Ldt_{Mt5}	No adduct	No adduct	No adduct	No adduct	No adduct	No adduct	No adduct	No adduct		
Ldt_{Mab1}	+366	+337, +335			+376, +421	+339, +384	No adduct	+86	+86	+86
Ldt_{Mab2}	No adduct	No adduct			+68	+383	+139	+86	+86	+86
Ldt_{Mav2}	No adduct	+355			+376, +420	+339	+278	+86		
Ldt_{Kp}	No adduct	No adduct			+376, +421	No adduct	No adduct	+86, +288	+86	+86
Ldt_{Cl}	No adduct	No adduct			+376, +421	+342, +386	+139	+86, +172	+86	+86
Ldt_{Pa}	No adduct	No adduct			No adduct	No adduct	No adduct	+86, +288	+86	
Abbu1	+366	+337, +353	+183	No adduct	+376, +421	+339, +384	+125	+86		
Abbu2	No adduct	No adduct	No adduct	No adduct	No adduct	No adduct	+138			
BlaC	No adduct	No adduct	No adduct	No adduct	No adduct	+338, +385	No adduct			

Molecular weights (Da) of β-lactams: Amoxicillin (A), 365.4; Cephalothin (C); 396.4; Doripenem (D), 420.1; Faropenem (F), 285.3; Aztreonam (Z), 435.4; Biapenem (B), 350.4; Tebipenem (Te), 383.5; A-C-Z-F and D-B-F-Te represent incubation of the enzymes with equimolar mixture of the indicated β-lactams. Abbvreviations for Ldt expressing strains: Mt = *M. tuberculosis*; Mab = *M. abscessus*; Mav = *M. avium*; Kp = *K. pneumoniae*; Cl = *E. cloacae*; Pa = *P. aeruginosa*. BlaC = β-lactamase C from *M. tuberculosis*. Blank cells indicate the experiment was not done.

UPLC-HRMS intact protein analysis revealed that carbapenems, including clinically used antibiotics such as doripenem are effective at forming covalent adducts with most Ldt proteins. Commonly prescribed imipenem and meropenem, however, did not form adducts with most Ldts. In many cases with carbapenems, the intact protein-carbapenem adducts were measured to be a lower molecular weight than predicted. For example, an adduct mass of +376 Da was observed for most doripenem-inhibited Ldts alongside the predicted adduct of +421 (MW doripenem = 421 Da). The difference between the two adducts is 45 Da, which we correlated to the loss of C_2H_4O (acetaldehyde). Mechanistically, retroaldol cleavage of the β-hydroxy-thioester is possible from the adduct thioester bond, as has been shown in the literature[11]. L,D-transpeptidases have a catalytic cysteine active site residue in comparison to D,D-transpeptidases, which use serine. The elimination of acetaldehyde has been observed in the literature for acylation by carbapenems of Ldts, further supporting our observation[11,13].

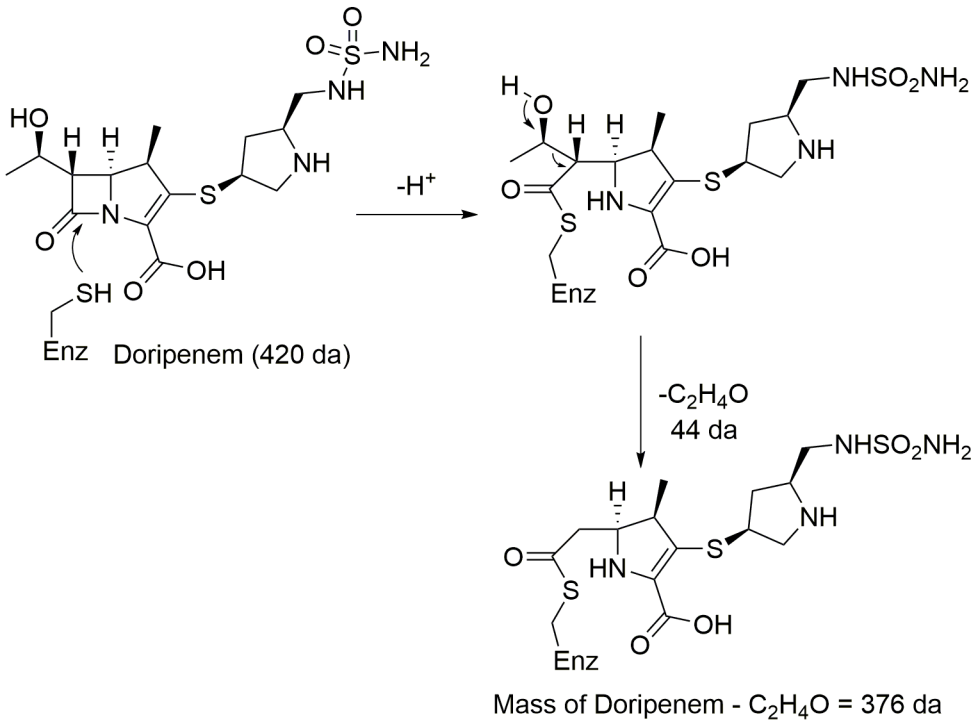

Scheme 5.1: Mechanism of retroaldol cleavage of acetylaldehyde from carbapenem adducts

In some cases, more complicated fragmentations take place post-inhibition. For example, the only doripenem-Ldt_{Mt2} adduct observed affords a mass of 123 Da greater than the native protein. In order to identify the covalently bound fragment, a crystal structure of the substrate-enzyme complex was obtained by Dr. Pankaj Kumar in the Lamichhane lab[9]. Modeling of possible 123 Da candidates for the doripenem fragment into the electron density map revealed that only the pyrrolidine ring from the bicyclic carbapenem core remains (Figure 5.1). To support the acylation structure that was observed by mass and crystallography, a mechanism was proposed in Scheme 5.2 to account for the loss of the C-2 sidechain and necessary saturation of the pyrrolidine ring. Bond angles were measured from the electron density modeling, giving confidence to assign the stereochemistry and 1,2-double bond as shown.

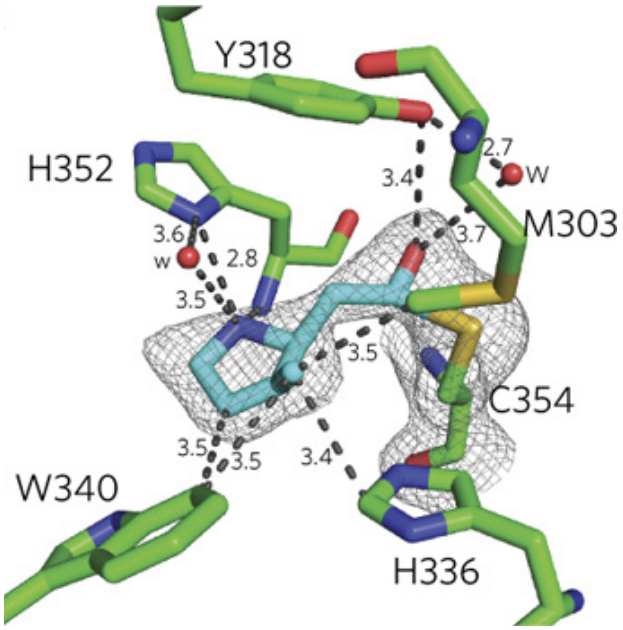

Figure 5.5: Adduct species for Doripenem-Ldt_{Mt2}

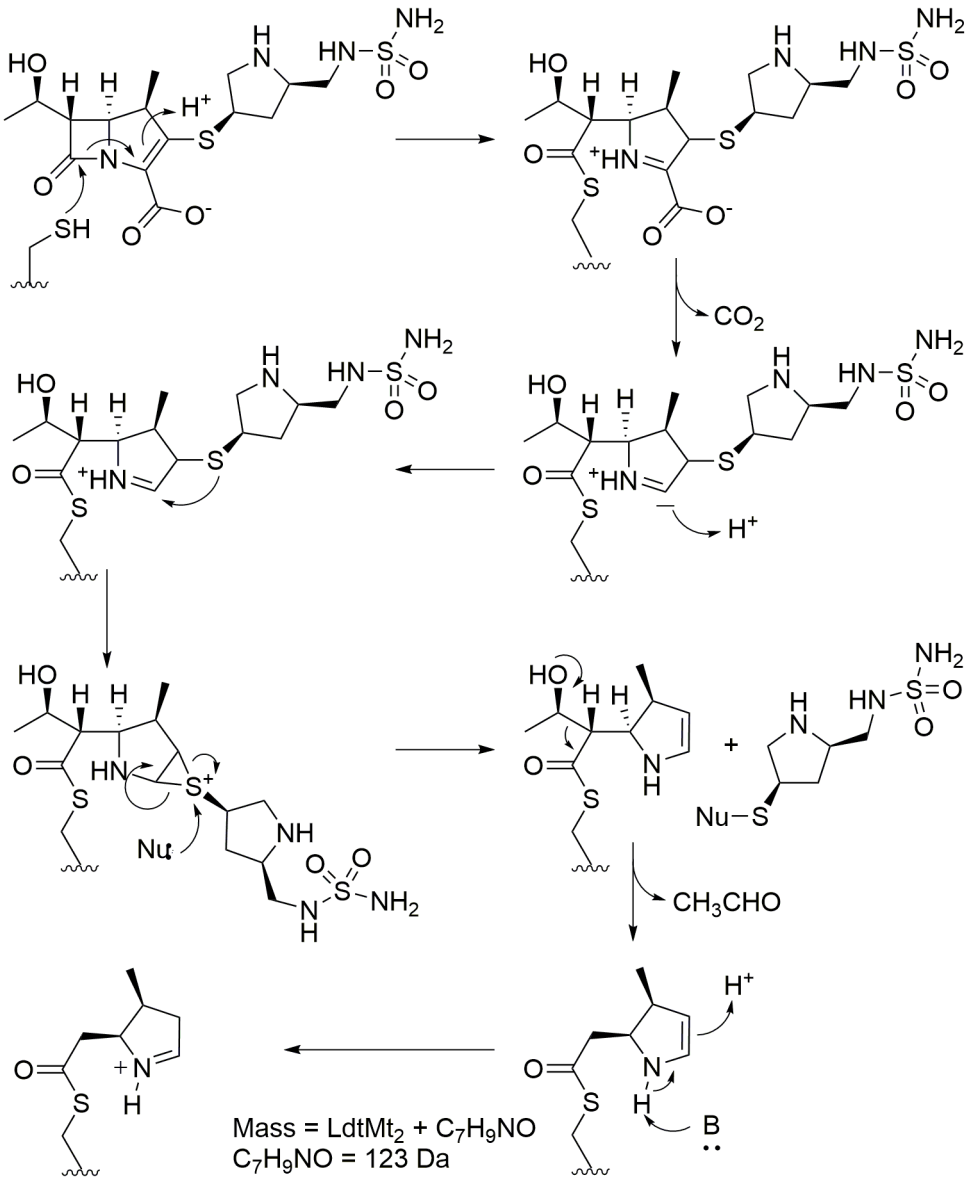

Scheme 5.2: Mechanism of pyrrolidine formation after degradation of the Doripenem-Ldt_{Mt2} adduct

Perhaps the most notable observation of the comprehensive UPLC-HRMS intact protein analyses was the efficiency of faropenem in the acylation of Ldts. A competition experiment involving the incubation of equimolar concentrations of faropenem, amoxicillin, cephalothin and aztreonam with Ldts was conducted. A similar experiment involved faropenem alongside the most potent carbapenems was similarily tested:

doripenem, biapenem and tebipenem. The +86 fragment derived from acylation by faropenem was the only major adduct found in all Ldts from both competition experiments. We proposed the mechanism of faropenem adduct degradation in Scheme 5.3. Initial fragmentation to cleave the thioether C-1/5 bond is parallel to the reaction of clavulanate with β-lactamases[14]. The result of this initial step is the formation of an aminal at the β-position to the thioester, which is susceptible to retro-aldol cleavage as previously described. The final acylation adduct is a (3*R*)-β-hydroxybutyroyl thioester, which matches the calculated mass increase of $C_4H_6O_2$ (86 Da).

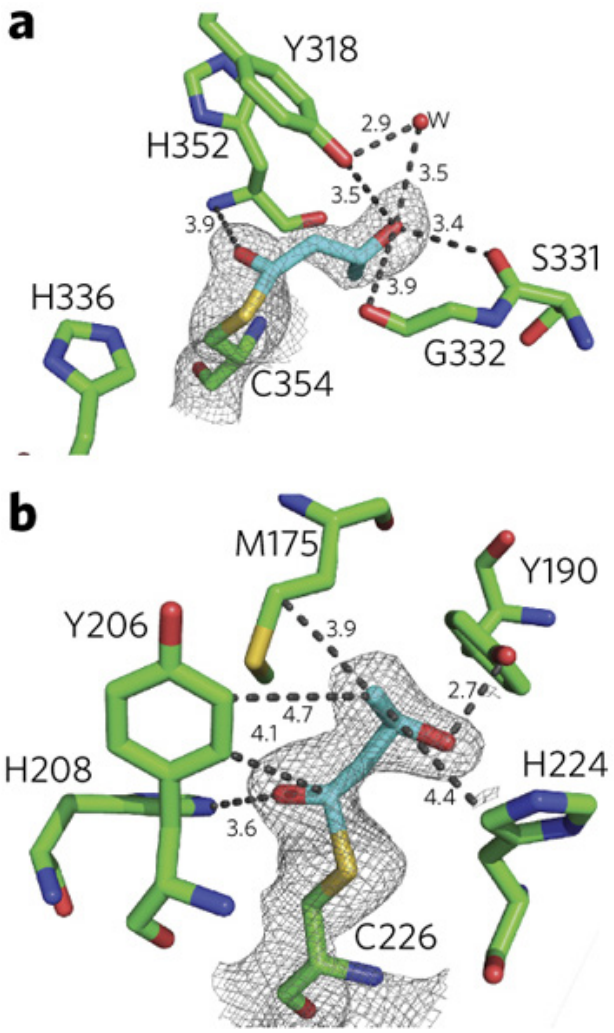

Figure 5.6: Adduct species for Faropenem with Ldt_{Mt1} (a) and Ldt_{Mt2} (b)[9].

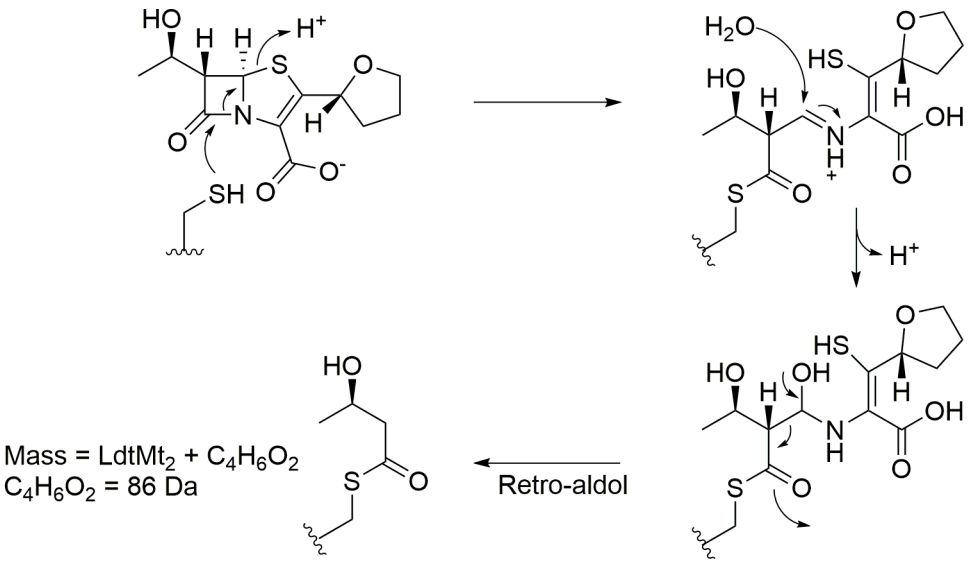

Scheme 5.3: Degradation of faropenem following acylation of Ldts.

Our collaborators next conducted investigations *in vivo*. The Lamichhane lab is equipped to perform extensive testing of antibiotics in a murine tuberculosis model, so the following experimentation was done by Dr. Amit Kaushik and Dr. Gyanu Lamichhane. Drugs with the best MIC values, doripenem, biapenem, tebipenem and faropenem, were injected into separate groups of infected mice twice daily for a course of 28 days. The results showed that a dose of 400 mg/kg biapenem was the most effective course of treatment. In combination with rifampin, biapenem was most effective in the reduction of *M. tuberculosis* cell-forming units (CFU) in murine lung tissue even when compared to the currently most aggressive regimen of isoniazid / rifampin[9].

Disappointingly, faropenem did not perform well *in vivo* when compared to its dominant activity *in vitro*. A few possibilities may explain failure of the drug *in vivo*: the C-2 sidechain of faropenem is small and lipophilic, potentially advantageous for permeating the greasy mycolic acid cell wall, but not polar enough to be as effective *in*

vivo as evidenced by comparison to carbapenems with positively charged C-2 side chains, like tebipenem and biapenem. Additionally, like imipenem, penems have been found to be especially susceptible toward degradation by mammalian renal dehydropeptidase I (RDH-I) therefore greatly reducing the drug's half-life *in vivo*[15,16].

The effectiveness of biapenem and tebipenem against Ldt_{Mt2}

With the Lamichhane lab's excellent *in vivo* results in hand, we further investigated the interactions of biapenem and tebipenem with Ldt_{Mt2} by ESI Mass spectrometry to confirm acylation. Following a five hour incubation of Ldt_{Mt2} with the carbapenems at high molar ratios (1:12.5, enzyme:carbapenem) the mass spectra of the reacted enzymes were analyzed (Table 5.2; Scheme 5.4). Tebipenem showed a Δ*m/z* of 384.5 Da corresponding to the expected mass of an intact tebipenem adduct to Ldt_{Mt2} after accounting for pyrroline tautomerization (Δ*m/z* of 384 Da). A peak corresponding to a Δ*m/z* of 339.5 was also observed (Table 5.2; Scheme 5.4). The 339.5 peak corresponds to a loss of 45 Da when compared to the intact species, matching the previously established loss of the hydroxyethyl group at C-6 and transfer of the proton from His336 to the adduct (Δ*m/z* of 339.5 Da) as explained mechanistically in Scheme 5.4. Surprisingly, when biapenem was incubated with Ldt_{Mt2}, a Δm/z of 139.5 Da was observed as a likely fragmentation product or from further degradation resulting from the ESI-TOF sampling conditions (exposure to trifluoroacetic acid, temperature 60 °C, ionization energy, etc.). Few biapenem degradation paths can be explained mechanistically that correspond to the observed adduct mass; however that this difference is unique from all other carbapenem adducts may speak to the ability of the C-2 sidechain

to act as a possible leaving group. The Ldt_{Mt2}-biapenem crystal structure, like in that of doripenem, provides electron density for a much smaller pyrrolidine adduct, confirming the hypothesis that the C-2 sidechain is no longer attached. A mechanism that is chemically sound could not be devised for biapenem fragmentation that gives a mass of 139.5 Da.

Mutational analysis of Ldt_{Mt2} active site residues

To probe the active site of Ldt_{Mt2} for mechanistic analysis, intact protein analysis was used to study inhibition of Ldt_{Mt2} mutants by carbapenems. The Lamichhane lab generated single amino acid mutations for the active site residues as follows: Y318A, Y318F, H336A, H336R, H336N, H352A, H352R, H352N, C354A and C354S. The active site residues, Tyr^{318}, His^{336}, His^{352} and Cys^{354} are thought, from crystal structure data[17], to be directly involved in the mechanism of transpeptidase activity. Cys^{354} is the active site residue for nucleophilic attack of the D-Ala amide bond, which forms thioesters with β-lactams. For the generation of acylation adducts of these mutants, tebipenem, biapenem and faropenem were studied. The cumulative results are shown in table 5.3. Of Tyr^{318}, His^{336}, His^{352} and Cys^{354}, the only critical residues are the base His^{336} and the nucleophile Cys^{354} as evidenced by no adduct formation with any β-lactam. Interestingly, tebipenem and faropenem were more resilient to mutation of Tyr^{318} and His^{352} than biapenem, which did not form adduct species with anything other than WT enzyme. Due to biapenem's particularity, simple mutations of Ldts could arise as a form of resistance more easily for biapenem than tebipenem or faropenem. Unfortunately,

H336A and H336R mutants did not form adducts analyzable by UPLC-HRMS, due to protein instability.

Table 5.3: Inhibition of Ld_{Mt2} mutants with tebipenem, biapenem, and faropenem

Protein	Tebipenem	Biapenem	Faropenem
WT	+339 +383	+138	+86
Y318A	+339 +383	No adduct	+86
Y318F	+339 +383	No adduct	+85
H336A	No data	No data	No data
H336R	No data	No data	No data
H336N	No adduct	No adduct	No adduct
H352A	+339 +385	No adduct	+86
H352R	No data	No data	+85
H352N	No data	No data	+86
C354A	No adduct	No adduct	No adduct
C354S	No adduct	No adduct	No adduct

Tebipenem is a potential therapeutic against Ldt_{Mav2} in *Mycobacterium avium*.

Additional focus was placed on the treatment of problematic pathogens other than *M. tuberculosis*. One particular focus was on the enzyme Ldt_{Mav2}, the major L,D-transpeptidase in *Mycobacterium avium*. *M. avium* is a more aggressive *mycobacterium* than *M. tuberculosis* and is notoriously difficult to treat with antibiotics, partially due to an even more efficient β-lactamase than BlaC in *M. tuberculosis* as well as high

resistance to most currently prescribed antibiotics. A first-world threat, *M. avium* is an increasing problem for patients that are immunocompromised, such as those with HIV/AIDS. High rates of *M. avium* infection is associated with high mortality rates[18,19].

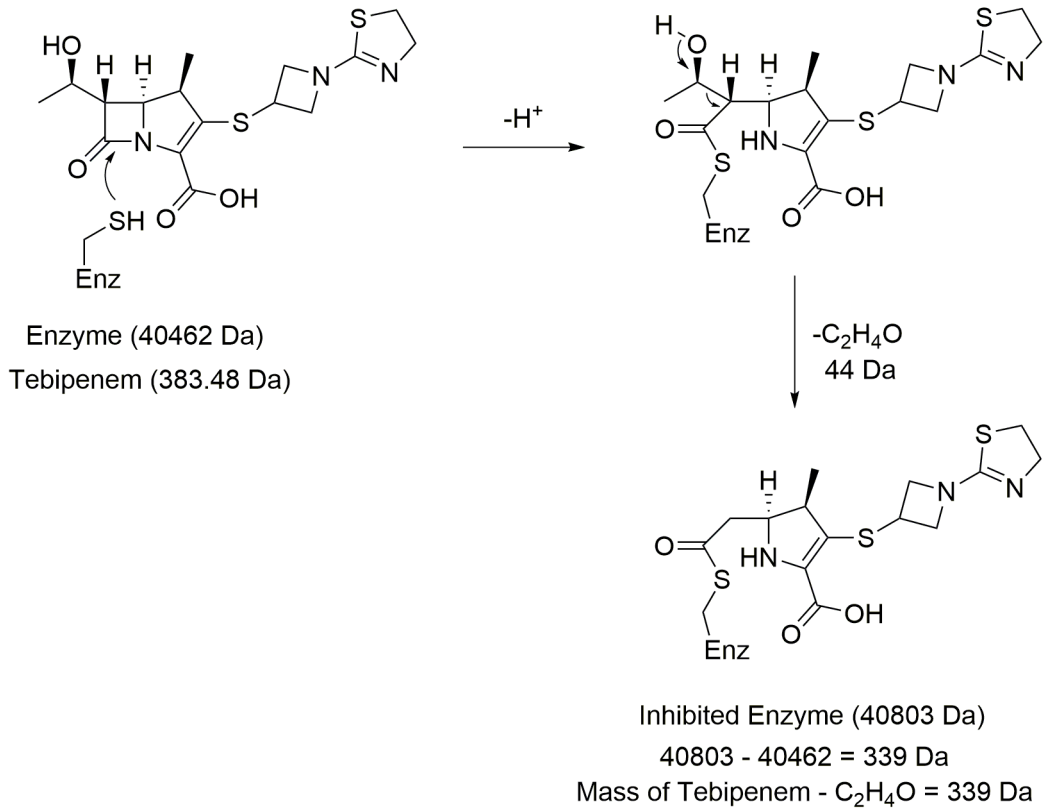

Enzyme (40462 Da)
Tebipenem (383.48 Da)

Inhibited Enzyme (40803 Da)
40803 - 40462 = 339 Da
Mass of Tebipenem - C_2H_4O = 339 Da

Scheme 5.4: Proposed mechanism of acylation of Ldt_{Mav2} by tebipenem

Dr. Rohini Mattoo obtained MIC_{90} values (Table 5.4), and *M. avium* showed resistance to most carbapenems in comparison to *M. tuberculosis*, with the exception of tebipenem, which was the only β-lactam with an MIC_{90} value in the effective therapeutic range, 4-8 μg/mL.

Table 5.4: MIC_{90} for β-lactams against *M. avium* (μg/mL). (+/- 1 Da)

	Drug	MIC_{90} pH 6.8	MIC_{90} pH 7.4
Control	Rifampin	4-8[20]	4-8
	Moxifloxacin	0.5-1	0.5-1
	Clarithromycin	2-4	1-2
β-lactams	Amoxicillin	>64	>64
	Ampicillin	>64	>64
	Cephalothin	>64	>64
	Cefoxitin	>64	>64
	Ertapenem	>64	>64
	Meropenem	>64	>64
	Imipenem	>64	>64
	Doripenem	>64	>64
	Biapenem	>64	>64
	Tebipenem	2-4	4-8
	Panipenem	>64	>64
	Faropenem	>64	>64

We studied the nature of the reaction between Ldt_{Mav2} and different sub-classes of β-lactams through UPLC-HRMS intact protein analysis. Amoxicillin and ampicillin were used as representatives of the penicillin sub-class, cephalothin and cefoxitin as representatives of the cephalosporins, and doripenem, biapenem, and tebipenem as carbapenems. Faropenem was the only penem tested. Dr. Matoo expressed and purified Ldt_{Mav2} and reacted the protein *in vitro* with the aforementioned inhibitors. I performed

intact protein analysis of adducts by UPLC-HRMS. While cephalothin, imipenem, doripenem, biapenem, faropenem and tebipenem formed covalent acyl adducts, we were unable to detect any reacted masses for amoxicillin, ampicillin, cefoxitin and meropenem (Table 5.2).

Incubation of Ldt_{Mav2} with tebipenem (MW=383.5 Da) produced a covalently bound acyl adduct of +339 Da (Table 5.2), in agreement with adducts formed with Ld_{Mt2} and other Ldts. Based on these data, we propose the mechanism for tebipenem adduct formation with Ldt_{Mav2} in Scheme 5.4. The sulfur atom of the putative catalytic cysteine (Cys349) attacks the carbonyl carbon of the β-lactam ring (Figure 5.4). Next, as in meropenem and tebipenem reactions with Ldt_{Mt2}[9], the hydroxyethyl group at C6 is lost resulting in an adduct of +339 Da. These data support the applicability of tebipenem as a potential treatment option against *M. avium*

Conclusion

The evidence for Ldt inhibition as a correlation to increased MIC_{90} is substantiated by these extensive crystallographic and mass spectrometric data. However, limitations are met *in vivo*, as evidenced by testing of our lead carbapenem, biapenem, with faropenem in the treatment of a mouse model of tuberculosis infection[9]. The data summarized in Table 5.3 suggests that faropenem is the most dominant drug in the inhibition of Ldts; however, does not perform well *in vivo*. We hypothesize that the C-2 sidechain and resulting RDH-1 susceptibility is the source of inefficacy *in vivo.* It is theorized that the optimally reactive penem structure against Ldts could be optimized for

in vivo administration if structural features from clinically successful antibiotics are incorporated.

Experimental

General methods for mass spectrometry analyses:

Ldt (2 μM) in 12.5 mM Tris buffer, pH 8 was incubated in the presence or absence of 50 μM antibiotic for 5 h at room temperature. Reactions were quenched by the addition of trifluoroacetic acid (TFA; final concentration, 0.1%). Samples were filtered through a 0.2-μm filter and analyzed by ultraperformance LC/MS at 60 °C. Ultraperformance liquid chromatography (LC)-high resolution MS samples were analyzed on a Waters Acquity H-Class ultraperformance LC system equipped with a multiwavelength ultraviolet-visible diode array detector in conjunction with a Waters Acquity BEH-300 ultraperformance LC column packed with a C_4 stationary phase (2.1 × 50 mm; 1.7 μm) in tandem with high resolution MS analysis by a Waters Xevo-G2 quadrupole-TOF electrospray ionization mass spectrometer.

The mobile phase was as follows: 0–1 min, isocratic 90% water + 10% ACN + 0.1% formic acid; 1–7.5 min, gradient to 20% water + 80% ACN + 0.1% formic acid; 7.5–8.4 min, isocratic 20% water + 80% ACN + 0.1% formic acid; 8.4–8.5 min, gradient to 90% water + 10% ACN + 0.1% formic acid; 8.5–10 min, isocratic 90% water + 10% ACN + 0.1% formic acid. The flow rate was 0.3 ml min^{-1}.

Intact protein analysis was performed using the following calculations for MaxEnt1 deconvolution: Resolution = 10000.0; Lock spray lock mass (Da) = 556.2771; MS mass

tolerance = 30 ppm; Time window in UPLC-chromatogram for protein analysis = 5.00-5.50 min; TIC threshold (Da) = 2000; Deconvolution *m/z* range (Da) = 800-2000; Protein MW range (Da) = [protein mass] ± 5 kd. Masses for inhibited proteins were obtained and adduct weights were calculated from subtraction of the uninhibited protein mass.

Bacterial strains, growth media and drugs:

The following bacterial strains were used in this study: *M. tuberculosis* H37Rv, *M. abscessus* (ATCC 19977), *M. avium* (strain 104; Clinical Microbiology; Johns Hopkins University), *A. baumannii* (strain 6M-1b; Clinical Microbiology, Johns Hopkins University), *K. pneumoniae* (ATCC 35657), *E. cloacae* (ATCC 13047), *P. aeruginosa* (PA14), *E. faecalis* (ATCC 19433) and methicillin-sensitive *S. aureus* (ATCC 29213). *M. tuberculosis* and *M. abscessus* were grown and assessed as previously described[21]. Cation-adjusted Mueller–Hinton broth was used to grow *A. baumannii*, *K. pneumoniae*, *E. cloacae*, *P. aeruginosa*, *E. faecalis* and *S. aureus* at 37 °C according to Clinical and Laboratory Standard Institute guidelines[22]. Rifampin, isoniazid and all β-lactams were obtained from commercial vendors. Compounds were 95–99% pure when random samples were analyzed using LC–MS.

Minimum Inhibitory Concentration and Checkerboard Titration Assay (done by Rohini Mattoo and Pankaj Kumar):

Minimum inhibitory concentration (MIC_{90}) of drugs against *M. tuberculosis, M. abcessus, and M. avium* was determined using the standard broth microdilution assay[23] using 96-well plates separately at pH 6.8 (Middlebrook 7H9 broth in the presence of 10%

OADC) and pH 7.4 (cation-adjusted Mueller-Hinton broth) in accord with the Clinical and Laboratory Standard Institute (CLSI) guidelines[22] as described[21]. MIC_{90} is expressed as a range between two concentrations, where higher concentration represents the lowest concentration at which bacterial growth could not be observed following incubation at 37 °C for seven days. Standard Checkerboard Titration assay[24] was used to assess combined activity of agents. Briefly, each well containing 105 CFU received two drugs each in two fold dilutions below their respective MIC_{90}. The suspensions were incubated at 37 °C and growth was evaluated as described above. Fractional Inhibitory Concentration (FIC) of a drug was calculated as described[24].

Cloning, overexpression, and purification of Ldts (done by Pankaj Kumar and Gyanu Lamichhane): L,D- and D,D-transpeptidases were cloned (excluding the *N*-terminal transmembrane anchoring domains), expressed and purified to enhance chances of obtaining *apo* and co-crystal structures with drugs. Desired gene fragments were cloned into the multiple cloning site in pET28a+ to afford a *N*-terminal His6-tagged protein cleavable by Tobacco Etch Virus (TEV)[12]. Single amino acid substitutions of Ldt_{Mt2} (fragment ΔN55) were constructed by site-directed mutagenesis as follows. Primers were designed so that mutations resulting in amino acid substitution were placed at the center of the oligo[9]. For each mutagenesis, two separate PCR reactions, each with forward or reverse primer, using New England BioLabs (NEB) high-fidelity buffer was used to amplify the pET28a+ vector carrying wild-type sequence for Ldt_{Mt2} (fragment ΔN55). DNA from the two reactions was combined, denatured at 95 °C, slowly renatured to 37 °C and digested with *Dpn*I as described. *Escherichia coli* DH5α(C2987H, NEB

labs) was used for cloning and manipulation of plasmids. *E. coli* BL21δε3 (C2527H, NEB labs) was used to overproduce proteins as described[8].

Cloning, overexpression, and purification of Ld_{Mav2} (done by Rohini Mattoo): Analysis for a potential membrane anchoring domain predicted a high likelihood of residues 13-32 as a transmembrane anchor domain[25]. Therefore, the *N*-terminal 24 residues were excluded to avoid the likely transmembrane anchor that could hinder solubilization and purification of the protein. Primers ATTGCCATATGGTGGGGGCAGTCGCCTGCGGCG and CAATACTCGAGTCAGGTGTTGGCGTTGCCCGC and Phusion polymerase (New England Biolabs) were used to amplify the region encoding residues 25-403 of Ldt_{Mav2}. The PCR product was cloned into pET28a+TEV to generate an *N*-terminal H6 tagged Ldt_{Mav2}. This expression plasmid, p1501RM, was sequenced to verify that the cloned DNA was identical in sequence to wild-type *ldtMav2*. *E. coli* BL21DE3 was used to overexpress Ldt_{Mav2} following induction with 500 µM IPTG for 22 hrs, 16 °C. Cells were harvested by centrifugation at 3,500 x g for 10 mins, 4 °C, lysed by sonication in a buffer containing 25 mM Tris-HCl (pH 8), 400 mM NaCl, 1 mM TCEP and protease inhibitor cocktail and centrifuged at 29,000 x g for 30 mins. The supernatant was interacted with Ni-NTA agarose on a column (BioRad) and washed with three column volumes 331 of 25 mM Tris-HCl (pH 332 8), 400 mM NaCl, 1 mM TCEP and 10 mM imidazole. Bound protein was eluted with 500 mM imidazole in the same lysis buffer and dialyzed at 4 °C in freshly prepared TEV protease against buffer containing 25 mM Tris-HCl (pH 8), 150 mM NaCl, 0.1 mM TCEP, 1 mM PMSF and 10% glycerol to enable cleavage of the N-

terminal H6 tag. The dialysis buffer was exchanged at least four times at 4 °C to ensure complete removal of imidazole. The cleaved protein was separated from TEV protease and any uncleaved protein by repeating Ni-NTA chromatography. The purity and homogeniety of the tagless Ldt_{Mav2} was assesed by 4-15% SDS PAGE. Vivaspin 20 columns were used to concentrate Ldt_{Mav2} to 10-20 mg/mL, flash frozen in liquid nitrogen and stored at -80 °C. The oligomeric status and homogeneity of the protein were analyzed by size exclusion chromatography using a Superose 12/300 GL column in the presence of dialysis buffer containing 25 mM Tris-HCl (pH 8), NaCl 150 mM, TCEP 0.1 mM, 1 mM PMSF and 10% glycerol on an AKTA FPLC (GE-Healthcare).

Evaluation of Carbapenems in mice (Done by Amit Kaushik and Gyanu Lamichhane): Female BALB/c mice, 4–5 weeks old (Charles River Labs), were used according to the protocol approved by the Johns Hopkins University Animal Care & Use Committee (MO15M25). An acute model of *M. tuberculosis* infection in mice to assess the activities of faropenem and biapenem was used. Using *M. tuberculosis* culture at exponential phase of growth, a suspension was prepared with an optical density (A_{600nm}) of 0.2 and infected mice by aerosolizing 10 ml of this suspension in a Glas-Col chamber. This high-dose infection resulted in implantation of 3.7 $\log_{10}$CFU in the lungs of each mouse. Treatment was initiated two days after infection, a time when *M. tuberculosis* bacilli are rapidly proliferating. While isoniazid (10 mg/kg) and rifampicin (10 mg/kg) were administered by oral gavage once daily (7 d per week), biapenem (200 mg/kg) and faropenem (200 mg/kg) were administered twice daily by subcutaneous injection. Five mice were sacrificed 1 d after infection, lungs homogenized and plated on

Middlebrook 7H11 selective medium to determine the actual infection burden. Next, five mice were sacrificed on the day of treatment initiation and at three weeks following initiation of treatment, the final time point, to determine bacterial burden in the lungs. Gross pathology of lungs and mouse body weights were recorded at each time point.

References

1. Papp-Wallace, K. M., Endimiani, A., Taracila, M. A. & Bonomo, R. A. Carbapenems: Past, Present, and Future. *Antimicrob. Agents Chemother.* **55,** 4943–4960 (2011).
2. Testero, S. A., Fisher, J. F. & Mobashery, S. in *Burger's Medicinal Chemistry and Drug Discovery* (John Wiley & Sons, Inc., 2010).
3. Mainardi, J. L. *et al.* Novel mechanism of beta-lactam resistance due to bypass of DD-transpeptidation in Enterococcus faecium. *J. Biol. Chem.* **275,** 16490–6 (2000).
4. Mainardi, J. L. *et al.* A novel peptidoglycan cross-linking enzyme for a β-lactam-resistant transpeptidation pathway. *J. Biol. Chem.* **280,** 38146–38152 (2005).
5. Lavollay, M. *et al.* The peptidoglycan of stationary-phase Mycobacterium tuberculosis predominantly contains cross-links generated by L,D-transpeptidation. *J. Bacteriol.* **190,** 4360–6 (2008).
6. Gupta, R. *et al.* The Mycobacterium tuberculosis protein LdtMt2 is a nonclassical transpeptidase required for virulence and resistance to amoxicillin. *Nat. Med.* **16,** 466–9 (2010).
7. WHO | Global tuberculosis report. *World Heal. Organ.* (2016).
8. Basta, L. A. B. *et al.* Loss of a functionally and structurally distinct LD-transpeptidase, LdtMt5, compromises cell wall integrity in mycobacterium tuberculosis. *J. Biol. Chem.* **290,** 25670–25685 (2015).
9. Kumar, P. *et al.* Non-classical transpeptidases yield insight into new antibacterials. *Nat. Chem. Biol.* **13,** 1–11 (2016).
10. Mattoo, R. *et al.* LdtMav2, a non-classical transpeptidase and susceptibility of Mycobacterium avium to carbapenems. *Futur. Microbiol* in press (2017).
11. Hugonnet, J.-E., Tremblay, L. W., Boshoff, H. I., Barry, C. E. & Blanchard, J. S. Meropenem-clavulanate is effective against extensively drug-resistant Mycobacterium tuberculosis. *Science..* **323,** 1215–1218 (2009).
12. Erdemli, S. B. *et al.* Targeting the Cell Wall of Mycobacterium tuberculosis:

Structure and Mechanism of L,D-Transpeptidase 2. *Struct. Des.* **20,** 1–13 (2012).

13. Drawz, S. M. *et al.* Inhibition of the Class C β-Lactamase from *Acinetobacter* spp.: Insights into Effective Inhibitor Design. *Biochemistry* **49,** 329–340 (2010).

14. Charnas, R. L., Fisher, J. & Knowles, J. R. Chemical studies on the inactivation of Escherichia coli RTEM β-lactamase by clavulanic acid. *Biochemistry* **17,** 2185–2189 (1978).

15. Volkmann, R. A. & O'Neill, B. T. in *Strategies and Tactics in Organic Synthesis* (ed. Lindberg, T.) **3,** 495–531 (Academic Press, Inc, 1991).

16. Mori, M., Hikida, M., Nishihara, T., Nasu, T. & Mitsuhashi, S. Comparative stability of carbapenem and penem antibiotics to human recombinant dehydropeptidase-I. *J. Antimicrob. Chemother.* **37,** 1034–6 (1996).

17. Li, W.-J. *et al.* Crystal structure of L,D-transpeptidase LdtMt2 in complex with meropenem reveals the mechanism of carbapenem against Mycobacterium tuberculosis. *Cell Res.* **23,** 728–31 (2013).

18. Kobayashi, T. *et al.* High Mortality of Disseminated Non-Tuberculous Mycobacterial Infection in HIV-Infected Patients in the Antiretroviral Therapy Era. *PLoS One* **11,** e0151682 (2016).

19. Raju, R. M., Raju, S. M., Zhao, Y. & Rubin, E. J. Leveraging Advances in Tuberculosis Diagnosis and Treatment to Address Nontuberculous Mycobacterial Disease. *Emerg. Infect. Dis.* **22,** 365–9 (2016).

20. Li, G. *et al.* Antimicrobial Susceptibility of Standard Strains of Nontuberculous Mycobacteria by Microplate Alamar Blue Assay. *PLoS One* **8,** e84065 (2013).

21. Kaushik, A. *et al.* Carbapenems and Rifampin Exhibit Synergy against Mycobacterium tuberculosis and Mycobacterium abscessus. *Antimicrob. Agents Chemother.* **59,** 6561–6567 (2015).

22. Desmond, E. *Susceptibility Testing of Mycobacteria, Nocardiae and Other Aerobic 565 Actinomycetes. Clinical Laboratory Standard Institute M24-A2.* (2011).

23. Gavan, T. L. & Town, M. A. A microdilution method for antibiotic susceptibility testing: an evaluation. *Am. J. Clin. Pathol.* **53,** 880–5 (1970).

24. Hsieh, M. H., Yu, C. M., Yu, V. L. & Chow, J. W. Synergy assessed by checkerboard. A critical analysis. *Diagn. Microbiol. Infect. Dis.* **16,** 343–9

25. Krogh, A., Larsson, B., von Heijne, G. & Sonnhammer, E. L. . Predicting transmembrane protein topology with a hidden markov model: application to complete genomes. Edited by F. Cohen. *J. Mol. Biol.* **305,** 567–580 (2001).

Chapter 6

Evolution of New Penems against *M. tuberculosis* and ESKAPE Pathogens

R.B. Woodward hypothesized that the increased β-lactam reactivity of cephalosporins combined with the potent inhibitory structure of penicillins could provide novel, highly reactive β-lactam antibiotics. The cephalosporin double bond in conjugation with the β-lactam amide was thought to be the source of increased acylation reactivity. Woodward's antibiotic, the penem, combined the structural features of the fused 5-membered ring of penicillin with the internal double bond in cephalosporin[1–4]. His group set out on the synthesis of 6-acylaminopenem-3-carboxylic acids and was successful in obtaining and characterizing these new molecules (Figure 6.1). Unfortunately, the antibacterial activity of these initial penems was disappointing. The concurrent discovery of carbapenems by Merck Sharp and Dohme, which had excellent broad spectrum bactericidal activity, drew pharmaceutical focus away from the 6-aminopenems. Researchers Dr. Michael S. Kellogg, Dr. Ernest S. Hamanaka, Dr. Robert L. Rosati and others at Pfizer, however, refined Woodward's penem using the newly discovered structural features of carbapenems to enhance potency. As a result of a tremendous effort utilizing the newest chemical methods, the penem group at Pfizer developed lead compounds that had potent broad-spectrum antibacterial activity, culminating in the advancement of CP-70,429, later named sulopenem, to clinical trials[5,6]. The project was abandoned at Pfizer at an advanced stage in the mid-1990s, possibly the result of lowered fiscal projections as competition by Merck's blockbuster carbapenem antibiotic, imipenem, would limit sales. Pfizer sold the rights of sulopenem

to Iterum Therapeutics, Ltd. in 2015, which plans to initiate phase 3 clinical trials by the end of 2017[7].

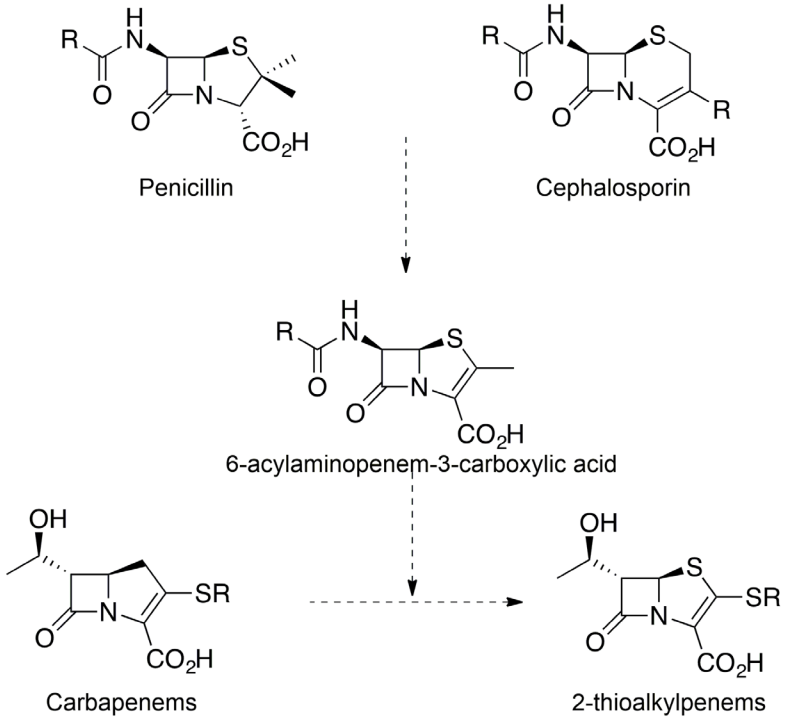

Figure 6.1: Evolution of 2-thioalkylpenems

With the passage of 20 years and the appearance of carbapenem-resistant organisms, another look at penems is warranted. Bacterial resistance to common orally-available drugs, such as penicillin and cephalosporin is increasingly more prevalent, and the desirability of both carbapenem availability and the development of new carbapenems is at an all-time high. However, the use of carbapenems requires intravenous administration, due to the high susceptibility of the carbapenem core to hydrolysis by stomach acid. Penems are more hydrolytically stable than carbapenems, and drugs such as these that would have the bactericidal potency of the carbapenems while retaining the possibility of oral administration would be extremely valuable.

The success of faropenem against L,D-transpeptidases *in vitro*[8] has led to attempts to develop new penems that could be effective therapeutics against tuberculosis and members of the ESKAPE pathogens. We began our push for new compounds by a thorough examination of penems in the literature. The work of Volkmann *et al.*[9] outlined the synthesis of sulopenem after early optimization of the C-2 thioether sidechain for resistance to the human enzyme renal dehydropeptidase 1 (DHP-1) responsible for degradation and removal of penems, like carbapenems, from the blood. As penems had been found by Pfizer to be often rendered ineffective *in vivo* due to their short half-lives in the presence of DHP-1, this structure was a breakthrough[10]. In our hands, we noticed a similar disadvantage in trials of faropenem as an antibiotic for the treatment of *M. tuberculosis* in a mouse model, and proposed that we could use C-2 sidechains that have proven to increase the resistance to degradation by DHP-1 in carbapenems. In the two decades since the sulopenem project at Pfizer was scrapped, development of new carbapenems have left us with promising structural modification to base the development of new penems. We decided that incorporation of the carbapenem substituent features that have been enhanced actively over 40 years of pharmaceutical research could generate better penem structures for the treatment of *Mycobacterial* infection *in vivo*. Testing penems with different carbapenem C-2 sidechains was our first goal in producing compounds for whole-cell *M. tuberculosis* grown-inhibition assays.

Synthesis of C-2 thioalkylpenems

Syntheses of penems had been achieved in the past from either simple starting materials or from penicillin[11–17]; however, we decided to take advantage of a synthesis

that incorporated the carbapenem commercial intermediate (3*S*,4*S*)-4-acetoxy-3-[(*S*)-1-(tert-butyldimethylsilyloxy)ethyl]-azetidin-2-one **1**, as a far lower cost of both starting material and time was expected with three contiguous stereocenters of the penem azetidinone core already in place. We hoped to develop a late stage intermediate with a leaving group at C-2 so that any C-2 thioalkyl nucleophile could be inserted, like Merck had developed in the synthesis of imipenem from a 2-oxo-carbapenam[18]. From the commercially-available azetidinone, the *N*-acyliminum species was reacted with triphenylmethylsulfide, as shown in the early penem literature[13,19] to produce the trityl-protected thioether **2** after recrystallization from methanol in 84% yield. Alkylation of the β-lactam nitrogen with allyl 2-bromoacetate occurred easily after deprotonation with potassium hydroxide in the presence of dicyclohexyl-18-c-6 to provide **3** in 90% yield. Deprotection of the trityl group occurred readily with silver (I) nitrate, a Lewis acid that has a high affinity to sulfur[13]. The resulting silver thiolate salt **4** was quenched with sodium sulfide, extracted into the organic phase with dichloromethane, and the crude concentrate was immediately reacted with *p*-nitrobenzoyl chloride to make the PNB-thioester **5** in 57% yield over two steps from **3**. The system was now primed for 5-*exo*-trig[20] cyclization of the α-carbon of the carboxymethyl amide to the thioester carbonyl by deprotonation with LiHMDS at -78 °C to provide intermediate **6**. Activation of the 2-oxopenem **6** by triflic anhydride produced reactive vinyl triflate, which formed the first 2-thioalkyl penem analogue after reaction with ethanethiol in the presence of an organic base[18]. Unlike the shelf-stable 2-oxocarbapenem intermediate in the synthesis of carbapenems, it was quickly found that the 2-oxopenem **6** was highly unstable and purification by chromatography or attempts at crystallization destroyed the compound.

The following transformation would only proceed with freshly distilled triflic anhydride on the crude 2-oxopenem, and the reaction proceeded in very poor yield (<20%). This unforeseen disaster occurred on precious material at the end of the synthesis, so as much product as possible was salvaged through reaction of the entire lot of **6** to ethanethiol derivative **7**. It was possible to resue our synthetic strategy, however. DiNinno and coworkers demonstrated that the displacement of thioalkyl sulfoxides was an optimal as a strategy for penem derivatization[21]. Selective oxidation of the 2-thioethyl chain of **8** was possible, albeit in low yield with *m*-CPBA to produce **9**. Sulfoxide **9** was converted reliably to penem allyl esters **10**-**14** before degradation of the sulfoxide could occur. Through these method four initial compounds were made using the sidechains from the synthesis of the carbapenems tebipenem, meropenem, and doripenem in addition to the ethanethiol derivative. Deprotection of the allyl ester with palladium followed by purification by HPLC provided penems **15**, **16**, **20**, and **21** in milligram quantities.

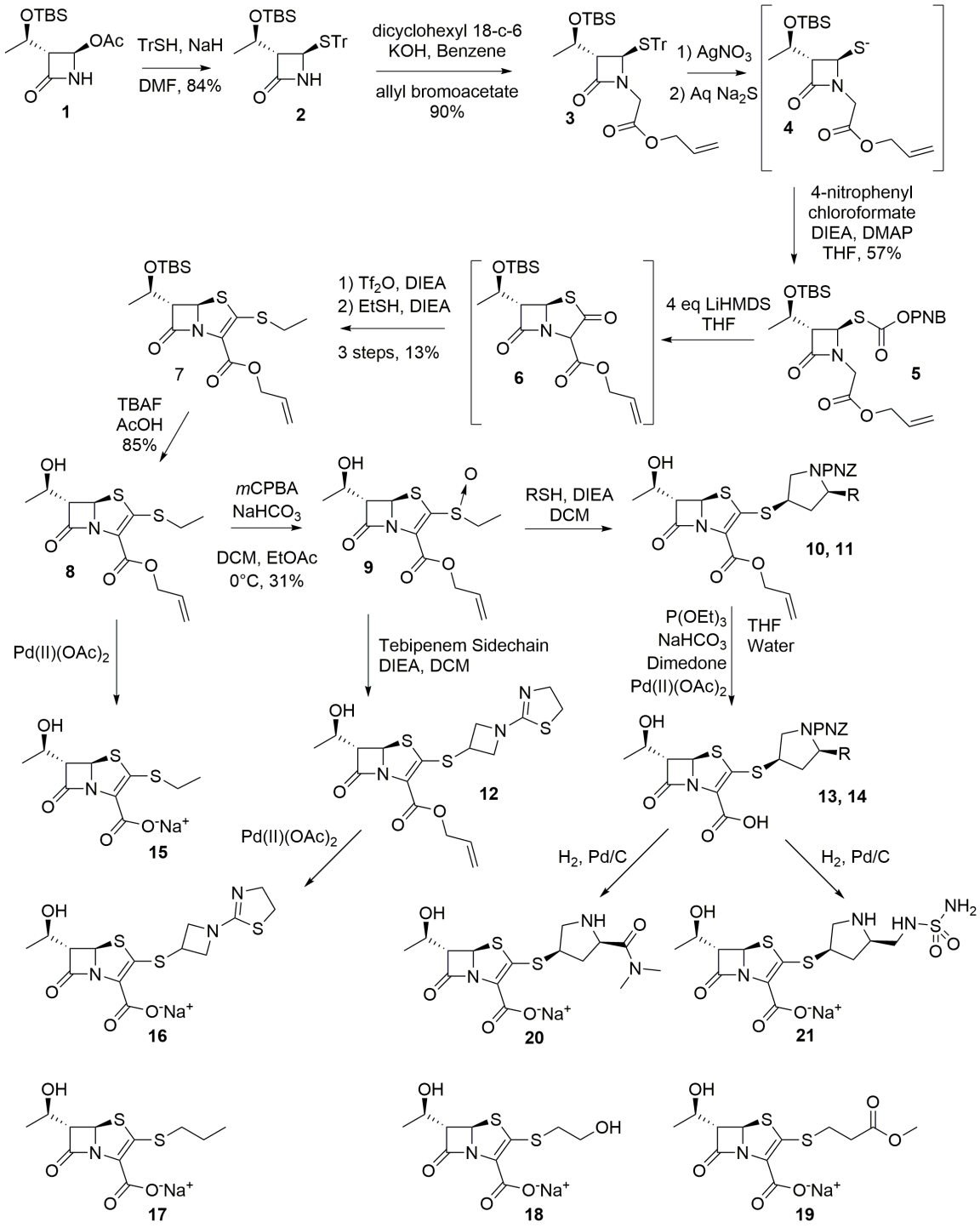

Scheme 6.1: Our first route to penems, following chemistry developed by Pfizer

Newly synthesized penems exhibit high potency against *M. tuberculosis*

MIC_{90} values were promising, as both **15** and **16** exhibited growth inhibition in the low micromolar range against wild-type *Mycobacterium tuberculosis* (Table 6.1). To validate our hypothesis that the 2-thioalkyl-penems form covalent adducts with Ldts, mass spectrometric analyses of covalent adducts were repeated as described previously with Ldts from *M. tuberculosis*, *M. absessus*, and ESKAPE pathogens (Table 6.2, Table 6.3). In addition, the adducts of **15** and **16** with Ldt_{Mt2} were crystallized by our collaborators with the Lamichhane Lab, namely Dr. Pankaj Kumar, and their respective diffraction data obtained at the Argonne National Laboratory in Illinois (Figure 6.3). nitrocefin-competition assay analyses of Ldt_{Mt2} *in vitro* showed greater inhibitory of **15** and **16** activity in comparison to penicillins, cephalosporins, and carbapenems (Figure 6.2).

Table 6.1: Spectrum of activity of the lead penem (**15**) series: (a) high potency (MIC in sub µg/mL range), (b) high potency and selectivity of **16** against *Mtb*.

A	MIC_{90} (µg/mL) vs. *Mtb* H37Rv
15	16-32
16	0.5-1
17	0.5-1
18	2-4
19	0.5-1
21	0.5-1
20	8-16

B	MIC_{90} (µg/mL)	
Pathogen	**16**	**Meropenem**
Mtb H37Rv	0.5	4.0
Rif-resistant *Mtb* 1	0.5	4.0
Rif-resistant *Mtb* 2	0.5	4.0
M. abscessus	1	128
A. baumannii	>64	16
E. faecalis	16	16
P. aeruginosa	4	0.25
K. pneumoniae	1	0.03

Table 6.2: A summary of antimicrobial MIC_{90} data for penems in the **15** series. *M.tb.* = *M. tuberculosis*, *M.ab.* = *Mycobacterium abscessus*, *E.cl.* = *Enterobacter cloacae*, *K.pn.* = *Klebsiella pneumoniae*, *A.ba.* = *Acinetobacter baumannii*, *P.ae.* = *Pesudomonas aeruginosa*, MRSA = Methicillin Resistant *Stapholococcus aureus*, MSSA = Methicillin Susceptible *Stapholococcus aureus*.

Drug	Antimicrobial Activities (µg/mL)							
	M. tb	*M.ab.*	MRSA	MSSA	*K. pn.*	*E. cl.*	*P. ae.*	*A. ba.*
15	16-32		0.5-1	0.5-1	1-2	16-32		
16	0.5-1	0.5-1	0.03-0.06	0.03-0.06	0.125-0.25	0.25-0.5	4-8	4-8
17	0.5-1				0.25-0.5	4-8		4-8
18	2-4				8-16			
19	0.5-1				8-16	4-8		16-32
21	0.5-1							
20	8-16				2-4	1-2	0.5-1	0.5-1

Table 6.3: Structures of synthetic penem antibiotics

	Chemical Structure & Description
15	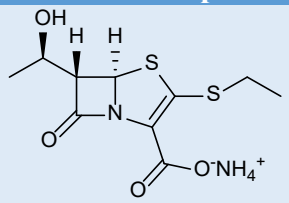
16	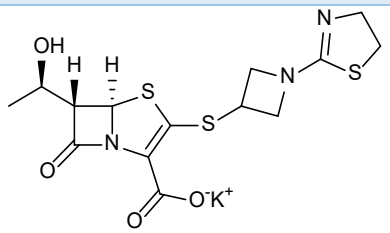
17	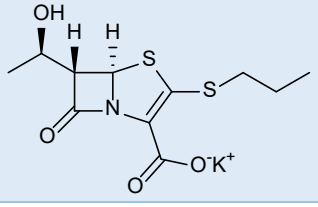

18	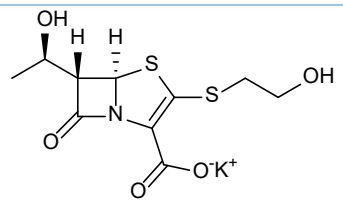
19	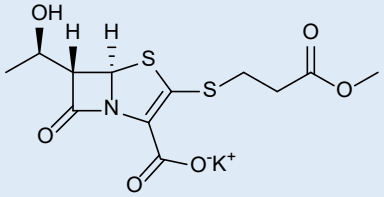
21	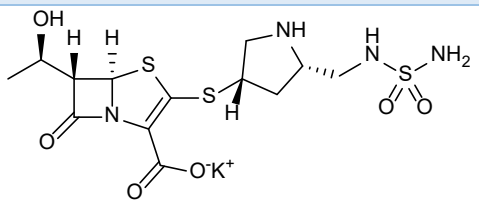
20	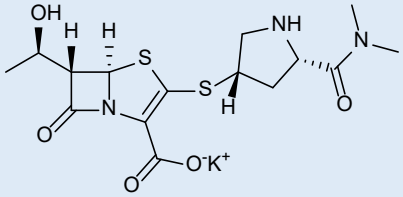

Although several new and evolved carbapenems have been recently assayed for their *in vitro* potencies against *M. tuberculosis* and other bacterial pathogens, our most successful program for *M. tuberculosis* has been the penems (**15-21**) as their potencies for this pathogen (Table 6.1, Table 6.2) have been superior to the carbapenems[8]. The carbapenem class exhibits broad-spectrum activity (potent against gram negatives and positives) while exhibiting lower potencies for *M. tuberculosis* than the penems (Table 6.1, Table 6.2).

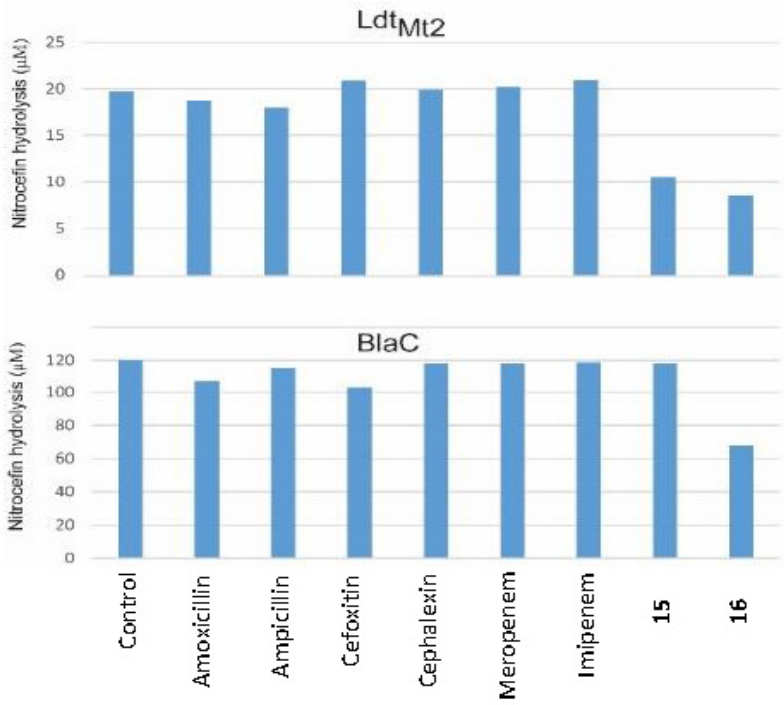

Figure 6.2: Nitrocefin hydrolysis by Ldt_{Mt2} and BlaC in the presence of various β-lactams and penems **15** and **16**, each at 200 μM.

16 **inhibits activity of Ld_{Mt2} and β-lactamase BlaC**

In addition to their inability to inhibit L,D-transpeptidases, the (otherwise potent broad-spectrum β-lactams) penicillins and cephalosporins lack clinically useful activity against *M. tuberculosis* due to their rapid hydrolysis by a strong β-lactamase, BlaC, of *M. tuberculosis*. Overcoming BlaC is important to any new agent with a β-lactam ring. Unlike penicillins and cephalosporins, carbapenems are only slowly hydrolyzed, enabling greater potency against *M. tuberculosis*[22]. In addition to resistance against BlaC hydrolysis, **16** is an effective inhibitor of BlaC activity, as evidenced by slowed hydrolysis of nitrocefin in a competition assay (Figure 6.2). **15** and **16** also inhibit Ldt_{Mt2} by covalently forming an acyl adduct (Figure 6.4, Table 6.4). We hypothesize that **16's**

more potent activity against BlaC than carbapenems contributes to its potent whole-cell activity against *M. tuberculosis*.

Penems form covalent adducts with Ldt_{Mt2} and inhibits activity

In 2012, the first crystal structure of Ldt_{Mt2} was reported[23]. Dr. Kumar obtained co-crystal structures with the new penems **15** and **16** (Figure 6.3) using established methods[8].

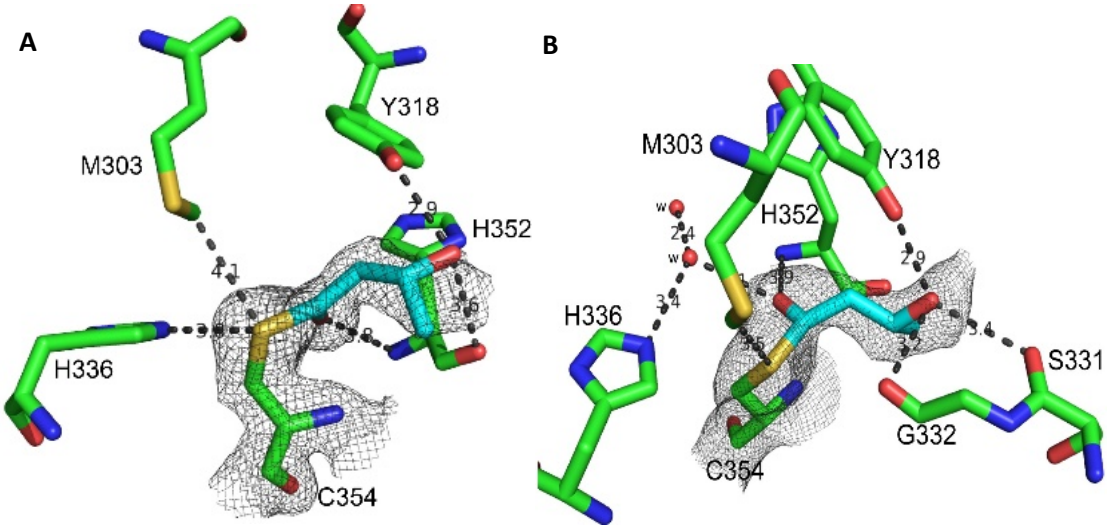

Figure 6.3: Crystal structures with Ldt_{Mt2} incubated with (a) **15**, and (b) **16** bound to Ldt_{Mt2}.

Unlike that of carbapenems, the reaction of **16** with *Mtb* L,D-transpeptidases Ldt_{Mt2} and Ldt_{Mt1}, proposed in Figure 6.4, is rapid and yields the inactivated enzymes bearing only (3*R*)-hydroxybutyryl covalently linked to the active site cysteine, Cys354 in Ldt_{Mt2} (Figure 6.3) (Cys226 in Ldt_{Mt1}). Nucleophilic attack by this cysteine on the reactive β-lactam is proposed to open the 4-membered ring followed by scission of the remaining thiazoline ring. Such a cleavage process is known for the analogous masked enol opening of clavulanate by seryl β-lactamases[24]. The resulting imine/iminium

species, again paralleling clavulanate cleavage, is proposed to hydrate to an aminal, whose facile retro-aldol scission affords the observed inactivated enzyme adduct. To determine whether carbapenems or our penems were more reactive with Ldt_{Mt2} and Ldt_{Mt1}, we incubated these enzymes with equimolar mixtures of doripenem, biapenem, tebipenem and **16** and assessed the identities and abundance of acyl-enzyme adducts (created when the β-lactam ring reacts with the active site cysteine) using ultra performance liquid chromatography-mass spectrometry (UPLC-MS) (Table 6.4). Although each carbapenem and **16** produced a unique adduct when reacted individually with the L,D-transpeptidases, acylation by **16** was the only adduct (+86 Da) detected in the competition assays, indicating that the Ldt_{Mt1} and Ldt_{Mt2} enzymes preferentially bound **16** over the other tested carbapenems, some of which (e.g., doripenem, biapenem and tebipenem) exhibit superior potency against *Mtb* compared to meropenem[22].

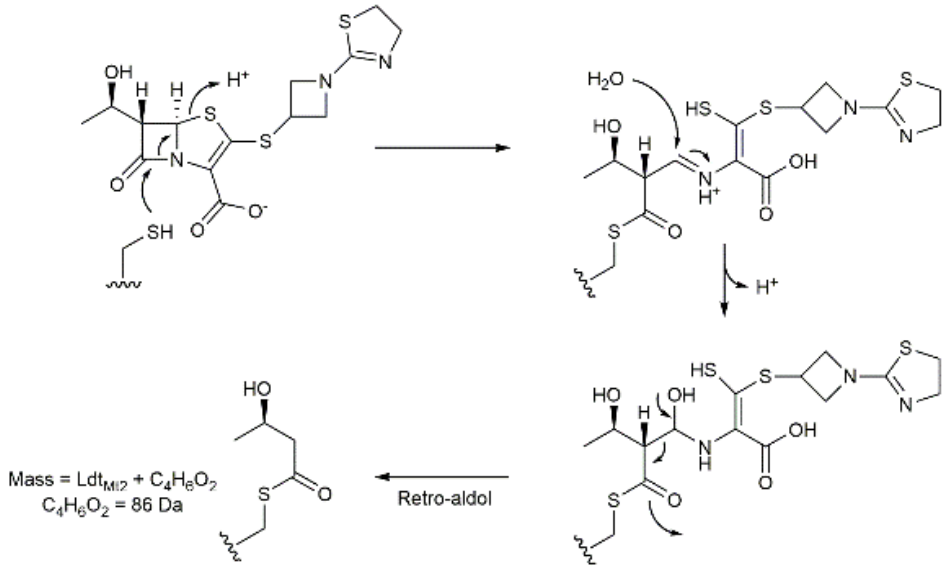

Figure 6.4: Proposed mechanism of acylation of Ldt_{Mt2} and Ldt_{Mt1} by [13,19].

Table 6.4: UPLC-HRMS Derived Mass data for Ldt/Penem adducts. Relative abundance denoted in brackets

Protein	Drug	Mass Difference (da)
Ldt_{Mt2}	**15**	+87
Ldt_{Mt2}	**16**	+86
Ldt_{Mab2}	**15**	+86
Ldt_{Mab2}	**16**	+86
Ldt_{Cl}	**15**	+86 +275
Ldt_{Cl}	**16**	+344 +387.5
Ldt_{Kp}	**15**	+86
Ldt_{Kp}	**16**	+342.5 +387.5

Strategies for a gram scale process to 16

Testing antibiotic efficacy in an *in vivo* tuberculosis model would require multiple grams of **16**, our lead compound. To produce a large amount of material, a different synthetic approach was needed due to the unacceptable ring closure and sulfoxidation yields outlined above. Pfizer's original process to sulopenem was first examined[9].

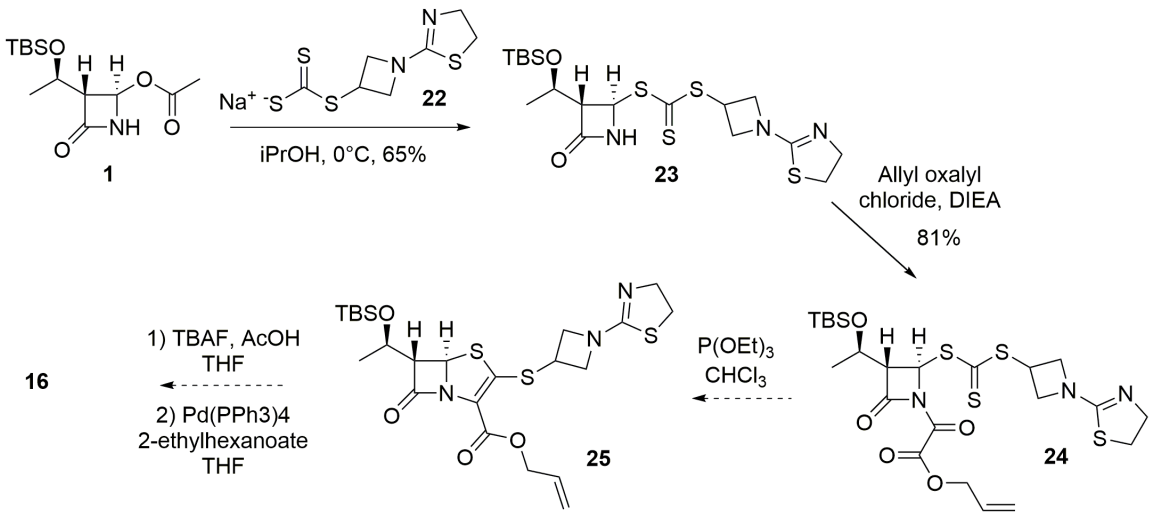

Scheme 6.2: Proposed synthesis of **16** using early incorporation of the tebipenem sidechain as the trithiocarbonate

Previously, sulfoxidation of the C-2 thiol **8** followed by conjugate addition / elimination proved successful, although it was inefficient as *m*-CPBA was a poor oxidizing agent in terms of regioselectivity. To avoid unacceptable yields on scale-up, the Pfizer synthesis of sulopenem served as a model to add the C-2 side chain as the first step, and ultimately yield the product in a much more efficient four steps from commecial starting materials. Generation of the trithiocarbonate **22** proceeded smoothly when using freshly generated sodium alkoxide from sodium metal in refluxing alcohol. The use of methanol or ethanol as the solvent in the subsequent reaction with the commercial 4-acetoxyazetidinone intermediate **1** yielded good conversion to product initially, however, upon workup and concentration yields plummeted. Especially on gram scales, reactions in methanol or ethanol caused significant degradation of the desired product. Elimination of the trithiocarbonate **22** by competing addition / elimination from the solvent alcohol was favored entropically through the release of carbon disulfide and the thiol sidechain. Examination of the work of Volkmann *et al.*[9] gave insight into the degradation, and the use of a sterically hindered solvent, such as isopropanol, significantly remedied the

problem. The use of isopropanol resulted in a good yield for reactions of less than 5 g of azetidinone **23**. On scale up to 20 g, however, the degradation problem was exacerbated as removal of such vast quantities of isopropanol required longer times and higher temperatures for vacuum distillation. The problem was solved when slow precipitation of the trithiocarbonate was allowed during low temperature removal of isopropanol solvent under high vacuum (<5 Torr). The addition of hexanes when approximately half the isopropanol remained facilitated precipitation, and ultimately led to a yield of 65% for **23** on a sufficient scale for multigram synthesis of **16**.

It was expected that the remaining highly precedented chemistry would proceed without issue, but another unforeseen roadblock was encountered as initial reaction with allyl oxalyl chloride failed. Despite resounding success across penem literature in the reaction of the azetidinone nitrogen with oxalyl chlorides, we found that elimination of the trithiocarbonate **22** occurred readily in the presence of organic bases such as triethylamine at 0 °C. Further examination of reaction products found that allyl oxalyl chloride had a preference to react with the thiourea group of the trithiocarbonate sidechain rather than the azetidinone nitrogen. We hypothesized that making a formal anion at the azetidinone nitrogen at low temperature in the presence of an electrophile would make that most acidic position the most nucleophilic, hence changing the preference of reaction. In a dry ice / acetone bath the addition of one equivalent allyl oxalyl chloride to **23** was followed by one equivalent LiHMDS in dichloromethane. Analysis of the crude reaction mixture by infrared spectroscopy revealed that our hypothesis was correct and the proper oxalamide **24** was formed, but only when the temperature was allowed to rise to -40 °C (data not shown). A control reaction was run

with diisopropylethylamine instead of LiHMDS and was found to produce the same result in higher yield at -40 °C. Our hypothesis was incorrect, as formal deprotonation of the β-lactam was not necessary. Conversely, reaction preferences were controlled by temperature. On scale up, the reaction proceeded without further issue to provide the oxalamide **24** in 81% yield. To our dismay, these efforts were for naught as all attempts at cyclization of the penem with triethylphosphite failed to produce the product penem **25**. It seemed that the first mechanistic step, addition of the triethylphosphate with the oxalamide carbonyl, was successful, however, the cyclization step did not proceed as expected. Degradation and polymerization products prevailed, although difficulty in separation of the myriad of product oils couldn't provide sufficient purity for characterization of any major product. At this point it was decided that the current route wouldn't produce a clear path forward, so attention was focused on other methods.

Our approach was an inefficient synthesis when compared to the original Pfizer route to sulopenem. Therefore an alternate route to sulopenem was tested as a basis for a different strategy. The new synthesis, published in 2011, focuses on the generation of an *n*-alkyltrithiocarbonate intermediate **28** in effort to favor conditions that avoid environmentally unfriendly solvents, achieve a lower cost of purification through precipitation and enable crystallization of intermediates resulting in higher yields[25]. Ultimately, improved yield alone made up for the increased number of synthetic steps. The keystone reaction that made this process successful was the development of a high-yielding sulfoxidation reaction of **30** that employs hydrogen peroxide urea complex as the oxidant in the presence of an expensive but recoverable solvent, 1,1,1,3,3,3-hexafluoroisopropanol (HFIP). The theory behind selective 2-thioalkylsulfoxidation is

that the 1-sulfur is protected by fluorine bonds with HFIP. Modifications to the process generated **16** successfully and on scale (Scheme 6.3).

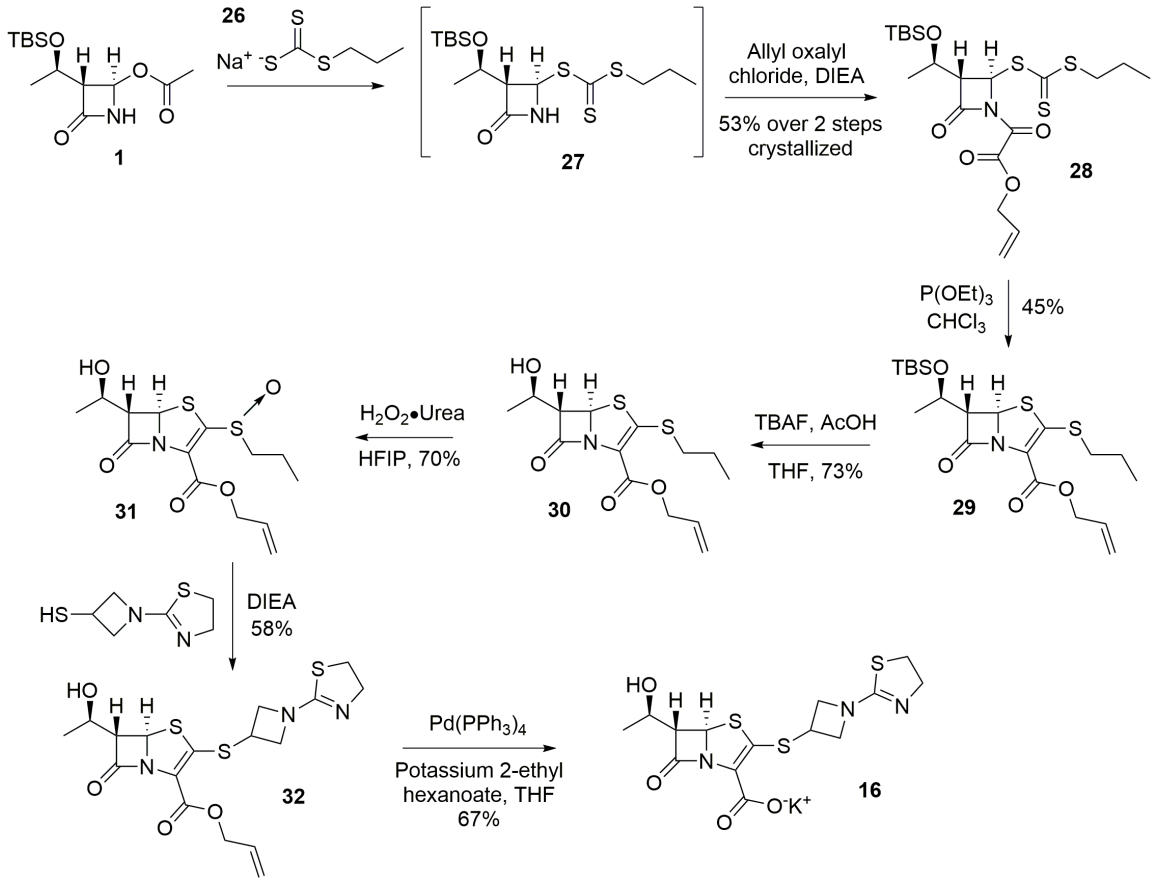

Scheme 6.3: Successful gram scale process to **16**

On a scale of 50g (3*S*,4*S*)-4-acetoxy-3-[(*S*)-1-(tert-butyldimethylsilyloxy)ethyl]-azetidin-2-one **1,** *n*-propyltrithiocarbonate **26** addition to **1** followed by reaction of resulting trithiocarbonate **27** with allyl oxalyl chloride provided the desired oxalamide **28** in 53% yield. Attempts at crystallization or chromatographic purification of the free amide **27** only gave opportunity for degradation. Immediate formation of the oxalamide **28** protected the compound from elimination of trithiocarbonate **26** at 0 °C in tert-butyl methyl ether (TBME). The best yield of cyclization was obtained from the slow addition of two equivalents triethylphosphite in refluxing alcohol-free chloroform to provide the

protected penem **29** as white crystals (isooctane) in 45% yield. At this point, TBS deprotection was favored as it was feared the thiourea functionality of the C-2 sidechain would be incompatible with either fluoride or acidic hydrolysis used for TBS protection. Another motive was that the high cost of purchased tebipenem side chain could be mitigated by adding it as late as possible in the sequence. Reasonable yields of 73% and 70% were achieved through TBAF deprotection and hydrogen peroxide / urea sulfoxidation to produce **30** and **31** respectively. **32** was produced in 58% yield from addition of tebipenem sidechain and subsequent elimination of *n*-propylsulfoxide from crystalline **31** (isooctane). At this point, the allyl ester of **32** was removed by catalytic palladium allyl transfer. It was found that anhydrous palladium transesterification to organic soluble potassium 2-ethylhexanoate in the presence of catalytic tetrakis(triphenylphosphane)palladium afforded **16** in 67% yield. This method was preferred to other procedures in the literature, such as those that use palladium acetate and sodium benzenesulfinate, due to the fortuitous spontaneous crystallization of our desired product from anhydrous tetrahydrofuran. The crystals obtained from the reaction mixture were spectroscopically pure if fresh, dry and anaerobically stored Pd(0)-tetrakis(PPh_3)$_4$ is used, however we were concerned by the presence of trace palladium byproducts visible as a deep red / brown color when **16** precipitate was dissolved in ddH_2O. Palladium is a hazard for any material to be administered to animals, so our concern was justified.

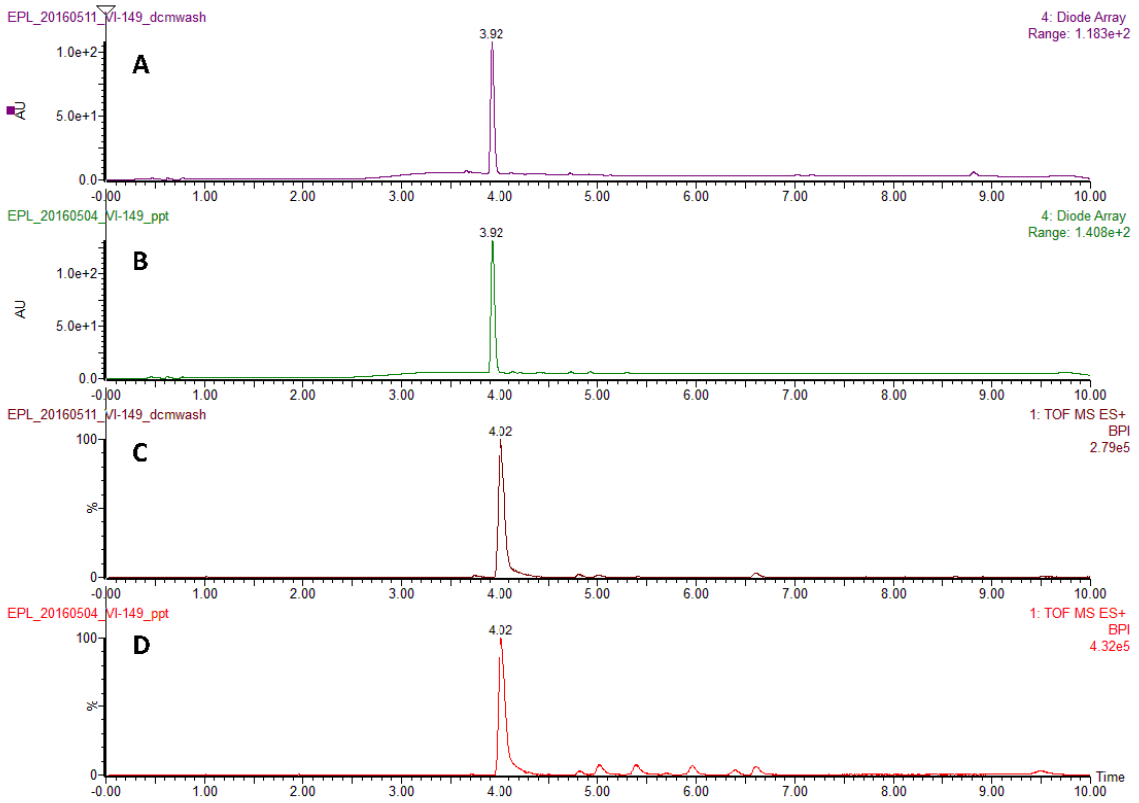

Figure 6.5: Comparison of **16** after (a: UV chromatogram, c: Total Ion Chromatogram) and before (b: UV chromatogram, d: Total Ion Chromatogram) organic extraction of phosphine-containing contaminants.

The palladium problem became a focused effort to remove the impurity as compound of pharmaceutical quality was needed. Initially, organic extracts of all contaminants were hoped to provide sufficient purification. UPLC-HRMS analysis confirmed that dichloromethane extraction removed the majority of contaminants as shown in Figure 6.5 however, injection under the skin of mice resulted in the formation of lesions and hair loss after multiple treatments: evidence that contamination still remained. At the suggestion of Dr. James Barrow at the Lieber Instutute for Brain Development (LIBD), purification of **16** from palladium impurity was made possible by the use of macroporous QuadraPure® thiourea resin that is specifically designed to bind palladium and other heavy metals. An aqueous sample of crude **16** that was incubated

with QuadraPure® thiourea resin for 2 h at RT and then purified by reverse-phase HPLC was injected under the skin in an acute toxicity study performed by Dr. Amit Kaushik in the Lamichhane lab. After 6 injections over 72 h, no skin irritation was observed.

For large scale purification, HPLC was necessary to ensure that no palladium contaminants remained. Through the help of Michael Poslusney in the lab of Dr. James Barrow, methodology to purify gram quantities of **16** was developed. In the presence of trifluoroacetic acid, the interaction between the colored palladium impurity and **16** was broken, and gradient elution of the colorless, pure compound was possible from C18 using a 5%-50% gradient of acetonitrile in water with 0.5% TFA.

Synthesis and activity of 5,6-*cis*-faropenem

Through *in vitro* analysis against Ld_{Mt2}, we wanted to discern if any value could be added from altering the C-6 stereochemistry of penem antibiotics. The compound 5,6-*cis*-faropenem **39** was synthesized using the established methods of Ishiguro and coworkers coupled with a key C-5 epimerization developed by the same group using UV radiation for epimerization[26–28].

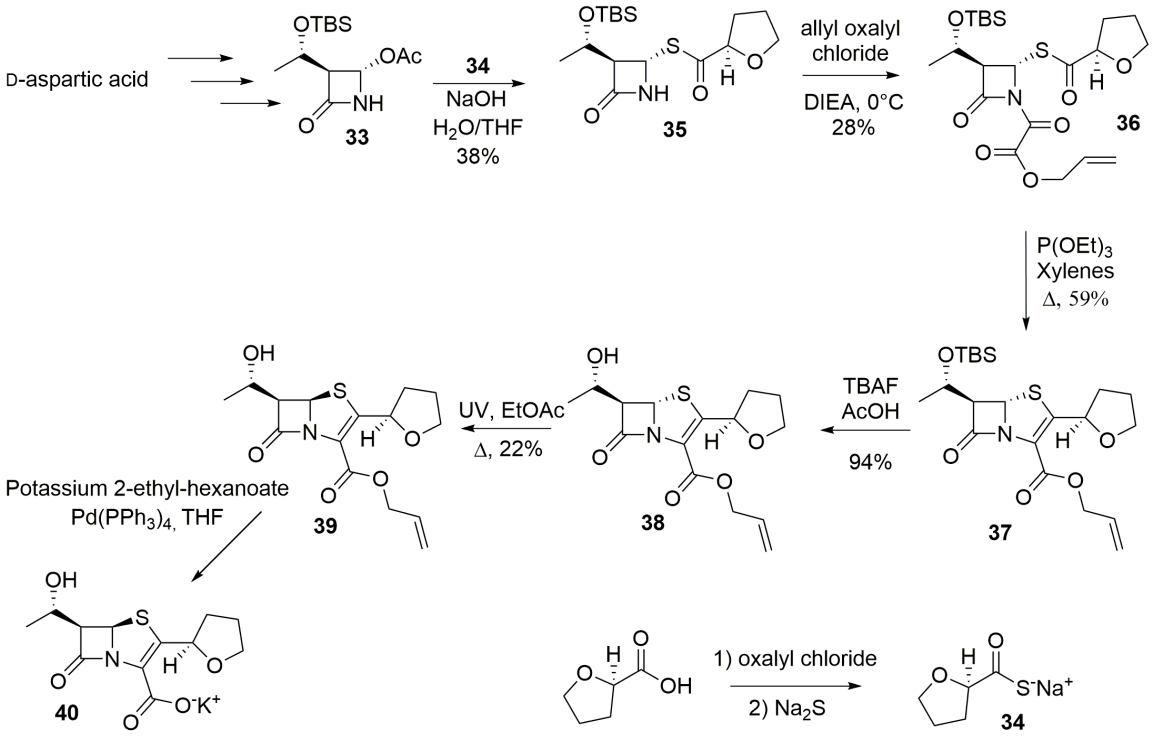

Scheme 6.4: Synthetic route to 5,6-cis-faropenem

Using D-aspartic acid, the azetidinone **33** was made by the route previously outlined in the Chapter 3. Preparation of the sodium 2-thiocarboxylatetetrahydrofuran nucleophile **34** was achieved by the addition of sodium sulfide to (*R*)-2-carboxy-tetrahydrofuranyl chloride. Addition of the thioester **34** to the *N*-acyliminium species generated from **33** in the presence of sodium hydroxide gave the thioester **35** in 38% yield. Lower than expected yield was obtained of **36** in the following reaction when one equivalent of allyl oxalyl chloride was added to **35** in the presence of diisopropylethylamine in dichloromethane at 0 °C. Carbene-mediated ring closure of **36** with triethylphosphite in refluxing xylenes provided **37** in 59% yield, and subsequent *O*-TBS deprotection with TBAF provided the free alcohol **38** in 94% yield. At this stage, UV irradiation of a solution of **39** in ethyl acetate using a quartz flask provided an equilibrium of 1:2 *cis* to

trans diastereomers which were separable by silica gel chromatography to give *epi*-faropenem allyl ester **40** in 22% yield[27]. Deprotection of the allyl ester was made possible by allyl transfer to 2-ethylhexanoate with tetrakis(triphenylphosphine)palladium in THF. This synthesis provided the desired product **40** in 6 steps from **33**, however poor yields plagued this route.

Our coworkers in the Lamichhane lab kindly tested *epi*-faropenem **40** with Ld_{Mt2} *in vitro* using a nitrocefin hydrolysis assay as previously described above and in Chapter 5[8]. The also tested 5,6-*cis*-faropenem against *M. tuberculosis* for MIC_{90} data. No binding to Ld_{Mt2} was observed and in comparison to faropenem, 5,6-cis-faropenem had poor activity (Table 6.4). None of the 5,6-*cis*-carbapenems synthesized in Chapter 3 had shown significant whole-cell MIC_{90} activity against *M. tuberculosis* (Table 6.5). The lesser potency of 5,6-cis-faropenem affirmed our belief that, against Ldts *cis*-penems are not of therapeutic potential.

Table 6.5: MIC_{90} data (µg/mL) for carbapenems and 5,6-cis-faropenem submitted for ESKAPE and *M. tuberculosis* testing. *M.tb.* = *M. tuberculosis*, *E.cl.* = *Enterobacter cloacae*, *K.pn.* = *Klebsiella pneumoniae*, *A.ba.* = *Acinetobacter baumannii*, *P.ae.* = *Pesudomonas aeruginosa*, MRSA = Methicillin Resistant *Stapholococcus aureus*, MSSA = Methicillin Susceptible *Stapholococcus aureus*.

Structure	*A.ba.*	*E.fa.*	*E.cl.*	*K.pn.*	MSSA	MRSA	*P.ae.*	*M.tb.*
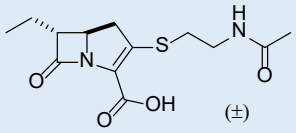	>64	>64	>64	>64	>64			>64
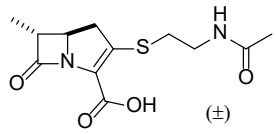	>64	>64	>64	>64	>64			>64
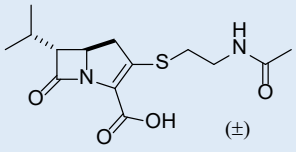	>64	>64	>64	>64	>64			>64

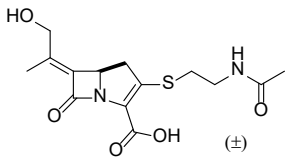	>64	>64	>64	>64	>64			>64
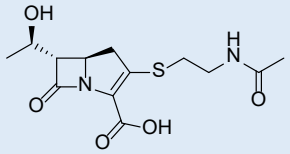	>64	>64	>64	>64	>64			>64
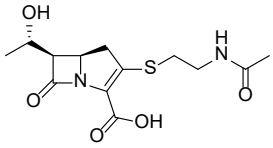	>64	>64	>64	>64	>64			>64
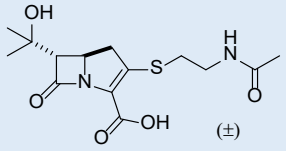	>64	>64	>64	>64	>64			>64
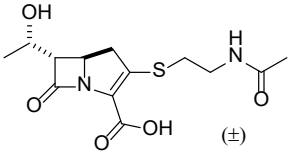	>64	>64	>64	>64	>64			10-20
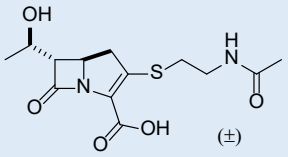	8-16	32-64	8-16	2-4	2-4	2-4	>64	10-20
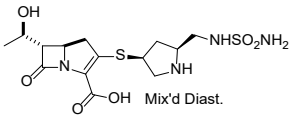	2-4	>64	>64	8-16	0.5-1	0.5-1	2-4	40-80
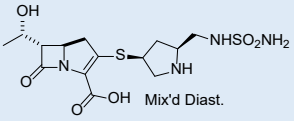		>64	>64				16-32	
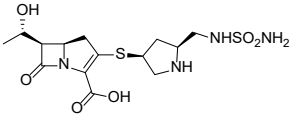								10-20
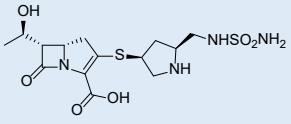	>64	>64	>64	>64	>64			>80

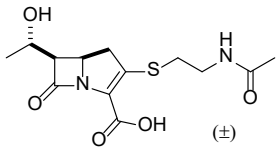	>64	>64	>64	>64	>64			>80
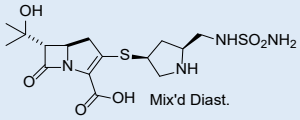	>64	>64	>64	>64	4-8			>80
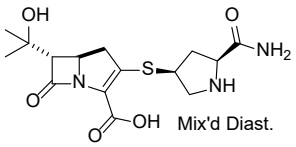	>64	>64	>64	>64	>64			>80
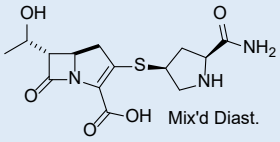	>64	>64	>64	>64	>64			>80
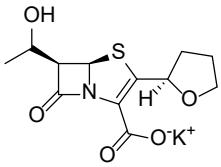	4-8	2-4	>64	32-64	4-8	4-8	>64	>64
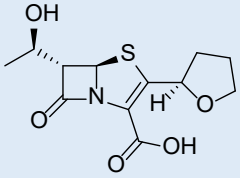	0.25-0.5	0.25-0.5	2-4	0.06-0.12	0.015-0.06	0.015-0.06	0.3-0.6	>80

Conclusion

Penems, in comparison to carbapenems, were found to be highly potent drugs against Ldts and as a result exhibited excellent bactericidal activity against *M. tuberculosis* in particular, as evidenced by MIC_{90} data (Table 6.1, Table 6.2). Against *Mycobacterium abscessus*, our lead compound, **16**, is the most potent antibiotic tested by our collaborators in the Lamichhane group. The high potency of **16** against *M. tuberculosis* and *M. abscessus* is attributed to its superior inhibitory activity against both Ldts and BlaC shown in colorimetric competition assays (Figure 6.2). Additional support

for covalent Ldt inhibition by **16** comes from intact protein analysis of Ldt-**16** adducts (Table 6.4). We have established that therapeutic potential exists for **16**, and to confirm its legitimacy as a clinical candidate, studies involving its use as a therapeutic in an animal model is required. To accommodate the multigram quantities necessary for such experiments, we have modified the Pfizer synthesis of sulopenem for the production of **16** on scale. We hope that *in vivo*, **16** is at least as effective as the carbapenems, and the limitations found with faropenem are no longer a concern[8]. To prevent low half-lives due to potential DHP-1 activity, we plan to co-administer cilastatin to **16** in a control experiment. Additionally, experiments where **16** is administered by gavage, rather than subcutaneous injection, would test if these drugs could be orally administered.

Penems currently have untapped potential in the market of highly potent late-stage broad-spectrum antibiotics. The development of new penems, such as **16**, is critical for their advantages of oral administration and activity against Ldts in comparison to carbapenems. For optimization, C-6 sidechain modification is not recommended, as the activites reported for 5,6-*cis*-penems and carbapenems are less potent than their 5,6-*trans*-counterparts. Future synthetic work should focus on the selection of the C-2 sidechain for better potency and bioavailability of the drugs *in vivo*.

Experimental

General methods:

Solvents and reagents were purchased from Sigma Aldrich or Fisher Scientific in purity of ≥98%. Silica gel chromatography was performed using 60Å silica gel from Sorbtech. Thin layer chromatography (TLC) was performed using 250 μm Analtech GHLF silica

plates. A Bruker Avance (Billerica, MA) 300 or 400 MHz spectrometer was utilized for all ^{1}H and ^{13}C NMR spectra, which are reported in parts per million (δ) referenced against a TMS standard or residual solvent peak. The JHU Chemistry Department Mass Spectrometry Facility determined exact masses by fast atom bombardment (FAB) or electrospray ionization (ESI).

Determination of antimicrobial activity (Work done by Lamichhane Group):

The standard broth dilution assay that is most widely used to determine Minimum Inhibitory Concentration (MIC) of a compound, which is recommended by the Clinical and Laboratory Standards Institute, was employed[29,30]. In this method, an axenic culture of a bacterial strain is grown to a defined growth phase in the appropriate culture broth. This primary culture is used to prepare a suspension with 10^6 live bacilli or colony-forming units per mL. Simultaneously, in a sterile 96-well plate, 100 µL of culture broth and a test compound are added in such a way that consecutive wells (across a row or column) contain 2 fold dilutions of the test compound. Next, 100 µL of the bacterial suspension is added to each well, the plate is incubated under appropriate conditions and growth or lack thereof is assessed at a defined time point. For *M. tuberculosis* the end point reading was taken at 2 weeks. For *M. abscessus* the end point reading was taken at 3 days, and for the rest of the pathogens the end point reading was obtained after overnight incubation according to the Clinical and Laboratory Standards Institute recommendations[30]. The lowest concentration at which bacterial growth is inhibited is reported as the MIC of the compound (Table 6.3).

UPLC-HRMS analysis of L,D-transpeptidase (Ldt)/penem adducts:

Penems (Table 6.4) were incubated with Ldts (2 μM) at 4 mM concentration in 400 μL of 25 mM Tris, pH 8, for 5 h at room temperature, quenched with 8 μL of freshly prepared 5% TFA and filtered through a 0.2 μm sterile membrane. 3 μL of each sample was injected into a Waters Aquity H-Class UPLC system equipped with a multi-wavelength ultraviolet-visible diode array detector in conjunction with a Waters Aquity BEH-300 UPLC column packed with a C4 stationary phase (2.1 x 50 mm, 1.7 μm) in tandem with HRMS analysis by a Waters Xevo-G2 Q-ToF ESI mass spectrometer. Solvent A = 0.1% formic acid in water, solvent B = 0.1% formic acid in acetonitrile. Mobile phase (A:B) = 0-1 min (90:10), 1-7.5 min (20:80), 7.5-8.4 min (20:80), 8.4-8.5 min (90:10), 8.5-10 min (90:10). Flow rate = 0.3 mL min^{-1}. T = 60 °C.

Penem synthetic methods:

(3*S*,4*R*)-3-((*R*)-1-((tert-butyldimethylsilyl)oxy)ethyl)-4-(tritylsulfanyl)azetidin-2-one (2). The preparation of **2** followed the procedures of *Leanza et al.*[13,19]. A suspension of sodium hydride in mineral oil (60%, 31.3 mmol, 1.25 g) was added to dimethylformamide (16 mL) and the solution was then added to a solution of trityl sulfide (8.65 g, 31.3 mmol) in dry dimethylformamide (20 mL). The resulting mixture was stirred for 2 h at 0 °C before it was slowly added to a solution of (3*R*,4*R*)-4-acetoxy-3-[(*R*)-1-(tert-butyldimethylsilyloxy)ethyl]azetidin-2-one **1** (5 g, 17.4 mmol) in dimethylformamide (16 mL) at 0 °C and was stirred for 2 h. The reaction mixture was quenched with saturated ammonium chloride, and the product mixture was extracted with diethyl ether and the organic layer was washed with water, brine and dried with

anhydrous sodium sulfate, filtered and concentrated *in vacuo*. The crude product was crystallized from hexanes to provide **2** as yellow needles (7.34 g, 84%). **2:** ^{1}H NMR (300 MHz, $CDCl_3$) δ 7.48 (d, *J* = 7.2 Hz, 6H), 7.29 (m, 9H), 4.53 (d, *J* = 2.6 Hz, 1H), 4.34 (s, 1H), 4.21 (m, *J* = 3.2 Hz, 1H), 3.10 (t, *J* = 2.3 Hz, 1H), 1.26 (d, *J* = 6.2 Hz, 3H), 0.73 (s, 9H), 0.01 (s, 3H), -0.05 (s, 3H). ^{1}H NMR matched the data reported by *Leanza et al.*[13,19].

Allyl 2-((3*S*,4*R*)-3-((*R*)-1-((tert-butyldimethylsilyl)oxy)ethyl)-2-oxo-4-trityl-sulfanyl-azetidin-1-yl)acetate (3). The preparation of **3** followed the procedures of *Leanza et al.*[13,19]. Dicyclohexyl-18-crown-6 (543 µL, 1.60 mmol) was added to a solution of **2** (8.1 g, 16.1 mmol) in benzene (80 mL). Potassium hydroxide pellets (1.5 g, 26.7 mmol) that were crushed in a mortar and pestle were added to the reaction mixture in one portion followed by the slow addition of allyl bromoacetate (3.0 mL, 24.0 mmol) in benzene (40 mL) over 5 min. The reaction mixture was stirred for 4.5 h, at which time the reaction was quenched with saturated ammonium chloride and extracted with ethyl acetate. The combined organic fractions were washed with brine and dried with anhydrous sodium sulfate, filtered and concentrated *in vacuo*. The crude oil was purified by silica gel chromatography (hexanes:ethyl acetate, 9:1) to provide **3** (8.77 g, 90%). **3:** ^{1}H NMR (400 MHz, $CDCl_3$) δ 7.47 (m, 6H), 7.27 (m, 9H), 5.84 (m, *J* = 3.6 Hz, 1H), 5.29 (m, 1H), 5.22 (m, 1H), 4.51 (m, 2H), 4.12 (m, 1H), 3.37 (q, *J* = 1.8 Hz, 1H), 3.33 (s, 2H), 3.10 (q, *J* = 1.6 Hz, 1H), 1.07 (d, *J* = 6.4 Hz, 3H), 0.77 (s, 9H), -0.01 (s, 3H), -0.05 (s, 3H). ^{1}H NMR matched the data reported by *Leanza et al.*[13,19].

Allyl 2-((2*R*,3*S*)-3-((*R*)-1-((tert-butyldimethylsilyl)oxy)ethyl)-2-(4-nitro-phenoxy-carbonyl-thio)-4-oxoazetidin-1-yl)acetate (5). The preparation of **5** followed the procedure of Philips and O'Neill[18]. Pyridine (1.37 mL, 17.02 mmol) followed by a

solution of silver nitrate (2.36 g, 13.89 mmol) in methanol (116 mL) was added to a solution of **3** (6.28 g, 10.4 mmol) in methanol (68 mL) at 0 °C and was shielded from light with aluminum foil and stirred for 30 min. The reaction mixture was concentrated *in vacuo* and redissolved in dichloromethane and water, and the organic layer was washed twice with water, dried with anhydrous sodium sulfate, filtered and concentrated *in vacuo*. The crude oil was dissolved in tetrahydrofuran (18.8 mL) and was added to a solution of *N*,*N*-dimethylaminopyridine (1.36 g, 11.17 mmol) and *p*-nitrophenylchloroformate (2.25 g, 11.17 mmol) in tetrahydrofuran (218 mL). A solution of diisopropylethylamine (1.95 mL, 11.17 mmol) in tetrahydrofuran (18.8 mL) was added to the reaction mixture and was stirred at 0 °C for 30 min during which time a precipitate formed. The reaction mixture was warmed to room temperature and stirred for an additional 5 min. The solution was filtered through Celite and the retentate was washed with ethyl acetate. The combined filtrates were washed with 1N HCl and the organic layer was directly concentrated *in vacuo*. The resulting black residue is best filtered before it is subjected to silica gel chromatography (dichloromethane) to provide **5** as a yellow oil (3.27 g, 57%). **5:** TLC (dichloromethane) = 0.2. ^{1}H NMR (400 MHz, $CDCl_3$) δ 8.26 (d, *J* = 9.2 Hz, 2H), 7.33 (d, *J* = 9.2 Hz, 2H), 5.85 (m, 1H), 5.51 (d, *J* = 2.5 Hz, 1H), 5.27 (m, 2H), 4.60 (m, 2H), 4.29 (t, *J* = 5.7 Hz, 1H), 3.31 (q, *J* = 2.5 Hz, 1H), 3.03 (s, 1H), 1.27 (d, *J* = 6.2 Hz, 3H), 0.86 (s, 9H), 0.08 (s, 3H), 0.07 (s, 3H). ^{1}H NMR matched the data reported by Philips and O'Neill[18].

Allyl (5*R*,6*S*)-6-((*R*)-1-((tert-butyldimethylsilyl)oxy)ethyl)-3-(ethylthio)-7-oxo-4-thia-1-azabicyclo[3.2.0]hept-2-ene-2-carboxylate (7). The preparation of **7** followed the procedures of Philips and O'Neill[18]. A solution of lithium hexamethylsilazane in

tetrahydrofuran (1 M, 37.5 mL) was added to a solution of **5** (4.9 g, 9.3 mmol) in tetrahydrofuran (336 mL) at -78 °C and was stirred for 30 min at this temperature. The reaction was quenched with acetic acid (1.1 mL, 18.6 mmol) and the mixture allowed to warm to room temperature. The reaction mixture was concentrated *in vacuo*, redissolved in diethyl ether and washed with saturated aqueous sodium bicarbonate, brine, dried over anhydrous sodium sulfate, filtered and concentrated *in vacuo*. The crude product was run through a short plug of silica gel (hexanes:ethyl acetate, 4:1). The 2-oxopenem intermediate was dissolved in dichloromethane (180 mL) and cooled to -78 °C. Diisopropylethylamine (6.4 mL, 36.8 mmol) was added followed by freshly distilled triflic anhydride (1.63 mL, 9.8 mmol) and the resulting solution was stirred at -78 °C for 1 h. Additional diisopropylethylamine (4.85 mL, 28 mmol) and ethanethiol (898 μL, 14.0 mmol) dissolved in dichloromethane (10 mL) were added to the vinyl triflate *in situ* and the reaction mixture was allowed to warm to room temperature over 2 h. The product was concentrated *in vacuo* and directly purified by silica gel chromatography (hexanes:ethyl acetate, 2:3) to provide an oil that solidified upon standing. The product can be recrystallized from isooctane to provide **7** as white needles (523 mg, 13%). **7:** TLC (hexanes:ethyl acetate, 1:1) = 0.3. ^{1}H NMR (300 MHz, $CDCl_3$) δ 5.68 (t, J = 1.7 Hz, 1H), 5.64 (d, J = 1.5 Hz, 1H), 5.38 (m, 1H), 4.86 (m, 1H), 4.65 (m, 1H), 4.25 (m, 1H), 4.12 (m, 1H), 3.69 (q, J = 2.1 Hz, 1H), 2.98 (m, 3H), 1.66 (m, 2H), 1.12 (d, J= 5.3 Hz, 3H), 0.92 (s, 9H), 0.08 (s, 6H). ^{1}H NMR matched the data reported by Philips and O'Neill[18].

Allyl (5*R*,6*S*)-6-((*R*)-1-hydroxyethyl-3-(ethylthio)-7-oxo-4-thia-1-azabicyclo-[3.2.0]-hept-2-ene-2-carboxylate (8). The preparation of **8** followed the procedures of Philips

and O'Neill[18]. A solution of tetra-*N*-butylammonium fluoride in tetrahydrofuran (1M, 3.66 mmol, 3.66 mL) was added to a solution of acetic acid (702 μL) and **7** (523 mg, 1.22 mmol) in tetrahydrofuran (10.5 mL) and was stirred for 2 h. The product mixture was partitioned into ethyl acetate (150 mL) and water (310 mL) and the pH was adjusted to 6 with potassium acetate. The aqueous layer was separated and washed twice with ethyl acetate (50 mL). The combined organic layers were dried with anhydrous sodium sulfate, filtered and concentrated *in vacuo*. The crude product was purified by a plug of silica gel (methanol:ethyl acetate, 3:17) to provide **8** as a white solid, which can be recrystallized from ethyl acetate/isooctane (427 mg, 85%). **8:** TLC (methanol:ethyl acetate, 3:17) = 0.9. ^{1}H NMR (400 MHz, $CDCl_3$) δ 5.96 (m, 1H), 5.64 (d, J = 1.5 Hz, 1H), 5.42 (m, 2H), 4.79 (m, 1H), 4.67 (m, 1H), 4.25 (quintet, J = 6.5 Hz, 1H), 3.71 (q, J = 2.8 Hz, 1H), 2.97 (m, 2H), 1.36 (d, J = 6.3 Hz, 3H), 1.25 (q, J= 4.9 Hz, 3H). ^{1}H NMR was in agreement the data reported by Philips and O'Neill[18].

Allyl (5*R*,6*S*)-3-(ethylsulfinyl)-6-((*R*)-1-hydroxyethyl)-7-oxo-4-thia-1-azabicyclo-[3.2.0]-hept-2-ene-2-carboxylate (9). The preparation of **9** followed the procedures of DiNinno *et al.*[21]. A solution of freshly crystallized *m*-chloroperbenzoic acid (232 mg, 1.35 mmol) in ethyl acetate (1.5 mL) was added to a solution of **8** (386 mg, 1.22 mmol) in dichloromethane (1.2 mL) and ethyl acetate (2.5 mL) and the resulting mixture was stirred for 30 min. The reaction mixture was decanted into a mixture of sodium bicarbonate (185 mg, 2.2 mmol) ethyl acetate (2.5 mL) and water (5 mL) and the suspension was stirred rapidly for 5 min. The organic layer was separated, concentrated *in vacuo* and directly purified by silica gel chromatography (hexanes:ethyl acetate, 1:1) to provide **9** (127 mg, 31%). **9:** TLC (hexanes:ethyl acetate, 1:1) = 0.15. ^{1}H NMR (300

MHz, $CDCl_3$) δ 5.91 (m, 1H), 5.72 (d, *J* = 1.7 Hz, 1H), 5.41 (m, 1H), 5.29 (q, *J* = 3.9 Hz, 1H), 4.71 (m, 2H), 4.20 (quintet, *J* = 6.5 Hz, 1H), 3.91 (m, 1H), 3.10 (m, 2H), 1.43 (t, *J* = 2.5 Hz, 3H), 1.34 (d, *J* = 6.3 Hz, 1H). ^{1}H NMR was in agreement with the data reported by DiNinno *et al.*[21].

Allyl 2-((3*R*,4*S*)-3-((*R*)-1-((tert-butyldimethylsilyl)oxy)ethyl)-2-oxo-4-(propylthio-carbonothioyl-thio)azetidin-1-yl)-2-oxoacetate (28). The preparation of **28** followed the procedures of Brenek *et al*.[25]. 1-Propanethiol (20.7 mL, 223 mmol) in methyl tert-butyl ether (100 mL) was slowly added to a suspension of 60% sodium hydride in mineral oil (14 g, 350 mmol) in methyl *tert*-butyl ether (MTBE) (500 mL) and the mixture was stirred for 1 h at which time carbon disulfide (20.93 mL, 348 mmol) was added and the resulting yellow slurry was stirred for 1 h. Magnesium sulfate (3 g) was added and the slurry was vacuum filtered under nitrogren through Celite to remove excess sodium hydride and the filter cake was rinsed with MTBE. (WARNING! The Celite filter pad contains trace amounts of MTBE in addition to large quantities of residual sodium hydride. This cake will spontaneously combust and on this scale can cause a significant flame. Great care must be taken to remove as much ether as possible. After filtering, keep the solids under nitrogen, suspend the filter cake in dichloromethane, cool to 0 °C and quench with isopropanol in the absence of oxygen). The filtrate containing **26** was transferred to a clean flask to which was added (3*R,*4*R*)-4-acetoxy-3-[(*R*)-1-(tert-butyldimethylsilyloxy)ethyl]azetidin-2-one **1** (50 g, 174 mmol) batchwise while stirring the solution rapidly. After 1 h, the slurry was filtered through a pad of silica gel and the solids were washed with methyl tert-butyl ether (200 mL). The filtrate containing **27** was cooled to -10 °C in a salt/ice bath to which was added allyl oxalyl

chloride (50 mL, 400 mmol) followed by a solution of triethylamine (56 mL, 400 mmol) in methyl tert-butyl ether (100 mL). The reaction mixture was warmed to room temperature and stirred for 1 h before it was quenched with water (100 mL). The organic layer was separated and washed twice with sodium bicarbonate (100 mL), dried with anhydrous sodium sulfate, filtered, diluted with heptanes (250 mL) and concentrated *in vacuo*. Once the majority of solvent was removed, additional heptanes (250 mL) was added and concentrated *in vacuo* to completion to ensure that no methyl tert-butyl ether remains. The crude oil is dissolveed in 400 mL isooctanes and crystallized at 4 °C for 16-24 h to provide **28** as yellow needles (45.8 g, 53%). **28:** TLC (hexanes:ethyl acetate, 7:3) = 0.4. MP = 65-67 °C. ^{1}H NMR (400MHz ,$CDCl_3$) δ = 6.76 (dd, *J* = 0.4, 3.5 Hz, 1H), 5.94 (tdd, *J* = 6.1, 10.6, 17.0 Hz, 1H), 5.39 (qd, *J* = 1.4, 17.0 Hz, 1H), 5.31 (qd, *J* = 1.0, 10.4 Hz, 1H), 4.78 (qd, *J* = 1.2, 6.1 Hz, 2H), 4.39 (dq, *J* = 2.5, 6.3 Hz, 1H), 3.56 (dd, *J* = 2.5, 3.5 Hz, 1H), 3.39 (dt, *J* = 3.7, 7.2 Hz, 2H), 1.76 (sxt, *J* = 7.4 Hz, 3H), 1.24 (d, *J* = 6.5 Hz, 3H), 1.03 (t, *J* = 7.4 Hz, 3H), 0.86 (s, 9H), 0.09 (s, 3H), 0.06 (s, 3H). ^{13}C NMR (101MHz, $CDCl_3$) δ = 218.3, 163.5, 159.1, 154.4, 130.4, 120.2, 67.4, 66.0, 64.5, 58.9, 38.9, 26.9, 25.6, 21.9, 21.3, 17.8, 13.4, -4.3, -5.3. HRMS (FAB), $C_{12}H_{34}NO_5S_3Si$ [$M+H^+$] calculated: 492.1368; found: 492.1370. ^{1}H and ^{13}C NMR is identical to the data reported in the literature[25].

Allyl (5*S*,6*R*)-6-((*R*)-1-((tert-butyldimethylsilyl)oxy)ethyl)-7-oxo-3-(propylthio)-4-thia-1-azabicyclo[3.2.0]hept-2-ene-2-carboxylate (29). The preparation of **29** was carried out by modification of the procedure of Brenek *et al*.[25]. A solution of triethylphosphite (38.7 mL, 233 mmol) in anhydrous ethanol-free chloroform (450 mL) was added over 24 h to a refluxing, stirring solution of **28** (45.8 g, 93 mmol) in

chloroform (1 L) using a 2L round-bottomed flask fitted with a Claisen adapter, reflux condenser and addition funnel. Once addition was complete, the solution was stirred for an additional 24 h, at which time additional triethyl phosphite (15 mL) was added in one portion. The mixture was stirred at reflux for 16 h, cooled to room temperature, and washed with aqueous HCl (0.1 N, 250 mL), saturated aqueous sodium bicarbonate (250 mL) and brine. The organic fractions were concentrated *in vacuo* and purified by silica gel chromatography (hexanes) to ensure the removal of triethylphosphite. The product oil crystallized from isooctane to produce **29** as white needles (18.57 g, 45%). **29:** TLC (hexanes:ethyl acetate, 7:3) = 0.5. m.p. = 104-105 °C. ^{1}H NMR (400MHz, $CDCl_3$) δ = 5.93 (tdd, *J* = 5.4, 10.7, 17.2 Hz, 1H), 5.59 (d, *J* = 1.4 Hz, 1H), 5.40 (qd, *J* = 1.6, 17.2 Hz, 1H), 5.22 (qd, *J* = 1.4, 10.4 Hz, 1H), 4.70 (tddd, *J* = 1.6, 5.5, 13.5, 28.2 Hz, 2H), 4.23 (td, *J* = 6.1, 11.5 Hz, 1H), 3.66 (dd, *J* = 1.6, 4.9 Hz, 1H), 2.91 (tdd, *J* = 7.4, 12.5, J_3 = 32.3 Hz, 2H), 1.74 (sxt, *J* = 7.4 Hz, 2H), 1.25 (d, *J* = 6.3 Hz, 3H), 1.03 (t, *J* = 7.3 Hz, 3H), 0.88 (s, 9H), 0.07 (s, 3H), 0.07 (s, 3H). ^{13}C NMR (101MHz, $CDCl_3$) δ = 172.1, 159.8, 131.9, 118.1, 117.0, 71.4, 65.3, 63.7, 37.9, 25.7, 23.3, 22.5, 17.9, 13.2, -4.3, -5.1. HRMS (FAB), $C_{20}H_{33}NO_4S_2Si$ [M^+] calculated: 443.1620; found: 443.1624. ^{1}H and ^{13}C NMR is identical to the data reported in the literature[25].

Allyl (5*S*,6*R*)-6-((*R*)-1-hydroxyethyl)-7-oxo-3-(propylthio)-4-thia-1-azabicyclo-[3.2.0]-hept-2-ene-2-carboxylate (30). A solution of **29** (10.2 g, 22.99 mmol) in tetrahydrofuran (64 mL) was added to a mixture of *tetra-N*-butylammonium fluoride (34.5 mmol) and acetic acid (12.5 mL, 218 mmol) in tetrahydrofuran (64 mL). The reaction mixture was stirred for 24 h before it was washed with saturated aqueous sodium bicarbonate. The aqueous layer was back extracted with dichloromethane and the

combined organic layers were washed with brine, dried with anhydrous sodium sulfate, filtered and concentrated *in vacuo*. The crude product was purified by silica gel chromatography (hexanes:ethyl acetate, 1:1) and the resulting oil crystallized from ethyl acetate/isooctane to provide **30** (5.5 g, 73%). **30:** TLC (hexanes:ethyl acetate, 7:3) = 0.2. m.p. = 85-86 °C. ^{1}H NMR (400MHz, $CDCl_3$) δ = 5.95 (tdd, *J* = 5.4, 10.6, 17.2 Hz, 1H), 5.63 (d, *J* = 1.6 Hz, 1H), 5.41 (qd, *J* = 1.5, 17.2 Hz, 1H), 5.23 (qd, *J* = 1.4, 10.6 Hz, 1H), 4.78 (tdd, *J* = 1.5, 5.4, 13.5 Hz, 1H), 4.66 (tdd, *J* = 1.4, 5.6, *J*$_3$ = 13.5 Hz, 1H), 4.24 (quin, *J* = 6.5 Hz, 1H), 3.70 (dd, *J* = 1.4, 6.8 Hz, 1H), 2.98 (td, *J* = 7.4, 12.7 Hz, 1H), 2.88 (td, *J* = 7.2, 12.5 Hz, 1H), 1.74 (sxt, *J* = 7.4 Hz, 2H), 1.35 (d, *J* = 6.3 Hz, 3H), 1.03 (t, *J* = 7.3 Hz, 3H). ^{13}C NMR (101MHz, $CDCl_3$) δ = 172.1, 159.8, 156.2, 131.9, 118.2, 116.7, 70.9, 65.5, 65.5, 64.0, 37.9, 23.3, 21.9, 13.2. HRMS (FAB), $C_{14}H_{19}NO_4S_2$ [M^+] calculated: 329.0756; found: 329.0753.

Allyl (5*S*,6*R*)-6-((*R*)-1-hydroxyethyl)-7-oxo-3-(propylsulfinyl)-4-thia-1-azabicyclo[3.2.0]hept-2-ene-2-carboxylate (31). Urea•hydrogen peroxide (1.62 g, 16.7 mmol) was dissolved in 1,1,1,3,3,3-hexafluoroisopropanol (16 mL) and added to a solution of **29** (5.0 g, 15.2 mmol) 1,1,1,3,3,3-hexafluoroisopropanol (20 mL) in one portion and the solution was stirred for 24 h. Heptanes (50 mL) was added to the product mixture and concentrated *in vacuo*. The process was repeated as necessary to remove all traces of fluorinated solvent prior to purification by silica gel chromatography (hexanes:ethyl acetate, 1:1). The resulting oil recrystallized from ethyl acetate/isooctane to provide **31** as a mixture of diasteromeric sulfoxides as yellow needles (4.63 g, 88%). **31:** TLC (hexanes:ethyl acetate, 1:1) = 0.2. m.p. = 90-93 °C. ^{1}H NMR (400MHz, $CDCl_3$) δ = 5.98 - 5.87 (m, 1H), 5.86 (d, *J* = 1.8 Hz, 0.33H), 5.71 (d, *J* = 1.8 Hz, 0.67H), 5.41

(qd, *J* = 1.6, 17.0 Hz, 0.33H), 5.43 (qd, *J* = 1.4, 17.2 Hz, 0.66H), 5.29 (qd, *J* = 1.2, 10.6 Hz, 1H), 4.77 (qdd, *J* = 1.6, 5.5, 13.3 Hz, 1H), 4.67 (qdd, *J* = 1.6, 5.7, 13.3 Hz, 1H), 4.27 - 4.14 (m, 1H), 3.92 (dd, *J* = 1.6, 6.8 Hz, 0.66H), 3.88 (dd, *J* = 2.0, 7.0 Hz, 0.33H), 3.21 - 3.04 (m, 1H), 2.99 (ddt, *J* = 7.0, 9.2, 13.3 Hz, 1H), 2.04 - 1.77 (m, 2H), 1.35 (d, *J* = 6.3 Hz, 3H), 1.11 (t, *J* = 7.4 Hz, 3H). ^{13}C NMR (101MHz, $CDCl_3$) δ = 172.7, 171.5, 164.4, 164.0, 158.2, 158.1, 130.8, 121.6, 121.4, 119.5, 119.5, 73.2, 73.2, 66.7, 66.7, 65.6, 65.4, 65.4, 63.4, 57.5, 57.0, 21.8, 16.5, 16.1, 13.0. FAB-MS analysis of sulfoxides **31** did not provide parent ions due to susceptibility to degradation.

General procedure for the addition of C-2 thiol side chains to the 2-ethylsulfinyl penem:

Allyl (5*S*,6*R*)-3-((1-(4,5-dihydrothiazol-2-yl)azetidin-3-yl)thio)-6-((*R*)-1-hydroxy-ethyl)-7-oxo-4-thia-1-azabicyclo[3.2.0]hept-2-ene-2-carboxylate (32). A solution of 1-(4,5-dihydro-2-thiazolyl)-3-azetidinethiol hydrochloride (tebipenem side chain) (3.10 g, 14.74 mmol) in acetonitrile (50 mL) followed by diisopropylethylamine (3.70 mL, 20.77 mmol) was added to a stirring solution of **31** (4.63 g, 13.4 mmol) in acetonitrile (100 mL) and the mixture was stirred for 2 h at 0 °C. The solution was diluted with brine and the aqueous layer was back extracted three times with ethyl acetate. The combined organic layers were dried with anhydrous sodium sulfate, filtered and concentrated *in vacuo*. The crude oil was purified by silica gel chromatography (methanol:dichloromethane, 1:40) to provide **32** as a yellow oil that became a glass under high vacuum (2.85 g, 50%).

32: TLC (methanol:dichloromethane, 1:19) = 0.3. ^{1}H NMR (400MHz, $CDCl_3$) δ = 5.94 (tdd, *J* = 5.4, 10.7, 17.2 Hz, 1H), 5.69 (d, *J* = 1.4 Hz, 1H), 5.41 (qd, *J* = 1.5, 17.1 Hz, 1H),

5.24 (qd, *J* = 1.2, 10.5 Hz, 1H), 4.77 (tdd, *J* = 1.4, 5.5, 13.4 Hz, 1H), 4.67 (tdd, *J* = 1.4, 5.6, 13.4 Hz, 1H), 4.40 (td, *J* = 8.4, 23.9 Hz, 3H), 4.19 (sxt, *J* = 6.5 Hz, 1H), 4.25 - 4.10 (m, 1H), 4.00 (t, *J* = 7.4 Hz, 2H), 4.06 - 3.90 (m, 2H), 3.72 (dd, *J* = 1.5, 6.9 Hz, 1H), 3.36 (t, *J* = 7.4 Hz, 2H), 1.33 (d, *J* = 6.5 Hz, 3H). ^{13}C NMR (101MHz, $CDCl_3$) δ = 172.2, 164.4, 159.5, 152.1, 131.6, 118.5, 117.6, 71.5, 65.8, 65.2, 65.0, 60.4, 59.3, 58.7, 36.2, 36.1, 21.9. HRMS (FAB), $C_{17}H_{22}N_3O_4S_3$ [M+H$^+$] calculated: 428.0773; found: 428.0765.

Allyl (5*R*,6*S*)-6-((*R*)-1-hydroxyethyl-3-(ethylthio)-7-oxo-4-thia-1-azabicyclo[3.2.0]hept-2-ene-2-carboxylate (8): The same procedure was followed as used to produce **32**. TLC (methanol:ethyl acetate, 3:17) = 0.9. ^{1}H NMR (400MHz, $CDCl_3$) δ = 5.96 (tdd, *J* = 5.4, 10.7, 17.2 Hz, 1H), 5.64 (d, *J* = 1.6 Hz, 1H), 5.42 (qd, *J* = 1.6, 17.2 Hz, 1H), 5.24 (qd, *J* = 1.6, 10.4 Hz, 1H), 4.79 (tdd, *J* = 1.4, 5.4, 13.4 Hz, 1H), 4.67 (tdd, *J* = 1.5, 5.5, 13.5 Hz, 1H), 4.25 (quin, *J* = 6.5 Hz, 1H), 3.71 (dd, *J* = 1.4, 6.8 Hz, 1H), 3.01 (qd, *J* = 7.2, 12.3 Hz, 1H), 2.94 (qd, *J* = 7.2, 12.5 Hz, 1H), 1.37 (t, *J* = 7.2 Hz, 3H), 1.36 (d, *J* = 6.3 Hz, 3H). ^{1}H NMR is identical to the data reported in the literature[25].

Allyl (5*R*,6*S*)-6-((*R*)-1-hydroxyethyl)-3-((2-hydroxyethyl)thio)-7-oxo-4-thia-1-azabicyclo[3.2.0]hept-2-ene-2-carboxylate (18 allyl ester): The same procedure was followed as used to produce **32**. ^{1}H NMR (400MHz, $CHCl_3$) δ = 5.95 (ddt, *J* = 5.4, 10.5, 17.2, 1H), 5.65 (d, *J* = 1.4 Hz, 1H), 5.41 (qd, *J* = 1.5, 17.2 Hz, 1H), 5.24 (qd, *J* = 1.3, 9.0 Hz, 1H), 4.78 (tdd, *J* = 1.4, 5.4, 13.4 Hz, 1H), 4.66 (tdd, *J* = 1.3, 5.6, 13.4 Hz, 1H), 4.23 (quin, *J* = 6.5 Hz, 1H), 3.86 (t, *J* = 6.2 Hz, 2H), 3.71 (dd, *J* = 1.5, 6.8 Hz, 1H), 3.14 (tq, *J* = 6.3, 14.0 Hz, 1H), 1.35 (d, *J* = 6.3 Hz, 3H). ^{13}C NMR (101MHz, $CHCl_3$) δ = 172.2,

159.8, 156.3, 131.8, 118.2, 116.7, 70.95, 65.4, 64.0, 37.8, 23.2, 21.7, 13.1.

Allyl (5*R*,6*S*)-6-((*R*)-1-hydroxyethyl)-3-((3-methoxy-3-oxopropyl)thio)-7-oxo-4-thia-1-azabicyclo[3.2.0]hept-2-ene-2-carboxylate (19 allyl ester): The same procedure was followed as used to produce **32**. ^{1}H NMR (400MHz, $CHCl_3$) δ = 5.97 (ddt, *J* = 5.3, 11.7, 17.2, 1H), 5.66 (d, *J* = 1.4 Hz, 1H), 5.40 (qd, *J* = 1.5, 17.2 Hz, 1H), 5.23 (qd, *J* = 1.3, 10.5 Hz, 1H), 4.77 (tdd, *J* = 1.4, 5.4, 13.4 Hz, 1H), 4.65 (tdd, *J* = 1.4, 5.5, 13.4 Hz, 1H), 4.23 (quin, *J* = 6.4 Hz, 1H), 3.72 (m, 1H), 3.71 (s, 3H), 3.21 (tq, *J* = 4.7, 11.7, 2H), 2.75 (m, 2H), 1.34 (d, *J* = 6.4 Hz, 3H). ^{13}C NMR (101MHz, $CHCl_3$) δ = 171.9, 171.2, 159.6, 154.1, 131.8, 118.3, 117.6, 71.2, 65.6, 64.3, 52.1, 34.6, 30.6, 21.9, 21.1.

Allyl (5*R*,6*S*)-6-((*R*)-1-hydroxyethyl)-3-(((3*R*,5*R*)-1-(((4-nitrobenzyl)oxy)carbonyl)-5-((sulfamoylamino)methyl)pyrrolidin-3-yl)thio)-7-oxo-4-thia-1-azabicyclo[3.2.0]hept-2-ene-2-carboxylate (10): The same procedure was followed as used to produce **32**. TLC (hexanes:ethyl acetate, 1:1) = 0.15. ^{1}H NMR (400MHz, MeOD) δ = 8.21 (d, *J* = 8.6 Hz, 2H), 7.56 (d, *J* = 6.1 Hz, 2H), 6.00 - 5.79 (m, 1H), 5.67 (d, *J* = 2.3 Hz, 1H), 5.37 (qd, *J* = 1.6, 17.0 Hz, 2H), 5.21 (qd, *J* = 1.0, 7.8 Hz, 1H), 5.27 - 5.15 (m, 2H), 4.28 - 4.15 (m, 1H), 3.85 - 3.72 (m, 1H), 3.70 (dd, *J* = 0.8, 7.0 Hz, 1H), 3.48 - 3.32 (m, 2H), 2.69 - 2.54 (m, 2H), 1.28 (d, *J* = 6.3 Hz, 3H). ^{13}C NMR (101MHz, 1:1 $CHCl_3$:MeOD) δ = 172.48, 159.3, 156.6, 146.8, 131.2, 127.6, 127.4, 122.9, 117.0, 115.6, 70.4, 65.0, 64.6, 64.4, 63.8, 57.2, 37.0, 33.5, 22.6, 20.4, 12.1.

Allyl (5*R*,6*S*)-3-(((3*R*,5*R*)-5-(dimethylcarbamoyl)-1-(((4-nitrobenzyl)oxy)carbonyl)pyrrolidin-3-yl)thio)-6-((*R*)-1-hydroxyethyl)-7-oxo-4-thia-1-azabicyclo[3.2.0]hept-2-ene-2-carboxylate (11): TLC (hexanes:ethyl acetate, 1:1) = 0.15. ^{1}H NMR (400MHz, $CDCl_3$) δ = 8.17 (d, *J* = 9.6 Hz, 2H), 7.50 (d, *J* = 8.8 Hz, 2H),

5.91 (tdd, *J* = 5.7, 10.4, 17.0 Hz, 1H), 5.66 (d, *J* = 1.4 Hz, 1H), 5.46 - 5.32 (m, 1H), 5.31 - 5.24 (m, 1H), 5.12 - 4.96 (m, 1H), 4.83 - 4.72 (m, 2H), 4.65 (td, *J* = 13.5, 17.2 Hz, 2H), 4.36 - 4.22 (m, 1H), 4.22 - 4.13 (m, 1H), 4.13 - 3.98 (m, 1H), 3.69 (dd, *J* = 1.5, 7.1 Hz, 1H), 3.60 - 3.31 (m, 3H), 3.08 (s, 3H), 2.96 (s, 3H), 2.83 - 2.68 (m, 1H), 2.64 (d, *J* = 11.9 Hz, 1H), 2.05 - 1.79 (m, 2H), 1.31 (d, *J* = 6.5 Hz, 3H). ^{13}C NMR (101MHz, 1:1 $CHCl_3$:MeOD) δ = 172.5, 171.4, 171.2, 156.5, 153.4, 152.9, 146.9, 143.4, 131.3, 127.4, 123.0, 117.2, 65.2, 56.4, 56.2, 55.6, 55.3, 40.2, 39.4, 36.2, 35.3, 34.4, 33.8, 12.3.

***S*-((2*S*,3*R*)-3-((*S*)-1-((tert-butyldimethylsilyl)oxy)ethyl)-4-oxoazetidin-2-yl)-(*R*)-tetrahydrofuran-2-carbothioate (35).** The preparation of **35** followed the procedure of Ishiguro *et al*.[26,28]. Thiocarboxylic acid **34** (2.94 g, 22.3 mmol) was added to a solution of 4-acetoxyazetidinone **33** (2 g, 6.96 mmol) in acetone (6 mL) and aqueous NaOH (1N, 11.97 mL). The reaction mixture was heated to 55 °C and stirred for 2 h while the pH was periodically monitored and maintained at pH = 8 with sodium bicarbonate. The organic layer was separated and the aqueous fraction extracted with ethyl acetate. The combined organic fractions were washed with saturated aqueous sodium bicarbonate and dried with brine before concentrated *in vacuo*. The crude product was purified by silica gel chromatography (hexanes:ethyl acetate, 4:1) to provide **35** as a colorless oil (970 mg, 39%). **35:** TLC (hexanes:ethyl acetate, 2:3) = 0.7. ^{1}H-NMR (300 MHz, $CDCl_3$) ^{1}H NMR (300 MHz, $CDCl_3$) δ 6.25 (s, 1H), 5.09 (d, *J* = 2.4 Hz, 1H), 4.48 (m, *J* = 2.7 Hz, 1H), 4.24 (m, *J* = 4.0 Hz, 1H), 4.04 (t, *J* = 5.7 Hz, 1H), 3.97 (m, *J* = 5.4 Hz, 1H), 3.18 (t, *J* = 3.2 Hz, 1H), 2.27 (m, *J* = 6.3 Hz, 1H), 1.95 (q, *J* = 6.8 Hz, 1H), 1.33 (d, *J* = 6.4 Hz, 3H), 0.88 (s, 9H), 0.09 (s, 3H), 0.03 (s, 3H). ^{1}H NMR matched the data reported by Ishiguro *et al*.[26,28].

Allyl 2-((3R,4S)-3-((S)-1-((tert-butyldimethylsilyl)oxy)ethyl)-2-oxo-4-(((R)-tetrahydrofuran-2-carbonyl)thio)azetidin-1-yl)-2-oxoacetate (36). The preparation of **36** followed the procedure of Ishiguro *et al*.[26,28]. Allyl oxalyl chloride (798 mg, 5.37 mmol) was added slowly to a solution of **35** (970 mg, 2.7 mmol) and trimethylamine (1.2 mL, 8.64 mmol) in dichloromethane (13.5 mL) at 0 °C. The reaction mixture was allowed to warm to room temperature and stirred for 2 h. The reaction was quenched with water and the pH of the aqueous layer was adjested to pH = 7.5 with aqueous sodium bicarbonate. The organic layer was separated, washed with water, dried with anhydrous sodium sulfate, filtered and concentrated *in vacuo*. The crude oil was purified by silica gel chromatography (hexanes:ethyl acetate, 7:3) to provide **36** as a colorless oil (290 mg, 28%). **36:** TLC (hexanes:ethyl acetate, 2:3) = 0.85. ^{1}H NMR (400 MHz, $CDCl_3$) δ 5.94 (m, *J* = 3.9 Hz, 1H), 5.62 (d, *J* = 3.4 Hz, 1H), 5.40 (d, *J* = 17.2 Hz, 1H), 5.32 (d, *J* = 10.3 Hz, 1H), 4.79 (q, *J* = 3.3 Hz, 1H), 4.53 (m, *J* = 3.9 Hz, 1H), 4.35 (m, *J* = 3.1 Hz, 1H), 4.07 (q, *J* = 7.1 Hz, 1H), 3.97 (m, *J* = 2.5 Hz, 1H), 3.45 (t, *J* = 3.2 Hz, 1H), 2.29 (m, *J* = 4.2 Hz, 1H), 2.20 (m, *J* = 4.4 Hz, 1H), 1.95 (m, *J* = 3.6 Hz, 1H), 1.37 (d, *J* = 6.4 Hz, 3H), 0.86 (s, *J* = 2.6 Hz, 9H), 0.16 (s, 3H), 0.05 (s, 3H). ^{1}H NMR matched the data reported by Ishiguro *et al*.[26,28].

Allyl (5S,6R)-6-((S)-1-((tert-butyldimethylsilyl)oxy)ethyl)-7-oxo-3-((R)-tetrahydrofuran-2-yl)-4-thia-1-azabicyclo[3.2.0]hept-2-ene-2-carboxylate (37). The preparation of **37** followed the procedure of Ishiguro *et al*.[26,28]. Triethyl phosphite (630 µL, 3.65 mmol) was added to a solution of **36** (285 mg, 0.75 mmol) in xylenes (15 mL) and the reaction mixture was fitted with a condenser and heated to reflux for 16 h. The solution was concentrated and the crude product directly purified by silica gel

chromatography (hexanes:ethyl acetate, 5:1) to provide **37** as a crude oil (150 mg, 59%). **37:** TLC (hexanes:ethyl acetate, 1:2) = 0.9. ^{1}H NMR (400 MHz, $CDCl_3$) δ 5.92 (m, 1H), 5.54 (d, *J* = 1.6 Hz, 1H), 5.40 (m, 2H), 5.23 (m, 1H), 4.68 (m, 2H), 4.21 (m, *J* = 4.7 Hz, 1H), 3.93 (q, *J* = 7.2 Hz, 1H), 3.82 (t, *J* = 7.4 Hz, 1H), 3.77 (q, *J* = 1.8 Hz, 1H), 3.65 (q, *J* = 2.3 Hz, 1H), 2.40 (m, *J*= 3.9 Hz, 1H), 1.95 (m, *J* = 7.0 Hz, 2H), 1.77 (m, *J* = 4.4 Hz, 1H), 1.24 (d, *J* = 6.2 Hz, 3H), 0.87 (s, 9H), 0.07 (s, 6H). ^{1}H NMR matched the data reported by Ishiguro *et al*. [26,28,31,32].

Allyl (5S,6R)-6-((S)-1-hydroxyethyl-7-oxo-3-((R)-tetrahydrofuran-2-yl)-4-thia-1-azabicyclo[3.2.0]hept-2-ene-2-carboxylate (38). The preparation of **38** followed the procedure of Ishiguro *et al*.[26,28]. A solution of tetra-*N*-butylammonium fluoride in tetrahydrofuran (1M, 0.67 mmol, 673 µL) was added to a solution of **37** (150 mg, 0.44 mmol) and acetic acid (110 mg, 1.94 mmol) in tetrahydrofuran (1.76 mL). The reaction mixture was stirred for 8.5 h at 50 °C. The reaction solution was poured into water (3.5 mL) and the mixture was extracted with ethyl acetate (3.5 mL). The combined organic fractions were washed with water, twice with saturated aqueous sodium bicarbonate, and brine before the solution was dried with anhydrous sodium sulfate, filtered and concentrated *in vacuo*. The crude oil was purified by silica gel chromatography (hexanes:ethyl acetate, 1:1) to provide the produce as a colorless oil (94.1 mg, 94%). **38:** TLC (hexanes:ethyl acetate, 1:2) = 0.9. ^{1}H NMR (400 MHz, $CDCl_3$) δ 5.94 (m, 1H), 5.52 (m, 1H), 5.39 (m, 2H), 5.26 (m, 1H), 4.76 (m, 1H), 4.65 (m, 1H), 4.22 (m , 1H), 3.96 (m, 1H), 3.83 (m, 1H), 3.71 (m, 1H), 2.43 (m, 1H), 1.96 (m, 2H), 1.80 (m, 2H), 1.40 (d, *J* = 6.4 Hz, 3H). ^{1}H NMR matched the data reported by Ishiguro *et al*.[26,28,31,32].

Allyl (5*R*,6*R*)-6-((*S*)-1-hydroxyethyl-7-oxo-3-((*R*)-tetrahydrofuran-2-yl)-4-thia-1-

azabicyclo[3.2.0]hept-2-ene-2-carboxylate (39). The preparation of **39** followed the procedure of Tanaka *et al*.[27,31,32]. A solution of **38** (94 mg, 0.289 mmol) in ethyl acetate (144 mL) in a quartz flask was stirred at room temperature in the presence of a high-pressure mercury 450 W Hanovia UV lamp. The mixture equilibrated to approximately a 2:1 ratio of **38**:**39** as observed by TLC after 90 min at which point the mixture was concentrated. The diastereomers were separated by silica gel chromatography (hexanes:ethyl acetate, 1:1) and crystallized from dichloromethane and hexanes to provide **39** as a white solid (30 mg, 32%). **39:** TLC (hexanes:ethyl acetate, 1:2) = 0.8. H NMR (400 MHz, $CDCl_3$) δ 5.51 (d, *J* = 4.0 Hz, 1H), 5.35-5.47 (m, 1H), 5.36 (t, *J* = 7.3 Hz, 1H), 5.28 (d, *J* = 11.2 Hz, 1H), 4.78 (dd, *J* = 5.9, 13.5 Hz, 1H), 4.65 (dd, *J* = 5.9, 13.5 Hz, 1H), 4.39-4.51 (m, 2H), 3.78-4.04 (m, 2H), 3.75 (d, *J* = 4.0 Hz, 1H), 2.35-2.55 (m, 1H), 1.72-1.87 (m, 4H), 1.23 (d, *J* = 5.9 Hz, 3H). ^{1}H NMR matched the data reported by Ishiguro *et al.*[31,32].

Potassium (5*R*,6*R*)-6-((*S*)-1-hydroxyethyl-7-oxo-3-((*R*)-tetrahydrofuran-2-yl)-4-thia-1-azabicyclo[3.2.0]hept-2-ene-2-carboxylate (*epi*-faropenem, 40). The preparation of **39** followed the procedure of Tanaka *et al*.[27,31,32]. A solution of **39** (30 mg, 0.092 mmol) in tetrahydrofuran (3 mL) was sparged with nitrogen for 30 min, at which point tetrakis(triphenylphosphine)palladium was added (9.2 mg, 0.0079 mmol) in a single portion. A solution of potassium 2-ethylhexanoate (26 mg, 0.119 mmol) in tetrahydrofuran (2 mL) was added and the resulting mixture was stirred for 1 h. The solution was diluted with water and extracted with diethyl ether. The organic layer was back extracted twice with water and the combined aqueous fractions were filtered and lyophilized. The crude product was purified by HPLC on a Phenomonex Luna C18(2)

stationary phase, 10 x 250 mm (acetonitrile:10 mM NH_4HCO_3 in water, 10:90; 1 mL/min; 6.5 min elution). **40:** ^{1}H NMR (300 MHz, D_2O) δ 8.73 (s, 1H), 5.73 (t, *J* = 6.8 Hz, 1H), 4.08 (m, 1H), 3.88 (q, *J* = 7.4 Hz, 1H), 2.50 (m, 1H), 2.03 (m, 3H), 1.84 (m, 1H), 1.39 (m, 2H), 1.24 (m, 2H), 0.83 (d, *J* = 3.1 Hz, 3H). ^{1}H NMR matched the data reported by Tanaka *et al.*[27,31,32].

General procedure for allyl deprotection with palladium(II) acetate: (5*R*,6*S*)-3-(ethylsulfinyl)-6-((*R*)-1-hydroxyethyl)-7-oxo-4-thia-1-azabicyclo-[3.2.0]-hept-2-ene-2-carboxylate (15). Palladium(II) acetate (1 mg, 0.003 mmol) and triethylphosphite (3.8 µL, 0.022 mmol) were sequentially added to a mixture of sodium bicarbonate (5.9 mg, 0.07 mmol), 5,5-dimethyl-cyclohexane-1,3-dione (5.9 mg, 0.042 mmol), water (168 µL) and tetrahydrofuran (422 µL) and vigorously stirred for 5 min. A solution of **8** (20 mg, 0.063 mmol) in tetrahydrofuran (85 µL) was added, and the reaction mixture was stirred while heating to 35°C for 45 min. The solution was diluted with water (500 µL) and dichloromethane (400 µL), washed three times with dichloromethane (5 mL) and the aqueous layer was added directly to a column of Diaion polystyrene resin (5 mL) and was eluted with water and the product-containing fractions were lyophilized to provide **15** as a white powder. **15:** ^{1}H NMR (400MHz, D_2O) δ = 5.72 (d, *J* = 1.4 Hz, 1H), 4.25 (quin, *J* = 6.3 Hz, 1H), 3.95 (dd, *J* = 1.4, 5.9 Hz, 1H), 3.14-2.90 (m, 2H), 1.34 (t, *J* = 7.3 Hz, 3H), 1.31 (d, *J* = 6.5 Hz, 3H). HRMS (FAB), $C_{10}H_{12}NO_4S_2$ [M-H$^+$] calculated: 274.0208; found: 274.0211; Δ 1.1 ppm. ^{13}C NMR was not obtained as the total amount of material was < 1 mg and compounds are not stable enough for 10+ h experiments at RT.

A general procedure for deallylation with palladium tetrakis:

Potassium (5*S*,6*R*)-3-((1-(4,5-dihydrothiazol-2-yl)azetidin-3-yl)thio)-6-((*R*)-1-hydroxyethyl)-7-oxo-4-thia-1-azabicyclo[3.2.0]hept-2-ene-2-carboxylate (16).

Tetrakis(triphenylphosphine)palladium (43 mg, 0.21 mmol) was added to a solution of **32** (1.8 g, 4.21 mmol) in freshly distilled tetrahydrofuran (84 mL) at which time the mixture became cloudy. A solution of potassium 2-ethylhexanoate (873 mg, 4.0 mmol) in tetrahydrofuran (16.8 mL) was added causing the reaction mixture to initially become clear. After stirring for 30 min, the solution became cloudy with the formation of yellow crystalline leaves. The reaction mixture is cooled to 4 °C and stirred for an additional 2 h. The precipitate is filtered and washed with cold tetrahydrofuran to provide **16** as an off-white powder (1.2 g, 66%). The precipitate may be re-dissolved in water and washed with dichloromethane to remove trace quantities of **32** and triphenylphosphine; the major impurities of the reaction. No evidence of palladium contamination was found by HRMS. **16:** ^{1}H NMR (400MHz, D_2O) δ = 5.71 (d, *J* = 1.0 Hz, 1H), 4.50 (td, *J* = 8.4, 20.9 Hz, 2H), 4.24 (quin, *J* = 6.5 Hz, 1H), 4.32 - 4.18 (m, 1H), 4.02 (ddd, *J* = 4.8, 9.0, 19.1 Hz, 2H), 3.93 (t, *J* = 8.0 Hz, 2H), 3.96 - 3.84 (m, 1H), 3.45 (t, *J* = 7.4 Hz, 2H), 1.30 (d, *J* = 6.5 Hz, 3H). ^{13}C NMR (101MHz, D_2O) δ = 175.4, 166.4, 143.6, 124.1, 69.4, 64.7, 63.8, 59.4, 59.0, 57.7, 51.1, 35.6, 35.1, 20.1. HRMS (UPLC), $C_{14}H_{18}N_3O_4S_3$ [$M+H^+$] calculated: 388.0456; found: 388.0457.

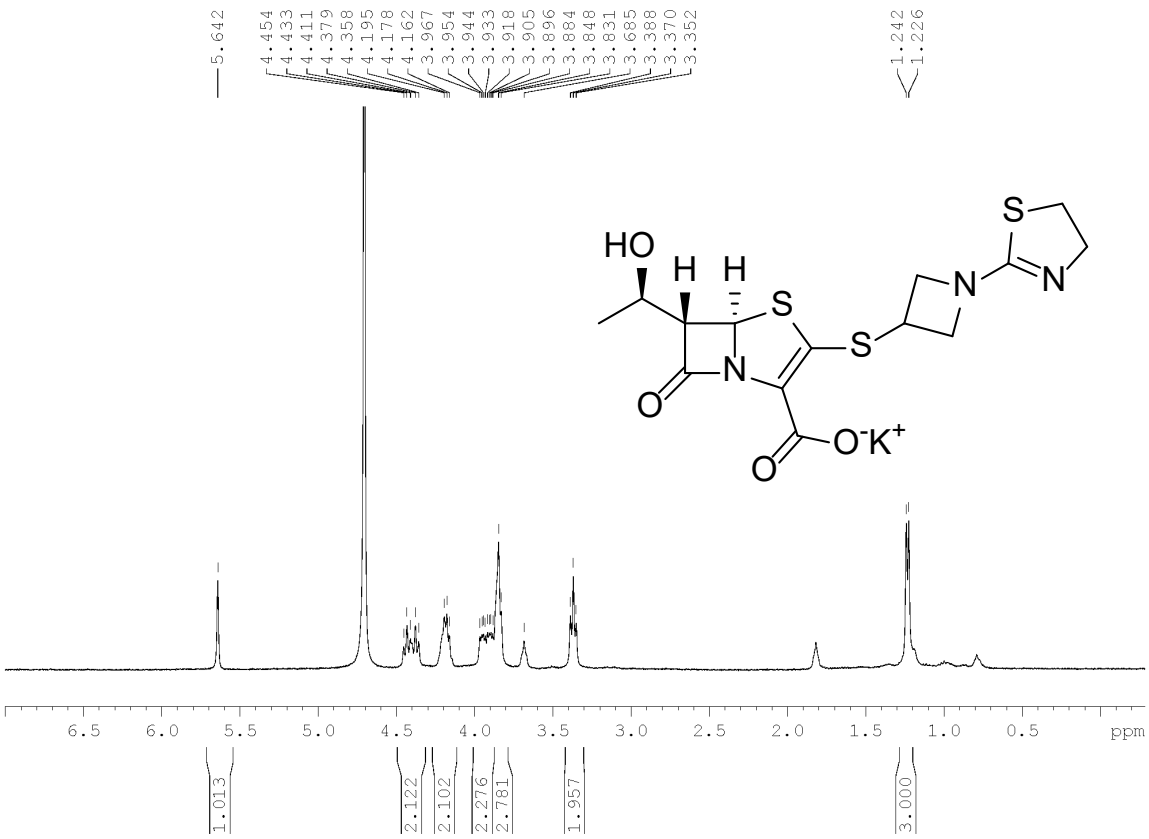

Potassium (5*R*,6*S*)-6-((*R*)-1-hydroxyethyl)-3-propylthio-7-oxo-4-thia-1-azabicyclo[3.2.0]hept-2-ene-2-carboxylate (17): From **30**; ^{1}H NMR (400MHz, D_2O) δ = 5.66 (d, *J* = 1.2 Hz, 1H), 4.25 (quin, *J* = 6.3 Hz, 1H), 3.89 (dd, *J* = 1.3, 6.0 Hz, 1H), 3.05 - 2.92 (m, 1H), 2.85 (td, *J* = 7.4, 13.0 Hz, 1H), 1.71 (dqd, *J* = 2.6, 7.3, 14.5 Hz, 2H), 1.31 (d, *J* = 6.5 Hz, 3H), 0.99 (t, *J* = 7.4 Hz, 3H). ^{13}C NMR (101MHz, D_2O) δ = 175.6, 166.8, 147.1, 123.3, 69.1, 64.7, 62.9, 37.2, 23.2, 20.1, 12.3. HRMS (UPLC), $C_{11}H_{15}NO_4S_2Na$ [M+Na^+] calculated: 312.0340; found: 312.0341.

Potassium (5*R*,6*S*)-6-((*R*)-1-hydroxyethyl)-3-((2-hydroxyethyl)thio)-7-oxo-4-thia-1-azabicyclo[3.2.0]hept-2-ene-2-carboxylate (18): ^{1}H NMR (400MHz, D_2O) δ = 5.67 (d, *J* = 1.4 Hz, 1H), 4.25 (quin, *J* = 6.3 Hz, 1H), 3.91 (dd, *J* = 1.5, 6.0 Hz, 1H), 3.82 (dt, *J* = 0.6, 6.5 Hz, 2H), 3.16 (td, *J* = 6.0, 14.1 Hz, 1H), 3.03 (td, *J* = 6.6, 14.1 Hz, 1H), 1.30 (d, *J*

= 6.5 Hz, 3H). HRMS (UPLC), $C_{10}H_{14}NO_5S_2$ [M+H$^+$] calculated: 292.0308; found: 292.0297. ^{13}C NMR was not obtained as the total amount of material was < 1 mg and compounds are not stable enough for 10+ h experiments at RT.

Potassium (5*R*,6*S*)-6-((*R*)-1-hydroxyethyl)-3-((3-methoxy-3-oxopropyl)thio)-7-oxo-4-thia-1-azabicyclo[3.2.0]hept-2-ene-2-carboxylate (19): ^{1}H NMR (400MHz, D_2O) δ = 5.69 (d, *J* = 1.8 Hz, 1H), 4.25 (quin, *J* = 6.3 Hz, 1H), 3.92 (dd, *J* = 1.5, 6.0 Hz, 1H), 3.72 (s, 3H), 3.25 (td, J_1 = 6.9, J_2 = 14.0 Hz, 1H), 3.10 (td, *J* = 7.1, 14.1 Hz, 1H), 2.83 (dt, J_1 = 1.8, 6.7 Hz, 2H), 1.31 (d, *J* = 6.5 Hz, 3H). HRMS (UPLC), $C_{12}H_{16}NO_6S_2$ [M+H$^+$] calculated: 334.0414; found: 334.0410; Δ 1.2 ppm. ^{13}C NMR was not obtained as the total amount of material was < 1 mg and compounds are not stable enough for 10+ h experiments at RT.

Potassium (5*R*,6*S*)-6-((*R*)-1-hydroxyethyl)-7-oxo-3-(((3*R*,5*R*)-5-(sulfamoylamino-methyl)pyrrolidin-3-yl)thio)-4-thia-1-azabicyclo[3.2.0]hept-2-ene-2-carboxylate (27): From **10**; ^{1}H NMR (400MHz, D_2O) δ = 5.71 (d, *J* = 1.4 Hz, 1H), 4.25 (quin, *J* = 6.4 Hz, 1H), 4.15 - 4.03 (m, 1H), 3.95 (dd, *J* = 1.5, 6.0 Hz, 1H), 3.81 - 3.70 (m, 2H), 3.64 (dd, *J* = 3.7, 11.7 Hz, 1H), 3.70 - 3.60 (m, 1H), 3.51 (dd, *J* = 7.0, 11.5 Hz, 1H), 3.49 (dd, J_1= 5.5, 7.4 Hz, 1H), 3.38 (dd, *J* = 8.6, 15.5 Hz, 1H), 2.76 - 2.64 (m, 1H), 1.30 (d, *J* = 6.5 Hz, 3H). HRMS (UPLC), $C_{13}H_{21}N_4O_6S_3$ [M+H$^+$] calculated: 425.0618; found: 425.0617. ^{13}C NMR was not obtained as the total amount of material was < 1 mg and compounds are not stable enough for 10+ h experiments at RT.

Potassium (5*R*,6*S*)-3-(((3*R*,5*R*)-5-(dimethylcarbamoyl)pyrrolidin-3-yl)thio)-6-((*R*)-1-hydroxyethyl)-7-oxo-4-thia-1-azabicyclo[3.2.0]hept-2-ene-2-carboxylate (20): From

11; ^{1}H NMR (400MHz, D_2O) δ = 5.69 (d, *J* = 1.4 Hz, 1H), 4.25 (quin, *J* = 6.3 Hz, 1H), 4.10 (q, *J* = 7.0 Hz, 1H), 3.91 (dd, *J* = 1.4, 6.3 Hz, 1H), 3.74 (dd, *J* = 3.9, 5.3 Hz, 2H), 3.64 (dd, *J* = 4.3, 5.1 Hz, 2H), 3.06 (s, 3H), 2.96 (s, 3H), 1.32 (d, *J* = 6.8 Hz, 3H). HRMS (UPLC), $C_{15}H_{22}N_3O_5S_2$ [M+H$^+$] calculated: 388.0995; found: 388.0994. ^{13}C NMR was not obtained as the total amount of material was < 1 mg and compounds are not stable enough for 10+ h experiments at RT.

References

1. Lang, M. *et al.* The penems, a new class of .beta.-lactam antibiotics. 2. Total synthesis of racemic 6-unsubstituted representatives. *J. Am. Chem. Soc.* **101,** 6296–6301 (1979).
2. Ernest, I., Gosteli, J. & Woodward, R. B. The penems, a new class of .beta.-lactam antibiotics. 3. Synthesis of optically active 2-methyl-(5R)-penem-3-carboxylic acid. *J. Am. Chem. Soc.* **101,** 6301–6305 (1979).
3. Pfaendler, H. R., Gosteli, J. & Woodward, R. B. The penems, a new class of .beta.-lactam antibiotics. 4. Syntheses of racemic and enantiomeric penem carboxylic acids. *J. Am. Chem. Soc.* **101,** 6306–6310 (1979).
4. Ernest, I. *et al.* The penems, a new class of .beta.-lactam antibiotics: 6-acylaminopenem-3-carboxylic acids. *J. Am. Chem. Soc.* **100,** 8214–8222 (1978).
5. Volkmann, R. A. & O'Neill, B. T. in *Strategies and Tactics in Organic Synthesis* (ed. Lindberg, T.) **3,** 495–531 (Academic Press, Inc, 1991).
6. Minamimura, M., Taniyama, Y. & Inoue, E. In Vitro Antibacterial Activity and ,-Lactamase Stability of CP-70,429, a New Penem Antibiotic. *Antimicrob. Agents Chemother.* 1547–1551 (1993).
7. Bloomberg.com. Iterum Therapeutics Limited: Private Company Information - Bloomberg. Available at: http://www.bloomberg.com/research/stocks/private/snapshot.asp?privcapId=31835 4064. (Accessed: 1st February 2017)
8. Kumar, P. *et al.* Non-classical transpeptidases yield insight into new antibacterials. *Nat. Chem. Biol.* **13,** 1–11 (2016).
9. Volkmann, R. A., Kelbaugh, P. R., Nason, D. M. & Jasys, V. J. 2-Thioalkyl Penems: An Efficint SYnthesis of Sulopenem, a (5R,6S)-6-(1(r)-hydroxyethyl)-2-[(cis-1-oxo-3-thiolanyl)thio]-2-penem Antibacterial. *J. Org. Chem* **57,** 4352–4361

(1992).

10. Mori, M., Hikida, M., Nishihara, T., Nasu, T. & Mitsuhashi, S. Comparative stability of carbapenem and penem antibiotics to human recombinant dehydropeptidase-I. *J. Antimicrob. Chemother.* **37,** 1034–6 (1996).

11. Girijavallabhan, V. M., Ganguly, A. K., McCombie, S. W., Pinto, P. & Rizvi, R. Synthesis of optically active penems. *Tetrahedron Lett.* **22,** 3485–3488 (1981).

12. Karady, S., Amato, J. S., Reamer, R. A. & Weinstock, L. M. Stereospecific conversion of penicillin to thienamycin. *J. Am. Chem. Soc.* **103,** 6765–6767 (1981).

13. Leanza, W. J. *et al.* An efficient synthesis of 2-substituted-thio-6-hydroxyethyl-penem-3-carboxylic acids via 2-thioxopenams. *Tetrahedron* **39,** 2505–2513 (1983).

14. Yishida, A., Hayashi, T., Takeda, N., Oida, S. & Ohki, E. 2-(Alkylthio)penem-3-carboxylic acids. IV. Synthesis of (hydroxyethyl)azetidinone precursors to 1-thia analogs of thienamycin. *Chem. Pharm. Bull. (Tokyo).* **29,** 2899–2909 (1981).

15. Hirai, K. *et al.* Synthesis of 1β-carbapenem derivative by aldol condensation method. *Tetrahedron Lett.* **22,** 1021–1024 (1981).

16. Fujimoto, K., Iwano, Y. & Hirai, K. From Penicillin to Penem and Carbapenem. VIII. Introduction of an Allyl Group at the C-4 Position of the Azetidinone Molecule, and the Synthesis of Dethiathienamycin. *Bull. Chem. Soc. Jpn.* **59,** 1363–1370 (1986).

17. Alpegiani, M. *et al.* Process for preparing optically active penems. (1985).

18. Phillips, D. & O'Neill, B. T. A convergent process to C-2 substituted peneme via addition of thiols and organocuprates to an O-triflylthioketene acetal. *Tetrahedron Lett.* **31,** 3291–3294 (1990).

19. Girijavallabhan, V. M., Ganguly, A. K., Pinto, P. & Versace, R. Synthesis of optically active penems. *J. Chem. Soc. Chem. Commun.* 908 (1983).

20. Evans, D. A. & Chapters, S. E. Rules for Ring Closure : Introduction Chemistry 206 Advanced Organic Chemistry Stereoelectronic Effects-3 'Rules for Ring Closure : Baldwin's Rules'. *Tetrahedron* 2003–2003 (2003).

21. DiNinno, F., Muthard, D. A., Ratcliffe, R. W. & Christensen, B. G. A convenient synthesis of racemic 6-hydroxyethyl-2-alkylthio-substituted penems. *Tetrahedron Lett.* **23,** 3535–3538 (1982).

22. Hugonnet, J., Tremblay, L. W., Boshoff, H. I., Barry, C. E. & Blanchard, J. S. Meropenem-Clavulanate Is Effective Against Extensively Drug- Resistant Mycobacterium tuberculosis. *Science.* **323,** 1215–1218 (2010).

23. Li, W.-J. *et al.* Crystal structure of L,D-transpeptidase LdtMt2 in complex with meropenem reveals the mechanism of carbapenem against Mycobacterium

tuberculosis. *Cell Res.* **23,** 728–31 (2013).

24. Charnas, R. L., Fisher, J. & Knowles, J. R. Chemical studies on the inactivation of Escherichia coli RTEM β-lactamase by clavulanic acid. *Biochemistry* **17,** 2185–2189 (1978).

25. Brenek, S. J. *et al.* Development of a practical and convergent process for the preparation of sulopenem. *Org. Process Res. Dev.* **16,** 1348–1359 (2012).

26. Ishiguro, M., Nishihara, T. & Tanaka, R. New Orally Active Penem Antibiotic: Farom. *Yakygaku Zashhi* **121,** 915–927 (2001).

27. Tanaka, R., Iwata, H. & Ishiguro, M. Synthesis of 5,6-cis-penems. *J. Antibiot. (Tokyo).* **43,** 1608–1610 (1990).

28. Ishiguro, M. *et al.* Studies on penem antibiotics. I. Synthesis and in vitro activity of novel 2-chiral substituted penems. *J. Antibiot. (Tokyo).* **41,** 1685–93 (1988).

29. Gavan, T. L. & Town, M. A. A microdilution method for antibiotic susceptibility testing: an evaluation. *Am. J. Clin. Pathol.* **53,** 880–5 (1970).

30. Desmond, E. *Susceptibility Testing of Mycobacteria, Nocardiae and Other Aerobic 565 Actinomycetes. Clinical Laboratory Standard Institute M24-A2.* (2011).

31. Ishiguro, M., Iwata, H., Tanaka, S. & Morishima, Y. Penem Derivative and Its Production. 1–6 (2001).

32. Ishiguro, M., Iwata, H., Tanaka, S. & Morishima, Y. Penem Derivative and its Production. 1–6 (1992).

Evan P. Lloyd

318 Birkwood Pl., Baltimore MD 21218
(412) 999-2382 ▪ elloyd5@jhu.edu

EDUCATION

Johns Hopkins University, Ph.D., Chemistry (Projected Feb. 2017), Baltimore, Maryland
Johns Hopkins University, M.A., Chemistry (Aug. 2012), Baltimore, Maryland
Carnegie Mellon University, B.S., Chemistry (Dec. 2009), Pittsburgh, Pennsylvania

RESEARCH EXPERIENCE

Johns Hopkins University, Department of Chemistry
Doctoral Research with Craig A. Townsend (June 2010 – current)

- New carbapenem and penem β-lactam antibiotics were developed for the treatment of multidrug-resistant ESKAPE pathogens with growth inhibitory activities in the clinically-useful low to sub μg/mL range. Potencies against *Mycobacteria* were improved >100 fold *vs.* FDA-approved carbapenems in the USA, and excellent activities against *M. abscessus* and *M. avium* have been demonstrated
- Lead optimization was guided by structure activity relationships, inhibitor–enzyme co-crystal structures and inhibitor adduct–protein mass spectrometry. This work was accomplished individually and as part of a larger team of biologists, pharmacologists, biophysicists and chemists at Johns Hopkins University and Medical School.
- Synthesized heat-, water- and pH-sensitive compounds with 3-6 stereogenic centers for enzyme activity assays providing data for multiple publications on enzymology.
- An oxygen-sensitive cobalamin-dependent radical SAM enzyme that is central to complex carbapenem biosynthesis was functionally characterized using a focused synthetic library of potential carbapenam(em) substrates and product standards.
- A new carbapenem-producing gene cluster from *Streptomyces argenteolus* ATCC 11009 was identified, the encoded biosynthetic proteins annotated and the carbapenems produced structurally characterized and compared to independently synthesized references.

Carnegie Mellon University, Department of Chemistry
Undergraduate Research with Terrence J. Collins (Sept. 2008 – June 2010)

- Green chemical methods were used for the selective oxidation of toxic and hazardous pollutants. Quantitative yields and kinetic rates of catalysis were analyzed by HPLC.

- New iron-tetra-amido macrocyclic ligand complexes (Fe-TAML) were synthesized concluding with the successful preparation of iron(III)$(NO_2)_2$ TAML D*, a powerful peroxidase enzyme mimic.

Medical College of Wisconsin, Department of Endocrinology
Undergraduate Research with Victor Drover (June 2008 – August 2008)

- Cloned and mutated constructs of encoded CD36 from genomic DNA and purified expressed protein to understand the role of human CD36 mutations in the regulation of fatty acid uptake. This work culminated in a formal presentation for the faculty of MCW.

PUBLICATIONS AND PATENTS

10. R. Mattoo, **E.P. Lloyd**, A. Kaushik, P. Kumar, J.L. Brunelle, C.A. Townsend, G. Lamichhane. "A molecular vulnerability in *Mycobacterium avium:* L,D-transpeptidase orthologue in *Mycobacterium avium* is constitutively expressed and inhibited by carbapenems." *Future Microbiol.,* (2017) *in press.*
11. P. Kumar, A. Kaushik, **E.P. Lloyd**, S-G. Li, R. Mattoo, N. Ammerman, D. Bell, A. Perryman, T. Zandi, S. Ekins, S. Ginell, C.A. Townsend, J. Freundlich, G. Lamichhane. "Non-classical transpeptidases yield insight into new antibacterials." *Nat. Chem. Biol.*, 2017, 13, 54-61.
12. D.R. Marous, **E.P. Lloyd**, A.R. Buller, T.L. Grove, A.J. Blaszczyk, S.J. Booker, C.A. Townsend. "Consecutive radical *S*-adenosylmethionine methylations form the ethyl side chain in thienamycin biosynthesis." *Proc. Natl. Acad. Sci. U.S.A.*, 2015, 112 (33), 10354-8.
13. L.A. Basta, A Ghosh, Y. Pan, J Jean, **E.P. Lloyd**, C.A. Townsend, G. Lamichhane, M.A. Bianchet. "Loss of a functionally and structurally distinct L,D-transpeptidase LdtMt5, compromises cell wall integrity in *Mycobacterium tuberculosis*." *J. Biol. Chem.*, 2015, 290 (42), 25670-85.
14. R. Li, **E.P. Lloyd**, K.A. Moshos, C.A. Townsend. "Identification and characterization of the carbapenem MM 4550 and its gene cluster in *Streptomyces argenteolus* ATCC 11009." *ChemBioChem*, 2014, 15 (2), 320-31.
15. M.J. Bodner, R.M. Phelan, M.F. Freeman, K.A. Moshos, **E.P. Lloyd**, C.A. Townsend. "Definition of the common and divergent steps in carbapenem β-lactam antibiotic biosynthesis." *ChemBioChem*, 2011, 12 (14), 2159-65.

Submitted or In Preparation:

16. Y.H. Pan, L.A. Basta, H.G. Saaverdra, **E.P. Lloyd**, P. Kumar, R. Mattoo, C.A. Townsend, M.A. Bianchet, G. Lamichhane. "Structural insight into the mechanism of inhibition of *Mycobacterium tuberculosis* L,D-transpeptidase 2 by Biapenem and Tebipenem." *Manuscript submitted for review.*
17. **E.P. Lloyd**, A. Kaushik, P. Kumar, H. Batchelder, T. Zandi, F. D'Andrea, E. Nuremberger, G. Lamichhane, C.A. Townsend. "Novel penems are effective against

multi-drug resistant ESKAPE pathogens and *Mycobacteria in vivo*." *Manuscript nearing submission.*

Patents

18. C.A. Townsend, **E.P. Lloyd**. "New Antibacterials Against D,D- and L,D-Transpeptidases." 2016. Provisional patent application.
19. G. Lamichhane, C.A. Townsend, R. Mattoo, P. Kumar, **E.P. Lloyd**. "L,D-transpeptidases of *Enterobacter cloacae*, *Klebsiella pneumoniae*, *Pseudomonas aeruginosa* and *Mycobacterium abscessus*." 2015. Provisional patent application.
20. G. Lamichhane, C.A. Townsend, N.M. Parrish, A. Kaushik, P. Kumar, **E.P. Lloyd**, S-G. Li, J. Freundlich, S. Ekins. "Novel Inhibitors of Bacterial Growth." U.S. Patent application US 62/288,532, filed November 2015. Patent Pending.

TEACHING EXPERIENCE

Johns Hopkins University

Teaching Assistant

Undergraduate Organic Chemistry I (Chemistry 03.205)	Fall 2010 – 2015
Undergraduate Organic Chemistry II (Chemistry 03.206)	Spring 2011

Head Teaching Assistant

Undergraduate Organic Chemistry II (Chemistry 03.206)	Spring 2012

MENTORING AND ADVISING EXPERIENCE

Research mentees:

Hunter Bachelder, Graduate Student, JHU Chemistry	2016-Present
Trevor Zandi, Graduate Student, JHU Biophysics	2016-Present
Erica Sinner, Graduate Student, JHU Chemical Biology Interface	2015-Present
Daniel Nguyen, Rotation Student, JHU Chemical Biology Interface	2014-2015
Currently a research associate at Genentech in San Jose, CA	
Victor Penaud, Masters Student, ENS Paris Chemistry	2013
Currently working at AP-HP Hopitaux de Paris	